

EDY LENIN TEJEDA MONTALVAN

Geotechnical properties of mixtures of water treatment sludge and residual lateritic soils from the State of São Paulo

Revised version

Concentration area:
Geotechnical Engineering

Advisor:
Prof. Dr. Maria Eugenia Gimenez Boscov

São Paulo
2021

EDY LENIN TEJEDA MONTALVAN

Geotechnical properties of mixtures of water treatment sludge and residual lateritic soils from the State of São Paulo

Revised version

Ph.D. Thesis presented to the Graduate Program in Civil Engineering at the Polytechnic School of the University of São Paulo, Brazil in partial fulfillment of the requirements to obtain the degree of Doctor of Science.

Concentration area:
Geotechnical Engineering

Advisor:
Prof. Dr. Maria Eugenia Gimenez Boscov

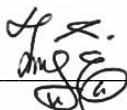
São Paulo
2021

AUTORIZO A REPRODUÇÃO E DIVULGAÇÃO TOTAL OU PARCIAL DESTE TRABALHO, POR QUALQUER MEIO CONVENCIONAL OU ELETRÔNICO, PARA FINS DE ESTUDO E PESQUISA, DESDE QUE CITADA A FONTE.

Este exemplar foi revisado e alterado em relação à versão original, sob responsabilidade única do autor e com a anuência de seu orientador.

São Paulo, 4 de fevereiro de 2021.

Assinatura do autor: _____



Assinatura do orientador: Marina Eugenia Gimenez Bonor

Catálogo-na-publicação

Montalvan, Edy Lenin Tejada

Geotechnical properties of mixtures of water treatment sludge and residual lateritic soils from the State of São Paulo / E. L. T. Montalvan -- versão corr. -- São Paulo, 2021.
233 p.

Tese (Doutorado) - Escola Politécnica da Universidade de São Paulo. Departamento de Engenharia de Estruturas e Geotécnica.

1.Lodo 2.Resíduos sólidos 3.Compactação dos solos 4.Resistência dos solos 5.Compressibilidade dos solos I.Universidade de São Paulo. Escola Politécnica. Departamento de Engenharia de Estruturas e Geotécnica II.t.

MONTALVAN, E. L. T. **Geotechnical properties of mixtures of water treatment sludge and residual lateritic soils from the State of São Paulo**. 2020. Thesis (PhD in Civil Engineering) – *Escola Politécnica, Universidade de São Paulo, São Paulo, 2020*.

Approval date: 11 / 11 / 2020

Evaluation committee:

Prof. Dr. (Thesis Advisor): **Maria Eugenia Gimenez Boscov**

Institution: Escola Politécnica, Universidade de São Paulo (USP), São Paulo, Brazil

Decision: Approved

Dr.: **António José Roque**

Institution: Laboratório Nacional de Engenharia Civil (LNEC), Lisboa, Portugal

Decision: Approved

Prof. Dr. **Gemmina di Emidio**

Institution: Ghent University (Gent), Ghent, Belgium

Decision: Approved

Prof. Dr. **Michéle Dal Toé Casagrande**

Institution: Universidade de Brasília (UnB), Brasília, Brazil

Decision: Approved

Prof. Dr. **Paulo Scarano Hemsí**

Institution: Instituto Tecnológico de Aeronáutica (ITA), São José dos Campos, Brazil

Decision: Approved

To my parents,

*Maria Betulia Montalvan and Raúl Guillermo Tejada,
who have always encouraged me to pursue my dreams.*

ACKNOWLEDGEMENTS

This thesis was only possible due to the guidance and motivation of my advisor professor Dr. Maria Eugenia Gimenez Boscov. I had the great opportunity to develop both my master's and doctoral research under her advisory. I am grateful for the support and patience, many days analyzing results, writing articles and correcting my written works. I am especially thankful for her friendship; I hope it will last for the rest of our days.

Special thanks to my family and to my girlfriend, Ana Figueroa, for all their love, motivation and support throughout my graduate career.

Many thanks to the technical staff of the Laboratory of Soil Mechanics (LMS), Antônio Heitzman and Valdineia dos Santos, without them my days in the laboratory would have been tougher. I really appreciate their support; my research work was immensely benefited from their experience.

Thanks to all professors and staff from the department of Structural and Geotechnical Engineering of the Polytechnic School, specially to prof. Faïçal Massad, prof. Fernando Marinho, prof. José Jorge Nader, prof. Marcos Massao Futai, prof. Avessani Neto, Maria Elizabete Santos, Rosangela Alves, and Wandréa Dantas. I am also grateful to prof. Paulo Hemsi, from the Aeronautics Institute of Technology (ITA), who has collaborated to the research project since the beginning.

Thanks to colleagues Kemmylle Ferreira (Master's of Science program), Aline Roque (Master's of Science program). Thanks also to Túlio Sawatani (Intern, from Environmental Engineering) and Rafaela Godoy (Intern, from Environmental Engineering), their assistance on the laboratorial testing was crucial.

Thanks to all friends from the LMS and the department Structural and Geotechnical Engineering: Adrian Torrico, Alex Novak, Aline, Ana Halabi, Juliana Keiko, Kemmylle Sanny, Thais Lada, Túlio Sawatani, Philippe Stankevicius, Luisa, Robinson, Gabriel Bellina, Moustafa, and all those who I may have forgotten to include.

Thanks to the São Paulo State Sanitation Company and the staff from Cubatão and Taiaçupeba water treatment plants who provided the sludge samples used in this research. Finally, I gratefully acknowledge financial support from the São Paulo Research Foundation (FAPESP, file numbers: 2013/50448-8 and 2017/24056-6).

ABSTRACT

MONTALVAN, E. L. T. **Geotechnical properties of mixtures of water treatment sludge and residual lateritic soils from the State of São Paulo**. 2020. Thesis (PhD in Civil Engineering) – Escola Politécnica, Universidade de São Paulo, São Paulo, 2020.

The most common practices for disposal of water treatment sludge (WTS) have generally been dumping into rivers, disposal in sanitary landfills, and discharge in sewage treatment plants. However, growing environmental concern and rigorous legislation have led to the search for more adequate disposal or recycling alternatives, such as, reuse in ceramic products, cement production, agriculture, earthworks, among others. Reuse of WTS in earthworks is a promising alternative, since large amounts of soil are used, which can be partly substituted by WTS as long as engineering properties are not significantly altered. This research investigated the geotechnical behavior of soils and WTS mixtures in different blending ratios in order to evaluate their suitability for geotechnical structures, as material for embankments, backfills, and bottom liners and covers of landfills. The studied soils and sludges comprise a lateritic clayey sand, a lateritic clay, a ferric sludge, and an alum sludge. Both sludges were chemically and mineralogically characterized by x-ray diffraction, x-ray fluorescence, scanning electron microscopy, loss on ignition, pH, cation exchange capacity, and organic matter. Geotechnical characterization of the soils and sludges comprised grain-size distribution, specific gravity of solids, and Atterberg limits. Each soil was mixed with each sludge at three different blending ratios, thus twelve mixtures were prepared. The geotechnical behavior of the mixtures was evaluated by the following tests: standard-effort Proctor compaction, oedometric compression, consolidated undrained triaxial compression, permeability, and unconfined compression. Moreover, volumetric shrinkage and soil-water retention tests were conducted. Besides, analyses by mercury intrusion porosimetry were carried out. Compelling results were obtained. Most of the mixtures presented compressibility and shear strength suitable for earthworks. Some mixtures presented adequate permeability for landfill liners, and all mixtures could be used as daily cover material in landfills. The final step for reuse would be the environmental evaluation of the mixtures, which was not in the scope of this thesis; apropos, physical-chemical characterization of the sludges indicates that environmental risk associated to release of contaminants is not to be expected. The results indicate that, from a structural point of view, WTS can be incorporated to local soils for geotechnical applications, provided the feasible mixtures are evaluated by means of typical geotechnical testing and criteria coherent with the intended application.

Keywords: water treatment sludge, soil-sludge mixtures, soil compaction, soil compressibility, hydraulic conductivity, shear strength

RESUMO

MONTALVAN, E. L. T. **Propriedades geotécnicas de misturas de lodo de estação de tratamento de água com solos residuais lateríticos do Estado de São Paulo**. 2020. Tese (Doutorado em Engenharia Civil) – Escola Politécnica, Universidade de São Paulo, São Paulo, 2020.

A destinação do lodo de estação de tratamento de água (ETA) tem sido comumente o descarte em rios, a disposição em aterros sanitários ou industriais e o lançamento na rede de esgoto. A legislação ambiental cada vez mais rigorosa tem levado à busca de alternativas mais econômicas e ambientalmente adequadas, como o reuso do lodo na indústria cerâmica, construção civil, agricultura, fabricação de cimento, obras de terra, entre outras. Obras de terra são uma alternativa promissora para o uso do lodo de ETA por utilizarem grande volume de solo, o qual pode ser parcialmente substituído por lodo desde que as propriedades geotécnicas não sejam significativamente alteradas. Esta pesquisa estudou o comportamento geotécnico de misturas de dois solos lateríticos com dois lodos de ETA, visando empregá-las como material para construção de obras geotécnicas, tais como revestimento de fundo, cobertura diária e cobertura final de aterros sanitários e industriais, aterros estruturais e reaterro de valas. Foram estudadas uma areia argilosa e uma argila. Os lodos foram provenientes de ETAs que usam coagulantes distintos, cloreto férrico e sulfato de alumínio. Os lodos foram caracterizados química e mineralogicamente por ensaios de difração de raios X, fluorescência de raios X, microscopia eletrônica de varredura, perda ao fogo, pH, capacidade de troca catiônica e matéria orgânica. Todos os materiais foram caracterizados geotecnicamente. Cada solo foi misturado a cada lodo em três proporções, resultando em 12 misturas. O comportamento geotécnico das misturas foi avaliado por ensaios de compactação, adensamento, permeabilidade, compressão triaxial e compressão simples. Determinaram-se, também, curvas de contração volumétrica e de retenção de água, e a distribuição porosimétrica por meio de intrusão de mercúrio. Os resultados foram promissores, pois a maioria das misturas apresentou compressibilidade e resistência adequadas para uso em aterros compactados. Algumas misturas apresentaram permeabilidade adequada para uso em revestimento de fundo e cobertura final de aterros sanitários, e todas as misturas podem ser utilizadas como material para cobertura diária. O último passo para o reuso seria a avaliação ambiental das misturas, fora do escopo desta tese; mesmo assim, a caracterização físico-química dos lodos indica que não há expectativa de risco potencial associado à liberação de contaminantes. Os resultados indicam que, do ponto de vista estrutural, lodos de ETA podem ser incorporados a solos locais em aplicações geotécnicas, desde que as misturas sejam avaliadas por meio de ensaios geotécnicos e de critérios coerentes com as aplicações desejadas.

Palavras-chave: lodo de estação de tratamento de água, misturas solo-lodo, compactação, compressibilidade, condutividade hidráulica, resistência ao cisalhamento

TABLE OF CONTENTS

1	INTRODUCTION	28
1.1	RESEARCH OBJECTIVES	30
2	LITERATURE REVIEW	31
2.1	WATER TREATMENT SLUDGE	31
2.1.1	<i>Water treatment process.....</i>	<i>31</i>
2.1.2	<i>Water treatment sludge production.....</i>	<i>33</i>
2.1.3	<i>Water treatment sludge quantification</i>	<i>35</i>
2.2	CHARACTERIZATION OF WATER TREATMENT SLUDGE.....	35
2.2.1	<i>Water distribution in WTS</i>	<i>36</i>
2.2.2	<i>Mineralogical composition.....</i>	<i>37</i>
2.2.3	<i>Chemical composition and characteristics.....</i>	<i>37</i>
2.2.4	<i>Geotechnical characterization.....</i>	<i>41</i>
2.3	WATER TREATMENT SLUDGE DISPOSAL AND REUSE	45
2.3.1	<i>Regulation and disposal</i>	<i>45</i>
2.3.2	<i>Beneficial reuse options.....</i>	<i>47</i>
2.4	REUSE OF WATER TREATMENT SLUDGE IN GEOTECHNICAL WORKS	48
2.4.1	<i>Waste landfills.....</i>	<i>49</i>
2.4.2	<i>Backfills.....</i>	<i>51</i>
2.4.3	<i>Embankments.....</i>	<i>51</i>
2.4.4	<i>Pavements.....</i>	<i>52</i>
2.5	COMPACTED SOILS IN GEOTECHNICAL WORKS.....	53
2.5.1	<i>Waste landfills.....</i>	<i>54</i>
2.5.2	<i>Embankments.....</i>	<i>59</i>
3	METHODOLOGY	64

3.1	MATERIALS	64
3.1.1	<i>Sludge from Cubatão WTP</i>	64
3.1.2	<i>Sludge from Taiaçupeba WTP</i>	65
3.1.3	<i>Clayey sand</i>	68
3.1.4	<i>Clay</i>	68
3.1.5	<i>Mixtures soil-WTS</i>	69
3.2	TESTING PROGRAM	73
3.2.1	<i>Sludge sampling</i>	73
3.2.2	<i>Mineralogical characterization</i>	75
3.2.3	<i>Chemical characterization</i>	76
3.2.4	<i>Organic matter removal</i>	76
3.2.5	<i>Geotechnical characterization</i>	77
3.2.6	<i>Compaction</i>	79
3.2.7	<i>Specimens preparation for consolidation, permeability and shear strength</i>	80
3.2.8	<i>Compressibility</i>	80
3.2.9	<i>Permeability</i>	80
3.2.10	<i>Shear strength</i>	81
3.2.11	<i>Specimens preparation for unconfined compression, suction, and porosimetry tests</i>	83
3.2.12	<i>Unconfined compression</i>	84
3.2.13	<i>Volumetric shrinkage</i>	84
3.2.14	<i>Mercury intrusion porosimetry (MIP)</i>	85
3.2.15	<i>Soil-water retention curves from suction tests</i>	86
3.2.16	<i>Soil-water retention curves from MIP</i>	89
4	RESULTS AND DISCUSSIONS	91
4.1	SLUDGE SAMPLING	91

4.2	MINERALOGICAL CHARACTERIZATION	94
4.2.1	<i>X-ray diffraction</i>	94
4.2.2	<i>Scanning electron microscopy</i>	97
4.3	CHEMICAL CHARACTERIZATION.....	101
4.3.1	<i>Chemical composition by X-ray fluorescence (XRF)</i>	101
4.3.2	<i>Chemical parameters</i>	103
4.4	GEOTECHNICAL CHARACTERIZATION	106
4.4.1	<i>Air-drying of sludge samples</i>	106
4.4.2	<i>Organic matter</i>	107
4.4.3	<i>Specific gravity and grain size distribution</i>	109
4.4.4	<i>Atterberg limits</i>	115
4.5	COMPACTION	117
4.6	COMPRESSIBILITY	125
4.7	PERMEABILITY	133
4.8	TRIAXIAL COMPRESSION.....	136
4.8.1	<i>Undrained shear strength</i>	136
4.8.2	<i>Shear strength in terms of effective stresses</i>	141
4.9	UNCONFINED COMPRESSION.....	146
4.10	VOLUMETRIC SHRINKAGE	148
4.11	MERCURY INTRUSION POROSIMETRY.....	151
4.12	SOIL-WATER RETENTION CURVES	156
4.12.1	<i>SWRC from suction tests</i>	156
4.12.2	<i>SWRC from MIP</i>	163
5	EVALUATION OF THE MIXTURES FOR USE IN EARTHWORKS.....	165
5.1	WASTE LANDFILLS.....	165
5.1.1	<i>BC mixtures</i>	166

5.1.2	<i>BT mixtures</i>	166
5.1.3	<i>CC mixtures</i>	166
5.1.4	<i>CT mixtures</i>	167
5.2	EMBANKMENTS.....	167
5.2.1	<i>BC mixtures</i>	169
5.2.2	<i>BT mixtures</i>	169
5.2.3	<i>CC mixtures</i>	169
5.2.4	<i>CT mixtures</i>	169
6	CONCLUSIONS	170
	REFERENCES	175
	APPENDIX A	191
	APPENDIX B	197
	APPENDIX C	203
	APPENDIX D	209
	APPENDIX E	212
	APPENDIX F	219
	APPENDIX G	231

LIST OF FIGURES

FIGURE 1 – CONVENTIONAL WATER TREATMENT PROCESS.	31
FIGURE 2 – COMMON RESIDUE STREAMS IN CONVENTIONAL WTPs.....	33
FIGURE 3 – FLOC SKELETON OF SLUDGE CLAY PARTICLES.	36
FIGURE 4 – FINAL DISPOSAL OF WTS IN BRAZIL: (A) PNSB 2008 ¹ ; (B) PNSB 2017 ²	47
FIGURE 5 – BENEFICIAL REUSE OPTIONS FOR WTS.	48
FIGURE 6 – SCHEMATICS OF: (A) CONVENTIONAL COMPACTION SPECIFICATION; (B) RECOMMENDED COMPACTION SPECIFICATION (DANIEL; BENSON, 1990).	56
FIGURE 7 – COMPACTION PARAMETERS OF SOILS USED FOR COMPACTED LANDFILL LINERS.	57
FIGURE 8- INFLUENCE OF RC ON DRY UNIT WEIGHT AND UNDRAINED SHEAR STRENGTH.	61
FIGURE 9 – COMPACTION PARAMETERS OF SOILS USED IN DIFFERENT EARTHWORKS.	62
FIGURE 10 – SHEAR STRENGTH ENVELOPES (EFFECTIVE STRESS) OF SOME COMPACTED BRAZILIAN SOILS.	63
FIGURE 11 – LOCATION OF CUBATÃO WTP.	66
FIGURE 12 – LOCATION OF TAIACUPEBA WTP.	67
FIGURE 13 – SAMPLING SITE OF THE CLAYEY SAND FROM BOTUCATU CITY.....	70
FIGURE 14 – SAMPLING SITE OF THE CLAY FROM CAMPINAS CITY.....	71
FIGURE 15 – SLUDGE SAMPLING METHODOLOGY AND TAGS MEANING.....	74
FIGURE 16 – (A) TAIACUPEBA WTS SAMPLES; (B) SAMPLES MIXING.....	74
FIGURE 17 – SCANNING ELECTRON MICROSCOPY EQUIPMENT.....	75
FIGURE 18 – OM REMOVAL PROCESS: (A) H ₂ O ₂ ADDITION AND HEATING; (B) FILTRATION; (C) OVEN-DRYING AND PULVERIZATION.	77
FIGURE 19 – DESCRIPTION OF WATER CONTENT OF SOIL-WTS MIXTURES.	79
FIGURE 20 – MINIATURE COMPACTION EQUIPMENT.	83
FIGURE 21 – MIP TEST: (A) CROSS-SECTIONAL VIEW OF MICROMERITICS PENETROMETER AND (B) TYPICAL PSD CURVES.	85

FIGURE 22 – SUCTION PLATE: (A) SCHEMATIC VIEW; (B) LABORATORY TEST.....	87
FIGURE 23 – PRESSURE CHAMBER: (A) SCHEMATIC VIEW; (B) USED IN THIS STUDY.	87
FIGURE 24 – FILTER PAPER METHOD.	88
FIGURE 25 - WATER AND SOLIDS CONTENT VARIATION: (A) CUBATÃO-WTS; (B) TAIACUPEBA-WTS.	91
FIGURE 26 – DESCRIPTIVE STATISTICS OF WATER CONTENT OF CUBATÃO WTS SAMPLES.	92
FIGURE 27 – DESCRIPTIVE STATISTICS OF WATER CONTENT OF TAIACUPEBA SAMPLES.	93
FIGURE 28 – X-RAY DIFFRACTION ANALYSIS OF TAIACUPEBA WTS POWDER: (A) DIFFRACTOGRAM; (B) IDENTIFIED PHASES.	96
FIGURE 29 - X-RAY DIFFRACTION ANALYSIS OF TAIACUPEBA WTS TREATED WITH HYDROGEN PEROXIDE: (A) DIFFRACTOGRAM; (B) IDENTIFIED PHASES.....	97
FIGURE 30 – IMAGES OF CUBATÃO WTS PARTICLES FROM SEM: (A) QUARTZ IN FINE SAND FRACTION WITH COATINGS; (B) (C) (D) CLAY MINERALS.	98
FIGURE 31 – SEM IMAGES OF TAIACUPEBA WTS PARTICLES.	99
FIGURE 32 – SEM IMAGES OF TAIACUPEBA WTS PRE-TREATED WITH H ₂ O ₂	101
FIGURE 33 – WATER CONTENT (W) AND SOLIDS CONTENT (SC) VARIATION DURING AIR-DRYING: (A) CUBATÃO SLUDGE ¹ ; (B) TAIACUPEBA SLUDGE ²	107
FIGURE 34 - SAMPLES FOR OM TESTS BY IGNITION AT 440 °C: A) CUBATÃO-WTS BEFORE IGNITION; B) TAIACUPEBA-WTS BEFORE IGNITION; C) CUBATÃO-WTS AFTER IGNITION; D) TAIACUPEBA-WTS AFTER IGNITION.	108
FIGURE 35 – GRADING CURVES OF CLAYEY SAND, CLAY, AND CUBATÃO WTS.	110
FIGURE 36 GRAIN SIZE DISTRIBUTION TESTS FOR TAIACUPEBA WTS WITH DIFFERENT DISPERSANTS.	111
FIGURE 37 – GSD CURVES FROM LASER ANALYSES: A) CUBATÃO-WTS; B) TAIACUPEBA-WTS.	112
FIGURE 38 – GSD CURVES OF CLAYEY SAND AND MIXTURES: (A) BC ¹ ; (B) BT ²	113
FIGURE 39 – GSD CURVES OF CAMPINAS CLAY AND MIXTURES: (A) CC MIXTURES; (B) CT MIXTURES.	114

FIGURE 40 – CASAGRANDE’S PLASTICITY CHART: (A) SOILS AND MIXTURES; (B) SLUDGES.	115
FIGURE 41 – COMPACTION CURVES OF: (A) CLAYEY SAND AND BT MIXTURES ¹ ; (B) CLAYEY SAND AND BC MIXTURES ² .	118
FIGURE 42 – COMPACTION CURVES OF: (A) CAMPINAS CLAY AND CT MIXTURES; (B) CAMPINAS CLAY AND CT MIXTURES.	119
FIGURE 43 – RELATIONSHIP BETWEEN OPTIMUM WATER CONTENT AND PLASTIC LIMIT.	119
FIGURE 44 – VARIATION OF COMPACTION PARAMETERS AS A FUNCTION OF WTS CONTENT FOR BC AND BT MIXTURES: (A) MAXIMUM DRY UNIT WEIGHT; (B) OPTIMUM WATER CONTENT.	120
FIGURE 45 – VARIATION OF COMPACTION PARAMETERS AS A FUNCTION OF WTS CONTENT FOR CC AND CT MIXTURES: (A) MAXIMUM DRY UNIT WEIGHT; (B) OPTIMUM WATER CONTENT	121
FIGURE 46 – VARIATION OF COMPACTION PARAMETERS AS A FUNCTION OF DESICCATION RATIO: (A) $\Gamma_{D_{MAX}}$ OF BC AND BT MIXTURES; (B) W_{OPT} OF BC AND BT MIXTURES.	122
FIGURE 47 – VARIATION OF COMPACTION PARAMETERS AS A FUNCTION OF DESICCATION RATIO: (A) $\Gamma_{D_{MAX}}$ OF CC MIXTURES; (B) W_{OPT} OF CC MIXTURES.	123
FIGURE 48 – VARIATION OF COMPACTION PARAMETERS WITH WTS ADDITION AND DESICCATION OF: (A) BC AND BT MIXTURES; (B) CC AND CT MIXTURES.	124
FIGURE 49 – COMPARISON OF OPTIMUM COMPACTION PARAMETERS.	125
FIGURE 50 – STRESS-STRAIN CURVES FROM OEDOMETRIC COMPRESSION TESTS OF BOTUCATU CLAYEY SAND AND BC MIXTURES.	126
FIGURE 51 – STRESS-STRAIN CURVES FROM OEDOMETRIC COMPRESSION TESTS OF BOTUCATU CLAYEY SAND AND BT MIXTURES.	126
FIGURE 52 – STRESS-STRAIN CURVES FROM OEDOMETRIC COMPRESSION TESTS OF CAMPINAS CLAY AND CC MIXTURES.	127
FIGURE 53 – STRESS-STRAIN CURVES FROM OEDOMETRIC COMPRESSION TESTS OF CAMPINAS CLAY AND CT MIXTURES.	127
FIGURE 54 - VARIATION OF COMPRESSION INDEX WITH WTS CONTENT.	129
FIGURE 55 - VARIATION OF SWELLING INDEX WITH WTS CONTENT.	129

FIGURE 56 – CORRELATIONS OF VIRGIN COMPRESSION INDEX (C_c) WITH STATE PARAMETERS: (A) C_c – LIQUID LIMIT (w_L); (B) C_c – INITIAL VOID RATIO (e_0).	130
FIGURE 57 – VARIATION OF CONSTRAINED MODULUS (M) WITH EFFECTIVE VERTICAL STRESS FOR BOTUCATU CLAYEY SAND AND BC MIXTURES.....	131
FIGURE 58 – VARIATION OF CONSTRAINED MODULUS (M) WITH EFFECTIVE VERTICAL STRESS FOR BOTUCATU CLAYEY SAND AND BT MIXTURES.	132
FIGURE 59 – VARIATION OF CONSTRAINED MODULUS (M) WITH EFFECTIVE VERTICAL STRESS FOR CAMPINAS CLAY AND CC MIXTURES.....	132
FIGURE 60 – VARIATION OF CONSTRAINED MODULUS (M) WITH EFFECTIVE VERTICAL STRESS FOR CAMPINAS CLAY AND CT MIXTURES.	133
FIGURE 61 – HYDRAULIC CONDUCTIVITY VARIATION WITH WTS CONTENT FOR: (A) CC^1 AND CT^1 MIXTURES; (B) BC^2 AND BT^1 MIXTURES.....	135
FIGURE 62 – UNDRAINED SHEAR STRENGTH (s_u) VERSUS CONSOLIDATION PRINCIPAL MAJOR STRESS (Σ'_{1c}) FOR CAMPINAS CLAY AND MIXTURES.	139
FIGURE 63 – UNDRAINED SHEAR STRENGTH (s_u) VERSUS CONSOLIDATION PRINCIPAL MAJOR STRESS (Σ'_{1c}) FOR BOTUCATU CLAYEY SAND AND MIXTURES.	139
FIGURE 64 – INFLUENCE OF WTS ADDITION ON DRY UNIT WEIGHT AND UNDRAINED SHEAR STRENGTH.....	140
FIGURE 65 – VARIATION OF UNDRAINED SHEAR STRENGTH (FOR $\Sigma'_{3c} = 50kPa$) WITH WTS CONTENT.	141
FIGURE 66 – EFFECTIVE STRESS PATHS FOR CAMPINAS CLAY AND: (A) CT MIXTURES; (B) CC MIXTURES.	142
FIGURE 67 – EFFECTIVE STRENGTH ENVELOPE FOR CAMPINAS CLAY, AND CC AND CT MIXTURES.	143
FIGURE 68 – EFFECTIVE STRESS PATHS FOR BOTUCATU CLAYEY SAND AND: (A) BT MIXTURES; (B) BC MIXTURES.....	144
FIGURE 69 – EFFECTIVE STRENGTH ENVELOPE FOR BOTUCATU CLAYEY SAND, AND BC AND BT MIXTURES.	145

FIGURE 70 – AS-COMPACTED UCS OF SOILS AND MIXTURES: (A) UCS VARIATION WITH WTS CONTENT; (B) STRENGTH REDUCTION RATIO (SRR) VARIATION WITH WTS CONTENT.	146
FIGURE 71 – VARIATION OF AS-COMPACTED UNDRAINED SHEAR STRENGTH WITH WTS CONTENT.	147
FIGURE 72 – COMPARISON OF UNDRAINED SHEAR STRENGTH FROM UC (AS-COMPACTED) AND CU TESTS (50 kPa CONFINING PRESSURE).	148
FIGURE 73 – VARIATION OF TOTAL VOLUMETRIC SHRINKAGE WITH: (A) WTS CONTENT; (B) COMPACTION MOISTURE.	149
FIGURE 74 – SHRINKAGE CURVES OF CAMPINAS CLAY AND CC MIXTURES.	150
FIGURE 75 – SHRINKAGE CURVES OF CAMPINAS CLAY AND CT MIXTURES.	150
FIGURE 76 – SHRINKAGE CURVES OF BOTUCATU CLAYEY SAND AND BC MIXTURES.	151
FIGURE 77 – SHRINKAGE CURVES OF BOTUCATU CLAYEY SAND AND BT MIXTURES.	151
FIGURE 78 – WATER CONTENT VARIATION OVER TIME OF SAMPLES DURING AIR-DRYING PRIOR MIP TESTS.	152
FIGURE 79 – RESULTS FROM MIP FOR THE CLAY AND CC MIXTURES: (A) CUMULATIVE VOLUME CURVES; (B) DERIVATIVE CURVES.	154
FIGURE 80 – RESULTS FROM MIP FOR THE CLAYEY SAND AND CC MIXTURES: (A) CUMULATIVE VOLUME CURVES; (B) DERIVATIVE CURVES.	155
FIGURE 81 – SWRCs OF CAMPINAS CLAY AND CC MIXTURES.	158
FIGURE 82 – SWRCs OF CAMPINAS CLAY AND CT MIXTURES.	159
FIGURE 83 – SWRC OF UNDISTURBED AND COMPACTED SAMPLES OF CAMPINAS CLAY.	160
FIGURE 84 – SWRCs OF BOTUCATU CLAYEY SAND AND BC MIXTURES.	161
FIGURE 85 – SWRCs OF BOTUCATU CLAYEY SAND AND BT MIXTURES.	162
FIGURE 86 – SWRCs ESTIMATED FROM MIP FOR THE CLAY AND CC MIXTURES.	164
FIGURE 87 – SWRCs ESTIMATED FROM MIP FOR THE CLAYEY SAND AND BC MIXTURES.	164
FIGURE 88 – COMPARISON OF STRENGTH ENVELOPES IN TERMS OF EFFECTIVE STRESSES.	168

FIGURE 89 – INFLUENCE OF PREVIOUS DRYING ON COMPACTION CURVES OF CC4:1 MIXTURES.	204
FIGURE 90 – INFLUENCE OF PREVIOUS DRYING ON COMPACTION CURVES OF CC3:1 MIXTURES.	204
FIGURE 91 – INFLUENCE OF PREVIOUS DRYING ON COMPACTION CURVES OF CC2:1 MIXTURES.	205
FIGURE 92 – INFLUENCE OF PREVIOUS DRYING ON COMPACTION CURVES OF CT3:1 MIXTURES.	205
FIGURE 93 – INFLUENCE OF PREVIOUS DRYING ON COMPACTION CURVES OF CT2:1 MIXTURES.	206
FIGURE 94 – INFLUENCE OF PREVIOUS DRYING ON COMPACTION CURVES OF CT1.5:1 MIXTURES.	206
FIGURE 95 – INFLUENCE OF PREVIOUS DRYING ON COMPACTION CURVES OF BT5:1 MIXTURES.	207
FIGURE 96 – INFLUENCE OF PREVIOUS DRYING ON COMPACTION CURVES OF BT4:1 MIXTURES.	207
FIGURE 97 – INFLUENCE OF PREVIOUS DRYING ON COMPACTION CURVES OF BT3:1 MIXTURES.	208
FIGURE 98 – OEDOMETRIC COMPRESSION CURVES OF CAMPINAS CLAY AND CC MIXTURES.	210
FIGURE 99 OEDOMETRIC COMPRESSION CURVES OF CAMPINAS CLAY AND CT MIXTURES.	210
FIGURE 100 - OEDOMETRIC COMPRESSION CURVES OF BOTUCATU CLAYEY SAND AND BT MIXTURES.	211
FIGURE 101 - OEDOMETRIC COMPRESSION CURVES OF BOTUCATU CLAYEY SAND AND BC MIXTURES.	211
FIGURE 102 – HYDRAULIC CONDUCTIVITY OF CAMPINAS CLAY.	213
FIGURE 103 – HYDRAULIC CONDUCTIVITY OF MIXTURE CC4:1.	213
FIGURE 104 – HYDRAULIC CONDUCTIVITY OF MIXTURE CC3:1.	214
FIGURE 105 – HYDRAULIC CONDUCTIVITY OF MIXTURE CC2:1.	214

FIGURE 106 – HYDRAULIC CONDUCTIVITY OF MIXTURE CT3:1.	215
FIGURE 107 – HYDRAULIC CONDUCTIVITY OF MIXTURE CT2:1.	215
FIGURE 108 – HYDRAULIC CONDUCTIVITY OF MIXTURE CT1.5:1.	216
FIGURE 109 – HYDRAULIC CONDUCTIVITY OF BOTUCATU CLAYEY SAND.	216
FIGURE 110 – HYDRAULIC CONDUCTIVITY OF MIXTURE BT5:1.	217
FIGURE 111 – HYDRAULIC CONDUCTIVITY OF MIXTURE BT4:1.	217
FIGURE 112 – HYDRAULIC CONDUCTIVITY OF MIXTURE BT3:1.	218
FIGURE 113 – RESULTS OF CIU TESTS ON CAMPINAS CLAY.	220
FIGURE 114 – RESULTS OF CIU TESTS ON CC4:1 MIXTURE.	221
FIGURE 115 – RESULTS OF CIU TESTS ON CC3:1 MIXTURE.	222
FIGURE 116 – RESULTS OF CIU TESTS ON CC2:1 MIXTURE.	223
FIGURE 117 – RESULTS OF CIU TESTS ON CT3:1 MIXTURE.	224
FIGURE 118 – RESULTS OF CIU TESTS ON CT2:1 MIXTURE.	225
FIGURE 119 – RESULTS OF CIU TESTS ON CT1.5:1 MIXTURE.	226
FIGURE 120 – RESULTS OF CIU TESTS ON BOTUCATU CLAYEY SAND.	227
FIGURE 121 – RESULTS OF CIU TESTS ON BT5:1 MIXTURE.	228
FIGURE 122 – RESULTS OF CIU TESTS ON BT4:1 MIXTURE.	229
FIGURE 123 – RESULTS OF CIU TESTS ON BT3:1 MIXTURE.	230
FIGURE 124 – STRESS-STRAIN CURVES FROM UC TESTS ON CAMPINAS CLAY AND CC MIXTURES.	232
FIGURE 125 – STRESS-STRAIN CURVES FROM UC TESTS ON CAMPINAS CLAY AND CT MIXTURES.	232
FIGURE 126 – STRESS-STRAIN CURVES FROM UC TESTS ON BOTUCATU CLAYEY SAND AND BC MIXTURES.	233
FIGURE 127 – STRESS-STRAIN CURVES FROM UC TESTS ON BOTUCATU CLAYEY SAND AND BT MIXTURES.	233

LIST OF TABLES

TABLE 1 – OBTAINED SOLIDS CONTENT FOR DIFFERENT DEWATERING METHODS.....	34
TABLE 2 – CHEMICAL COMPOSITION OF SOME BRAZILIAN WATER TREATMENT SLUDGE	38
TABLE 3 – TYPICAL COMPOSITION OF WATER TREATMENT SLUDGE FOR DIFFERENT COAGULANTS.....	39
TABLE 4 – CATION EXCHANGE CAPACITY OF SOME COMMON SOIL COLLOIDS.....	40
TABLE 5 – GEOTECHNICAL CHARACTERISTICS OF WTS FROM DIFFERENT COUNTRIES.	44
TABLE 6 – RECOMMENDED CRITERIA FOR SOIL SUITABILITY AS LANDFILL LINER MATERIAL. ...	55
TABLE 7 – INVESTIGATED SOIL-WTS MIXTURES.....	72
TABLE 8 – STANDARDS FOR GEOTECHNICAL CHARACTERIZATION TESTS.	77
TABLE 9 – CONCENTRATION OF DISPERSING AGENTS AND SAMPLE MASS USED IN HYDROMETER TESTS FOR TAIACUPEBA WTS.	78
TABLE 10 – MAXIMUM HYDRAULIC GRADIENTS RECOMMENDED BY ASTM D5084/16.....	81
TABLE 11 – MINERALOGICAL COMPOSITION OF STUDIED SOILS AND WTS.	94
TABLE 12 – CHEMICAL COMPOSITION (SEMI-QUANTITATIVE) OF SOILS AND SLUDGES (PERCENT BY DRY MASS).....	102
TABLE 13– CHEMICAL PARAMETERS OF STUDIED SOILS AND WTS.	105
TABLE 14 – GEOTECHNICAL CHARACTERIZATION OF TESTED SOILS, SLUDGES AND MIXTURES.	117
TABLE 15 – SUMMARY OF SAMPLES CHARACTERISTICS AND INDEXES COMPUTED FROM OEDOMETRIC COMPRESSION TESTS.	128
TABLE 16 – SUMMARY OF PERMEABILITY TEST SAMPLES, TESTING CONDITIONS, AND RESULTS.	134
TABLE 17 – CHARACTERISTICS OF SPECIMENS AND PARAMETERS FROM TRIAXIAL COMPRESSION TESTS (CU) ON CAMPINAS CLAY AND MIXTURES.	137
TABLE 18 – CHARACTERISTICS OF SPECIMENS AND PARAMETERS FROM TRIAXIAL COMPRESSION TESTS (CU) ON BOTUCATU CLAYEY SAND AND MIXTURES.	138

TABLE 19 – MOHR-COULOMB EFFECTIVE SHEAR STRENGTH PARAMETERS OF SOILS AND MIXTURES.	143
TABLE 20 – POROSITY AND VOID RATIO VALUES COMPUTED FROM MIP AND AS-COMPACTED CONDITION.	153
TABLE 21 SUMMARY OF HYDRAULIC CONDUCTIVITY, UNDRAINED SHEAR STRENGTH AND VOLUMETRIC SHRINKAGE OF THE STUDIED MIXTURES.	165

LIST OF ACRONYMS

ABNT	Brazilian Association of Technical Standards <i>Associação Brasileira de Normas Técnicas</i>
ASCE	American Society of Civil Engineers
ASTM	American Society for Testing Materials
AWWA	American Water Work Association
CONAMA	National Environmental Council <i>Conselho Nacional do Meio Ambiente</i>
DNIT	National Department of Transport Infrastructure <i>Departamento Nacional de Infraestrutura de Transportes</i>
EMBRAPA	Brazilian Agricultural Research Corporation <i>Empresa Brasileira de Pesquisa Agropecuária</i>
FAPESP	São Paulo Research Foundation <i>Fundação de Amparo à Pesquisa do Estado de São Paulo</i>
IBGE	Brazilian Institute of Geography and Statistics <i>Instituto Brasileiro de Geografia e Estatística</i>
PAN-ICSD	PANalytical Inorganic Cristal Structure Database
PNRS	National Solid Waste Policy <i>Política Nacional de Resíduos Sólidos</i>
SABESP	Basic Sanitation Company of the State of São Paulo <i>Companhia de Saneamento Básico do Estado de São Paulo</i>
UN	United Nations
USEPA	US Environmental Protection Agency

LIST OF ABBREVIATIONS AND SYMBOLS

A	Skempton's activity
\bar{A}_f	Skempton's pore-pressure coefficient A at failure
ACZ	Acceptable compaction zone
AEV	Air-entry value
Al	Aluminum
a_v	Coefficient of compressibility
B	Skempton's pore-pressure coefficient B
BOD	Biochemical oxygen demand
c	Cohesion intercept
c'	Effective cohesion intercept
CAU	Consolidated Anisotropically Undrained
CBR	California Bearing Ratio
C_c	Compression index
CCL	Compacted clay liner
CEC	Cation Exchange Capacity
CH	Fat clay
CIU	Consolidated Isotropically Undrained
CL	Lean clay
C_s	Swelling index
CU	Consolidated Undrained
D	Specimen diameter
D	Grain diameter
D	Pore diameter
d	Intercept of failure envelope for effective stress path

DAF	Dissolved air flotation
e	Void ratio
e_0	Initial void ratio
e_{MIP}	Void ratio calculated from MIP test
EDS	Energy Dispersive Spectroscopy
Fe	Iron
G_s	Specific gravity of solids
GSD	Grain-size distribution
Hg	Mercury
i	Hydraulic gradient
k	Hydraulic conductivity
k_{20}	Hydraulic conductivity at 20°C
k_f	Hydraulic conductivity at field
L	Height
LMS	Laboratory of Soil Mechanics <i>Laboratório de Mecânica dos Solos</i>
LOI	Loss on ignition
M	Constrained or confined modulus
MCT	Tropical-compacted-miniature <i>Miniatura-compactado-tropical</i>
MH	Elastic silt
MIP	Mercury intrusion porosimetry
ML	Silt
n	Porosity
n_e	Maximum cumulative intruded mercury volume
n_i	Cumulative intruded mercury volume at any pressure
n_{MIP}	Porosity calculated from MIP test

NOM	Natural organic matter
NP	Non-plastic
NTU	Nephelometric Turbidity Unit
OC	Organic carbon
OH	Organic silt
OM	Organic matter
P	Pressure
p	Mean total stress
p'	Mean effective stress
PACl	Poly-aluminum chloride
PI	Plasticity index
PSD	Pore size distribution
PVC	Polyvinyl chloride
Q	Flow
q	Half deviator stress
RC	Relative compaction
S	Saturation or total saturation
SC	Clayey sand
SC	Solids content
S_e	Effective saturation
S_u	Undrained shear strength
SEM	Scanning Electron Microscopy
SFBW	Spent filter backwashing water
SHMP	Sodium hexametaphosphate
SiBCS	Brazilian Soil Classification System <i>Sistema Brasileiro de classificação de solos</i>
SM	Silty sand

SOM	Soil organic matter
SP	São Paulo
S_r	Residual saturation
SS	Suspended solids
STPP	Sodium tripolyphosphate
SWRC	Soil-water retention curve
T	Turbidity
TCLP	Toxicity characteristic leaching procedure
T_{Hg}	Surface tension of Mercury
TSP	Trisodium phosphate
TSPP	Tetrasodium pyrophosphate
T_w	Surface tension of water
u_a	Air pressure
UCS	Unconfined compression strength
USA	United States of America
USCS	Unified Soil Classification System
UU	Unconsolidated Undrained
u_w	Water pressure
VS	Volumetric shrinkage
V_v	Voids volume
w	Water content or gravimetric water content
w_0	Initial water content
w_i	Water content after partial or total dehydration
w_L	Liquid limit
w_{opt}	Optimum water content
w_p	Penetrometer weight (MIP test)

WRC	Water Research Centre
W_s	Sample weight (MIP test)
WTP	Water treatment plant
WTS	Water treatment sludge
wts	Sludge content
XRD	X-Ray Diffraction
ZAVC	Zero-Air-Voids-Curve
γ_d	Dry unit weight
$\gamma_d \text{ máx}$	Maximum dry unit weight
$\theta_{\text{Hg-s}}$	Angle of contact between mercury and soil particles
θ_w	Volumetric water content
θ_{w-s}	Angle of contact between water and soil particles
$(\sigma_1 - \sigma_3)$	Deviator stress
σ'_v	Vertical effective stress
σ_{3c}	Minor principal confining stress
σ_c	Confining pressure
σ'_c	Effective confining pressure
φ	Friction angle
φ'	Effective friction angle
Δu	Increment in pore pressure
$\Delta \sigma_3$	Increment in confining pressure
β	Slope of failure envelope for effective stress path
ε_a	Axial strain
σ'_1	Major principal effective stress
σ'_3	Minor principal effective stress
σ'_1/σ'_3	Effective principal stress ratio

1 INTRODUCTION

Drinking or potable water is produced by treatment of raw water collected from different sources, like rivers, lakes, groundwater, and reservoirs. The treatment process of raw water consists, generally, in the addition of chemical compounds in order to remove impurities such as microorganisms, organic matter, and soil particles present in the water.

Water treatment plants (WTPs) generate large amounts of a by-product composed of sedimented impurities, chemical compounds and water. Because of high water content, this by-product is usually known as water treatment sludge (WTS) or drinking-water sludge. Declaration of access to safe water as human right by the United Nations (UN, 2010) and rapid population growth in urban areas have contributed to an increasing demand on potable water, thus increasing WTS production at the same rate. For example, the São Paulo State Sanitation Company (*Companhia de Saneamento Básico do Estado de São Paulo*, SABESP) manages 240 WTPs, which produce 119,000 L/s of potable water (SABESP, 2019a) for the majority of São Paulo State population (circa 45 million inhabitants) and, approximately, 90 tons/day of WTS dry solids (IWAKI, 2017).

According to the National Sanitation Survey Report (IBGE, 2010), among the 2098 Brazilian WTPs, 67.4% release WTS into rivers and 0.3% into the sea, 22.1% do land application, 4.0% dispose of WTS in sanitary landfills, and the remainder percentage apply other methods. In Brazil, however, WTS is classified as solid waste (ABNT, 2004), and it cannot be disposed of in water streams without adequate treatment to meet the minimum water quality required by legislation (CONAMA, 2011). A concern and big challenge for sanitation companies, therefore, is the adequate and economically feasible destination of WTS. Disposal in sanitary landfills is expensive and unwanted because WTS impacts negatively the stability of the waste mass. On the other hand, destination to sewage treatment plants overcharges the system with a different material. Hence, an upsurge in research of sustainable recycling of WTS has occurred in the last decades.

Some of the alternatives for disposal and recycling of WTS are: composting and agriculture (SILVA, FERNANDES, 1998; VERLICCHI; MASOTTI, 2000), coagulant recovery (PETRUZZELLI et al., 2000), brick making (RODRIGUES; HOLANDA, 2015),

ceramic products (TEIXEIRA et al., 2011), cement production (CHEN, H.; MA; DAI, 2010), landfill cover (KAMON et al., 2000), earthworks (RAGHU et al., 1987; SOCKANATHAN, 1991; SILVA; HEMSI, 2018; ROQUE; CARVALHO, 2006; MONTALVAN; BOSCOV, 2018), among many others. Reviews on beneficial reuse alternatives of WTS have been presented by Cornwell (2006); Babatunde and Zhao (2007); Breesem et al. (2014); Ahmad, Ahmad and Alam (2016); and Gomes et al. (2019).

Reuse in geotechnical structures is a promising alternative, since earthworks use large amounts of soil that can be partly substituted by WTS, raw or treated with cement, lime, soil, or polymers.

Some researchers have investigated the geotechnical behavior of raw and treated WTS. One of the biggest concerns when using raw WTS is its high water content, which yields low shear strength and high compressibility, impairing field workability. Researches using WTS mixed with lime or soil have been successful to some extent (WANG; HULL; JAO, 1992; ALDEEB et al., 2003). Some investigations have been conducted using dry WTS (ROQUE; CARVALHO, 2006; WATANABE et al., 2011), since air- or oven-dried WTS is generally a good geotechnical material, however WTS dewatering and drying is difficult, expensive and time-consuming. Few investigations have studied the behavior of raw wet WTS mixed with soil as a candidate material for geotechnical works.

The present research investigates the geotechnical behavior of raw wet WTS mixed with natural soils, aiming at the evaluation of the maximum amount of sludge that can be added to a soil and maintaining acceptable hydromechanical behavior for geotechnical structures. The purposes are to enhance the reuse of waste and to preserve natural resources, i.e. natural soils. This work will bring valuable insight into the knowledge and understanding of how WTS incorporation into soils influences its geotechnical behavior.

This research is part of the FAPESP–SABESP Research Project (File number: 13/50448-8), titled “Feasibility of the use of water treatment sludge as construction material for landfill covers and embankments” (“*Viabilização da utilização do lodo de ETA como material de cobertura de aterros sanitários e na construção de aterros em solos compactados*”).

1.1 RESEARCH OBJECTIVES

The main objective is to assess the possibility of reusing WTS in geotechnical applications by evaluating the WTS content that can be incorporated into residual lateritic soils usually applied in earthworks while guaranteeing that the mixtures still maintain adequate geotechnical behavior.

The specific objectives include:

- a) to determine the geotechnical characteristics and properties of soil-WTS mixtures at several ratios using two different lateritic soils and two different WTS.
- b) to evaluate the influence of type of soil, type of sludge and blending ratio on the geotechnical behavior of the mixtures.
- c) to assess the geotechnical feasibility of the mixtures as construction material for different geotechnical works.

2 LITERATURE REVIEW

2.1 WATER TREATMENT SLUDGE

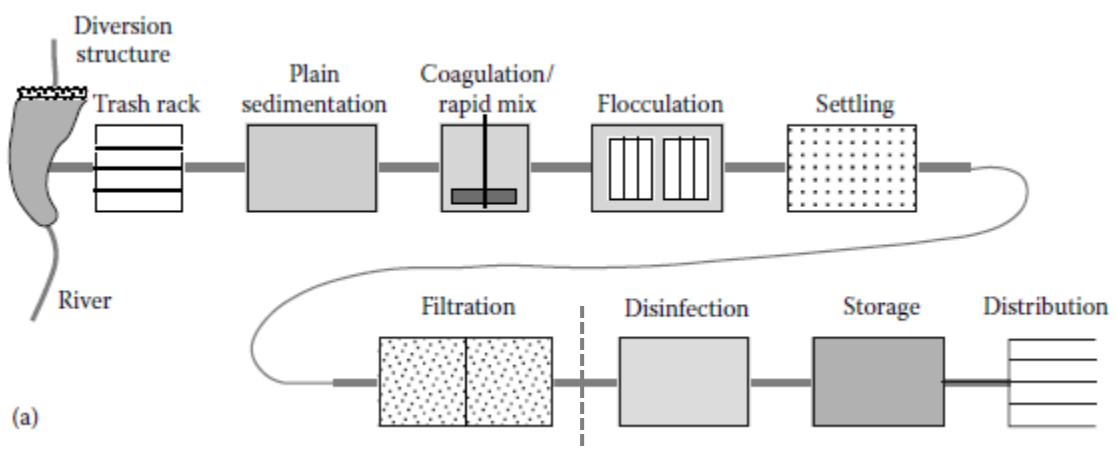
2.1.1 Water treatment process

The purpose of water treatment plants (WTPs) is to produce safe water for human use and consumption. The water to be treated may be any water, e.g. surface water, groundwater, wastewater, seawater or brackish water. Natural fresh water (raw water) contains several impurities such as suspended solids (mineral and organic), microorganisms, dissolved salts (ions) and dissolved gasses (KAISHA, 1985), and needs to be treated.

Any water treatment process is conducted by means of a 'train treatment', a succession of unit processes. The train treatment may include unit processes such as screening, sedimentation, flotation, coagulation, filtration, adsorption, ion exchange, gas transfer, biological reactions and disinfection (HENDRICKS, 2011).

There are several configurations for the train treatment in WTPs, since the necessary unit processes depend on the quality of raw water. The most common train treatment for potable water is the 'conventional treatment', presented in Figure 1, but considerable variations are likely.

Figure 1 – Conventional water treatment process.



Source: Hendricks (2011, p.8).

IBGE (2010) reported that 69.2% of the total volume of potable water produced in Brazil in 2008 was treated by the conventional treatment process. Conventional treatment includes the following unit processes: coagulation/rapid mix, flocculation,

sedimentation (settling), and filtration, usually followed by disinfection, fluoridation, and pH correction.

Coagulation is defined as the reaction between a chemical compound and suspended solids (SS) in water to bring them together and form a “microfloc” (HENDRICKS, 2011). Raw waters contain several types of fine particles and colloids, mainly mineral particles (e.g. clay fraction), organic matter (e.g. natural organic matter, NOM), and microorganisms (e.g. viruses, bacteria, algae etc.). These particles generally have negative electrical surface charge; thus, they repel each other and remain dispersed in water. In the coagulation process, a coagulant is added to water in order to destabilize/neutralize the negative charge of colloids, followed by a rapid mix to promote the formation of microflocs.

The most widely used coagulants in water treatment are sulfate or chloride salts that contain the metal ions Al^{+3} or Fe^{+3} , such as aluminum sulfate or “alum” ($\text{Al}_2(\text{SO}_4)_3 \cdot 14\text{H}_2\text{O}$), ferric chloride ($\text{FeCl}_3 \cdot \text{XH}_2\text{O}$), and ferric sulfate ($\text{Fe}_2(\text{SO}_4)_3 \cdot \text{XH}_2\text{O}$) (EDZWALD, 2011). These coagulants form insoluble aluminum and iron hydroxides (HSIEH; RAGHU, 1997). Other coagulants such as polyaluminum chloride (PACl) and polymers are also commonly used. Some WTPs practice water softening for the removal of calcium and magnesium, i.e. lime and soda ash are added to water in order to achieve chemical precipitation of calcium and magnesium.

The next stage is flocculation. The purpose is to bring about collision of particles and microflocs formed in the coagulation process, causing microflocs to grow into “floc” particles. The larger the floc particles, the more efficient the removal of suspended solids in the subsequent unit processes of sedimentation (settling) and filtration.

Clarification of water, i.e. removal of particles, begins with gravity settling (sedimentation) of floc particles, which accumulate in the bottom of the sedimentation basin or clarifier. Dissolved air flotation (DAF) is an alternative to sedimentation to improve flocs removal. The sedimentation unit process is the main source of sludge in a WTP. Sludge is produced when the sedimented material is washed from the bottom of the clarifiers.

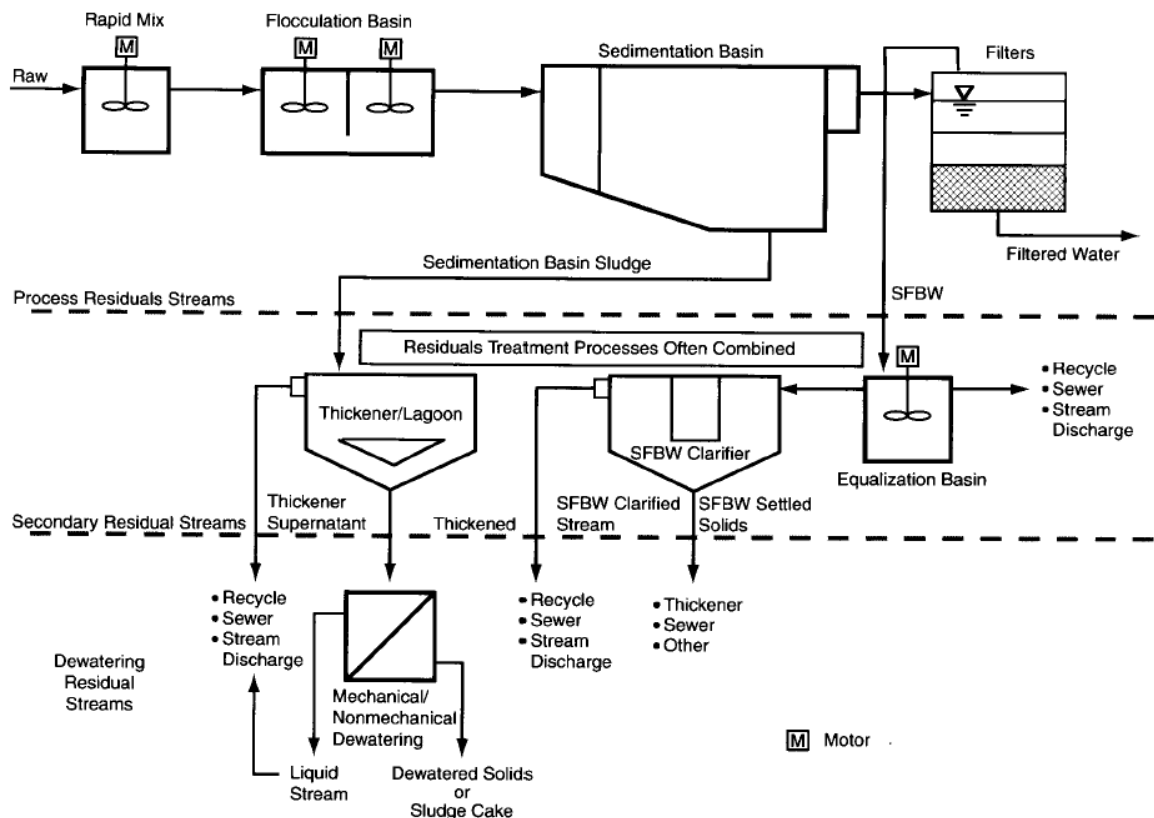
After coagulation-mixing and flocculation-settling, particles still suspended in water are removed by rapid filtration process, consisting of passage of water through a granular media bed. Larger floc particles deposit in the space pores of the granular

bed, and this initial clogging retains smaller particles. Eventually, the granular bed is completely clogged and needs cleaning. Backwash is the process used to clean the filter and consists of a reverse flow of water (upward) through the granular media, also generating sludge. Filtration closes the conventional water treatment process.

2.1.2 Water treatment sludge production

The term "water treatment sludge" describes the residue generated by washing sedimentation basins and filters in water treatment plants, since other types of residues are also produced in the water treatment process. According to Cordeiro (1999), the major sources of residues in water treatment plants are: sedimentation basin (coagulation sludge), filter media (backwash sludge), and tanks for chemicals storage. Figure 2 shows the major residual streams in conventional WTPs.

Figure 2 – Common residue streams in conventional WTPs



Source: Cornwell; Macphee, and Mutter (2003).

The coagulation sludge from the sedimentation basin contains about 1 to 2% of solids. It is destined to a thickening tank to reduce volume and increase solids content.

Coagulation and spent filter backwashing water (SFBW) are usually combined. However, some WTPs recycle SFBW by discharging it into an equalization tank, and then into a thickening tank. For a lime softened sludge, the solids content may vary between 2 and 10%. Solids content of coagulation and lime sludge from the thickening tank are likely to be in the range of 3 to 15% and 10 to 30%, respectively (PIZZI, 2010).

The thickened sludge is then subjected to a dewatering process, mechanical or non-mechanical, to produce the final sludge cake. The solids content of the sludge cake depends on the dewatering method. The non-mechanical methods include sand drying beds, solar drying beds, dewatering lagoons, freeze-thaw beds and geotextile bags. The mechanical dewatering methods embrace centrifuges, plate and frame filter presses, diaphragm filter presses, belt filter presses and vacuum filters. Table 1 presents the sludge solids content obtained for different dewatering methods.

Table 1 – Obtained solids content for different dewatering methods.

Dewatering method	Solids content (%)	
	Lime sludge	Coagulant sludge
Gravity thickening	15-30	3-4
Centrifuge	55-65	18-25
Belt filter press	NE ^a	15-22
High solids belt press	NE ^a	25-30
Vacuum filter	45-65	NA ^b
Pressure filter	55-70	25-45
Drying bed	~50	20-25
Dewatering lagoon	50-60	7-15

^aNE= not estimated; ^bNA= not applicable.

Source: Cornwell (2006, p.78)

WTS is usually named according to the major coagulant or softening chemical compound used on the treatment process, e.g. alum sludge, ferric sludge, lime sludge or polymer sludge for, respectively, aluminum sulfate, ferric chloride or ferric sulfate, lime and polymer.

2.1.3 Water treatment sludge quantification

Equations used to estimate WTS production depend on the type and amount of coagulant. In Brazil, WTPs usually use aluminum sulfate or ferric chloride as coagulant.

In a WTP that uses alum coagulant for the removal of suspended solids, the sludge production can be estimated by Equation (1) (CORNWELL, 2006).

$$S = Q \cdot (0.44Al + SS + A) \quad (1)$$

Where:

S= sludge production (kg/d by dry weight)

Q= plant flow (ML/d)

Al= alum dose (mg/L)

SS= suspended solids (mg/L)

A= additional chemicals added (polymer, clay, or activated carbon in mg/L)

In WTPs where iron coagulant is used, the amount of sludge is estimated by Equation (2) (CORNWELL, 2006).

$$S = Q \cdot (2.9Fe + SS + A) \quad (2)$$

Where:

Fe= iron coagulant dose (mg/L)

2.2 CHARACTERIZATION OF WATER TREATMENT SLUDGE

Sludge composition is somewhat homogeneous in a WTP (HSIEH; RAGHU, 1997). However, physicochemical characteristics of sludge may vary largely from one WTP to another. The main aspects that influence WTS characteristics are raw water quality, treatment process, type and dosage of chemicals, and dewatering method.

An important characteristic of WTS is solids content, which is inversely proportional to water content. Solids content is defined as the ratio of solids weight to total weight (solids and water), and water content is the ratio of water weight to solids weight. Solids content (SC) is commonly used in sanitary engineering, and water

content (w) is typically used in geotechnical engineering. Equations (3) and (4) express the relationship between these two parameters.

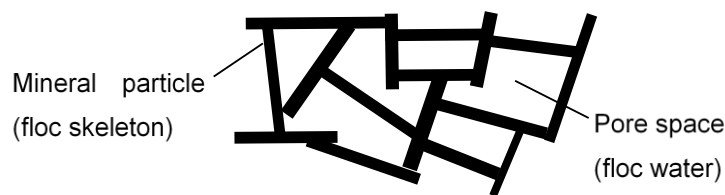
$$SC (\%) = \left[\frac{1}{1 + \frac{w(\%)}{100}} \right] * 100 \quad (3)$$

$$w (\%) = \left[\frac{100}{SC(\%)} - 1 \right] * 100 \quad (4)$$

2.2.1 Water in WTS

In the flocculation process, suspended solids aggregate forming flocs with an edge-to-face linkage of particles, as shown in Figure 3. This floc structure is called salt-type (LAMBE; WHITMAN, 1969).

Figure 3 – Floc skeleton of sludge clay particles.



Source: modified from Hsieh and Raghu (1997, p.7).

Hsieh and Raghu (1997) classify the water in WTS into four categories: free water, floc water, capillary water and adsorbed water.

Free water refers to the water that can move freely by gravity. Floc water is defined as free water trapped inside the pore spaces of the floc structure. Capillary water is held by surface tension. Adsorbed water is considered part of the molecular structure of the solids.

A different distribution of water in sludge has been proposed by Cornwell, 1978 (apud CORNWELL, 2006), with only three categories of water: free water, hydrogen-bound water, and chemically bound water. Free water can be removed by low-pressure mechanical methods or simple drainage, the second category is water linked to the flocs through hydrogen binding, and the third one is water bound by covalent bonds to chemical floc particles.

2.2.2 Mineralogical composition

Several authors have determined the mineralogical composition of different WTS by X-ray diffractometry, reporting the occurrence of the minerals boehmite, calcite, feldspars, gibbsite, goethite, illite, graphite, gypsum, kaolinite, magnesite, quartz, rhodochrosite, ringwoodite, among others (BASIM, 1999; ROQUE; CARVALHO, 2006; TEIXEIRA et al., 2011; MONTALVAN, 2016). The most ubiquitous mineral in WTS is quartz (SiO_2), also the most commonly occurring mineral in soils (MITCHELL; SOGA, 2005).

2.2.3 Chemical composition and characteristics

Chemical composition analyses by X-ray diffractometry of WTS from different Brazilian WTPs have shown that silicon, aluminum and iron are the major occurring elements, as presented in Table 2. Babatunde and Zhao (2007), analyzing WTS from several countries, mention the same major elements, including calcium among the elements with highest concentration in WTS. The great occurrence of quartz particles explains the predominance of silicon. Aluminum and iron generally have two main sources, clay minerals and coagulants (metal salts), while in tropical lateritic soils additional important sources are the aluminum and iron oxides.

Table 3 presents a data compilation of typical chemical composition of WTS for different coagulants. Concentration of metals, especially heavy metals, is important for environmental safety or toxicity evaluation of waste disposal. Metals often found in coagulation sludge include aluminum, arsenic, occasionally cadmium, chromium, copper, iron, lead, manganese, nickel, and zinc (EDZWALD, 2011). Some studies have shown that WTS contains low concentrations of these metals, usually below the maximum allowable limits (ROQUE; CARVALHO, 2006); however, chemical analyses should be performed in every case.

Table 2 – Chemical composition of some Brazilian water treatment sludge

Chemical compound	Chemical composition (percent by dry weight)									
	São Leopoldo WTP ^a	Campos dos Goytacazes WTP ^b	Passaúna WTP ^c	Tamanduá WTP ^d	Cubatão WTP ^e	Caçapava do Sul WTP ^f	Leopoldina WTP ^g	Curitiba WTP ^h	Rio de Janeiro WTP ⁱ	Botafogo WTP ^j
Coagulant	Alum	-	Alum	PACl	Ferric	Alum	Alum	-	PACl	Alum-PACl
SiO ₂	34.80	35.92	15.55	24.10	18.3	17.80	26.84	15.6	50.80	24.10
Al ₂ O ₃	22.30	31.71	13.07	31.60	8.89	16.50	26.33	31.1	32.60	33.80
Fe ₂ O ₃	6.60	12.79	4.15	18.60	46.00	11.10	24.00	6.6	11.50	37.70
TiO ₂	0.94	1.10	0.19	2.20	0.42	0.80	1.26	0.3	1.50	1.08
MnO	0.17	0.09	0.22	-	0.21	0.39	1.11	0.2	-	0.28
MgO	0.69	0.37	0.15	-	0.44	-	0.32	0.1	1.20	0.29
CaO	0.40	0.10	0.43	-	1.59	0.44	0.14	0.3	0.30	0.15
K ₂ O	0.57	0.58	0.06	0.30	1.00	0.72	0.34	0.2	1.60	0.45
Na ₂ O	0.23	0.06	0.04	-	0.10	-	0.03	-	-	-
P ₂ O ₅	-	0.35	0.26	-	0.25	0.34	0.31	0.3	-	0.46
SO ₃	-	-	-	2.80	0.24	0.43	-	0.8	-	1.45
FeO	2.90	-	-	-	-	-	-	-	-	-
LOI	28.0	16.9	49.8	20.4	22.0	-	19.3	44.5	-	41.1

LOI= Loss on ignition at 1000 °C.

Source: ^a(SANTOS et al., 2000); ^b(OLIVEIRA; MACHADO; HOLANDA, 2004); ^c(HOPPEN et al., 2005); ^d(TARTARI et al., 2011); ^e(MONTALVAN, 2016); ^f(PASINI; DA SILVA; DA SILVA, 2017); ^g(PINHEIRO; ESTEVÃO; SOUZA, 2014); ^h(ANDRADE et al., 2016); ⁱ(MARTINS; YOKOYAMA; ALMEIDA, 2014); ^j(SIQUEIRA JÚNIOR, 2011).

Table 3 – Typical composition of water treatment sludge for different coagulants

Parameter	Sludge type		
	Alum sludge	Ferric sludge	Lime sludge
Aluminum (% dry weight)	29.7 ± 13.3	10.0 ± 4.8	0.5 ± 0.8
Iron *(% dry weight)	10.2 ± 12.0	26.0 ± 15.5	3.3 ± 5.8
Calcium (% dry weight)	2.9 ± 1.7	8.32 ± 9.5	33.1 ± 21.1
Magnesium (% dry weight)	0.89 ± 0.80	1.6	2.2 ± 1.04
SiO ₂ (% dry weight)	33.4 ± 26.2	-	54.57
pH	7.0 ± 1.4	8.0 ± 1.6	8.9 ± 1.8
BOD ₅ (mg/L)	45 (2 – 104)	ND	ND ^a
P (% dry weight)	0.35	0.36	0.02
Zinc (mg/kg)	33.9 ± 28.0	18.7 ± 16.0	2.5 ± 0.7
Lead (mg/kg)	44.1 ± 38.2	19.3 ± 25.3	1.87 ± 0.02
Cadmium (mg/kg)	0.5	0.48 ± 0.26	0.44 ± 0.02
Nickel (mg/kg)	44.3 ± 38.4	44.3 ± 38.4	0.98 ± 0.52
Copper (mg/kg)	33.72 ± 32.5	18.7 ± 25.8	3.6 ± 3.1
Chromium (mg/kg)	25.0 ± 20.1	25.7 ± 21.6	1.3 ± 0.2
Cobalt (mg/kg)	1.06	1.61 ± 1.10	0.67 ± 0.05
Total solids (mg/L)	(2500 – 52,345)	(2132 – 5074)	ND ^a

^aND= No Data.

Source: Babatunde and Zhao (2007).

Hsieh and Raghu (1997) determined toxicity potential of coagulant sludge from different WTPs based on the Toxicity Characteristic Leaching Procedure (TCLP) and the materials met TCLP requirements. Metals content in WTS is expected to be below this criteria in most cases (USEPA, 1996).

Table 2 also presents values of loss on ignition (LOI) at 1000 °C. The investigated WTS presented high LOI values, from 16.9 to 49.8%, indicating high percentage of volatile solids. Volatiles are generally related to organic matter; however, some inorganic solids may also volatilize at such temperature. Thus, additional methods should be used to determine the organic matter (OM) content.

The solids in WTS comprise soil particles and organic matter from raw water, and chemical compounds from the treatment process. The amount and proportion of soil particles and organic matter in WTS depend on the quality of raw water. Water from rivers, for example, usually contains predominantly soil particles, especially in rainy seasons because of the erosion of rocks and soils. On the other hand, water from

reservoirs or lagoons generally present low content of soil particles and high content of organic matter, e.g. algae (HSIEH; RAGHU, 1997).

Soil organic matter (SOM) is the organic fraction of the soil and consists of three primary parts: small plant residues and small living organisms (fresh), decomposing organic matter, and stable organic matter (humus) (USDA, 2020). Humic substances (humus, humic and fulvic acids), the stabilized or mineralized organic matter, are highly varying combinations of organic molecules (carbohydrates, amino acids, and fatty acids) and are also highly resistant to further microbial degradation (ADEY; LOVELAND, 2007). SOM has high water retention capacity and can hold up to 20 times its weight in water (STEVENSON, 1994). This feature impairs sludge dewatering.

Hsieh and Raghu (1997) observed that organic matter content in WTS is strongly dependent on the source of water: sludge from WTPs that use water from rivers showed low percentage of volatile solids (3 to 17%), related to low organic matter content. On the other hand, sludge from WTPs that treat water from reservoir presented high percentage of volatile solids (14 to 63%), indicating high OM content.

Another important chemical characteristic is the cation exchange capacity (CEC), defined as the capacity of soils to adsorb and exchange cations. The CEC of a colloid is related to its surface area and surface charge (TAN, 2010). SOM has high CEC, 150 to 300 $\text{cmolc}\cdot\text{kg}^{-1}$ according to (SPARKS, 2003), and 100 to 400 $\text{cmolc}\cdot\text{kg}^{-1}$ according to (FOTH, 1991). Table 4 presents typical values of CEC for some common colloids, such as SOM, clay minerals and aluminum and iron oxides (sesquioxides).

Table 4 – Cation exchange capacity of some common soil colloids.

Soil colloid	CEC ($\text{cmolc}\cdot\text{kg}^{-1}$)
Humus	200
Vermiculite	100-150
Smectite	70-95
Illite	10-40
Kaolinite	3-15
Sesquioxides	2-4

Source: Tan (2010).

CEC of natural soils, usually composed of several minerals, varies with nature and quantity of colloids, generally between 3 to 35 $\text{cmolc}\cdot\text{kg}^{-1}$ (BRADY; WEIL, 2016). CEC of highly organic soils may be 30 to 70% that of SOM (SPARKS, 2003).

The CEC of WTS is highly influenced by mineralogy, chemical composition and organic matter content. Hsieh and Raghu (1997) reported CEC values of different WTS varying from 23 to 136 $\text{cmolc}\cdot\text{kg}^{-1}$, with average of 82 $\text{cmolc}\cdot\text{kg}^{-1}$, higher than typical values for inorganic soils or soils with low organic matter content. The authors pointed out that the CEC values were apparently related to the organic matter content.

pH is another chemical parameter to be considered for WTS disposal. Basic condition ($\text{pH} > 7$) favors metals immobilization and impairs biodegradation, while acidic condition ($\text{pH} < 7$) facilitates metals leaching (USEPA, 1986). Nonetheless, solubility of some metal hydroxides is increased for pH greater than 8. Hsieh and Raghu (1997) reported pH for alum and ferric WTS ranging from 6.3 to 7.8, and for lime WTS ranging from 7.5 to 11.8. Babatunde and Zhao (2007) presented pH of alum, ferric and lime WTS equal to 7.0 ± 1.4 , 8.0 ± 1.6 , and 8.9 ± 1.8 , respectively (Table 3), which agree with those reported by Hsieh and Raghu (1997). For WTS from Brazilian WTPs, researchers have reported pH values ranging from 5.9 to 8.3 (PORTELLA et al., 2003; GUERRA, 2005; GERVASONI, 2014; MONTALVAN, 2016; RAMIREZ et al., 2018).

2.2.4 Geotechnical characterization

Geotechnical characterization and classification generally consist in determining specific gravity of solids, grain size distribution, and Atterberg limits. For WTS, index properties are mainly influenced by treatment process, raw water source, raw water quality, type of coagulant, and dewatering method employed in WTPs.

Water quality varies seasonally in almost every WTP, hence, it is expected that WTS characterization will vary significantly over a year. Watanabe et al. (2011) determined specific gravity of solids and Atterberg limits for samples of PAC WTS from a Japanese WTP collected over a period of two and a half years. Specific gravity values varied from 2.40 to 2.61, and liquid limit and plasticity index values varied, respectively, from 83 to 511%, and from 23 to 325%.

Grain-size distribution and organic matter content of WTS also varies seasonally: Teixeira et al. (2011) reported large variations of clay, silt and sand fractions, and of organic matter in WTS samples collected during a year.

Specific gravity of solids of WTS is influenced mainly by inorganic particles, coagulant type, and organic matter content. Specific gravity of WTS with high content of inorganic particles (clay, silt, and sand particle fractions) would be expected to be similar to that of natural soils (2.60 to 2.70). On the other hand, peats and organic soils usually have low values of specific gravity due to the high content of organic matter (HUAT et al., 2014), and the same is expected for WTS with high organic content (HSIEH; RAGHU, 1997; BASIM, 1999).

Vandermeijden and Cornwell (1998) determined the specific gravity of alum sludges (37 samples), ferric sludges (9 samples), PACl sludges (5 samples), and lime sludges (9 samples), and reported values varying, respectively, from 2.04 to 2.94 (average of 2.35), from 2.08 to 2.84 (average of 2.43), from 2.08 to 2.56 (average of 2.33), and from 2.26 to 2.71 (average of 2.50). In general, alum and ferric sludges tend to have higher values of specific gravity.

Table 5 presents the geotechnical characterization and classification of WTS from different countries. Properties vary largely, specific gravity of solids has been reported as being as low as 1.52 and as high as 2.95. Values of plasticity index and liquid limit in Table 5 are as high as 322 and 617, respectively. On the other hand, some WTS have even been reported as non-plastic.

Geotechnical characteristics of WTS are also affected by laboratorial testing procedures, e.g. drying may drastically alter index properties. Characterization of WTS as non-plastic usually occurs when samples are dried prior to testing. Wang; Hull and Jao (1992), Vandermeijden and Cornwell (1998), Hsieh and Raghu (1997) and Montalvan (2016) reported that drying WTS samples caused particles bonding/cementation, which could not be broken even after a long period of soaking in water or dispersing agent. Basim (1999) studied the influence of drying temperature (from 60 to 555 °C) on the specific gravity of WTS samples and observed that the higher the temperature, the higher the specific gravity of solids. According to the author, organic matter oxidation is the main factor responsible for such behavior.

Hsieh and Raghu (1997) tried to determine the grain-size distribution of twenty-one (21) samples of WTS by hydrometer tests. The dry preparation method of samples (drying prior testing) failed to yield adequate results because of particles cementation. The wet preparation method (no drying prior testing) was successful in some cases, whereas some WTS were not completely deflocculated by the dispersing agent. The authors concluded that the hydrometer test is not adequate for determining the grain-size distribution of WTS.

Table 5 – Geotechnical characteristics of WTS from different countries.

Coagulant	Country	w (%)	w _L (%)	PI (%)	G _s	USCS	Reference
Lime	USA	226	-	NP	1.90	SM	(RAGHU et al., 1987)
Alum	USA	714	550	311	2.26	CH	(WANG; HULL; JAO, 1992)
Alum	USA	549	617	230	2.27	-	(HSIEH; RAGHU, 1997)
Ferric	USA	452	429	322	2.71	-	(HSIEH; RAGHU, 1997)
Lime	USA	329	330	130	2.38	-	(HSIEH; RAGHU, 1997)
Lime	USA	45	35.5	4	2.67	-	(HSIEH; RAGHU, 1997)
Lime	USA	282	207	74	2.67	-	(HSIEH; RAGHU, 1997)
Alum	USA	~67	468	306	2.06	-	(ALDEEB et al., 2003)
Alum	USA	~67	542	298	1.97	-	(ALDEEB et al., 2003)
Alum	Portugal	478.2	107	26	2.27	MH	(ROQUE; CARVALHO, 2006)
Lime	USA	203 - 300	125 - 135	40 - 43	-	-	(WU; ZHOU; GALE, 2007)
Alum	Ireland	340	490	250	1.86	OH	(O'KELLY; QUILLE, 2009)
Alum	Ireland	570-700	550	270-290	1.83-1.99	OH	(O'KELLY; QUILLE, 2009)
Alum	Ireland	300	430	105	1.90	OH	(O'KELLY; QUILLE, 2009)
PACl	Japan	300 - 488	83 - 511	23 - 325	2.40 - 2.61	-	(WATANABE et al., 2011)
Alum	USA	70	281	88	1.52 - 2.10	CH	(KOMLOS et al., 2013)
Ferric	Brazil	350	239	158	2.85 - 2.95	MH	(MONTALVAN, 2016)
Alum	Brazil	94	NP	NP	2.09 – 2.10	ML	(DELGADO, 2016)
Ferric	Brazil	15	NP	NP	2.75	-	(GONÇALVES et al., 2017)

SC= Solids content; w= water content; w_L= liquid limit; PI= plasticity index; G_s= specific gravity of solids; NP= non-plastic.

The influence of drying prior testing on grain-size distribution of WTS was also studied by Watanabe et al. (2011). The grain-size distribution of a PACI WTS was found to be dependent on initial water content: the drier the sludge, the lower the fines content. This suggests the occurrence of progressive particles cementation.

These results indicate that conventional characterization tests are not completely adequate for WTS characterization. Vandermeijden and Cornwell (1998) proposed modifications to the hydrometer test: no drying prior testing and use a sample with solids mass of approximately 10 g instead of the 50-g sample recommended by the standards to improve dispersion.

2.3 WATER TREATMENT SLUDGE DISPOSAL AND REUSE

2.3.1 Regulation and disposal

In Brazil, the National Policy for Solid Waste (PNRS, Act 12,305/2011) defines guidelines for an integral management of solid waste as well as the responsibilities of waste generators. This act aims to safeguard public health, improve environment quality, reduce waste generation, promote waste recycling, enforce adequate waste disposal, and to protect the environment.

NBR 10004 (ABNT, 2004) is the Brazilian standard for solid waste classification, which is based on potential risk to the environment and public health. According to this standard, solid waste includes residues at liquid or semi-solid state that are generated by activities from industry, households, hospitals, agriculture, and public services, including sludge from water treatment plants. Waste can be classified as class I (Hazardous) and class II (Non-hazardous). Class II is subdivided into two categories, non-inert (class II A) and inert (class II B). Class II A waste is non-hazardous but may present solubility concentrations higher than admissible values defined by NBR 10004.

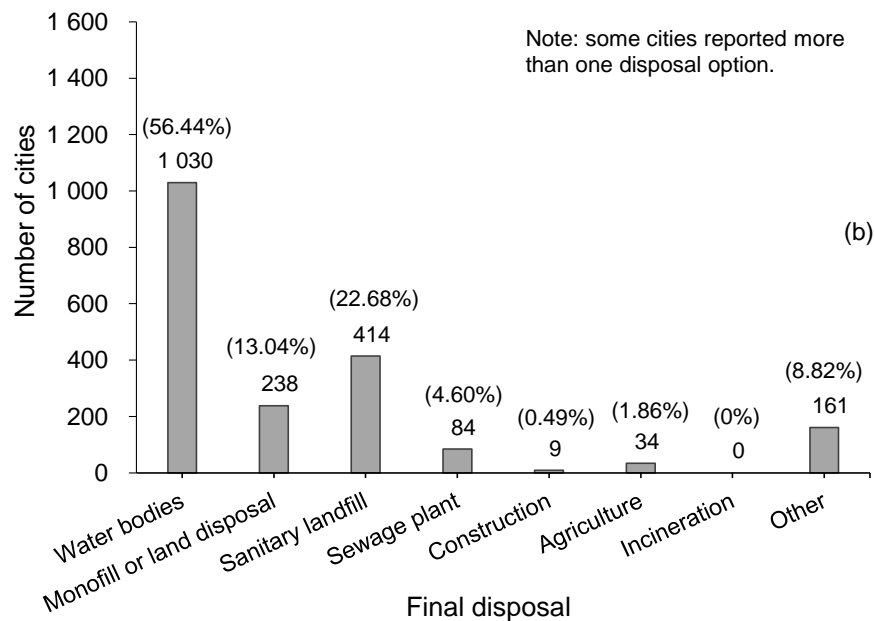
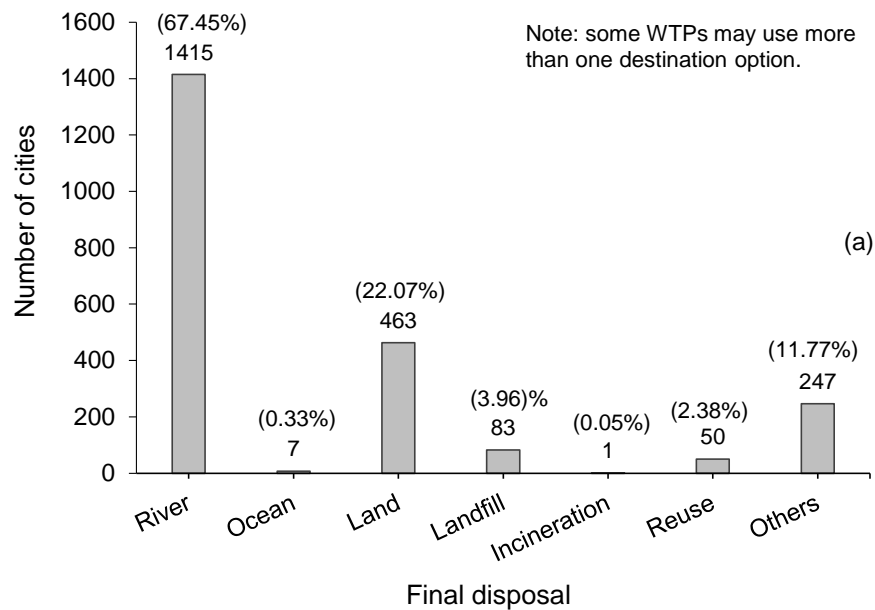
The few existing Brazilian studies on WTS classification have indicated class II A solid waste, i.e. non-hazardous and non-inert (ABOY, 1999; GUERRA, 2005; DELGADO, 2016; GODOY et al., 2019). In most cases, WTS presented solubility concentration for only one or two pollutants higher than the admissible threshold for inert waste.

According to Brazilian regulations, class II A solid waste must be disposed of safely. In Brazil, however, WTS is commonly discarded in rivers without previous

treatment (IBGE, 2010), even though the National Committee for the Environment – CONAMA (Resolution No. 430/2011) regulates the requirements (treatment, characteristics and quality) necessary for disposal of effluents in rivers.

Among the main options for WTS destination are discharge in sewage treatment plants, landfill disposal, land disposal, ocean dumping and incineration (HSIEH; RAGHU, 1997). In most countries, as in Brazil, environmental legislation does not allow direct discharge in water courses or water bodies.

Figure 4 shows the statistics of WTS disposal in Brazil, according to the National Survey of Basic Sanitation – PNSB 2008 (IBGE, 2010) and PNSB 2017 (IBGE, 2020). From the 2008's survey, over 67.5% of WTP that generated WTS discarded it in rivers despite illegality. From the 2017's survey, around 56% of WTPs disposed WTS into water bodies. According to these surveys, there was a reduction about 10% in the disposal of WTS into water bodies. Nevertheless, the 2017's survey comprises a lower number of WTPs than 2008's survey.

Figure 4 – Final disposal of WTS in Brazil: (a) PNSB 2008¹; (b) PNSB 2017².

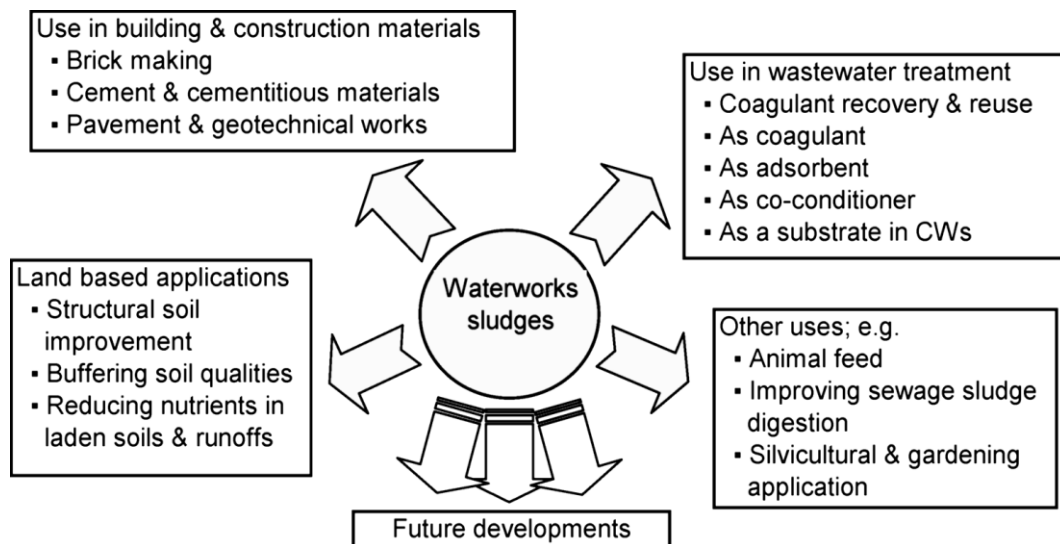
Source: modified from ¹IBGE (2010) and ²IBGE (2020).

2.3.2 Beneficial reuse options

Several beneficial reuse alternatives for WTS have been proposed and studied. Babatunde and Zhao (2007) classify WTS reuse options into four main categories: use in wastewater treatment process, use as construction material, use in land-based applications, and others (Figure 5).

Among the specific alternatives for reuse of WTS are: composting and agriculture (SILVA; FERNANDES, 1998; VERLICCHI; MASOTTI, 2000), coagulant recovery (PETRUZZELLI et al., 2000), brick making (RODRIGUES; HOLANDA, 2015), ceramic products (TEIXEIRA et al., 2011), cementitious material (GODOY, L. G. G. de et al., 2019), cement production (CHEN, H.; MA; DAI, 2010), landfill cover (KAMON et al., 2000), landfill liner (RAGHU et al., 1987; SOCKANATHAN, 1991; SILVA, A. dos S.; HEMSI, 2018), embankments (MONTALVAN; BOSCOV, 2018; ROQUE; CARVALHO, 2006). More details about disposal and reuse of WTS can be found in Cornwell (2006); Babatunde and Zhao (2007); Breesem et al. (2014); Ahmad, Ahmad and Alam (2016); and Gomes et al. (2019).

Figure 5 – Beneficial reuse options for WTS.



Source: Babatunde and Zhao (2007).

2.4 REUSE OF WATER TREATMENT SLUDGE IN GEOTECHNICAL WORKS

Some authors have studied the possibility of using WTS as construction material for geotechnical works such as sanitary landfill covers, landfill liners, backfills, embankments, and road pavement structures. WTS has been investigated in different conditions, namely, dry, wet, alone or blended with sludge-amendment materials such as soil, fly ash, lime, and cement.

2.4.1 Waste landfills

Raghu et al. (1987) evaluated the feasibility of using WTS as sanitary landfill liner. WTS samples were collected from a WTP in New Jersey, US, which uses lime and alum in the coagulation process. WTS was oven-dried prior testing and classified as silty sand; oven-drying may have turned the material non-plastic. The laboratory compaction was easy, indicating that there would not be compaction difficulties in the field. The hydraulic conductivity determined from consolidation tests carried out on compacted samples (modified Proctor effort) was about 10^{-9} m/s. The physical integrity and permeability of the samples were unaltered after soaking in leachate from a local sanitary landfill for seven, fourteen, and twenty-eight days. Pinhole tests showed that the compacted WTS was non-dispersive. Raghu et al. (1987) concluded that the studied WTS was feasible to be used as material for sanitary landfills liner.

Aldeeb et al. (2003) investigated the engineering properties of two alum WTS mixed with clayey soil aiming at use as construction material for sanitary landfill cover. Samples were collected from two WTPs located in the City of Arlington, Texas, USA. After partial oven drying at 70 to 80 °C, WTS samples with solids content about 60% presented high plasticity index, low dry unit weight, and low undrained shear strength. To enhance WTS engineering properties, a clayey soil (90% finer than 2 μ m) was added in different ratios (WTS% / soil%): 60/40, 40/60, 20/80, and 0/100. Atterberg limits, compaction, unconfined compression and direct shear strength tests were conducted. The lower the WTS percentage, the lower the plasticity and the higher the dry unit weight. Since the plasticity index of WTS decreases with soil addition, handling of WTS blended with soil becomes easier at field. The mixture 20/80 presented the highest undrained shear strength and could be used as material for landfill cover.

Roque and Carvalho (2006) studied a sludge from a WTP from Portugal in order to evaluate the possibility of using WTS for geotechnical works. Chemical analyses according to the Portuguese environmental legislation were conducted on samples of wet WTS and its eluate. WTS complied with the inert waste category, while the eluate presented fifteen out of nineteen parameters lower than the maximum admissible values for inert waste category, and all parameters complied with non-hazardous waste category. Geotechnical tests were carried out on samples oven dried at 50 to 60 °C. Index properties of the sludge are presented in Table 5. Compaction tests with standard and modified Proctor effort yielded maximum dry unit weight equal to 6.3 and

7.5 kN/m³, respectively, and optimum water content 84 and 71%, respectively, different from compacted natural soils. Permeability tests on rigid-wall permeameter were performed using water and leachate from a sanitary landfill. For water, hydraulic conductivity of samples compacted at $-12\% \leq w - w_{opt} \leq 9\%$ under standard effort varied in the range $0.9 - 2.7 \times 10^{-7}$ m/s, and compacted at $-10\% \leq w - w_{opt} \leq 9\%$ under modified effort, in the range $0.2 - 1.6 \times 10^{-8}$ m/s. For leachate, hydraulic conductivity values for samples compacted at $w_{opt} - 5\%$ and $w_{opt} - 10\%$ under modified effort were, respectively, 1.2 and 9.3×10^{-10} , i.e. were reduced 17 to 133 times. Effective shear strength parameters were determined by consolidated undrained (CU) triaxial compression tests: cohesion intercept equal to 77 kPa and effective friction angle equal to 44°. One-dimensional consolidation test showed that the compacted WTS had low compressibility. Roque and Carvalho (2006) suggested that, based on chemical and permeability results, the studied WTS could be employed as construction material for sanitary landfill covers and liners.

Hidalgo et al. (2017) performed leaching and solubility tests on six WTS from different Spanish WTPs to confirm the suitability for disposal in an inert waste landfill. All WTS presented values below legal limits and were classified as inert waste.

Silva and Hemsli (2018) studied the influence of solids content on compaction behavior and undrained shear strength of a ferric WTS aiming at a possible use as material for sanitary landfill daily cover. Water content of WTS samples varied from 225 to 300%, and liquid limit and plasticity index varied, respectively, from 221 to 240% and from 71 to 154%. Compaction by the dry method (beginning at the dry side) showed the typical one-hump curve. However, when compacted by the wet method (beginning at the wet side), the dry unit weight of WTS increased gradually as the water content decreased, similar to the behavior reported by Wang et al. (1992) and Hsieh and Raghu (1997). The undrained shear strength, determined from unconfined compression tests, increased exponentially with increasing solids content, with values very close to those reported by Wang et al. (1992). The authors concluded that for reuse as daily cover in sanitary landfills, the studied WTS must be dewatered to a solids content of about 50% (water content circa 100%), which corresponds to undrained shear strength of 10 kPa. This is the minimum strength considered by the authors as necessary for spreading the material in the field by usual earthwork equipment.

2.4.2 Backfills

Fortes et al. (2006) investigated the technical feasibility of using WTS from Taiapuêba WTP, located in Suzano, São Paulo, Brazil, with lime addition as backfill for trenches. WTS dewatered first by centrifuge and subsequently at drying beds presented water content of 19.7%. The sludge was characterized as Class II A (non-hazardous and non-inert waste) according to NBR 10004 (ABNT, 2004). Compaction and California Bearing Ratio (CBR) tests were conducted on samples blended with lime and soil. WTS with 3% lime presented maximum dry unit weight of 8.7 kN/m³, optimum water content of 51%, CBR of 17% and expansion value of 0.25%. WTS with 45% soil and 5% lime presented dry unit weight of 12.5 kN/m³, optimum water content of 32.6%, CBR of 19% and expansion value of 0.17%. According to a local standard (IR-01/2004), the minimum acceptable CBR value for backfill material of trenches for flexible pavements restoration is 12% and the maximum expansion value is 2% (PREFEITURA DO MUNICÍPIO DE SÃO PAULO, 2004). Fortes et al. (2009) conducted further studies with addition of 3 and 5% hydrated lime, and 3 and 5% Portland cement. Unconfined compression, diametral compression and CBR tests were performed on samples with different curing times. The authors concluded that, considering strength, WTS stabilized with lime and cement can be used in earthworks, such as backfill material for trenches, and road pavement sub-base and subgrade.

2.4.3 Embankments

Wang, Hull and Jao (1992) studied the compaction, compressibility, and shear strength properties of a WTS and mixtures with additives, namely, lime, fly ash and soil (clayey sand), for possible use as material for embankment construction. Sludge samples were collected at a WTP located in Chesapeake, Virginia, US, which uses aluminum sulfate as coagulant. The index properties of the untreated sludge are presented in Table 5. All mixtures were prepared with WTS at natural water content and additive content of 60% (dry mass basis). Compaction curves under standard Proctor effort did not present the typical one-hump curve, dry unit weight was highest near zero moisture and decreased with water content increment. The compression index of the mixtures, determined from one-dimensional consolidation tests, varied from 3.5 to 4.0, indicating that they are highly compressible, as compression index for most natural clays is lower than 1.0 (MITCHELL; SOGA, 2005). The effective friction

angle of untreated WTS, determined from Consolidated Undrained (CU) triaxial compression test, ranged from 42 to 44°, similar to values reported by other authors (ROQUE; CARVALHO, 2006; O'KELLY, 2008; O'KELLY; QUILLE, 2010). The undrained shear strength of mixtures, determined by fall cone penetration tests, was initially very low, however increased substantially with increasing solids content. The authors concluded that stabilization of WTS by additives such as lime, fly ash and soil, effectively enhances its workability. Even though the mixtures showed higher compressibility and lower shear strength than required for embankment construction, those properties may be further improved by increasing the additive content and/or reducing WTS water content prior to mixing.

The high shear strength and low compressibility of the compacted WTS studied by Roque and Carvalho (2006) indicated its feasibility, under proper design, for embankment and pavement construction, especially as material for light embankments on soft soils due to its low dry unit weight, approximately half of that of natural soils.

Montalvan (2016) studied mixtures of a sandy soil with ferric WTS aiming at use in geotechnical works. Compaction, one-dimensional consolidation, permeability and shear strength tests were carried out. The sludge was collected at Cubatão WTP, located in the State of São Paulo, Brazil. Mixtures of soil/WTS were prepared using three WTS contents by wet mass: 16.7%, 20.0% and 25.0%. WTS was not previously dried, with water content about 350%, and the soil was air-dried to hygroscopic water content. WTS addition reduced maximum dry unit weight, increased compressibility, lowered permeability, and reduced undrained shear strength. Nonetheless, final parameters were still acceptable for earthworks. From a hydro-mechanical viewpoint, soil/WTS mixtures are feasible as construction material for backfills, landfill covers, landfill liners, and embankments. However, environmental evaluations are needed.

2.4.4 Pavements

Coelho et al. (2015) evaluated the possibility of using WTS mixed with a clayey soil and a sandy soil, as construction material for subgrade, sub-base, and base in road pavement. WTS samples were collected at Cafezal WTP, located in Londrina, Paraná, Brazil, dewatered in a geotextile, and finally air-dried. The sludge content in the mixtures (by wet mass) was 50% for the clayey soil and 25% for the sandy soil. WTS addition did not significantly alter the compaction parameters of the soils,

probably because of the low quantity of added solids and previous air-drying. Most investigated WTS have been reported to suffer irreversible changes after drying, such as plasticity loss and formation of highly cemented clods (WANG; HULL; JAO, 1992; HSIEH; RAGHU, 1997; MONTALVAN, 2016; WATANABE et al., 2011). Compacted samples of the soils and mixtures were subjected to CBR tests and expansion by immersion in water. The WTS/clayey soil mixture presented CBR 42% lower and expansion potential 747% higher than the values obtained for the soil. The WTS/sandy soil mixture presented CBR 58% lower and expansion potential 200% higher than the values of the soil. According to the minimum requirements for road pavements, both soils and mixtures presented admissible values only for subgrade category.

Delgado (2016) studied the feasibility of WTS addition to clayey and sandy soils, and to rock dust, as material for road pavement sub-base. The sludge was collected at Guandu WTP, located in the State of Rio de Janeiro, Brazil, which uses aluminum sulfate as main coagulant. Mixtures were prepared using WTS at 94% water content. WTS was classified as waste class II A (non-hazardous and non-inert). According to Delgado (2016), addition of 5 to 15% WTS by wet mass would not represent an environmental issue in roadway structures. Cyclic triaxial compression tests were carried out to determine the resilient modulus. For WTS/soil mixtures, the resilient modulus decreased with increasing WTS content. For WTS/rock dust, the resilient modulus initially increased, up to 5% WTS content, probably due to granulometric stabilization, as the rock dust had low fines content (~2 %) and WTS contained high fines content (~84 %). The author concluded that WTS/soil mixtures were not adequate for sub-base construction, WTS/rock dust mixtures with 5% WTS could be used as sub-base of low-traffic roads, and a high resilient modulus could be achieved for WTS/rock dust mixtures with WTS content up to 15% by adding 2% of cement.

2.5 COMPACTED SOILS IN GEOTECHNICAL WORKS

Geotechnical works, such as backfills, landfills, embankments (for earth dams, highways, and buildings foundation), and road pavements, use soil as construction material. Soils randomly dumped are usually unsuitable for geotechnical works; they are highly compressible, unstable, and sometimes have permeability higher than desirable. Thus, soils must be densified, what is generally achieved by mechanical stabilization (compaction). Compaction homogenizes the soil mass and greatly

enhances its hydromechanical behavior, i.e. compressibility, permeability, and shear strength, which are the most important soil properties for earthworks design.

Following, a discussion is presented about typical hydromechanical behavior and requirements for acceptability of compacted soils in different geotechnical structures.

2.5.1 Waste landfills

The bottom liner, the daily cover and the final cover are fundamental protection components of sanitary landfills. The bottom liner and the final cover usually have the same specification in terms of permeability. The daily cover, however, usually does not have a permeability specification, but a minimum undrained shear strength of 10 kPa has been considered necessary for adequate workability and spreading of the material in the field (SILVA and HEMSI, 2018).

For bottom liners and final covers, permeability has major importance. Since permeability must be low, compacted layers of clayey soils (CCL – compacted clay liner) are usually employed. Formerly, sand-bentonite mixtures have also been used, but nowadays inadequate local soil for CCL is frequently substituted by geosynthetic clay liners.

Most environmental agencies recommend or require a maximum hydraulic conductivity value of 1×10^{-9} m/s for bottom liner and final cover (NRA, 1992; USEPA, 1993; ROCCA; IACOVONE; BARROTTI, 1993; QASIM; CHIANG, 1994; BOSCOV, 2008; DANIEL, 2012). Murray, Dixon, and Jones (1998) compiled several criteria recommended by different authors for the evaluation of soil suitability as construction material for landfill liners (Table 6).

Benson, Zhai, and Wang (1994), analyzing a database of compacted bottom liners from 67 landfills in North America, tried to establish requirements for Atterberg limits, percentage of fines and clay, and activity, in order to screen proper soils for CCLs, i.e. to achieve compacted hydraulic conductivity equal or smaller than 1×10^{-9} m/s. They proposed minimum recommended values for liquid limit (20%), plasticity index (7%), fines percentage (30%), clay fraction percentage (15%), and Skempton's activity (0.3). These values are similar to those presented in Table 6. Some authors suggest that compacted clay liners should also attend to chemical requirements. For

instance, Rocca, Iacovone and Barrotti (1993) recommend a pH higher than 7 for industrial waste landfills, and according to Hsieh and Raghu (1997), the New Jersey Administrative code of 1988 prescribes a minimum CEC value of $35 \text{ cmolc}\cdot\text{kg}^{-1}$.

Table 6 – Recommended criteria for soil suitability as landfill liner material.

Parameter	Reference	Criteria
Plasticity	DOE (1995)	$10\% < IP < 30\%$
	Daniel (1993)	$PI < 7-10\%$
	NRA (1992)	$w_L < 90\%$; $IP < 65\%$
	Murray et al. (1992)	$PI > 12\%$
	Gordon (1987)	$PI > 15\%$
	Williams (1987)	$PI > 15\%$
Fines percentage	Daniel (1993)	Silt and clay $> 20-30\%$
	NRA (1992)	Clay $> 10\%$
	Gordon (1987)	Clay and silt $> 50\%$
Activity (PI / %Clay)	DOE (1995)	$A > 0.3$

Source: Murray; Dixon and Jones (1998).

The specifications for field compaction usually include acceptable relative compaction (RC) and water content deviation ($w_{\text{field}} - w_{\text{opt}}$) (Figure 6a), defined by the designer and controlled in the field. Minimum dry unit weights for CCLs are typically defined by 95% of maximum dry unit weight of standard Proctor effort ($RC \geq 95\%$), and 90% of maximum dry unit weight of modified Proctor effort ($RC \geq 90\%$). The range for acceptable water content for landfill liners and covers is usually about 0 and 4% wet-of-optimum (DANIEL; BENSON, 1990).

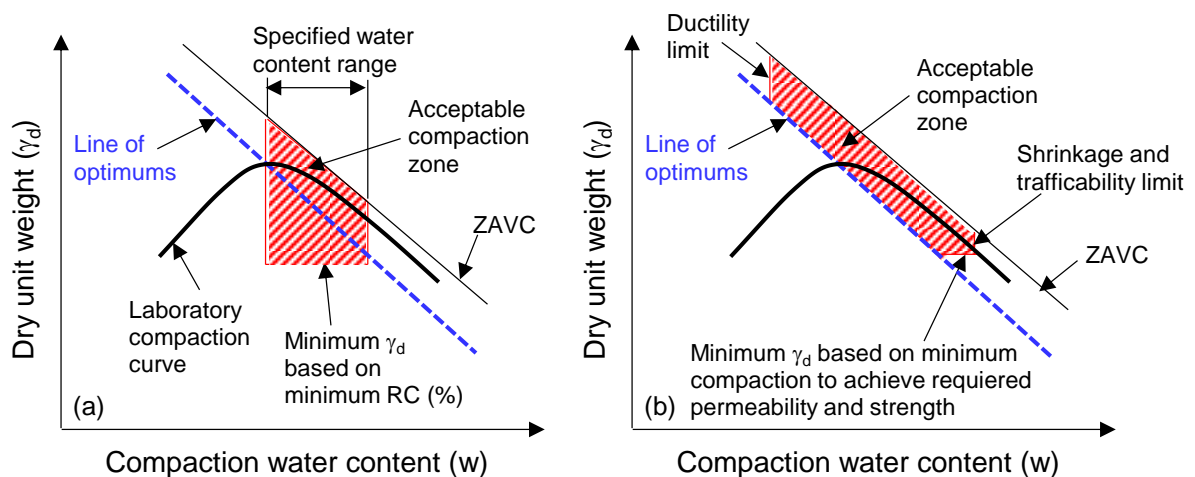
Daniel and Benson (1990) proposed a methodology to define the “acceptable zone” for compacted liners and covers. The procedure consists in defining water content and dry unit weight ranges that produce the required hydraulic conductivity using different compaction efforts, and then modifying this compaction range in order to account for other factors, such as shrinkage and strength (Figure 6b). This kind of approach is similar to that proposed by other authors for compaction specifications in earthworks (PARSONS; BODEN, 1979; TRENTER; CHARLES, 1996; PINTO, 2006). The lower limit for moisture is usually dictated by permeability or ductility requirement, and the upper limit is often dictated by shear strength or shrinkage, as illustrated in

Figure 6b. An undrained shear strength of 40 to 50 kPa is typically required in earthworks, values lower than that may compromise stability and make handling, compaction and trafficability more difficult (MURRAY; RIX; HUMPHREY, 1992).

A database of 85 compacted liners from different sites in the United States and Canada, 8 actual in-service liners and 77 test pads, was compiled by Benson, Daniel and Boutwell (1999) to evaluate field performance. The authors believe the database captured the results of 50–75% of all test pads constructed in North America where large-scale field hydraulic conductivity tests have been carried out until that year. Compacted liners using soil-bentonite mixtures were not included. A wide variety of soils is comprised in the database. The liquid limit (w_L) varies from 21 to 101, the fines content varies from 48 to 99%, and the clay content (%finer < 2 μm) varies from 16 to 57%. Almost all soils were classified as CL or CH by the USCS.

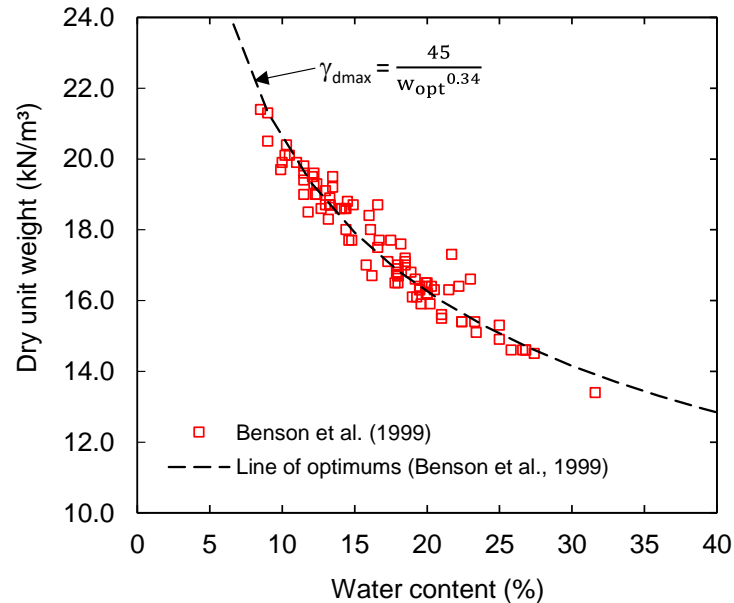
Most liners were designed by conventional percent compaction specification (Figure 6a). Maximum dry unit weight and optimum water content values of soils from the database are plotted in Figure 7. Although all liners in the database were constructed aiming to achieve hydraulic conductivity equal or lower than 1×10^{-9} m/s, 26% of them presented higher values.

Figure 6 – Schematics of: (a) conventional compaction specification; (b) recommended compaction specification (DANIEL; BENSON, 1990).



Source: modified from Benson et al. (1999).

Figure 7 – Compaction parameters of soils used for compacted landfill liners.



Source: modified from Benson et al. (1999).

Benson, Daniel and Boutwell (1999) observed that RC and water deviation requirements do not guarantee that the liner will present acceptable hydraulic conductivity and recommended that the compaction specifications must warrant that soil is compacted on or above the line of optimums.

Compaction parameters and hydraulic conductivity values for tropical lateritic soils may differ from those of the database for similar Atterberg limits and fines content. Compacted lateritic clays may not achieve hydraulic conductivity lower than 10^{-9} m/s, which could be explained by the typical porous fabric due to particles aggregation and clusters formation; indeed, several Brazilian earth dams display hydraulic conductivity near 10^{-8} m/s (BOSCOV et al., 2011). On the other hand, lateritic sands and clayey sands may present hydraulic conductivities similar to lateritic clays ($\leq 10^{-8}$ m/s) when compacted at or above optimum water content (NOGAMI; VILLIBOR, 1995b).

Daniel and Wu (1993), worried with shrinkage-induced cracking due to desiccation of compacted soil liners and covers in arid areas, proposed to use the recommended compaction specification by Daniel and Benson (1990) in order to meet the requirements of low hydraulic conductivity and minimal shrinkage potential. They considered three criteria for definition of the acceptable zone: hydraulic conductivity (k) not higher than 1×10^{-9} m/s; volumetric shrinkage (VS) not higher than 4%; and unconfined compressive strength (UCS) not less than 200 kPa. Other criteria could be

adequate for different projects. The maximum volumetric shrinkage strain of 4% was based on Kleppe and Olson (1985), who reported that compacted mixtures of clay and sand with shrinkage strain greater than 4 to 5% may develop cracks, and with shrinkage strain greater than 10% may undergo severe cracking.

Osinubi and Nwaiwu (2006) compared, by laboratorial testing, the conventional compaction specifications (Figure 6a) and that recommended by Daniel and Benson (1990) (Figure 6b) for the design of compacted liners and covers using lateritic soils from Nigeria. These authors outlined deficiencies of the conventional compaction specifications already described by other authors (BENSON; DANIEL; BOUTWELL, 1999; DANIEL; BENSON, 1990), and pointed out that the proposed approach is applicable and advantageous for lateritic soils.

Albrecht and Benson (2001) studied how drying cycles, compaction conditions, and soil composition affect shrinkage and cracking of compacted clayey soils due to desiccation. Specimens were compacted at optimum, dry- and wet-of-optimum, and saturated before desiccation. Their results confirmed an expected lower volumetric shrinkage of specimens compacted close to optimum water content; and that volumetric shrinkage tends to increase with the increase of saturated water content and decrease with the increase of dry unit weight, although the results showed great dispersion. Results, however dispersed, showed a trend in accordance with the expected increase of volumetric shrinkage with increasing clay fraction content (% finer < 2 μm) and plasticity index. The authors suggested that, to diminish shrinkage effects, compacted soil covers should be constructed using soils with low clay fraction content and low plasticity index, near optimum water content and with high compactive effort. Nonetheless, the authors did not consider that rigid soil covers may develop cracks due to tension caused by the large differential settlements of landfilled waste.

Moreover, desiccation considerably affects hydraulic conductivity of compacted clayey soils. Permanent alteration of soil structure usually occur during initial drying or first drying-wetting cycle (BERNUCCI, 1987; FREDLUND; RAHARDJO, 1993; ALBRECHT; BENSON, 2001). Albrecht; Benson (2001) compared four North American soils (marine sediments, residual soil and glacial soil) that showed very similar and high volumetric shrinkage strain after the first drying cycle (~15%) when compacted wet-of-optimum using standard compactive effort: after three drying-wetting cycles, two soils (PI = 46% and 32%) suffered severe cracking, one soil (PI =

11%) presented no visible cracks, and other (PI = 26%) presented intermediate cracking pattern and area. The cracked probes showed significant increase of the hydraulic conductivity compared to as-compacted probes (up to three orders of magnitude). The authors explain that wet-of-optimum hydraulic conductivity is controlled by microscale pores, while cracks developed by the drying cycle create a macroscale pore structure that henceforth controls the hydraulic conductivity. Desiccation cracking is even more significant for tropical soils, for which shrinkage may even be a classifying parameter (Godoy and Bernucci, 2002).

The major function of compacted landfill covers is to protect from rainfall infiltration and gas leakage to atmosphere. Thus, evaluation of landfill covers performance comprises two important aspects: soil water retention curve (SWRC), and shrinkage behavior or cracking potential (BIZARRETA; DE CAMPOS, 2012). The SWRC permits the estimation of unsaturated hydraulic conductivity, necessary to model water flow through compacted covers and liners under unsaturated conditions.

2.5.2 Embankments

In Brazil, the compaction specifications of several embankments have been adopted considering the conventional specification: water content of $w_{opt}-1\%$ to $w_{opt}+2\%$ (percentage point) and relative compaction (RC) varying from 95% to 102% (PINTO, 2006; MARINHO; SOTO; GIRITANA JUNIOR, 2015). These values are usually defined based on Proctor compaction with standard effort as reference.

The technical specification 108-ES (BRASIL, 2009) of the National Department of Transport Infrastructure (DNIT) requires highway embankments to be constructed with soils without organic matter, CBR $\geq 2\%$, expansion less or equal than 4%, compaction criteria: water content deviation of $\pm 3\%$ and RC $\geq 100\%$. However, the final layer of the embankment (subgrade) must present better mechanical properties, i.e. expansion $\leq 2\%$ and CBR $> 6\%$.

In the case of embankments for foundation of low-rise buildings or simple structures, where slope failure or instabilities are not likely to occur, the dry unit weight (or void ratio) of the compacted soil is the most important aspect to be considered, since it is closely related to the compressibility of the embankment (PINTO, 2006): the lower the dry unit weight, the higher the compressibility.

Compression index (C_c) of natural clays is usually lower than 1.0, and in most cases lower than 0.5 (MITCHELL; SOGA, 2005). For compacted soils, compression index is even lower. Based on Brazilian literature, compression index of compacted Brazilian residual soils is about 0.15 (ASSIS; HERNANDEZ; COLMANETTI, 2014). The compacted lateritic soil used in Tucuruí earth dam presented compression index value of 0.19 (DIB; ONO, 1985), and those soils studied by Pozzebon (2017), used in highway embankments, showed values ranging between 0.16 and 0.44 (mean of 0.31).

For the analysis of end-of-construction stability of embankments, the undrained shear strength must be considered for design purposes. For drained conditions and long-term stability analyses, effective strength parameters are used. Acceptability of compacted cohesive soils in earthworks is frequently based on undrained shear strength (TRENTER, 2001). The specification of a minimum undrained shear strength is generally governed by stability or trafficability. A wide range of minimum undrained shear strength values is indicated in the literature. According to Trenter (2001), a range of 50 to 60 kPa is often considered as an acceptable value for satisfactory equipment maneuvering without soil rutting. According to Murray, Rix, and Humphrey (1992), a minimum undrained strength of 40 to 50 kPa is typically required for earthworks. Ranges of specified undrained strength for the clay core at some earth dams in England have been reported to vary from 42 to 110 kPa (KENNARD et al., 1979).

The undrained shear strength behavior of compacted cohesive soils can be compared to that of overconsolidated (OC) clays. The undrained shear strength (s_u) of OC soils is related to the pre-consolidation pressure (σ'_p), and s_u of compacted soils is influenced by the compaction-induced stresses. The relationship between s_u and σ'_p is usually defined by the SHANSEP method using equation 5 (LADD; FOOTT, 1974):

$$\left(\frac{s_u}{\sigma'_{v0}}\right) = \left(\frac{s_u}{\sigma'_{v0}}\right) \left(\frac{\sigma'_p}{\sigma'_{v0}}\right)^m \quad (5)$$

Where σ'_{v0} is the *in situ* or initial effective vertical stress; and m is a material constant.

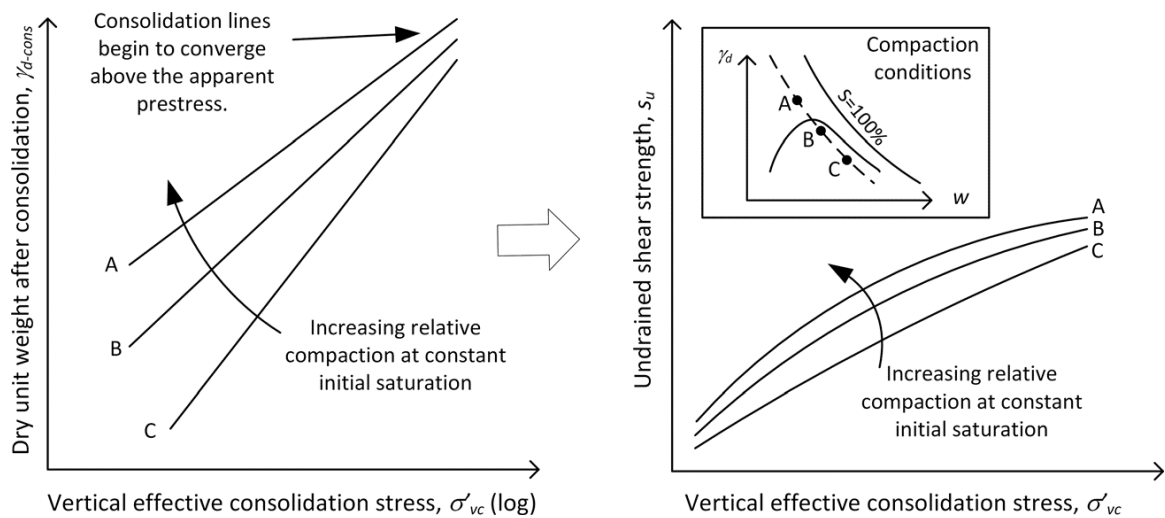
However, since the compaction-induced pre-stress is not easily or accurately determined for compacted soils, a two-parameter power function, developed for OC clays, can be used instead (Vandenberge, Daniel R.; Duncan; Brandon, 2015), as defined by Equation 6:

$$s_{u-oc} = c p_a \left(\frac{\sigma'_{1c}}{p_a} \right)^d \quad (6)$$

Where c is a parameter controlling the overall slope of the fit; b is a parameter controlling the curvature of the fit; σ'_{1c} is the effective major principal consolidation stress; and p_a is the atmospheric pressure (same units as stress and strength).

Vandenberge; Brandon, and Duncan (2014) indicate that dry unit weight and undrained shear strength are influenced by relative compaction (RC) at constant initial saturation as shown in Figure 8. The authors focused the variation of dry unit weight due to relative compaction or compactive efforts. This approach may be interesting for evaluating the compaction and strength behavior of mixtures of soil and WTS, for which the dry unit weight varies along the line-of-optimums due to WTS content.

Figure 8- Influence of RC on dry unit weight and undrained shear strength.



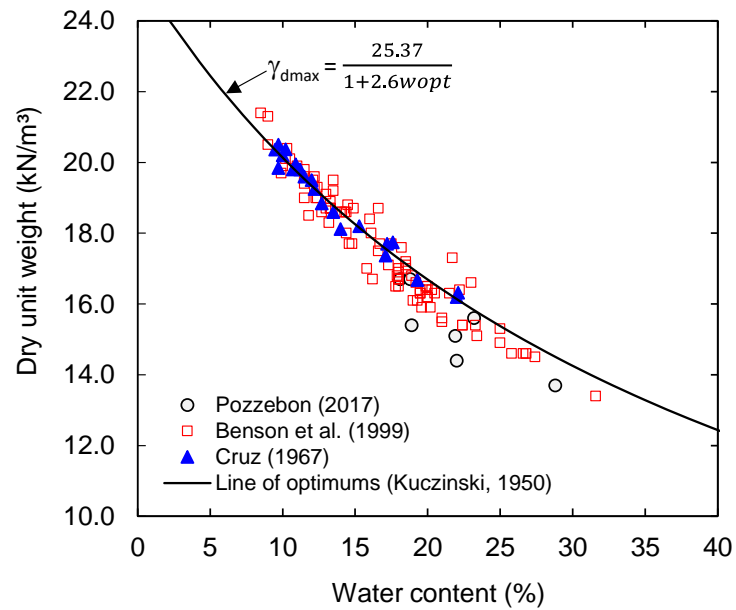
Source: Vandenberge, Brandon and Duncan (2014)

Cruz (1967) presented a compilation of geotechnical properties of several compacted Brazilian residual soils applied in embankment dams. The compaction parameters of these soils are presented in Figure 9, plotted with those from the database compiled by Benson, Daniel and Boutwell (1999) of North American soils used in compacted landfill liners, and some Brazilian residual saprolitic soils studied by Pozzebon (2017).

The soils studied by Pozzebon (2017) were used as material for construction of highway embankments in the State of São Paulo, Brazil. It can be noted that those

soils used for earth dams, fine lateritic soils (CRUZ, 1967), presented higher dry unit weight than those used in highway embankments, saprolitic soils (POZZEBON, 2017), and they align closely to the Kuczinski's line-of-optimums. This line of optimums was obtained from more than one thousand compaction curves of Brazilian soils (MASSAD, 2016).

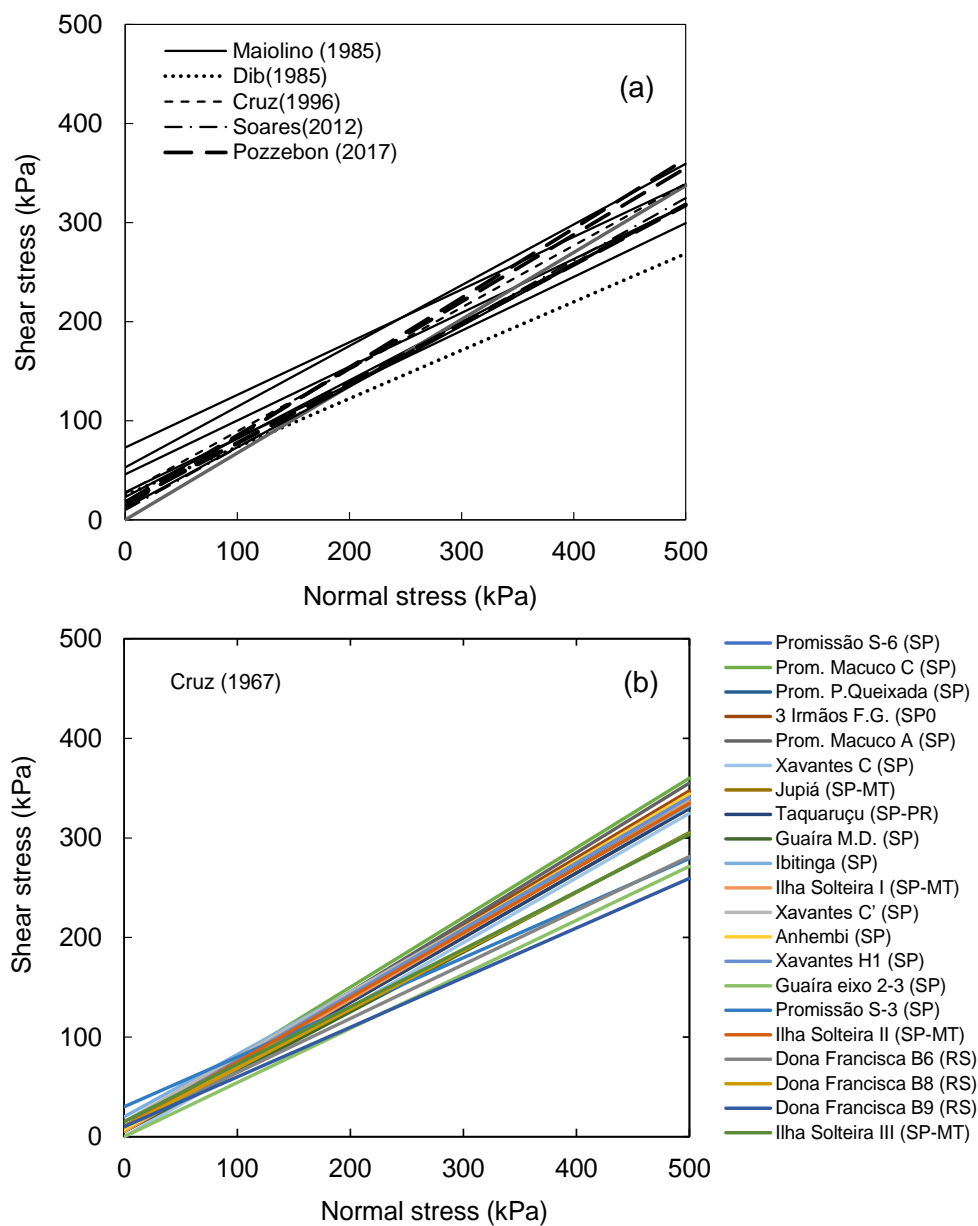
Figure 9 – Compaction parameters of soils used in different earthworks.



Source: adapted from Cruz (1967); Benson et al. (1999); Pozzebon (2017).

The shear strength envelope for effective stresses of different compacted Brazilian soils is presented in Figure 10. Effective cohesion values varied from 0 to 73 kPa. Effective angle of internal friction varied from 26 to 35 degrees. Most of the structures constructed with these compacted soils presented good performance. Hence, those values are a good reference for geotechnical behavior comparison among Brazilian soils.

Figure 10 – Shear strength envelopes (effective stress) of some compacted Brazilian soils.



Source: adapted from references indicated inside the charts.

3 METHODOLOGY

This chapter describes the materials and methods employed along the research. There are two subchapters, Materials and Testing Program. Materials subchapter contains a description of the studied materials, two WTS and two residual soils. Testing program subchapter describes methods, procedures, and equipment used for sampling of the materials and for the execution of tests.

3.1 MATERIALS

The studied materials comprise two WTS from different WTPs (raw water from river and reservoir) and two residual lateritic soils, a clayey sand and a clay. These soils were selected because they cover large areas of the State of São Paulo according to the Brazilian Soils Map (IBGE, 2001). The two WTPs were selected by SABESP's recommendation because of high WTS generation, and also because of different raw water sources (river and reservoir). Mixtures of soils and WTS were prepared at several ratios aiming to investigate the influence of WTS addition on the geotechnical behavior and properties of the soils.

3.1.1 Sludge from Cubatão WTP

The Cubatão WTP, operated by SABESP, produces 4.5 m³/s of potable water. This WTP supplies water to a population of approximately 1.5 million people of the *Baixada Santista*, a metropolitan area located on the coast of the State of São Paulo, which includes Brazilian most important harbor, petrochemical industry, and seaside resorts (MONTALVAN; BOSCOV, 2016). Figure 11 shows the location map of Cubatão WTP.

Raw water is collected from the Cubatão River, which presents turbidity of 800 NTU and 8,000 cells of filamentous algae/mL. The Cubatão WTP contains 14 filters, washed every 18 hours during 40 minutes (MONTALVAN; BOSCOV, 2016).

This WTP uses ferric chloride as coagulant. The major sludge generation points are the sedimentation basins and filters. WTS produced in these points is sent to a thickening tank, where it reaches solids content of 2 to 4%. The final step is dewatering by centrifuges, generating circa 60 tons per day of WTS with 20 to 25% of solids content. The sludge is currently being disposed of in a local industrial waste landfill.

Samples of Cubatão WTS were collected right after centrifuge dewatering. The sampling procedure is described in detail in section 3.2.1 – Sludge sampling.

3.1.2 Sludge from Taiaçupeba WTP

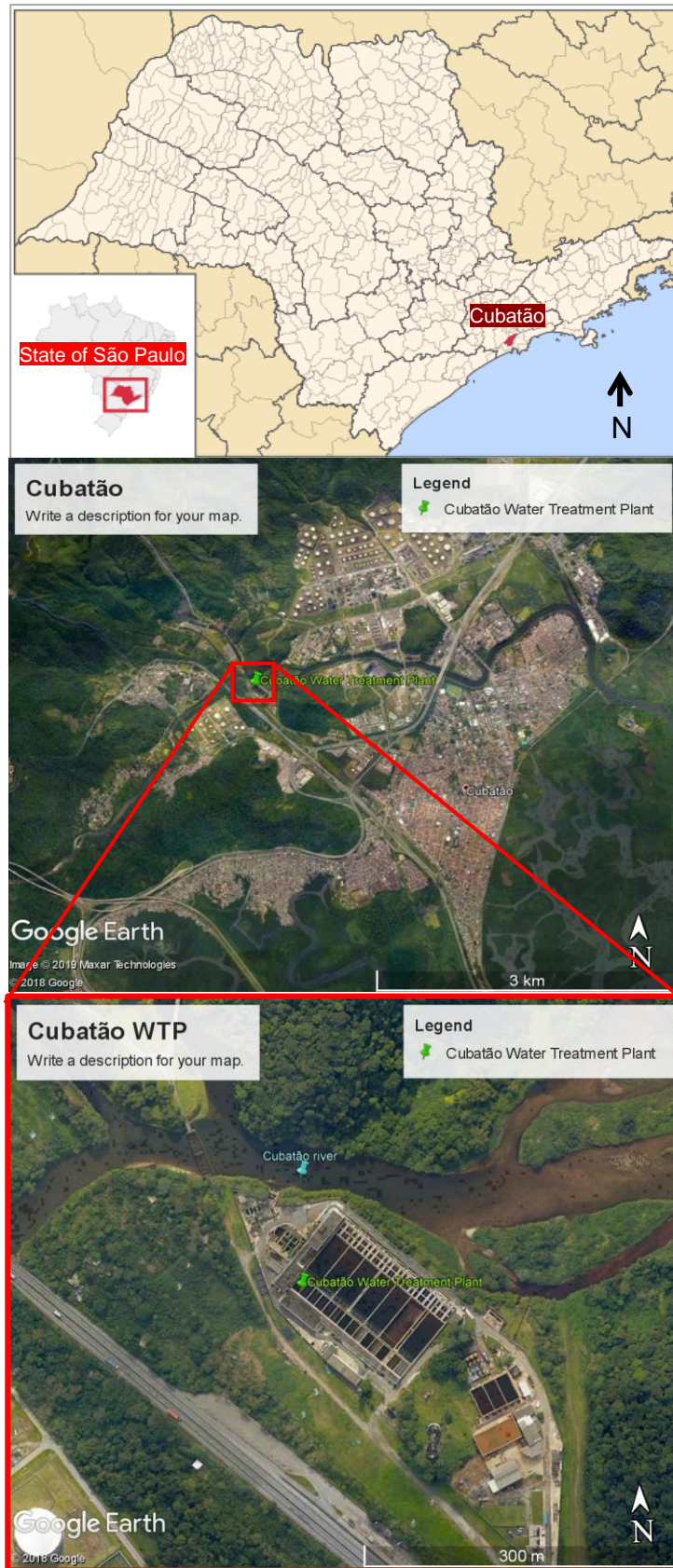
The Taiaçupeba WTP is located in the city of Suzano, part of São Paulo Metropolitan Region (SPMR), and integrates the Upper Tietê Production System of SABESP, which is responsible for supplying water to SPMR's East Zone and to some of the municipalities in the upper Tietê River basin, like Poá, Suzano, Brás Cubas, Mogi das Cruzes and Arujá. Figure 12 shows the regional and local view of the location of Taiaçupeba WTP.

The Taiaçupeba WTP has currently a water production capacity of 15 m³/s (SABESP, 2019b). This WTP treats raw water, collected from the Taiaçupeba reservoir, by the conventional treatment process. The coagulation process employs aluminum sulfate and a polymer of high molecular weight (superfloc 8392).

WTS collected from the sedimentation basins and filters backwashing is sent to an equalization tank (solids content of about 2%), then to a thickening tank, from there to belt filters where it receives polymer coagulant (solids content of 4%), and finally to centrifuges, where WTS is dewatered to a solids content of approximately 16 to 18%. WTS is further air-dried and disposed of in engineered cells inside the WTP or sent to an external landfill.

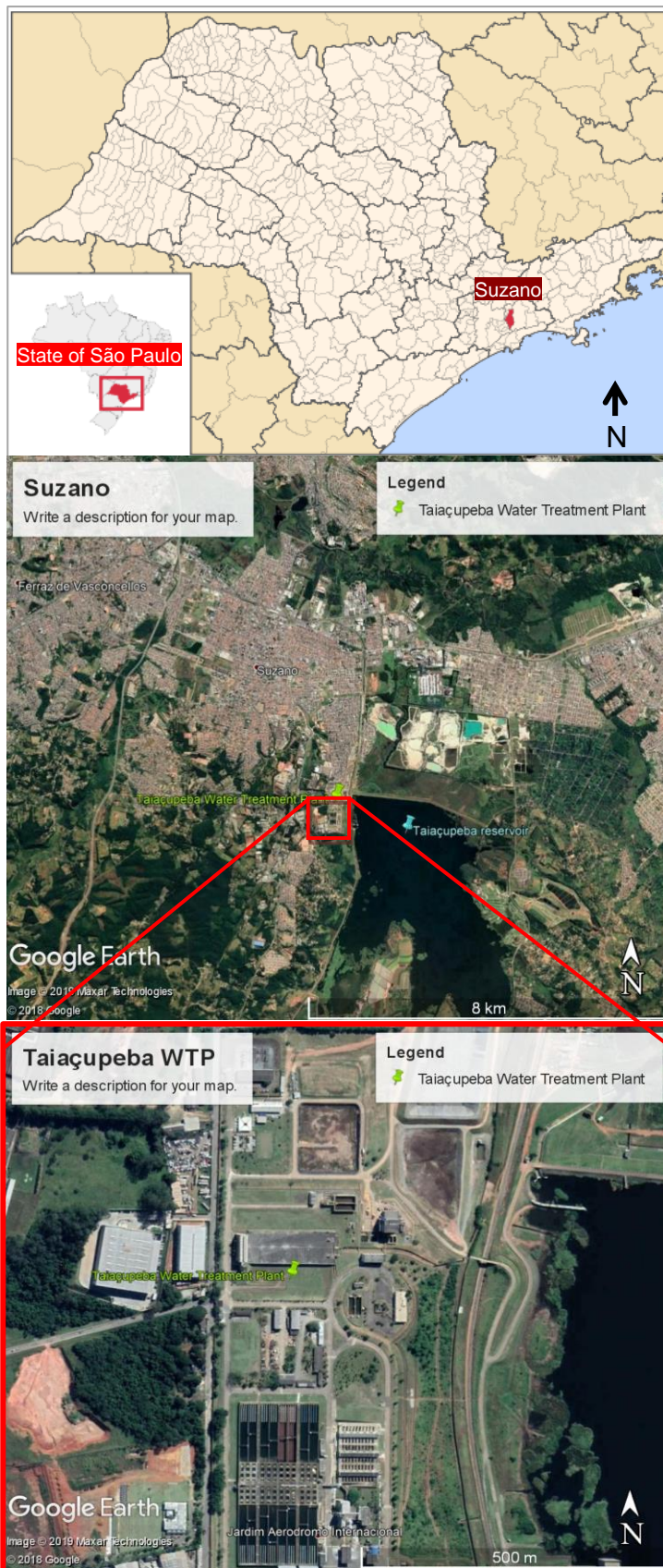
Samples were collected directly after centrifuge dewatering. A detailed description of the sampling procedure is presented in Section 3.2.1 – Sludge sampling.

Figure 11 – Location of Cubatão WTP.



Source: modified from Wikimedia Commons Contributors (2017b) and Google Earth (2019).

Figure 12 – Location of Taiacupeba WTP.



Source: modified from Wikimedia Commons Contributors (2017c) Google Earth (2019).

3.1.3 Clayey sand

Samples of this soil were collected at Botucatu city in the State of São Paulo. Figure 13 shows regional and local view of the sampling site.

This region presents stratigraphy with characteristics from the Botucatu and Pirambóia Geological Formations interspersed with igneous rocks (basalts and diabases) from outcrops of the Serra Geral Formation (PINTO et al., 1993). The Botucatu Formation comprises mostly sandstones of eolian origin, which altered by weathering to a fine to medium sandy soil (BASSO; PARAGUASSÚ, 2006). The Botucatu sandy soil is usually classified as lateritic with red-yellow color and fines content (particles < 75µm) lower than 20% (PINTO et al., 1993). This soil is rich in metal oxides and the major occurring minerals are quartz, kaolinite, gibbsite, and hematite (ZANON, 2014).

This soil has been classified in previous studies as following:

- a) clayey sand (SC) according to Unified Soil Classification System – USCS (ZANON, 2014; MONTALVAN; BOSCOV, 2016).
- b) *latossolo vermelho* (ZANON, 2014) according to the Brazilian Soil Classification System – SiBCS (SANTOS et al., 2018), corresponding approximately to oxisol from the Soil Taxonomy of the US Department of Agriculture (SOIL SURVEY STAFF, 1999).
- c) lateritic clayey sand (LA') according to MCT (Miniature-Compacted-Tropical) Classification System (NOGAMI; VILLIBOR, 1995b).

The *latossolo vermelho* (oxisol) is the soil class with major occurrence in the state of São Paulo, covering approximately 52% of its area (IBGE, 2001).

3.1.4 Clay

This soil was collected at the Agronomic Institute of Campinas, located in Campinas city, in the State of São Paulo. Figure 14 shows regional and local view of the location of the sampling site.

This region consists of basic migmatites with occurrence of intrusive rocks from the *Serra Geral* Geologic Formation (diabase rocks). The soil of this region, formed by weathering of diabase, is classified as *latossolo roxo* (ZUQUETTE, 1987), approximately equivalent to oxisol from the US Soil Taxonomy System. This soil is a reddish lateritic clay with relatively high content of aluminum and iron oxides. Its major occurring minerals are quartz, kaolinite, gibbsite, hematite, magnetite, and ilmenite (GABAS; SARKIS; BOSCOV, 2014; HEMSI, 2001).

This soil has been classified in previous studies as:

- a) a silt of medium compressibility (ML-MH), according to the USCS (HEMSI, 2001; GABAS; SARKIS; BOSCOV, 2014)
- b) *latossolo roxo* according to the SiBCS, corresponding approximately to oxisol from the Soil Taxonomy of the US Department of Agriculture (SOIL SURVEY STAFF, 1999).
- c) lateritic clay (LG') according to the MCT Classification System (NOGAMI; VILLIBOR, 1995b).

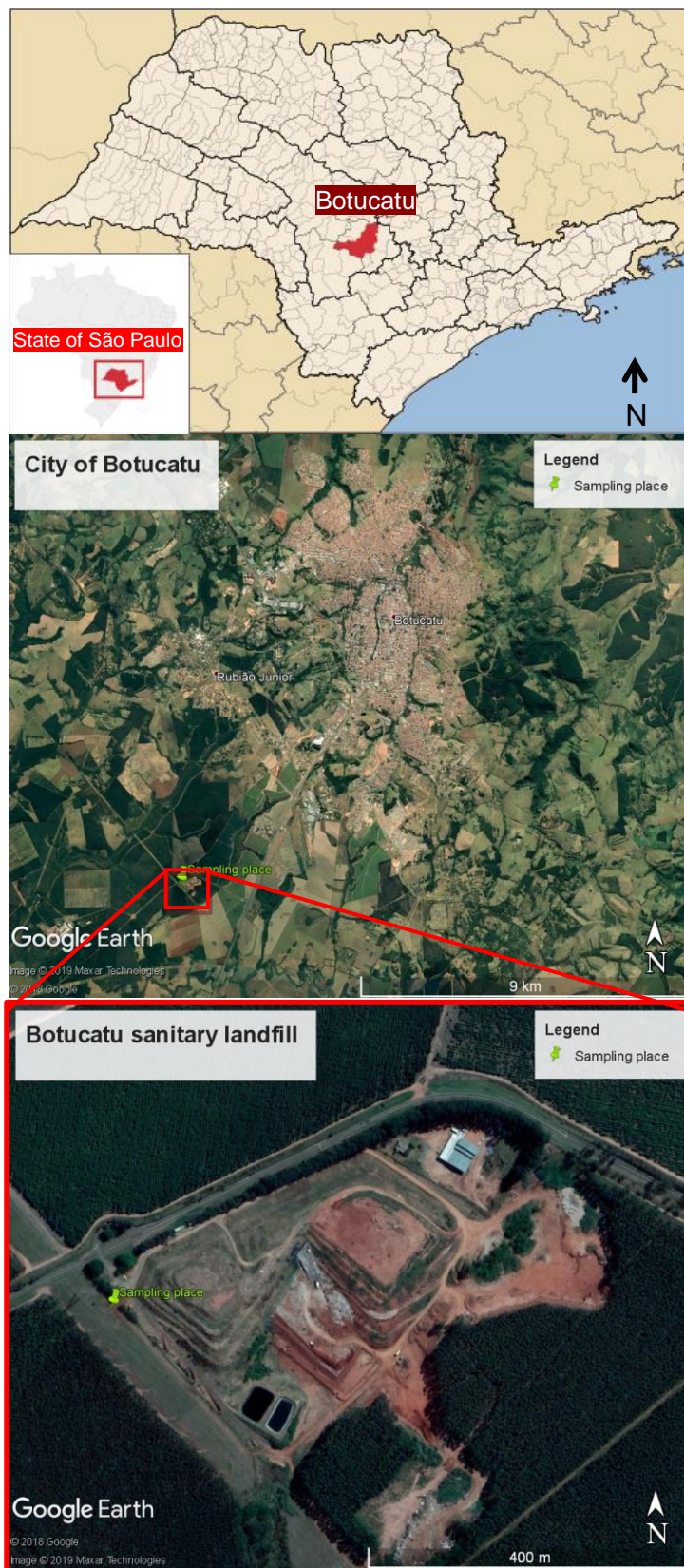
3.1.5 Mixtures soil-WTS

Mixtures were prepared using soils at the hygroscopic water content (air-dried), and WTS at its 'natural' water content (after centrifuge dewatering), since drying usually alters WTS properties (XIA, 1994; BASIM, 1999; MONTALVAN, 2016).

Three blending ratios of soil/WTS by wet mass were selected according to arbitrary workability/compactability of the resulting mixture. Table 7 presents the mixtures used in this study.

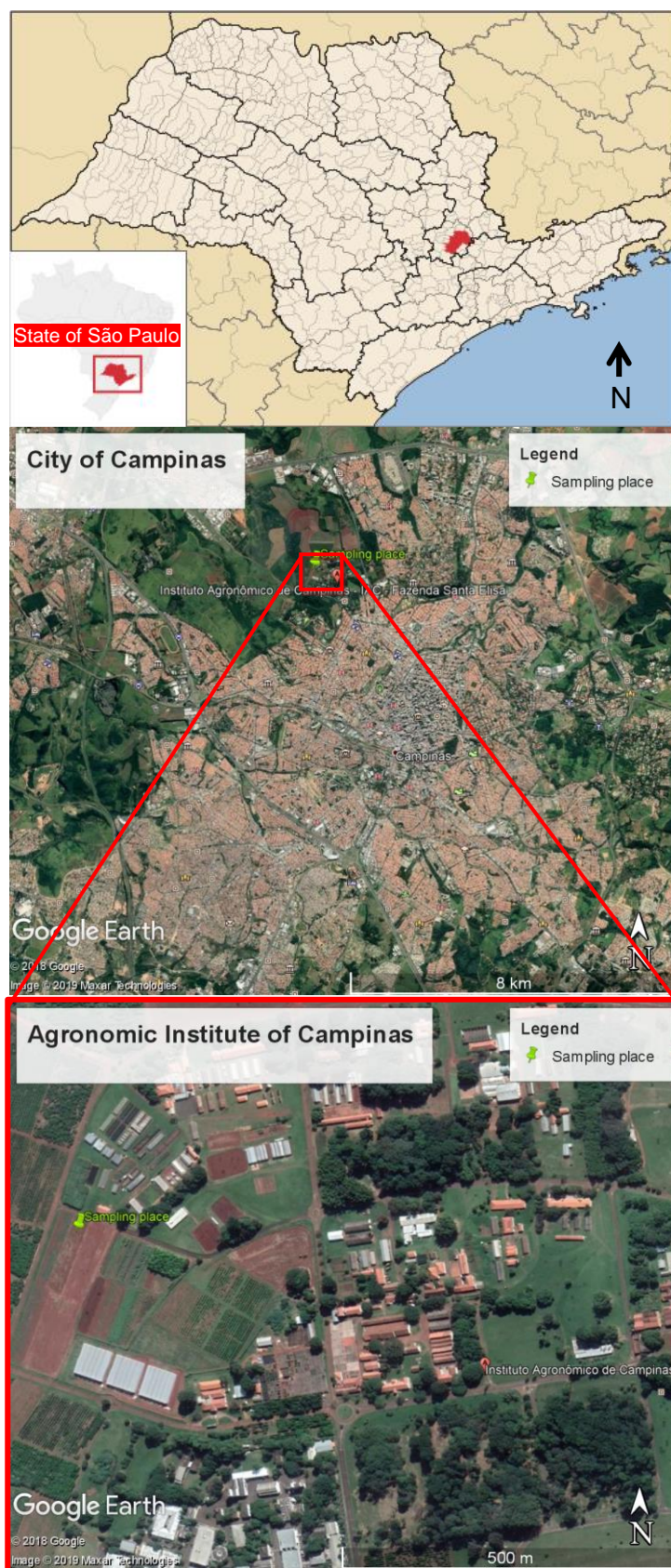
The soil/WTS ratio by wet mass is the relation of soil mass (at hygroscopic or residual moisture) to sludge mass (at natural moisture), very convenient for the preparation of mixtures at the laboratory. On the other hand, WTS content by dry mass represents the percentage of WTS solids in relation to the total solids of the mixture, i.e. soil and WTS solids, more useful for the analysis of test results.

Figure 13 – Sampling site of the clayey sand from Botucatu city.



Source: modified from Wikimedia Commons Contributors (2016) and Google Earth (2019).

Figure 14 – Sampling site of the clay from Campinas city



Source: modified from Wikimedia Commons Contributors (2017) and Google Earth (2019).

Some geotechnical tests with mixtures BC5:1, BC4:1, and BC3:1 (Table 7) were carried out previously by Montalvan (2016). Geotechnical tests with CC mixtures and BT mixtures were carried out in collaboration with, respectively, Ferreira (2020) and Roque (2020).

Table 7 – Investigated soil-WTS mixtures.

Sample	Clayey sand	Clay	Cubatão sludge	Taiapuêba sludge	Soil/WTS ratio by wet mass (kg/kg)	WTS content by dry mass (%)
Clayey sand	✓				-	0.0
Clay		✓			-	0.0
C-WTS			✓		0.0	100.0
T-WTS				✓	0.0	100.0
BC5:1	✓		✓		5.0	4.5
BC4:1	✓		✓		4.0	5.6
BC3:1	✓		✓		3.0	7.5
CC4:1		✓	✓		4.0	7.0
CC3:1		✓	✓		3.0	9.3
CC2:1		✓	✓		2.0	13.9
BT5:1	✓			✓	5.0	3.4
BT4:1	✓			✓	4.0	4.2
BT3:1	✓			✓	3.0	5.7
CT3:1		✓		✓	3.0	5.7
CT2:1		✓		✓	2.0	8.5
CT1.5:1		✓		✓	1.5	11.3

C-WTS = Cubatão WTS; T-WTS = Taiapuêba WTS; B = Botucatu clayey sand; C = Campinas clay. For mixtures, the first letter stands for the soil, the second for WTS, and the numbers, for soil/WTS ratio (for example: BC5:1 = mixture of Botucatu clayey sand with Cubatão WTS at soil/WTS ratio of 5:1 by wet mass)

3.2 TESTING PROGRAM

3.2.1 Sludge sampling

The sludge sampling procedure for both Cubatão and Taiaçupeba WTPs consisted in collecting daily samples of approximately 7 kg, from Monday to Friday, during four weeks (total of twenty samples). This procedure aimed at the preparation of a unique sample, representative of a month of sludge production of each WTP. Such procedure was recommended by Tsugawa et al. (2019) based on the Theory of Sampling.

The sampling procedure was conducted as follows:

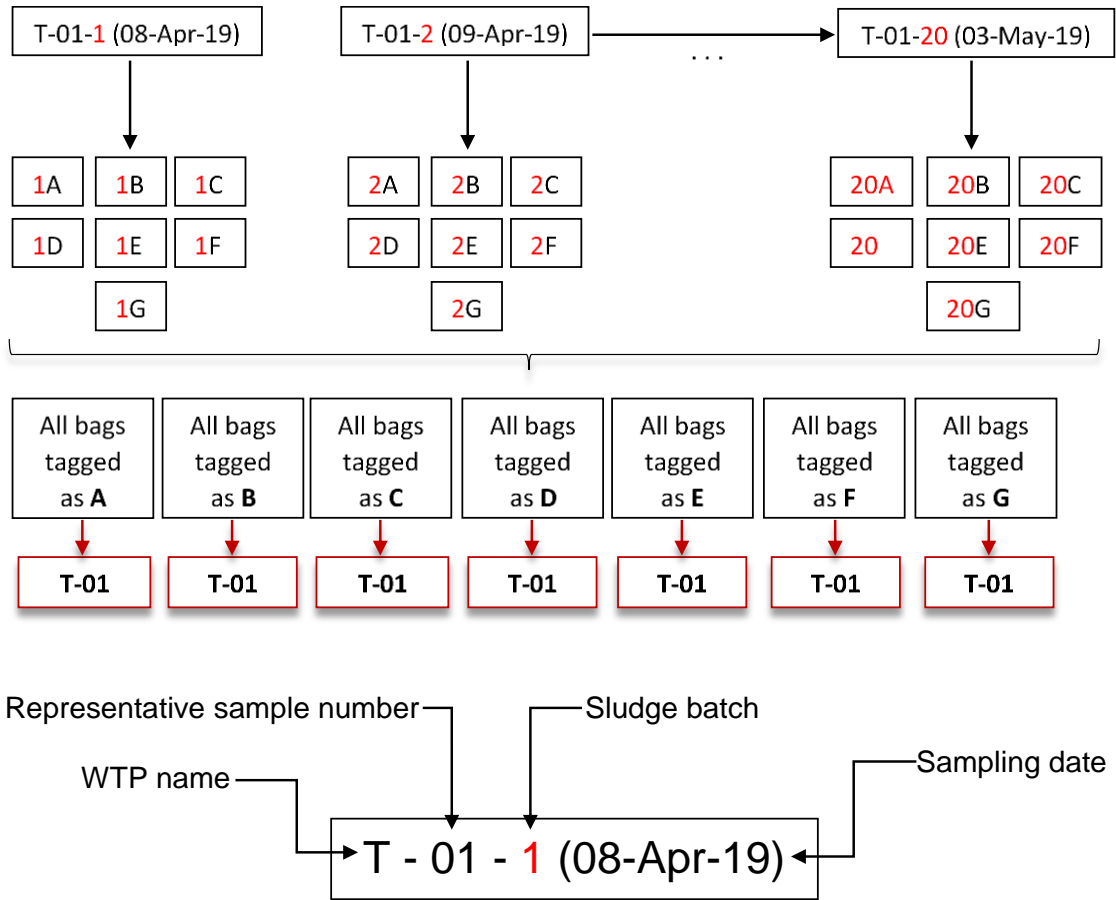
1. Sludge samples of approximately 7 kg were collected after centrifuge dewatering in the WTP, stored in plastic bags, and tagged with date and sample number (numbers from 1 to 20).
2. Transportation of samples, every week, from the WTP to the Laboratory of Soil Mechanics of the Polytechnic School, University of Sao Paulo (LMS-EPUSP).
3. Determination of water content of each sample after homogenization in a mixer. Then, each sample was divided into 7 smaller samples of 1 kg. These smaller samples were tagged with the sample number plus a letter from A to G. For example, 1A, 1B, 1C, and so on.
4. In order to obtain a representative sample, all samples tagged with the same letter were mixed together.

Cubatão sludge samples were collected from January 29 to February 23, 2018, while Taiaçupeba sludge samples, from April 8 to May 3, 2019.

Figure 15 illustrates the sampling method and description of tags used to identify the sample bags of Taiaçupeba sludge. The same method was used to sample Cubatão WTS. Figure 16 shows WTS samples and WTS homogenization by mixer.

Water content of all samples was determined by drying the samples at 105 °C. The WTS samples were also dried at this temperature, according to test method B of ASTM-D2974 standard (ASTM, 2000) and following recommendation of O'Kelly and Sivakumar (2014), although NBR-6457 (ABNT, 1986) recommends organic soils should be dried at 60 °C.

Figure 15 – Sludge sampling methodology and tags meaning.



Source: prepared by the author.

Figure 16 – (a) Taiapuêba WTS samples; (b) Samples mixing.



Source: author.

3.2.2 Mineralogical characterization

Mineralogical characterization analyses were conducted only for Taiapuêba WTS since all other materials have been previously characterized. The analyses were conducted at the Laboratory of Technological Characterization of the Polytechnic School, University of Sao Paulo (LCT-EPUSP).

The mineral composition was determined by X-ray diffraction (XRD) with Phillips diffractometer MPD 1880 and scanning electron microscopy (SEM) with FEI Quanta m600 FEG microscope, equipped with a Bruker X-ray energy dispersion spectrometer (EDS) Quantax 400 (technology SDD – Silicon Drift Detector) and the software Sprit. Tested samples were oven-dried at 35 °C prior testing.

Identification of crystalline phases was conducted by comparing the obtained diffractogram to those of the International Centre of Diffraction Data and the PANalytical Inorganic Crystal Structure Database (PAN-ICSD, 2007).

Microscopic analyses were carried out by collection of backscattered electron images and specific chemical analyses (EDS) for the compositional characterization of particles. The SEM analyses were conducted on oven-dried (35 °C) and pulverized sample, glued to a double-sided carbon tape and coated with platinum (Figure 17). The platinum coating is used because the SEM analyses need to be performed on a conductor material.

Figure 17 – Scanning Electron Microscopy Equipment.



Source: author.

3.2.3 Chemical characterization

Chemical composition analyses of Cubatão WTS and Taiaçupeba WTS were performed at LCT-EPUSP. It consisted of X-ray fluorescence (XRF) by a spectrometer Axios-Advanced PANalytical by standardless analysis from fluor to uranium, and loss on ignition (LOI) at 1020 °C for two hours. The analyses were conducted on samples oven-dried at 35 °C.

Analyses for chemical parameters of the two soils and the two sludges were carried out at the Laboratory of Soil Analysis of the *Luiz de Queiroz* College of Agriculture (LSO-ESALQ-USP), University of São Paulo. The analyses, conducted on air-dried samples, comprised determination of pH in water and KCl, P, K, Ca, Mg, Al, Al+H, exchangeable bases, cation exchange capacity (CEC), saturation by exchangeable bases, saturation by aluminum following EMBRAPA methods (DONAGEMA et al., 2011). Additionally, organic matter and organic carbon analyses were conducted by the Walkley-Black method, recommended by the Agronomic Institute of Campinas (IAC, 2009).

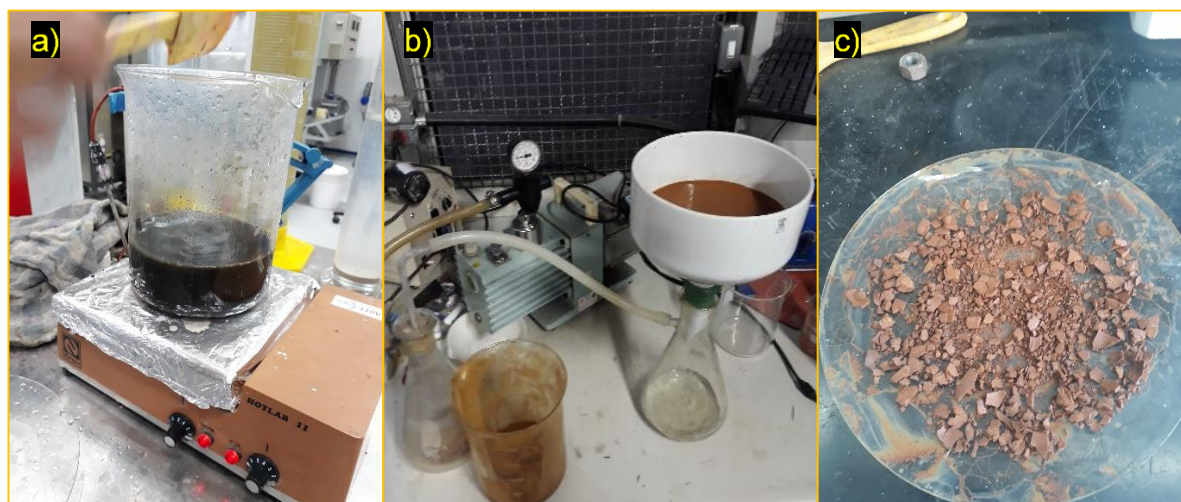
3.2.4 Organic matter removal

Several authors have conducted geotechnical characterization tests on WTS samples without testing difficulties. However, some WTS with high content of organic matter may present unusual behavior that impair the execution of tests following soil standards, e.g. hydrometer tests for particle size analysis (HSIEH; RAGHU, 1997).

According to ASTM-D7928-17 (ASTM, 2017b) and EMBRAPA methods for soil analysis (DONAGEMA et al., 2011), hydrogen peroxide and moderate heat can digest organic matter. Pretreatments to remove organic matter by chemical reagents have been used to analyze soil mineral phase for different purposes (MIKUTTA et al., 2005).

Herein, sludge samples that presented testing difficulties due to the high content of organic matter were treated by hydrogen peroxide H₂O₂ (30% concentration). The treatment process consisted in diluting a sludge sample in distilled water pre-heated at 60 °C, then adding H₂O₂ by small quantities and continuous mixing and heating. The organic matter was considered completely digested when effervescence no longer occurred. The treated sample was then washed, filtrated by a vacuum pump, oven dried, and pulverized. Figure 18 illustrates the treatment process.

Figure 18 – OM removal process: (a) H₂O₂ addition and heating; (b) filtration; (c) oven-drying and pulverization.



Source: author.

3.2.5 Geotechnical characterization

The geotechnical characterization comprises grain-size distribution (GSD), specific gravity of solids (G_s), Atterberg limits (liquid limit and plastic limit), and organic matter content by ignition. All tests were performed according to procedures of the Brazilian Association of Technical Standards (ABNT). Table 8 presents the corresponding standard for each test and its equivalent to the American Society of Technical Standards (ASTM).

Table 8 – Standards for geotechnical characterization tests.

Test	ABNT	ASTM
Particle-size distribution	ABNT-NBR 7181/1988	ASTM D422-07
Liquid limit	ABNT-NBR 6459/1984	ASTM D4318-17e1
Plastic limit	ABNT-NBR 7180/1988	ASTM D4318-17e1
Specific gravity of solids	ABNT-NBR 6508/1984	ASTM D854 - 14
Organic matter content	ABNT-NBR 13600/1996	ASTM D2974 - 14

Source: author

Soil samples were air-dried prior to geotechnical characterization tests. On the other hand, WTS samples were used at their natural water content (as collected from the centrifuge), since several authors have pointed out the influence previous drying

exerts on geotechnical characteristics of WTS (WANG et al., 1992; XIA, 1994; BASIM, 1999; WATANABE et al., 2011; MONTALVAN, 2016).

The grain-size distribution tests were conducted by sieving and sedimentation (hydrometer method). The first is applicable to particle sizes greater than 75 μm , and the second for smaller particles. Soils and mixtures were tested by the standard procedure using sodium hexametaphosphate (SHMP) (NaPO_3)₆ as dispersing agent. Cubatão WTS was also tested without dispersing agent (only distilled water) to evaluate the flocculation effect of the coagulant (ferric chloride). Taiaçupeba WTS, whose high content of organic matter impaired the execution of the hydrometer test, was tested using different dispersing agents and different sample masses described in Table 9. The GSD of Cubatão and Taiaçupeba WTS was also determined by laser analyses using wet and dry (powder) samples.

Table 9 – Concentration of dispersing agents and sample mass used in hydrometer tests for Taiaçupeba WTS.

Dispersing agent	Dispersing agent concentration (g.L^{-1})	Approximate dry mass of tested sample (g)
Sodium hexametaphosphate (SHMP)	45.7	40
SHMP	45.7	10
SHMP	91.4	10
Trisodium phosphate (TSP)	40.0	40
TSP	80.0	40
Tetrasodium pyrophosphate (TSPP)t	40.0	40
TSPP	80.0	40
Sodium tripolyphosphate (STPP)	40.0	40
STPP	80.0	40

Source: author.

Soil samples for the Atterberg limits were prepared by the dry method (drying prior to test), while WTS and mixtures samples were prepared by the wet method. Liquid limit tests were carried out using the Casagrande's apparatus, and plastic limit tests were conducted by the hand method.

In order to determine the organic matter content, 100g-samples of the soils and the sludges were oven dried at 105 °C and their water content was computed. The oven-dried samples were then ignited in a muffle furnace at 440 °C during 24h, following NBR 13600/1996 (ABNT, 1996).

3.2.6 Compaction

Compaction tests under standard Proctor effort followed NBR 7182 (ABNT, 1998), equivalent to ASTM standard D698-12e2 (ASTM, 2012).

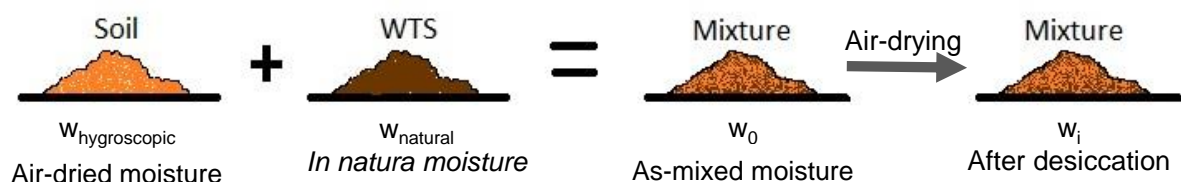
Compaction of soils was conducted using air-dried samples (method A of ASTM D698) and reuse of material. Although disadvised by some standards, material reuse was necessary in this study due to the great number of compaction tests to be conducted. Each test uses approximately 3 kg of material.

Compaction of mixtures was carried out with and without previous drying. Montalvan (2016) showed that previous air-drying alters compaction parameters (maximum dry unit weight and optimum water content) of soil-WTS mixtures and that there is a linear correlation between compaction parameters and desiccation ratio, a parameter defined according to Equation (7). In order to evaluate the effect of previous drying on compaction parameters, compaction tests for each mixture were conducted at three different desiccation ratios.

$$\text{Desiccation ratio (\%)} = \frac{w_0 - w_i}{w_0} \times 100 \quad (7)$$

Where w_0 is the water content before desiccation (as-mixed water content) and w_i is the water content after desiccation, as illustrated in Figure 19. A desiccation ratio of 0% ($w_i = w_0$) means that the mixture did not lose any water prior to compaction, whereas a desiccation ratio of 100% ($w_i = 0\%$) means complete loss of moisture.

Figure 19 – Description of water content of soil-WTS mixtures.



Source: author.

Compaction tests with Cubatão and Taiapuêba WTS were not conducted. Compaction behavior of Cubatão WTS and Taiapuêba WTS, however, had already been studied by Silva and Hemsí (2018) and Fortes et al. (2009), respectively.

3.2.7 Specimens preparation for consolidation, permeability and shear strength

Soils and mixtures specimens were compacted at optimum compaction parameters at standard effort. However, some mixtures were compacted at as-mixed moisture, as they already were slightly wet-of-optimum and air-drying was avoided unless strictly specified (see 3.2.6). After compaction, the specimens were extruded from the compaction mold, wrapped tightly with PVC film (plastic wrap), then wrapped with aluminum foil, and then stored in a polystyrene box (foam box). The box containing the specimen was stored in a temperature-controlled room (20 ± 2 °C) for 24 hours. Specimen compaction quality was controlled using maximum water content deviation of $\pm 1\%$ (percentage point) and minimum relative compaction (RC) of 95%.

3.2.8 Compressibility

Oedometric compression tests were carried out on specimens carved from compacted samples of the soils and the mixtures prepared as described in 3.2.7. The compression tests were performed according to NBR 12007 (ABNT, 1990), equivalent to ASTM D2435 (ASTM, 2011a).

The test conditions were: specimen inside a stainless steel ring of 71.3 mm diameter and 20.0 mm height, inundation with distilled water at initial loading, incremental loading (load increment ratio of 1), and loading interval of 24 h (Method A of ASTM-D2453). The applied vertical stresses were: 10, 20, 40, 80, 160, 320, 640, 1280, and 2560 kPa. Unloading path was also recorded.

3.2.9 Permeability

The hydraulic conductivity (k) of compacted soils and mixtures was determined by constant head permeability tests in flexible-wall permeameter. Since there is no Brazilian standard for this test, the procedures followed ASTM D5084 (ASTM, 2016). Tests were conducted with specimens of 70 mm height (L) and 70 mm diameter (D). Saturation of specimens was achieved by backpressure, ranging from 500 to 700 kPa, considering adequate saturation at B-value (equation (8)) equal or greater than 0.96.

$$B = \frac{\Delta u}{\Delta \sigma_3} \quad (8)$$

Where, Δu is the measured increment in pore water pressure caused by an increment $\Delta\sigma_3$ in confining pressure.

Three confining pressures were used (50, 100 and 200kPa) in order to evaluate permeability variation with voids ratio. However, as tests duration was too long (20 to 30 days), some samples were only tested under confining pressure of 50 kPa. Constant head permeation of tap water was allowed until steady flow rate was reached.

The maximum hydraulic gradient recommended by ASTM D5084 (ASTM, 2016) is presented in Table 10. Compacted clay liners in sanitary landfills are subjected to a maximum hydraulic gradient ranging from 5 to 10 according to (Sarsby, 2000), and about 2 according to Edelman, Hertweck, and Amann (1999). Bagchi (2004) recommends laboratory permeability tests of compacted liners to be performed under the following conditions: 90 to 100% saturation, low confining pressure, and low hydraulic gradient (maximum 10) to simulate field conditions.

Permeability tests were initially carried out using hydraulic gradient equal to 10. However, a hydraulic gradient of 20, which still complies with ASTM D5084, was used for samples with very low permeability in order to decrease test duration.

Table 10 – Maximum hydraulic gradients recommended by ASTM D5084/16.

Hydraulic conductivity (m/s)	Recommended maximum hydraulic gradient
1×10^{-5} to 1×10^{-6}	2
1×10^{-6} to 1×10^{-7}	5
1×10^{-7} to 1×10^{-8}	10
1×10^{-8} to 1×10^{-9}	20
Less than 1×10^{-9}	30

Source: ASTM (2016, p.11)

3.2.10 Shear strength

Isotropically consolidated undrained (CIU) triaxial compression tests with measurement of pore pressure were carried out on three specimens, 38 mm diameter and 76 mm height (L/D ratio = 2), with effective confining pressures of 50, 100, and 200 kPa. Since there is no Brazilian standard for triaxial tests, they were performed according to ASTM standard D4767 (ASTM, 2011b).

Specimen saturation (B-value higher than 0.96) was achieved by backpressure ranging from 500 to 700 kPa. Specimens were consolidated by applying a difference between confining pressure and backpressure equal to the specified effective consolidation pressure. Measurements of volume change were recorded until full dissipation of pore pressure (end of primary consolidation).

After consolidation, the shearing stage was conducted applying a strain rate of 1%/h for clayey samples and 3%/h for sandy samples.

Proper failure criterion for strain-hardening soils, such as cohesive compacted soils, can be difficult to select or define, particularly for undrained strength (Seed et al., 1960). Although the maximum deviator stress is often used to define failure for undrained triaxial tests, the deviator stress increases steadily up to high strains for strain-hardening soils, therefore its maximum value depends mainly on test length. The undrained strength in this study was defined as the maximum deviator stress that occurred up to axial strain of 17%.

Two-parameter power function curves (equation 6) were fitted to values of undrained shear strength for all tested soils and mixtures.

The effective strength parameters, cohesion intercept (c') and friction angle (φ'), were determined from the effective stress paths using the maximum effective stress ratio $(\sigma'_1/\sigma'_3)_{\max}$ as failure criterion. Seed; Mitchell; Chan, (1960) suggested the maximum effective principal stress ratio is possibly the most adequate failure criterion to define the shear strength envelope in terms of effective stresses. Although the maximum principal stress ratio and the maximum deviator stress in CU triaxial tests usually do not occur at the same axial strain, they generally yield similar values of effective friction angle and cohesion intercept (Lade, 2016).

The effective cohesion intercept (c') and the effective friction angle (φ') were calculated from the effective stress paths using the following equations:

$$c' = \frac{d}{\cos(\varphi')} \quad (9)$$

$$\varphi' = \sin^{-1}[\tan(\beta)] \quad (10)$$

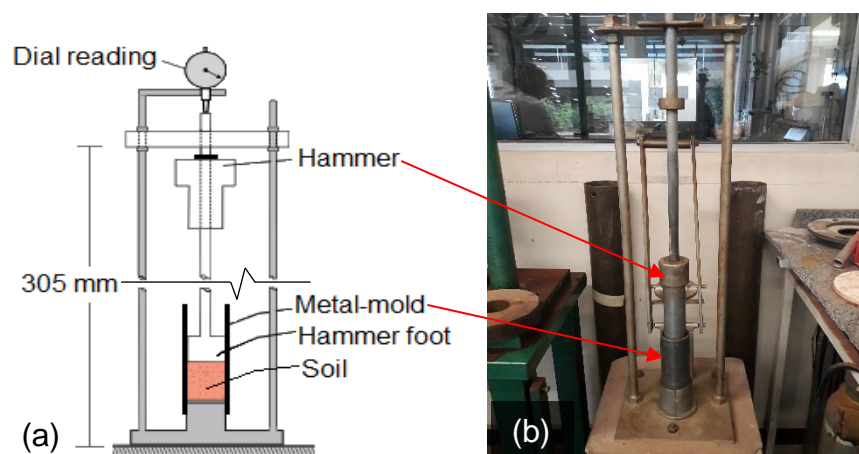
Where, d is the intercept of the failure envelope plotted on the stress path diagram (p' - q), and β is the slope angle of the failure envelope.

3.2.11 Specimens preparation for unconfined compression, suction, and porosimetry tests

Soils and mixtures samples for mercury intrusion porosimetry (MIP) tests and suction tests were compacted at optimum water content ($W_{opt} - 1\% < W < W_{opt} + 1\%$) and maximum dry density ($RC > 95\%$).

Samples were compacted dynamically in a cylindrical metal mold of 50 mm diameter and 50 mm height using a miniature compaction equipment (Figure 20). Chu and Davidson (1960) first proposed this equipment as an equivalent substitute for Proctor's when a great number of specimens are needed (for instance, to determine the minimum necessary additive content to stabilize soils by unconfined compression tests), thus saving time and material due to the smaller dimensions of the specimens. The compactive effort of five blows per side of the specimen has been found to be equivalent to the standard effort of Proctor compaction (CHU; DAVIDSON, 1960; NOGAMI; VILLIBOR, 1985). Miniature compaction is applicable only to soils with grain-size smaller than 2 mm. This equipment have been extensively used in Brazil for MCT soil classification system for road construction (NOGAMI; VILLIBOR, 1991, 1995b).

Figure 20 – Miniature compaction equipment.



Source: (a) Modified from Villibor and Nogami (2009, p.43); (b) author.

Samples for MIP tests were previously air-dried, although some researchers suggest freeze-drying to reduce shrinkage strains caused by the drying process. However, since compacted lateritic soils at optimum water content generally undergo

low shrinkage (Bernucci, 1987), air-drying was considered acceptable. These samples were carved to fit the sample cup, approximately 15 mm diameter and 20 mm height.

Samples for suction tests were trimmed using a PVC ring with 37.5 mm diameter and 20 mm height.

3.2.12 Unconfined compression

Unconfined compression tests were carried out following NBR 12770 (ABNT, 1992) at strain rate of 1.0 %/min. Three equally compacted specimens were tested for each soil and mixture. Since L/D ratio of the specimens was equal to 1, and the NBR 12770 recommends ratio equal to or higher than 2, a correction factor of 0.69 was applied to the maximum axial stress, based on the correction equation suggested by Güneşli and Rüşen (2016):

$$UCS_{(L/D=2)} = \frac{UCS_{(L/D)}}{\left[1.83 - 0.39 \left(\frac{L}{D}\right)\right]} \quad (11)$$

Where, $UCS_{(L/D=2)}$ is the standard unconfined compression strength; $UCS_{(L/D)}$ is the measured UCS for tested samples with L/D ratio.

3.2.13 Volumetric shrinkage

Compacted specimens of 50 mm height and 50 mm diameter were air dried and their dimensions and weight were measured over time to compute void ratio and water content. These parameters were used to construct the shrinkage curve of the samples.

The total volumetric shrinkage at the end of desiccation was computed for each sample, defined as:

$$Volumetric\ shrinkage = \frac{(\Delta V)_{max}}{V_0} \quad (12)$$

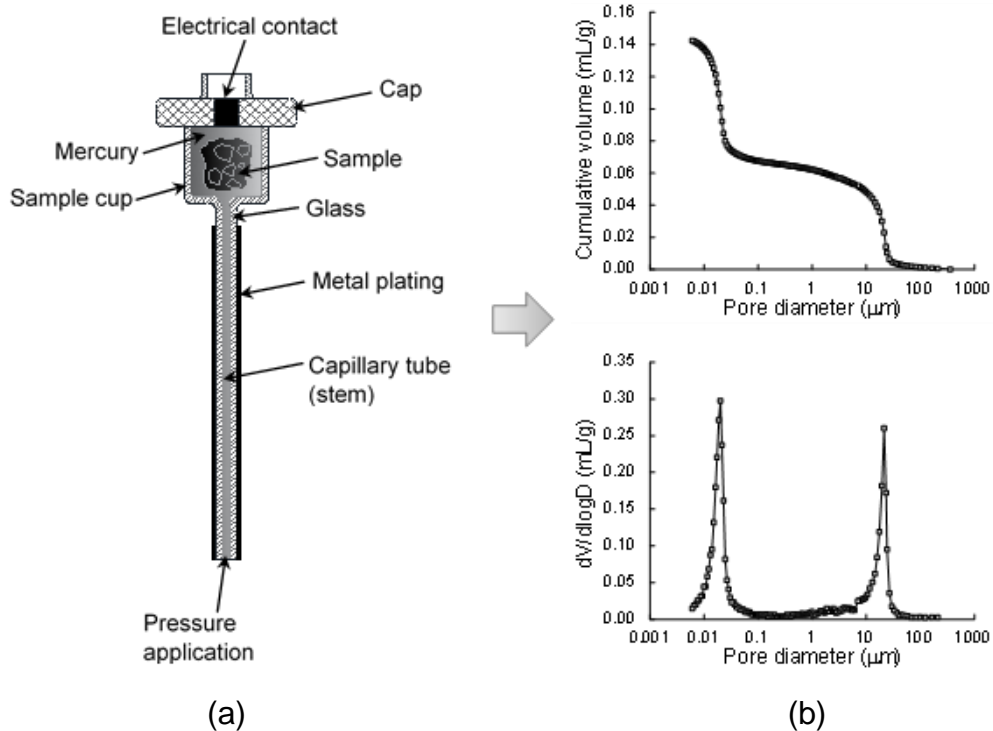
Where ΔV_{max} is the maximum volume change; V_0 is the initial volume of the specimen.

3.2.14 Mercury intrusion porosimetry (MIP)

The MIP tests were conducted at the Laboratory of the Research Foundation for Physics and Chemistry of the University of São Paulo (FAFQ-USP), Campus São Carlos, employing a Micromeritics Porosizer 9320 equipment with capability to measure pore diameters varying approximately from 0.006 μm to 70 μm .

Mercury does not wet most substances (non-wetting property) and has a high surface tension, thus an external pressure is necessary for mercury to intrude pores. MIP equipment comprises a penetrometer and a pump for pressure supply. The penetrometer consists of a sample cup bonded to a metal-clad, a precision-bore, and a glass capillary stem, as illustrated in Figure 21a.

Figure 21 – MIP test: (a) Cross-sectional view of Micromeritics penetrometer and (b) Typical PSD curves.



Source: modified from Micromeritics Instrument Corporation (2019).

The following samples characteristics can be determined from MIP results: dry unit weight (bulk density), specific gravity of solids (skeletal density), and effective porosity (n_e). First, penetrometer weight (W_p) and sample weight (W_s) are measured. The soil specimen is placed into the sample cup, vacuum is applied, and the cup and penetrometer are filled with mercury. The weight of the set (penetrometer plus sample

and mercury) is determined and used to calculate the volume of the sample, which allows the computation of bulk density. At the end of the MIP test, mercury intrusion measurements allow to determine the total intruded volume or effective voids volume, and the effective porosity of the sample. The skeletal density (solids density) can only be computed after calculating the real volume of solids. As the tested samples were air-dried prior testing, they contained a residual water content. The porosity must be corrected to determine the volume of solids (discounting the volume of residual water).

MIP results are generally presented in two types of graph: cumulative volume (V) versus pore diameter (D), and differential-log volume ($dV/d\log D$) versus pore diameter (D), as illustrated in Figure 21b. The latter type of graph, known as derivative curve (Bruand and Prost, 1987), is useful for determining high frequency macropores and micropores.

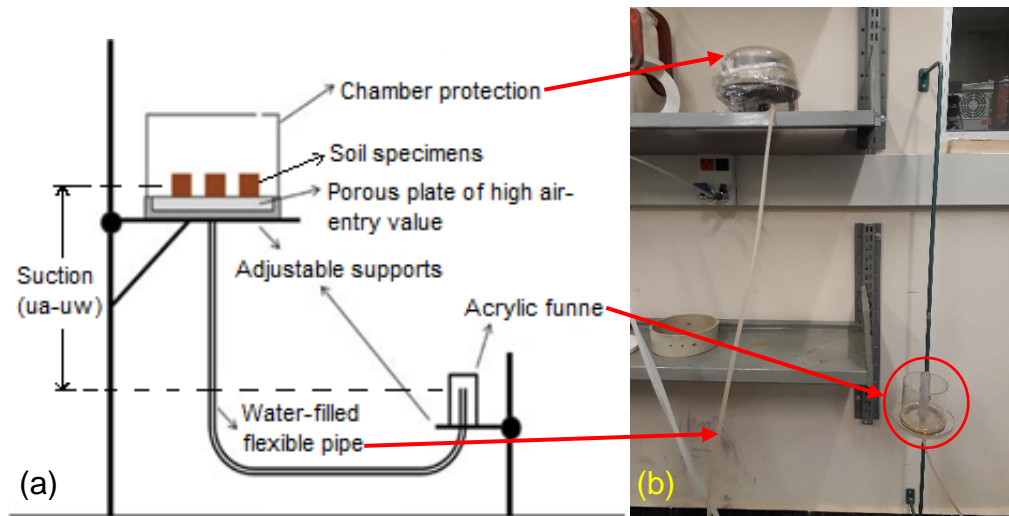
3.2.15 Soil-water retention curves from suction tests

Suction tests were carried out using a combination of three methods, namely, suction plate, pressure chamber (axis translation technique), and contact filter paper. The first two methods allow to measure and control suction, the filter paper method only permits to measure suction values up to 30 000 kPa.

Soil-water retention curves (SWRC) were determined by the drying path. The first stage was saturation of the specimens, achieved by applying a very small water head (no greater than 0.5 cm) during at least a week.

Suction tests initiated in the suction plate (Figure 22), which allowed the application of increasing suction values from 0 to 30 kPa. The applied suction values were 0.1, 0.2, 0.4, 0.7, 1, 2, 4, 7, 10, 20, and 30 kPa. Each suction value was maintained until water drainage ceased (2 to 3 days), i.e. suction equilibrium was reached. Then the specimen was weighed for water content computation and its dimensions were measured for volume change calculation. Following, a suction increment was applied, and the procedure was repeated.

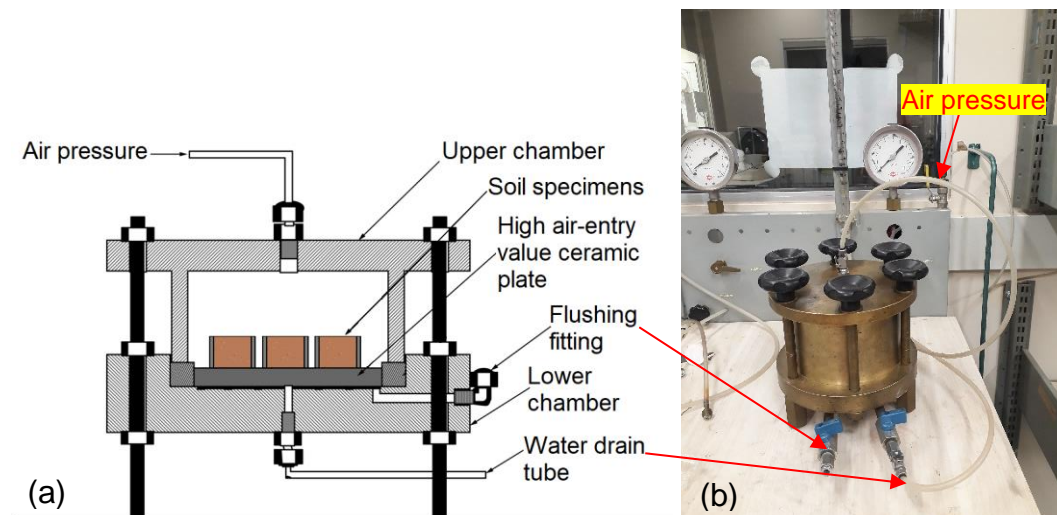
Figure 22 – Suction plate: (a) Schematic view; (b) laboratory test.



Source: (a) modified from Marinho et al. (2015, p.237); (b) author.

The axis translation technique was used to apply suction values from 30 to 500 kPa. Figure 23b shows the pressure chamber used in the tests. The applied air pressure corresponds to the suction value; therefore, the applied suction is easily controlled. For most samples, six suction values were applied: 50, 70, 100, 200, 300, and 500 kPa.

Figure 23 – Pressure chamber: (a) schematic view; (b) used in this study.



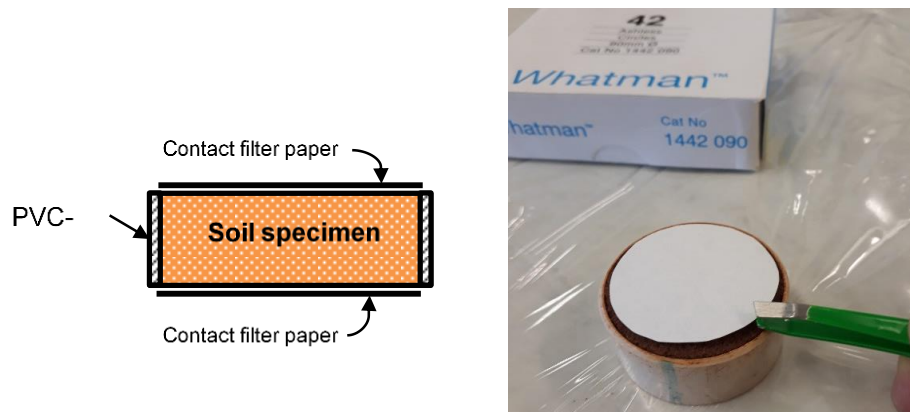
Source: (a) modified from ASTM (2016b, p.6); (b) author.

The contact filter paper method was employed for soil matric suction values greater than 500 kPa. Quantitative filter paper Whatman No.42 was used, always

handled utilizing tweezers as shown in Figure 24. The procedure consists in placing two filter papers in contact with the soil, one on each side of the specimen. Once the filter papers are placed, the specimen is wrapped tightly with a PVC film (plastic wrap), then wrapped with aluminum foil, and finally put in a polystyrene box (foam box). The box containing the specimens is stored in a temperature-controlled room (20 ± 2 °C) for a minimum of seven days in order to allow suction equilibration.

When suction equilibrium is achieved, the filter papers are removed from the specimens and quickly placed in a plastic bag. The mass of the plastic bags (tare) and wet filter papers are determined in a scale of 0.0001 g readability. Filter papers are then oven dried at 105 °C, for a minimum period of four hours, and their dried mass is measured. Finally, the water content of the filter papers is calculated and used for suction determination using calibration equations.

Figure 24 – Filter paper method.



Source: prepared by the author.

Soil matric suction values were calculated using the calibration equations proposed by Chandler et al. (1992), defined as follows:

$$w_{\text{paper}} \leq 47\% \Rightarrow \text{suction (kPa)} = 10^{4.84 - 0.0622w(\%)} \quad (13)$$

$$w_{\text{paper}} > 47\% \Rightarrow \text{suction (kPa)} = 10^{6.05 - 2.48 \log w(\%)} \quad (14)$$

Where, w is the water content of the filter paper in percentage (%).

3.2.16 Soil-water retention curves from MIP

Prapaharan et al. (1985) suggested a method to determine the soil-water retention curve (SWRC) of compacted soil using pore size distribution (PSD) obtained by MIP. The method consists in using Washburn's (1921) capillary equation to determine the soil matric suction:

$$P = \frac{-2 \cdot T \cdot \cos\theta}{r} \quad (15)$$

Where, P is the pressure required to force mercury into a capillary pore of radius r; T is the surface tension of mercury (4.84×10^{-4} N/mm at 25°C), and θ the angle of contact between mercury and soil particles, ranging from 139 to 147° (Diamond, 1970). An important assumption is that mercury intrusion is equivalent to water desorption (drying path), thus PSD from MIP can be used for estimation of SWRC using equation (13) for matric suction computation:

$$\frac{-4T_{hg} \cos(\theta_{m-soil})}{P} = \frac{-4T_w \cos(\theta_{w-soil})}{(u_a - u_w)} \quad (16)$$

Where T_w is the surface tension of water, and θ_w the angle of contact between water and soil particles. Since all the parameters are known in this equation, matric suction ($u_a - u_w$) can be easily calculated. The following relation between matric suction and mercury intrusion pressure was obtained:

$$(u_a - u_w) = 0.196 \cdot P \quad (17)$$

The effective saturation is calculated using the maximum cumulative mercury volume (n_e) and the cumulative volume at each pressure increment (n_i).

$$S_e(\%) = \frac{n_e - n_i}{n_e} \cdot 100 \quad (18)$$

Mascarenha et al. (2008) indicated that water content for air-dried samples should be corrected due to hygroscopic moisture. On the other hand, MIP equipment has a maximum pressure limit, therefore there is a minimum pore diameter that can be intruded. Sun et al. (2016) suggested that estimated water content from MIP should be corrected due to non-intruded pores. If the volume of non-intruded pores is greater

than the volume of residual water, only correction for non-intruded pores is necessary (SIMMS; YANFUL, 2002).

The exact volume of non-intruded pores filled by residual water is difficult to know, since there may also be non-connected pores (dead-ended). By assuming that the volume occupied by residual water is the only non-intruded volume, the residual saturation can be determined and used to calculate real saturation (S). The relation between effective saturation (S_e) and real or total saturation is defined using residual saturation (S_r) as follows:

$$S_e (\%) = \left[\frac{S - S_r}{1 - S_r} \right] \cdot 100 \quad (19)$$

Then,

$$S (\%) = [S_e \cdot (1 - S_r) + S_r] \cdot 100 \quad (20)$$

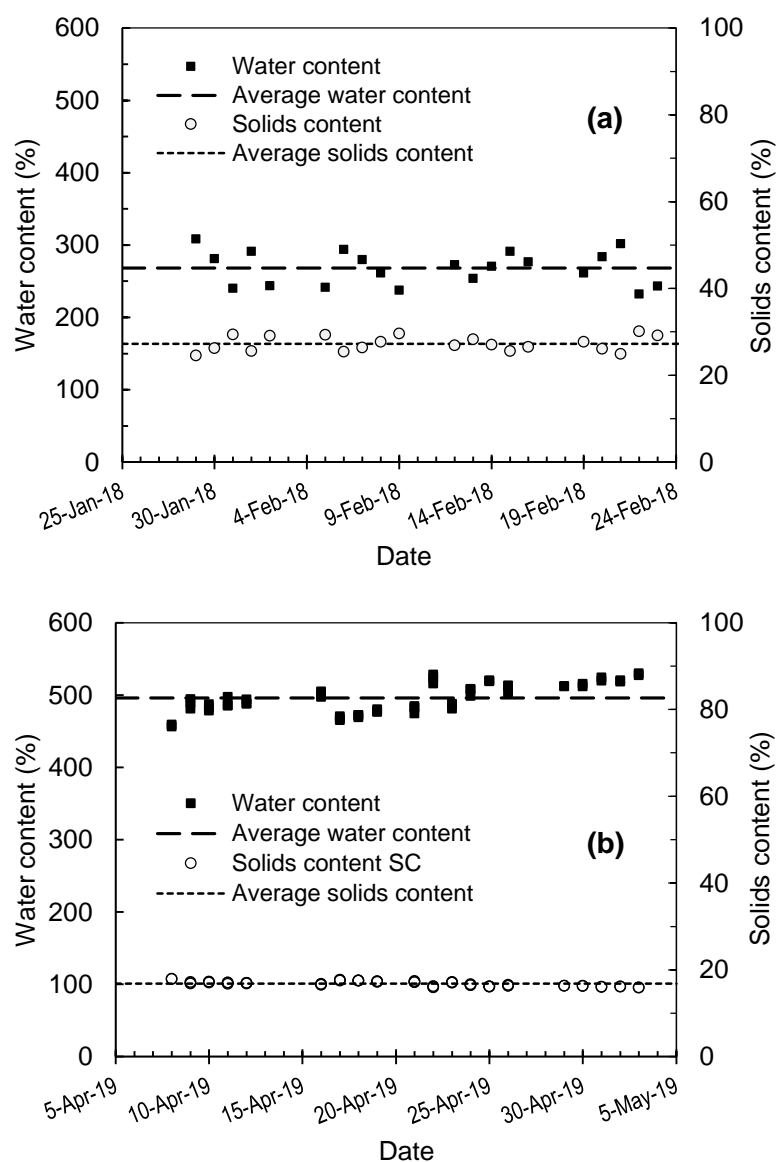
4 RESULTS AND DISCUSSIONS

Tests results are presented in the same order as in 3.2 (Testing program).

4.1 SLUDGE SAMPLING

The variation of water content of WTS Cubatão and WTS Taiacupeba along one month is presented in Figure 25.

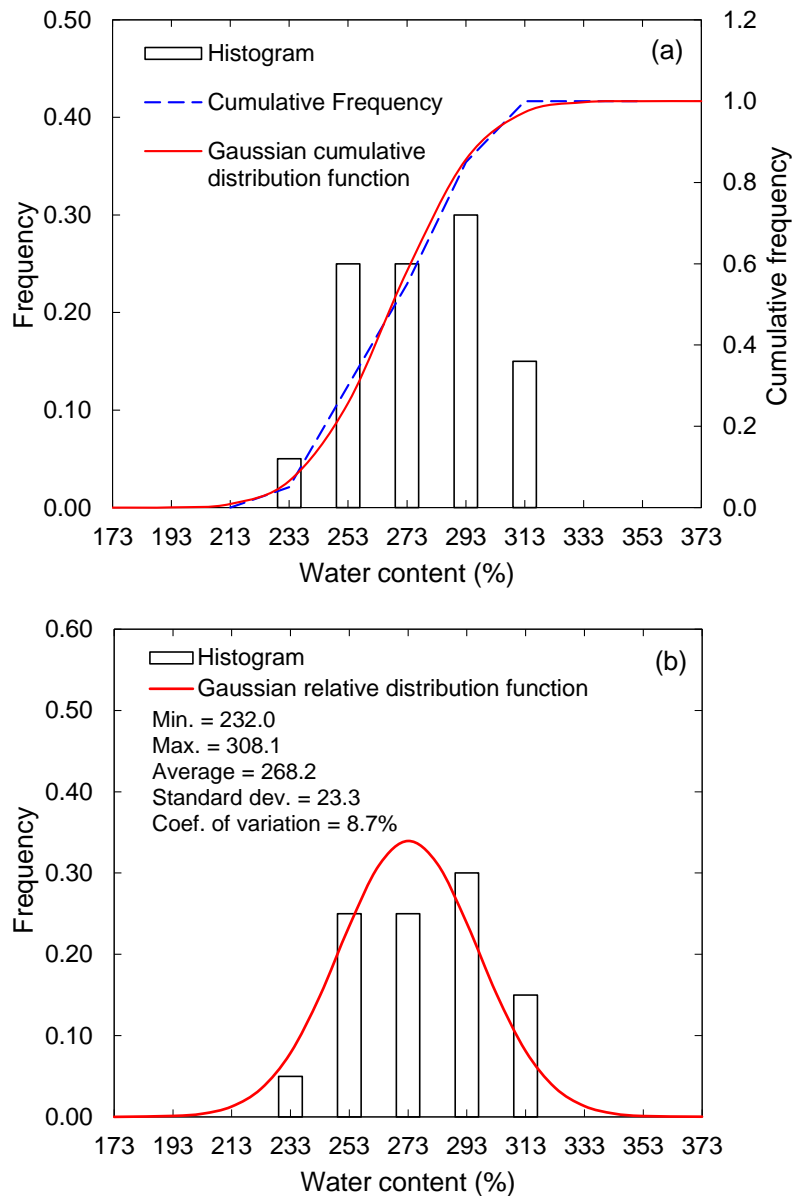
Figure 25 - Water and solids content variation: (a) Cubatão-WTS; (b) Taiacupeba-WTS.



Source: author.

The average water content and solids content of Cubatão samples were equal to 268.2 and 27.3 %, respectively. Figure 26 presents the descriptive statistics of the water content of Cubatão WTS samples. The minimum and maximum values, standard deviation and coefficient of variation are 232.0, 308.1, 23.3, and 8.7 %, respectively.

Figure 26 – Descriptive statistics of water content of Cubatão WTS samples.

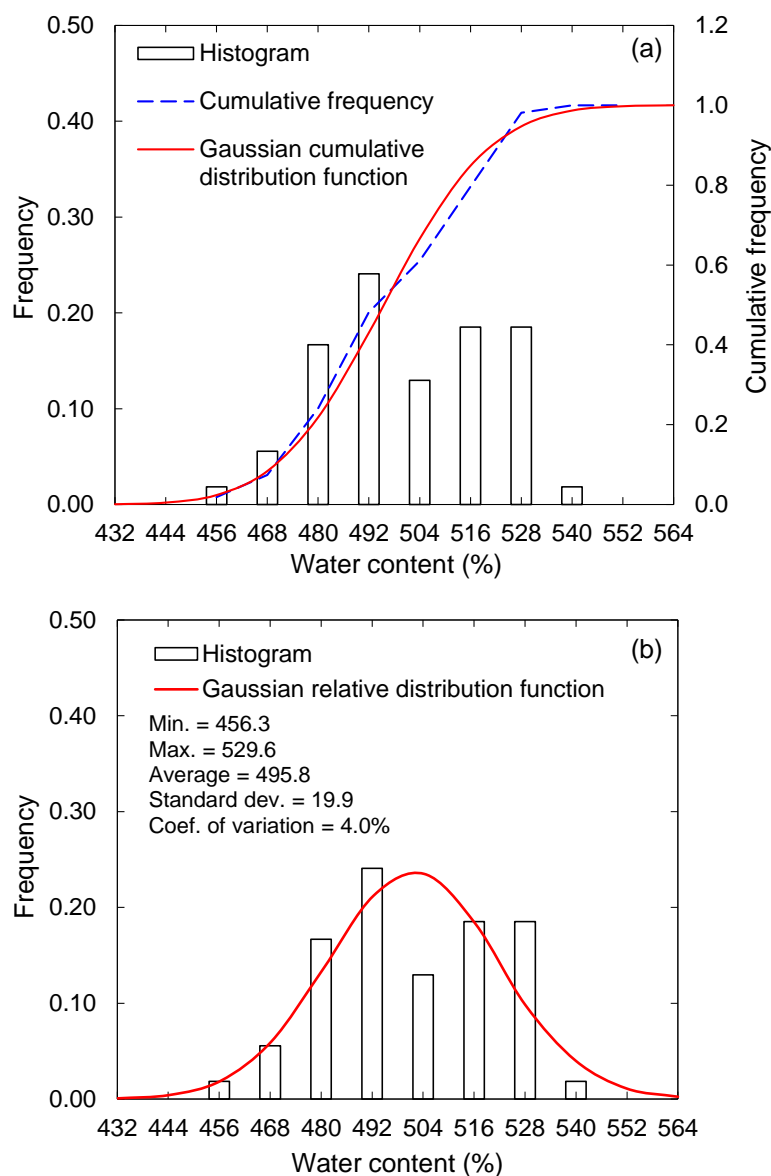


Source: author.

Samples of Taiapuêba WTS presented average water content equal to 495.8% and average solids content of 16.8%. Figure 27 contains the descriptive statistics of the water content of Taiapuêba WTS samples. The maximum and minimum values,

standard deviation and coefficient of variation are 456.3, 529.6, 19.9, and 4.0%, respectively.

Figure 27 – Descriptive statistics of water content of Taiiaçupeba samples.



Source: author.

Both Cubatão and Taiiaçupeba WTPs use centrifuge for sludge dewatering, however, the average water content of Taiiaçupeba samples (495.8%) was almost twice that of Cubatão samples (268.2%). This is associated to physicochemical characteristics of raw water and to coagulants. Taiiaçupeba WTP collects raw water from a reservoir and uses aluminum sulfate and a polymer as coagulants, whereas Cubatão WTP collects water from a river and uses ferric chloride. WTS generated from

treatment of raw water from reservoirs usually contains high content of organic matter (HSIEH; RAGHU, 1997) and is therefore more difficult to dewater. On the other hand, the coefficient of variation of Taiacupeba samples (4.0%) was half that of Cubatão samples (8.7%).

4.2 MINERALOGICAL CHARACTERIZATION

4.2.1 X-ray diffraction

Table 11 presents the mineralogical composition of Botucatu clayey sand, Campinas clay, and Cubatão and Taiacupeba WTS, obtained by XRD analyses.

Table 11 – Mineralogical composition of studied soils and WTS.

Clayey sand ¹	Clay ²	Cubatão WTS ³	Taiacupeba WTS ⁴	Taiacupeba WTS ** ⁴
Quartz SiO ₂	Quartz SiO ₂	Quartz SiO ₂	Amorphous phase	Amorphous phase
Kaolinite Al ₂ Si ₂ O ₅ (OH) ₄	Kaolinite Al ₂ Si ₂ O ₅ (OH) ₄	Goethite FeO(OH)	Quartz* SiO ₂	Gibbsite * Al(OH) ₃
Gibbsite Al(OH) ₃	Gibbsite Al(OH) ₃	Muscovite KAl ₂ (AlSi ₃ O ₁₀)(OH) ₂	Gibbsite* (Al(OH) ₃)	Kaolinite * Al ₂ Si ₂ O ₅ (OH) ₄
Hematite Fe ₂ O ₃	Hematite Fe ₂ O ₃	Kaolinite Al ₂ Si ₂ O ₅ (OH) ₄	Kaolinite* Al ₂ Si ₂ O ₅ (OH) ₄	
Anatase TiO ₂	Magnetite Fe ₃ O ₄			
	Ilmenite FeTiO ₃			

*Possible occurrence; **organic matter removed by H₂O₂.

Source: ¹Zanón (2014); ²Gabas et al. (2014) ; ³Montalvan (2016); ⁴The author.

Quartz, kaolinite, gibbsite, and hematite occur in both soils. Quartz is predominantly present in sand and silt fractions of most soils. Kaolinite is the most common clay mineral found in the clay fraction of Brazilian lateritic soils (NOGAMI; VILLIBOR, 1995b). The crystalline aluminum and iron (hydr)oxides such as gibbsite, hematite, and goethite are also of common occurrence in the fine fraction of lateritic soils.

According to Montalvan (2016), Cubatão WTS presents mineralogical composition typical of residual soils from the *Serra do Mar* region (FURIAN et al., 2002), where the Cubatão River's basin is located.

Taiapuêba WTS showed predominance of amorphous phase and only likely presence of crystalline phases (quartz, gibbsite, and kaolinite). Figure 28 shows the diffractogram of Taiapuêba WTS, in which no well-defined diffraction peaks can be observed. Amorphous solid materials such as organic matter, glasses and several polymers do not generate sharp diffraction peaks and produce significant scattered intensities in the wide-angle range (CULLITY; STOCK, 2014). This behavior was observed in the diffractogram of Taiapuêba WTS.

There are three main likely sources of amorphous material in Taiapuêba WTS: organic matter, expected because raw water comes from a reservoir, amorphous aluminum or iron (hydr)oxides from the coagulant, and the polymer of high molecular weight that Taiapuêba WTP uses for sludge coagulation and dewatering improvement.

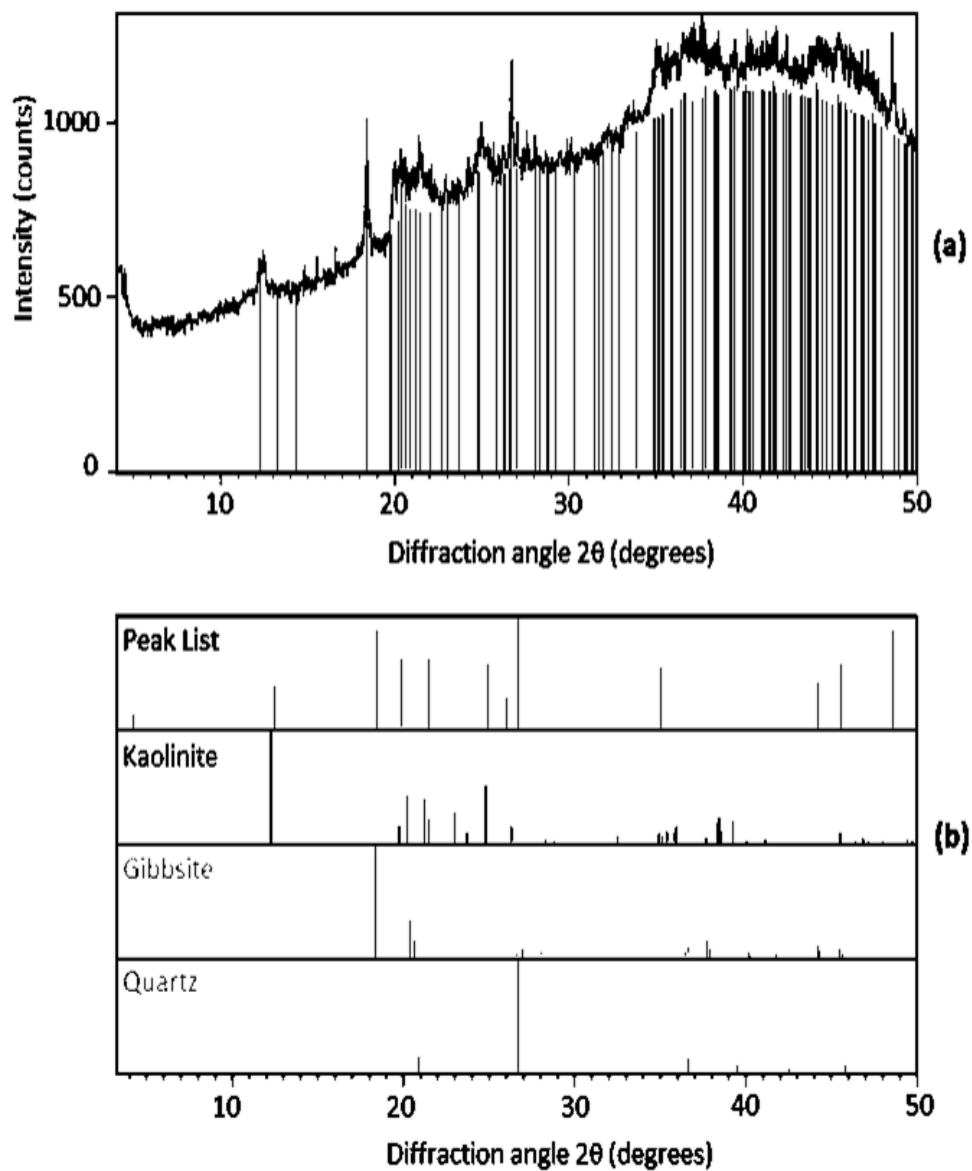
In order to better identify the crystalline phases of Taiapuêba WTS, a sample was treated by hydrogen peroxide to remove organic matter, as described in 3.2.4, and then subjected to XRD analysis.

Figure 29 displays the diffractogram obtained for this sample, which also indicates major occurrence of amorphous material and only possible presence of kaolinite and gibbsite.

The hydrogen peroxide treatment of Taiapuêba WTS does not seem to have been successful in removing organic matter and polymer. It is possible that part of organic material was removed, but amorphous substances remained covering mineral particles, therefore impairing the identification of crystalline phases.

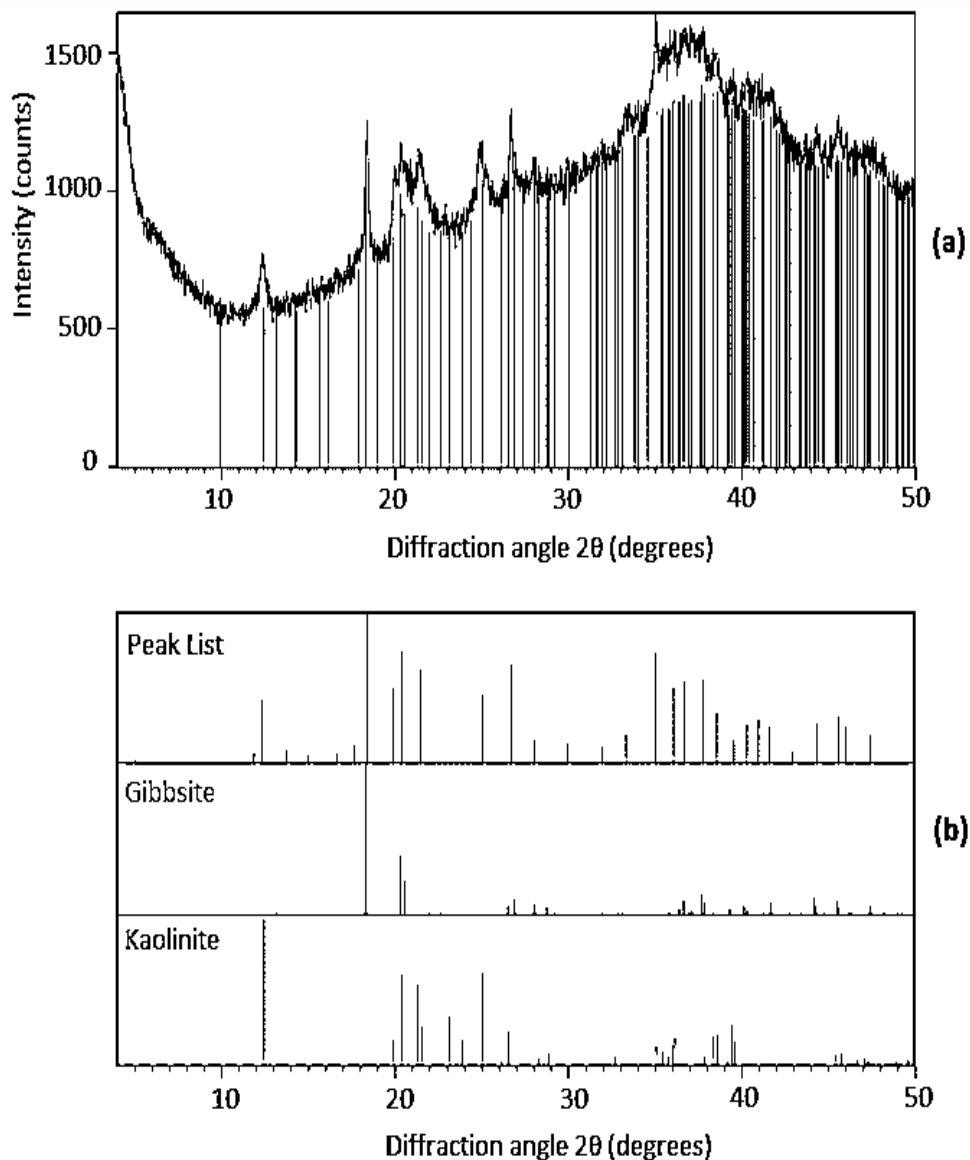
Results from Scanning Electron Microscopy (SEM) and x-ray fluorescence (XRF) help to understand the mineralogical and chemical composition of this material.

Figure 28 – X-ray diffraction analysis of Taiapuêba WTS powder: (a) Diffractogram; (b) identified phases.



Source: author.

Figure 29 - X-ray diffraction analysis of Taiapuêba WTS treated with hydrogen peroxide: (a) Diffractogram; (b) identified phases.

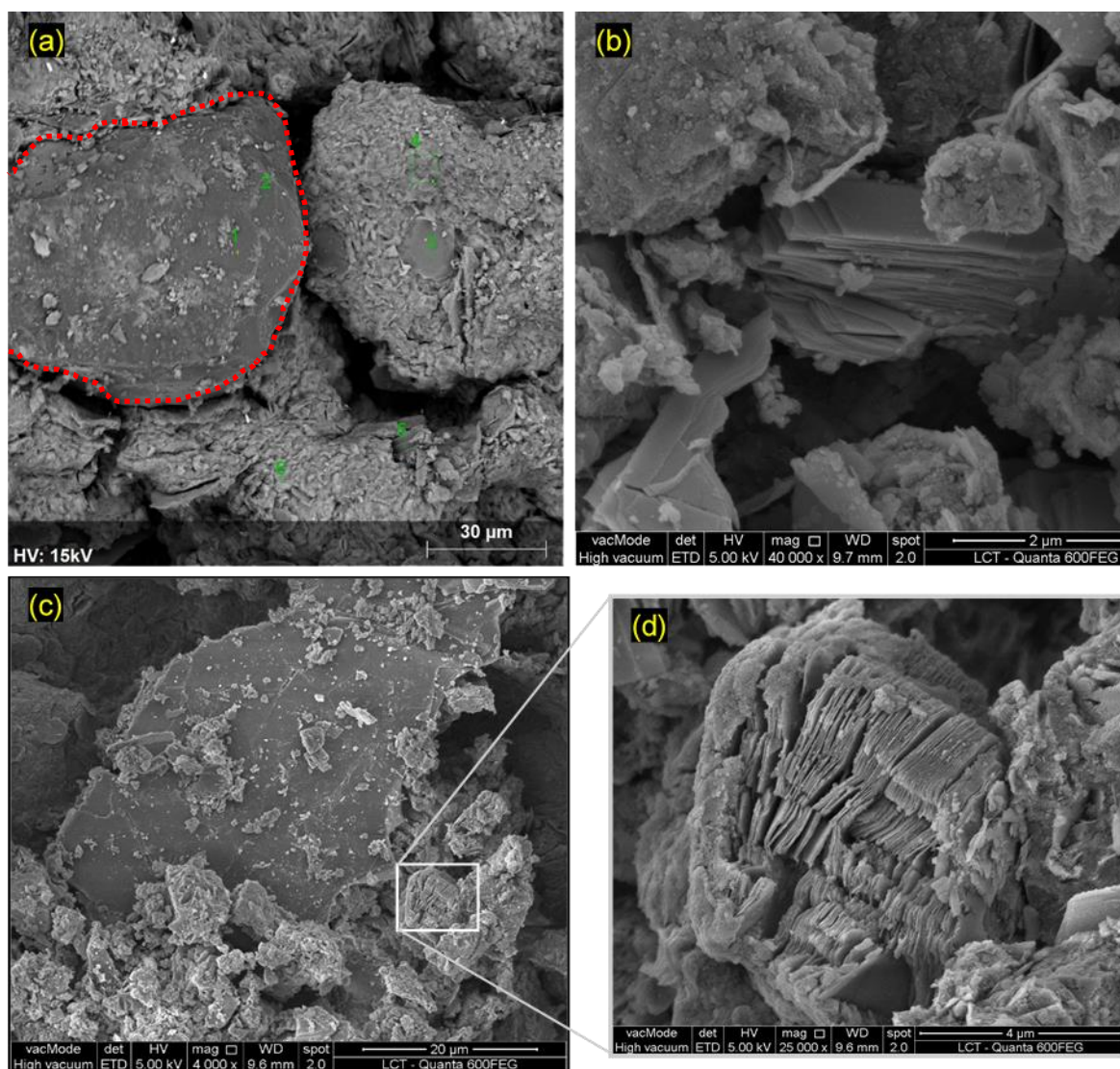


Source: author.

4.2.2 Scanning electron microscopy

SEM images of Cubatão WTS are depicted in Figure 30. The presence of quartz particles in the fine sand fraction can be observed. These particles present coatings of clay minerals and aluminum and iron (hydr)oxides (Figure 30a). Some flake-shaped particles observed in Figure 30b and 30d are likely to be clay minerals.

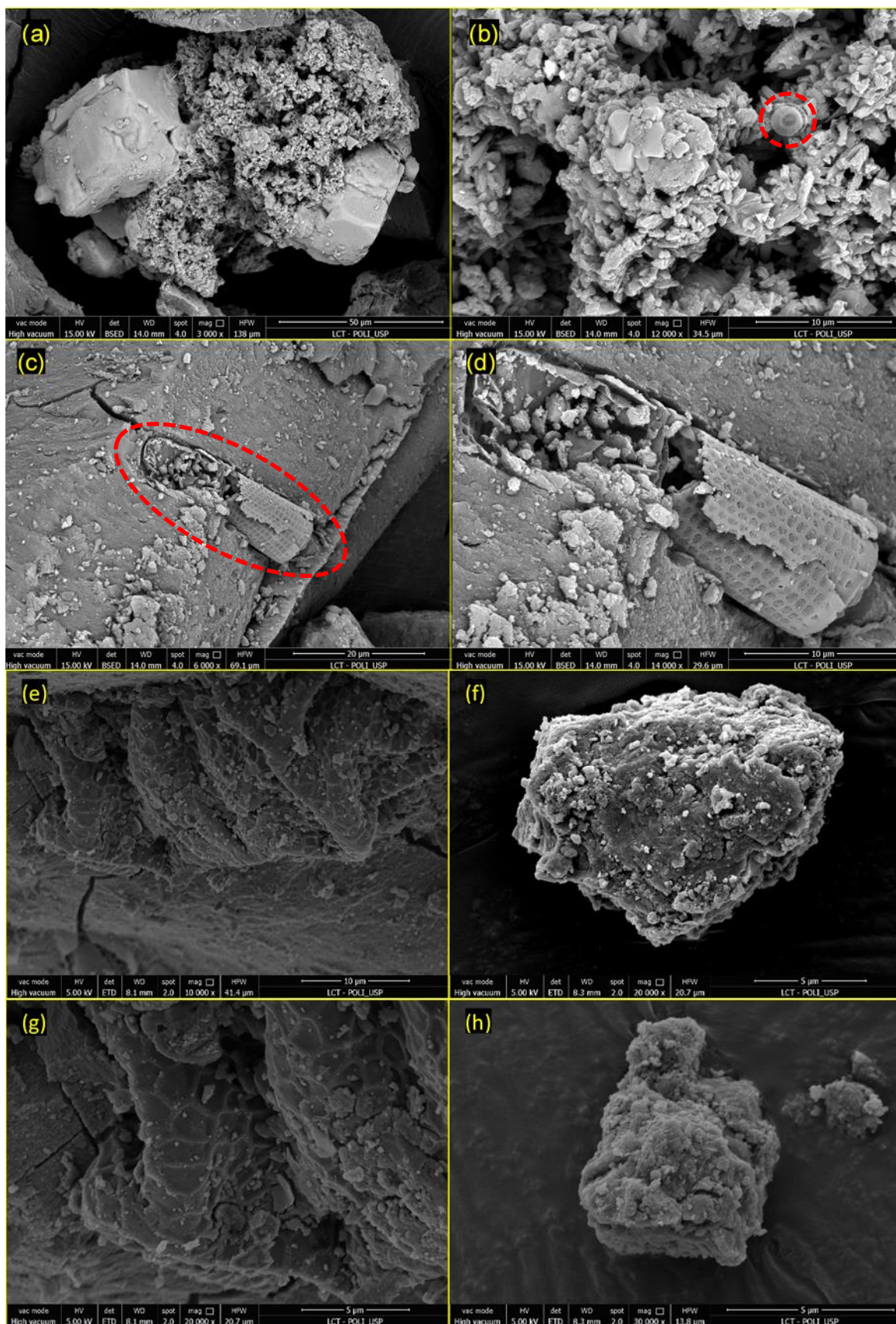
Figure 30 – Images of Cubatão WTS particles from SEM: (a) Quartz in fine sand fraction with coatings; (b) (c) (d) clay minerals.



Source: modified from Montalvan (2016).

SEM images of Taiaçupeba WTS showed unusual particles, coatings of amorphous material, coatings of aluminum and iron (hydr)oxides, and complex aggregations and clusters, as displayed in Figure 31. Such results are consistent with those from XRD analysis, which indicated major occurrence of amorphous material. Figure 31a and Figure 31b show a cluster of aggregated particles of different size and shape. The cube-shaped particle in Figure 31a could be a feldspar particle (KAlSi_3O_8 – $\text{NaAlSi}_3\text{O}_8$ – $\text{CaAl}_2\text{Si}_2\text{O}_8$) because of its shape and size around 50 μm. Energy dispersive x-ray spectroscopy (EDS) analyses conducted on particles depicted in Figure 31b detected major occurrence of Ca, Na, and Cl in the chemical composition.

Figure 31 – SEM images of Taiaçupeba WTS particles.



Source: author.

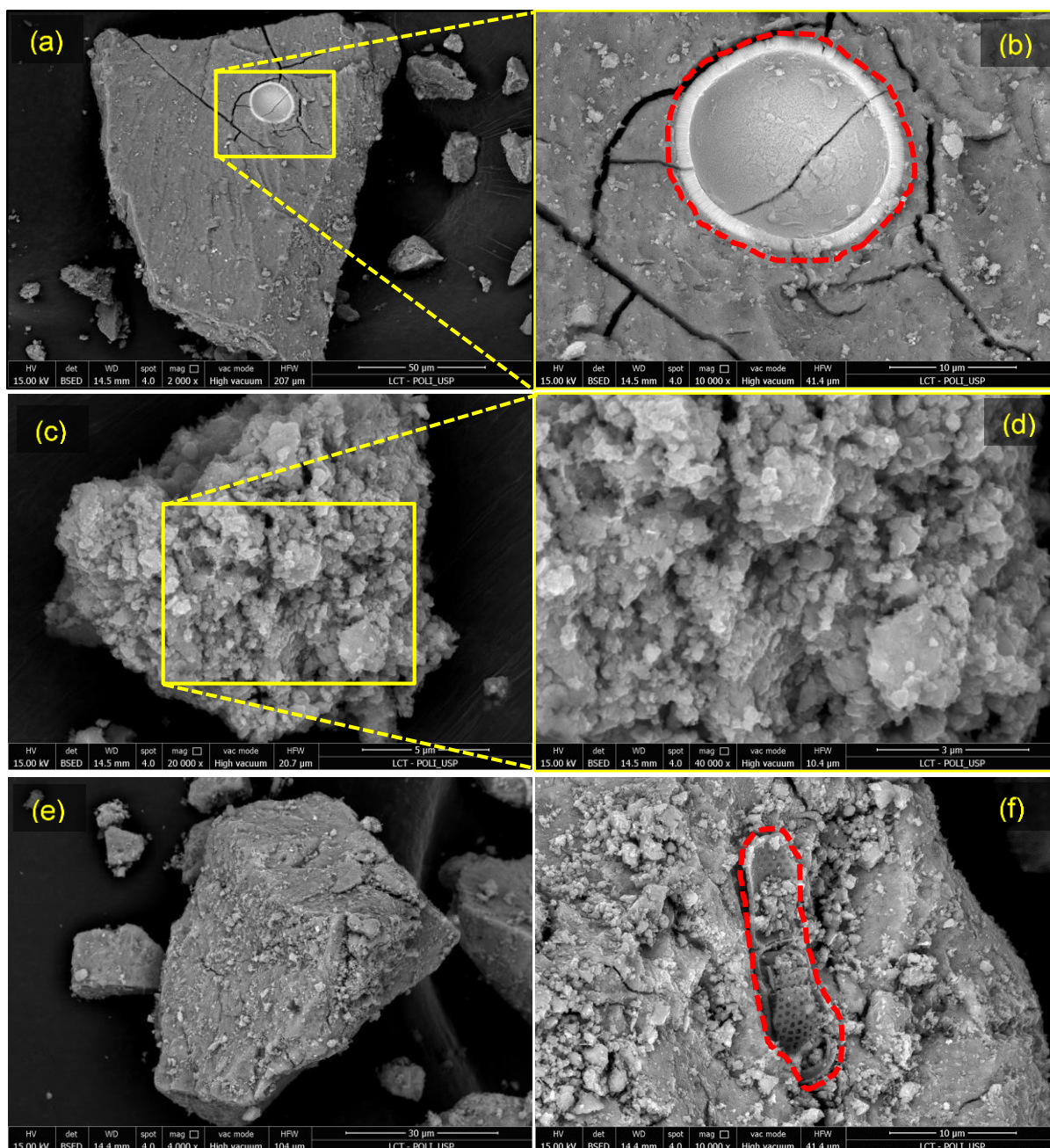
Figure 31c and Figure 31d portray a folded flake-shaped structure with dimensions about of 20 μm long and less than 1 μm thick. EDS analyses on this particle indicated its chemical composition contains Si, Al, and Fe, as shown in APPENDIX A. The particles marked inside a circle in Figure 31b and 31c are likely to be diatoms. The presence of diatoms in Taiacupeba-WTS could be explained by algae presence in the reservoir water.

Figure 31e to Figure 31h seem to be entirely coated aggregations. Coatings in Figure 31e and Figure 31g form a kind of honeycomb network; they could be long chains of polymer. Coatings in Figure 31f and Figure 31h look like metal (hydr)oxides, as those occurring in lateritic soils. EDS analyses identified occurrence of mainly iron (Fe) and aluminum (Al) in most particles, suggesting (hydr)oxides coatings. More SEM images and EDM analyses of Taiacupeba-WTS are presented in APPENDIX A.

SEM images of Taiacupeba WTS pre-treated with hydrogen peroxide are shown in Figure 32. Clusters/aggregations are similar to those of the non-treated sample, indicating that either the treatment did not completely remove organic matter or that coatings of amorphous material, such as metal (hydr)oxides, are still present.

The cluster shown in Figure 32b resembles metal (hydr)oxides. The particles marked with red dashed line in Figure 32b and 32f are probably diatoms, very similar to those observed in the untreated samples of Taiacupeba WTS.

Another interesting aspect is the formation of fissures in some particles clusters (Figure 32a and 32b), also observed in the non-treated sample (Figure 31c, 31e and 31g). The fissures appeared after focusing the electrons beam on the particles. One hypothesis is that the electrons beam heated the particles causing the formation of fissures, a behavior not commonly observed in crystalline phases (minerals).

Figure 32 – SEM images of Taiapuêba WTS pre-treated with H₂O₂.

Source: author.

4.3 CHEMICAL CHARACTERIZATION

4.3.1 Chemical composition by X-ray fluorescence (XRF)

The chemical composition of soils and WTS from XRF analyses is presented in Table 12. Aluminum and iron occurred in high percentage in all materials (measured as Al₂O₃ and Fe₂O₃, respectively). Aluminum and iron were expected to occur

significantly in both soils due to their lateritic nature, and in both WTS because of the coagulants used in water treatment (ferric chloride and aluminum sulfate).

The clayey sand showed high silicon content (68.1% SiO₂), as expected, since the sand fraction is large and DRX analyses detected occurrence of quartz. The clay presented a lower content of Si (31.1% SiO₂), also expected due to the smaller sand fraction and higher fines content composed predominantly of metal oxides. Cubatão and Taiaçupeba WTS presented low silicon content, 18.3 and 4.87%, respectively. As Cubatão WTS results from the treatment of raw water from a river that flows through residual soils derived from gneiss, a higher percentage of silica than Taiaçupeba (reservoir) WTS was anticipated.

Interestingly, for both soils and WTS, the content of silica is inversely proportional to loss on ignition (LOI). LOI values for Botucatu clayey sand, Campinas clay, Cubatão WTS and Taiaçupeba WTS were 6.11, 14.2, 22.0, and 52.6 %, respectively. Taiaçupeba WTS presented a considerably high value of LOI.

Table 12 – Chemical composition (semi-quantitative) of soils and sludges (percent by dry mass).

Element	Clayey sand ¹	Clay ²	Cubatão WTS ³	Taiaçupeba WTS ⁴	Taiaçupeba WTS* ⁴
SiO ₂	68.1	31.1	18.3	4.87	4.39
Al ₂ O ₃	16.5	23.9	8.89	29.6	37.4
Fe ₂ O ₃	7.17	24.4	46.0	12.3	16.7
MnO	0.03	0.141	0.21	0.32	0.23
MgO	0.04	0.17	0.438	<0.10	0.16
CaO	0.02	0.09	1.59	0.49	0.57
Na ₂ O	-	<0.02	0.10	<0.10	0.13
K ₂ O	0.04	0.03	1.00	<0.10	0.19
TiO ₂	1.55	5.21	0.417	0.17	0.26
P ₂ O ₅	0.05	0.14	0.249	0.45	0.78
LOI	6.11	14.2	22.0	52.6	39.1

LOI= Loss on ignition; *Sample treated by hydrogen peroxide

Source: ¹Zanón (2014); ²Gabas et al. (2014) ; ³Montalvan (2016); ⁴author.

The clayey sand presented aluminum oxides content about twice that of iron oxides (16.5 and 7.17%, respectively). On the other hand, the clay showed similar values for aluminum and iron oxides (23.9 and 24.4%, respectively), and higher than those of the clayey sand. The chemical composition of these soils is in accordance with the mineralogical composition from XRD analyses.

The iron content in Cubatão WTS was high (46.0% Fe_2O_3) and the aluminum content was relatively low (8.89% Al_2O_3). Conversely, Taiacupeba WTS presented higher content of aluminum than of iron (29.6 Al_2O_3 and 12.3% Fe_2O_3). The chemical composition of both WTS is coherent with the coagulants used in water treatment process: ferric chloride and aluminum sulfate, respectively.

Finally, the chemical composition of Taiacupeba WTS treated by hydrogen peroxide did not differ significantly from the non-treated or fresh WTS. Aluminum and iron oxides increased, respectively, from 29.6 to 37.4%, and from 12.3 to 16.7%. On the other hand, LOI decreased from 52.6 to 39.1%, indicating that hydrogen peroxide treatment only removed 13.5% of organic material. However, that value is close to the organic carbon content (OCC) determined by the Walkley-Black method (Table 13).

During ignition at 1020 °C, oxidation or volatilization of substances other than organic matter probably takes place. For instance, pore water and adsorbed water are driven off at temperatures ranging from 100 to 300 °C. Oxidation of carbonates and organic matter occurs in the range of 250 to 450 °C. Removal of interlayer water of some minerals (e.g. halloysite) and crystal lattice water (*dehydroxylation*, with destruction of the mineral structure) occurs in the range of 500 to 1000 °C. Besides, formation of new crystals (*crystallization*) may occur between 800 to 1000 °C (MITCHELL; SOGA, 2005).

4.3.2 Chemical parameters

Chemical parameters are presented in Table 13. Botucatu clayey sand and Campinas clay presented pH values (in H_2O) equal to 4.7 and 5.0, which corresponded to strongly-acid soil class (SANTOS et al., 2018). Cubatão WTS and Taiacupeba WTS presented pH (in H_2O) of 7.0 and 6.4, respectively, corresponding to practically-neutral class (SANTOS et al., 2018). The literature has reported pH values of some Brazilian WTS varying from 5.9 to 8.3 (PORTELLA et al., 2003; GUERRA, 2005; GERVASONI, 2014; MONTALVAN, 2016; RAMIREZ et al., 2018).

A relatively simple method for determining whether the net charge of soil colloids is negative, zero, or positive, is the analysis of soil pH in KCl and in water. The difference between the two pH values is termed ΔpH (SOIL SURVEY STAFF, 1999):

$$\Delta\text{pH} = \text{pH}_{(\text{KCl})} - \text{pH}_{(\text{H}_2\text{O})} \quad (21)$$

Depending on the net surface charge, the value of ΔpH can be positive, zero, or negative. A positive value indicates the predominance of positively charged colloids. A negative value, on the contrary, indicates the predominance of negatively charged colloids (TAN, 2010). All tested materials presented negative ΔpH (Table 13).

CEC of Botucatu clayey sand was $27.2 \text{ mmolc}\cdot\text{kg}^{-1}$ ($2.72 \text{ cmolc}\cdot\text{kg}^{-1}$), and CEC of Campinas clay, $76.3 \text{ mmolc}\cdot\text{kg}^{-1}$ ($7.63 \text{ cmolc}\cdot\text{kg}^{-1}$). These are low values, which are common for Brazilian lateritic soils (Fadigas et al., 2002).

According to the SiBCS (SANTOS et al., 2018), the chemical activity of the clay fraction of a soil can be determined using equation (22):

$$\text{Clay Activity (cmolc}\cdot\text{kg}^{-1}) = \frac{\text{CEC (cmolc}\cdot\text{kg}^{-1}) * 1000}{\text{Clay fraction (g}\cdot\text{kg}^{-1} < 2 \mu\text{m})} \quad (22)$$

Clay activity values higher than $27 \text{ cmolc}\cdot\text{kg}^{-1}$ correspond to high chemical activity. Using data from the geotechnical characterization (Table 14), the clay activity for Botucatu clayey sand is $9.4 \text{ cmolc}\cdot\text{kg}^{-1}$, and for Campinas clay, $14.7 \text{ cmolc}\cdot\text{kg}^{-1}$. Therefore, the clay fraction of both soils has medium to low chemical activity.

CEC values of Cubatão WTS and Taiaçupeba WTS were, respectively, 325.5 and $73.3 \text{ mmolc}\cdot\text{kg}^{-1}$ (32.5 and $7.3 \text{ cmolc}\cdot\text{kg}^{-1}$). Hsieh and Raghu (1997) reported CEC values for different WTS from the US varying from 23 to $136 \text{ cmolc}\cdot\text{kg}^{-1}$, with average of $82 \text{ cmolc}\cdot\text{kg}^{-1}$. WTS with higher organic matter usually has high CEC, since CEC of organic matter ranges from 150 to $300 \text{ cmolc}\cdot\text{kg}^{-1}$ (SPARKS, 2003). Nonetheless, although Taiaçupeba WTS has higher organic matter content (26.7%) and LOI (52.6%) than Cubatão WTS (2.4% and 22.0% , respectively), it presented lower CEC.

The clay activity of Cubatão WTS ranged from 36.8 to $41.7 \text{ cmolc}\cdot\text{kg}^{-1}$, i.e. high activity, and of Taiaçupeba-WTS, from 9.2 to $10.5 \text{ cmolc}\cdot\text{kg}^{-1}$, i.e. low activity.

Table 13– Chemical parameters of studied soils and WTS.

Parameter	Clayey sand ¹	Clay ¹	Cubatão sludge ²	Cubatão sludge ¹	Taiapuèba sludge ¹
pH (in H ₂ O)	4.7	5.0	7.2	7.0	6.4
pH (KCl 1 mol·L ⁻¹ solution)	4.5	4.4	6.7	5.9	5.6
ΔpH	-0.2	-0.6	-0.5	-1.1	-0.8
P (mg·kg ⁻¹)	<2	<2	1.2	<2	4.2
K ²⁺ (mmolc·kg ⁻¹)	<0.5	2.2	<0.3	1.5	2.5
Ca ⁺ (mmolc·kg ⁻¹)	2	21	226	266	32
Mg ²⁺ (mmolc·kg ⁻¹)	0.4	4	20	45	4
Na ⁺ (mmolc·kg ⁻¹)	<0.2	<0.2	5	4	14.8
Al ³⁺ (mmolc·kg ⁻¹)	3	1	<1	1	1
H ⁺ + Al ³⁺ (mmolc·kg ⁻¹)	25	49	<10	9	20
Exchangeable bases (mmolc·kg ⁻¹)	2.2	27.3	252.2	316.5	53.3
CEC (mmolc·kg ⁻¹)	27.2	76.3	255.2	325.5	73.3
Base saturation (%)	8	36	99	97	73
Aluminum saturation (%)	58	4	0	0	2
Organic matter (g·kg ⁻¹)	9	25	26	24	267
Organic carbon (g·kg ⁻¹)	5	14	15	14	155

Source: ¹author; ²Montalvan (2016).

Organic matter contents of Botucatu clayey sand and Campinas clay were low, 0.9 and 2.5%, respectively. The organic carbon of these soils was consequently low, 0.5 and 1.4%, respectively (organic carbon is computed assuming that organic matter consists of 58% organic carbon).

The SiBCS (SANTOS et al., 2018) classifies organic soils considering two conditions: (i) organic matter influences soil properties and behavior more than the mineral phase; and (ii) the organic carbon content of an air-dried sample is higher than or equal to 80 g·kg⁻¹ (8.0 %). The organic carbon content of Cubatão WTS was 1.4 %, and of Taiapuèba WTS, 15.5 %. Thus, Taiapuèba WTS could be classified as organic soil according to the SiBCS criteria.

4.4 GEOTECHNICAL CHARACTERIZATION

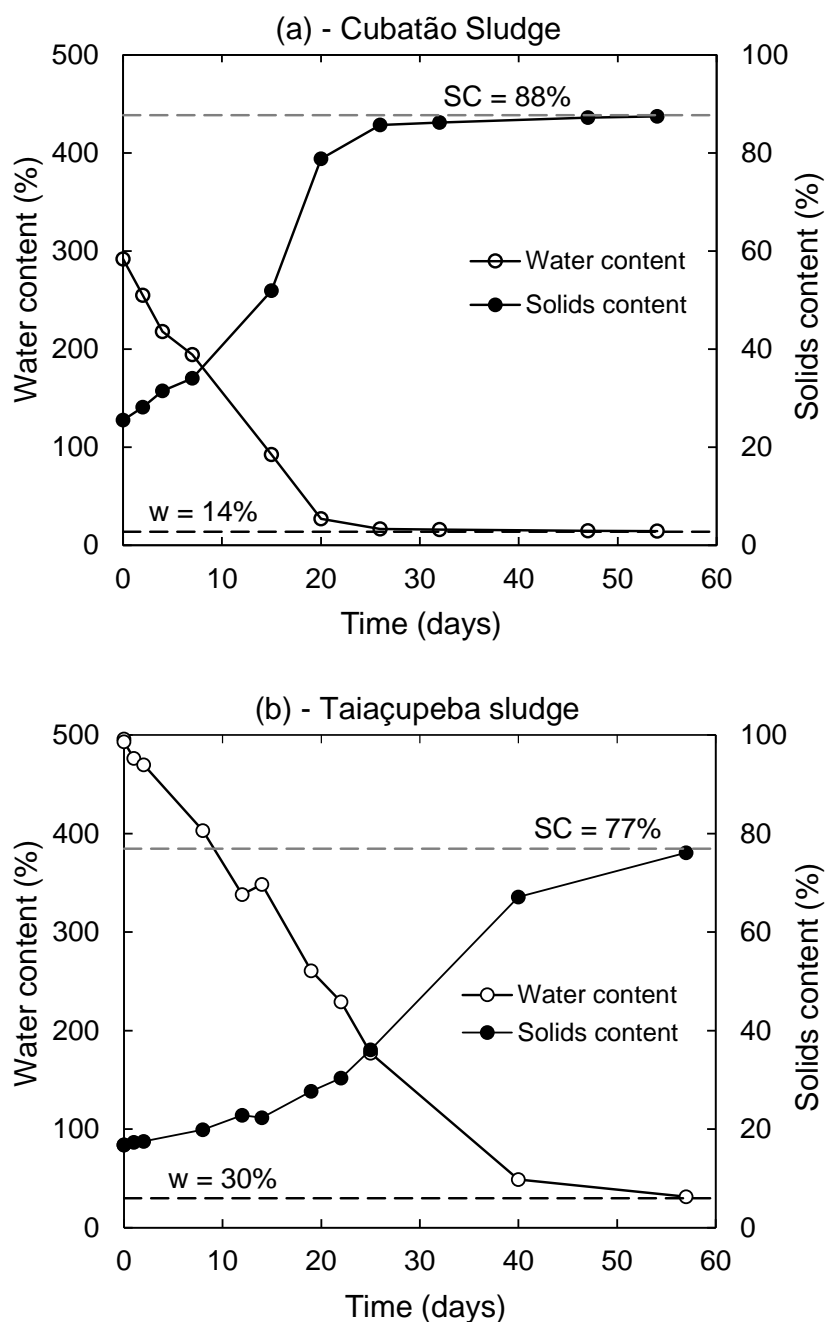
4.4.1 Air-drying of sludge samples

Samples of Cubatão WTS and Taiaçupeba WTS were air-dried over two months. The decrease of water content and increase of solids content with time is depicted in Figure 33. Cubatão WTS reached moisture constancy ($w \sim 14\%$) after approximately 30 days. Taiaçupeba WTS, however, after 30 days still presented water content of 140% and after 60 days, about 30%. Those results suggest that Taiaçupeba WTS is more hydrophilic than Cubatão WTS.

During air-drying, both WTS underwent strong cementation of particles. The cementation was irreversible, even after long periods of soaking in water and dispersant (sodium hexametaphosphate). Moreover, the materials completely lost plasticity. Similar behavior was reported for other WTS (WANG; HULL; JAO, 1992; HSIEH; RAGHU, 1997; BASIM, 1999).

Such results indicate that WTS should not be dried prior testing unless it will be reused or studied in dry state. Since this study aims at the utilization of WTS in fresh wet state, tests were executed without previous drying.

Figure 33 – Water content (w) and solids content (SC) variation during air-drying: (a) Cubatão sludge¹; (b) Taiapuêba sludge².



Source: ¹modified from Montalvan (2016); ²author.

4.4.2 Organic matter

The organic matter content determined by ignition at 440 °C for Botucatu clayey sand, Campinas clay, Cubatão WTS and Taiapuêba WTS was 3.5, 11.7, 19.2, and 49.0%, respectively. These values are roughly similar to those of LOI (Table 12). Figure 34 shows WTS samples prior and after ignition.

Figure 34 - Samples for OM tests by ignition at 440 °C: a) Cubatão-WTS before ignition; b) Taiaçupeba-WTS before ignition; c) Cubatão-WTS after ignition; d) Taiaçupeba-WTS after ignition.



Source: author.

NBR 6502 (ABNT, 1993) defines an organic soil as a homogeneous mixture of decomposed organic matter and mineral compounds, generally black or dark gray-colored. However, this standard neither defines nor suggests any value of organic matter content as reference for classification of organic soils.

The USCS defines that a fine-grained soil is an organic silt or clay if organic matter is present in sufficient quantity to influence the liquid limit as follows: the liquid limit after oven drying is less than 75% of the liquid limit of the original sample determined before oven drying.

The SiBCS defines organic soils as those containing organic carbon content higher than 8%. According to Huat et al. (2014), in geotechnical engineering, soils with organic matter content higher than 20% are defined as organic soils. This definition is basically founded on the mechanical behavior of soils, since it is generally accepted that when a soil has organic content higher than 20%, the mechanical criteria for mineral soils can no longer be universally applied.

Hence, in this work a soil was considered as organic if one of the following criteria is met: organic content determined by ignition at 440 °C higher than 20%

(HUAT et al., 2014), or organic carbon higher than 8% (SANTOS et al., 2018). Based on these criteria, Taiaçupeba WTS is the only tested material classified as organic soil.

4.4.3 Specific gravity and grain size distribution

Specific gravity of solids (G_s) of Botucatu clayey sand was equal to 2.69 for the first sampling (Montalvan, 2016) and 2.80 for the second sampling. Campinas clay presented G_s about of 2.98. These values agree with the mineralogical and chemical composition of the soils. The clayey sand presented G_s value closer to that of quartz (2.65), its major mineral (silica represents almost 70% of its composition, Table 3). The second and higher value is likely due to a greater content of clay mineral and metal oxides. The clay has higher specific gravity, and the mineralogical and chemical composition indicated the occurrence of iron oxides with high specific gravity, such as hematite ($G_s= 5.0-5.3$), magnetite ($G_s= 5.2$), and ilmenite ($G_s= 4.0-4.79$). Moreover, aluminum and iron oxides in the clay composition account for nearly 50% (Table 12).

For Cubatão WTS, G_s varied between 2.94 and 2.97 (average 2.95). For Taiaçupeba WTS, G_s ranged from 2.37 to 2.45 (average 2.42). These values can also be explained by the chemical composition. Cubatão WTS comprises 46% iron oxides and 22% LOI (Table 12). The high content of iron oxides in Cubatão WTS can be responsible for its high specific gravity of solids.

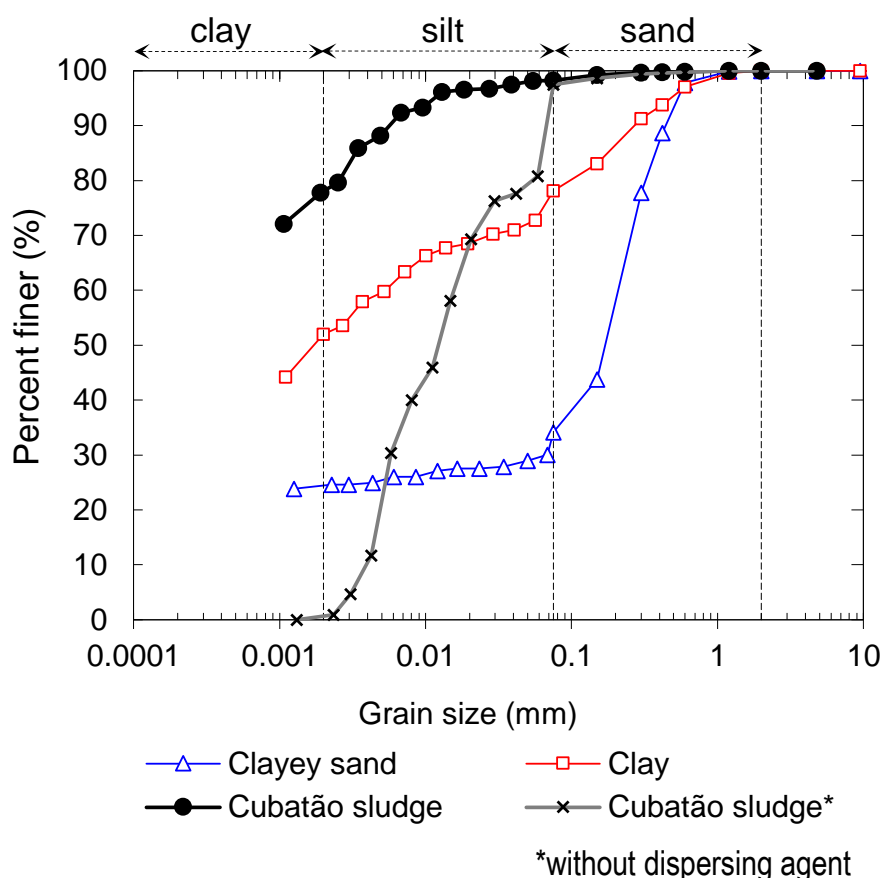
On the other hand, Taiaçupeba WTS consists of only 12.3% iron oxides and 52.6% LOI (Table 12). The low specific gravity of solids of Taiaçupeba WTS is coherent with the large percentage of LOI. Organic soils usually have low specific gravity of solids due to the large percentage of organic matter (HUAT et al., 2014). Also, some authors have related low specific gravity of WTS to high content of volatiles (HSIEH; RAGHU, 1997; BASIM, 1999). Table 5 shows values of G_s as low as 1.90 and as high as 2.95 for WTS from different countries.

Grading curves of the clayey sand, the clay and Cubatão WTS are presented in Figure 35. The grain size distribution of the clayey sand consists of nearly 35% fines (diameter < 75 μm) and 65% sand fraction. The clay contains roughly 80% fines and 20% sand fraction.

Cubatão WTS presented only 2% of sand fraction, and 98% of fines. The grading curve of Cubatão WTS determined without dispersing agent also indicated

nearly 98% of fines. However, the clay fraction (% finer < 2 μm) was depleted to less than 1%, whereas the grading curve determined with dispersant presented 78% of clay fraction. The coagulant agent present in the WTS (ferric chloride) is responsible for the agglomeration of clay particles, which is reversed by the dispersing agent used in the hydrometer test.

Figure 35 – Grading curves of clayey sand, clay, and Cubatão WTS.

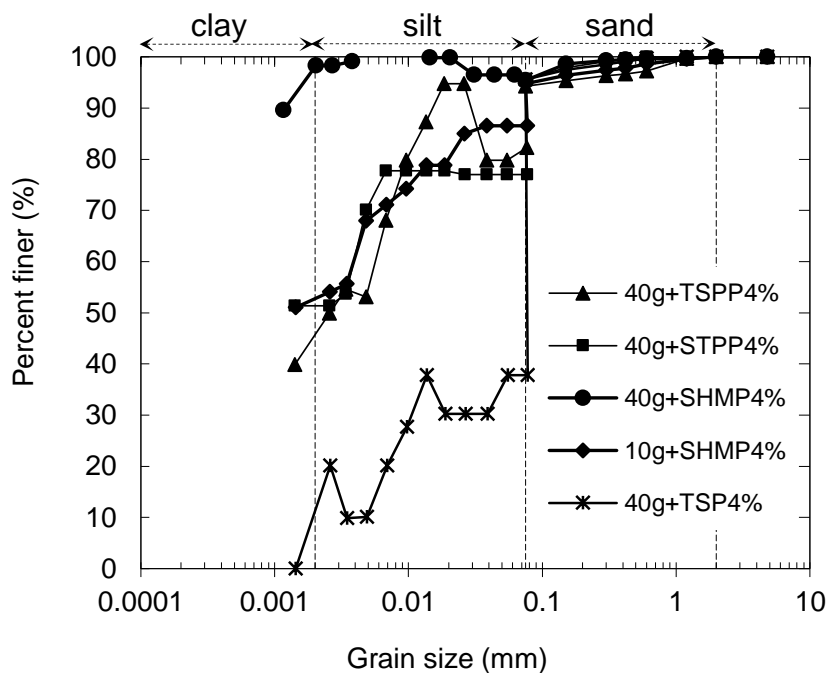


Source: prepared by the author.

Figure 36 displays the unsuccessful results from hydrometer tests with Taiapuêba WTS. These tests were conducted using different dispersants in several conditions (see details in Table 9). However, none of the dispersants yielded completely satisfactory results. The sludge remained permanently dispersed in water, and even after 24 hours there was almost no sedimentation of particles. Besides, the density of the fluid (WTS-water suspension) sometimes seemed to increase based on the hydrometer readings. The test conducted with 10-g (dry mass) and 4% SHMP was the only to present a fairly coherent behavior, however, not entirely satisfactory. The

sieving analysis show that Taiapuêba WTS comprises about of 95% fines and 5% sand fraction, similar to Cubatão WTS.

Figure 36 Grain size distribution tests for Taiapuêba WTS with different dispersants.



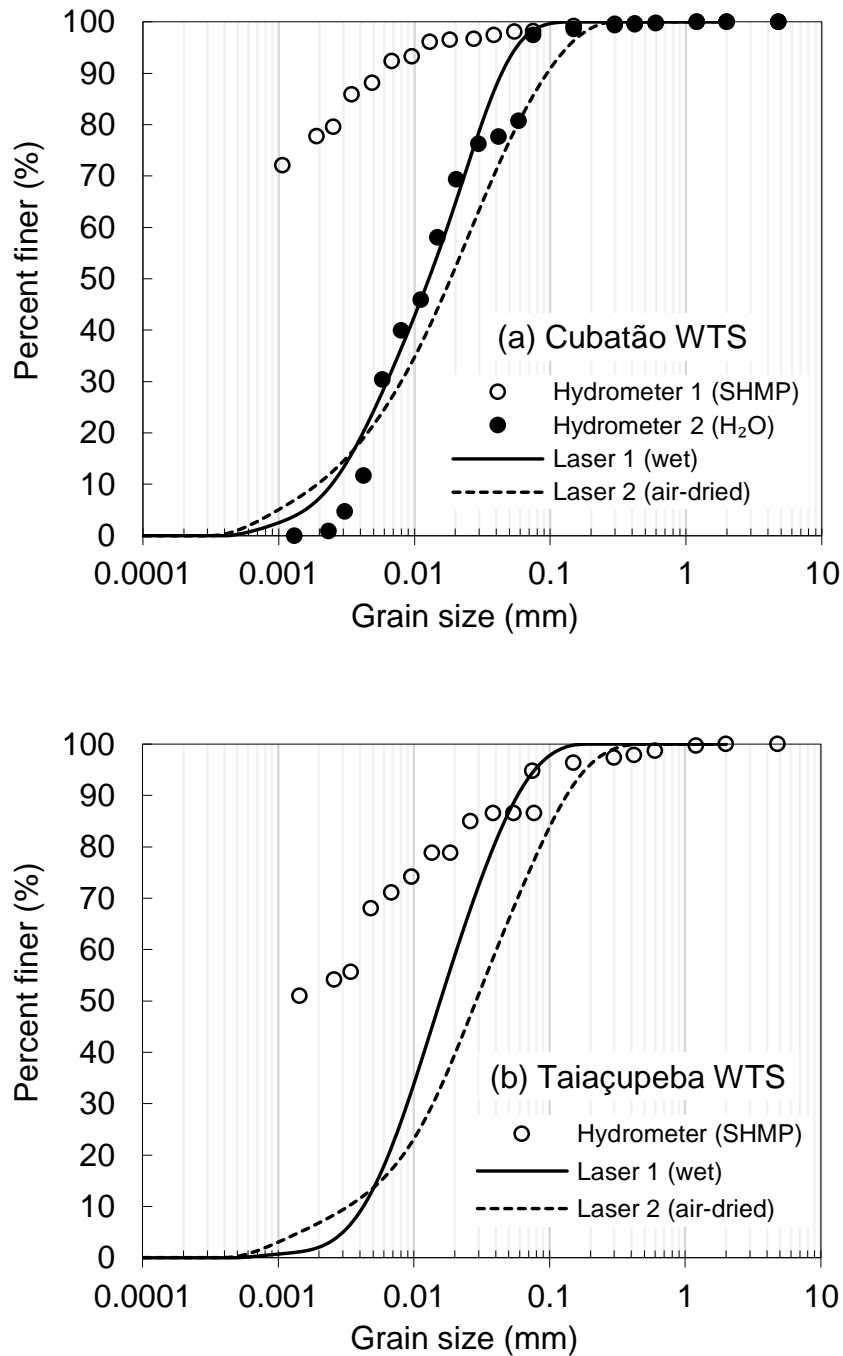
TSP = Trisodium phosphate; TSP4% = 4% Trisodium phosphate; STPP = Sodium tripolyphosphate; STPP4% = 4% Sodium tripolyphosphate; SHMP = Sodium hexametaphosphate; SHMP4% = 4% Sodium hexametaphosphate; TSP4% = 4% Trisodium phosphate

Source: author.

On the other hand, GSD curves by laser analyses of Cubatão-WTS were similar to that from hydrometer analysis without dispersing agent, as shown in Figure 37, although the laser analyses were conducted using calgon as dispersing agent.

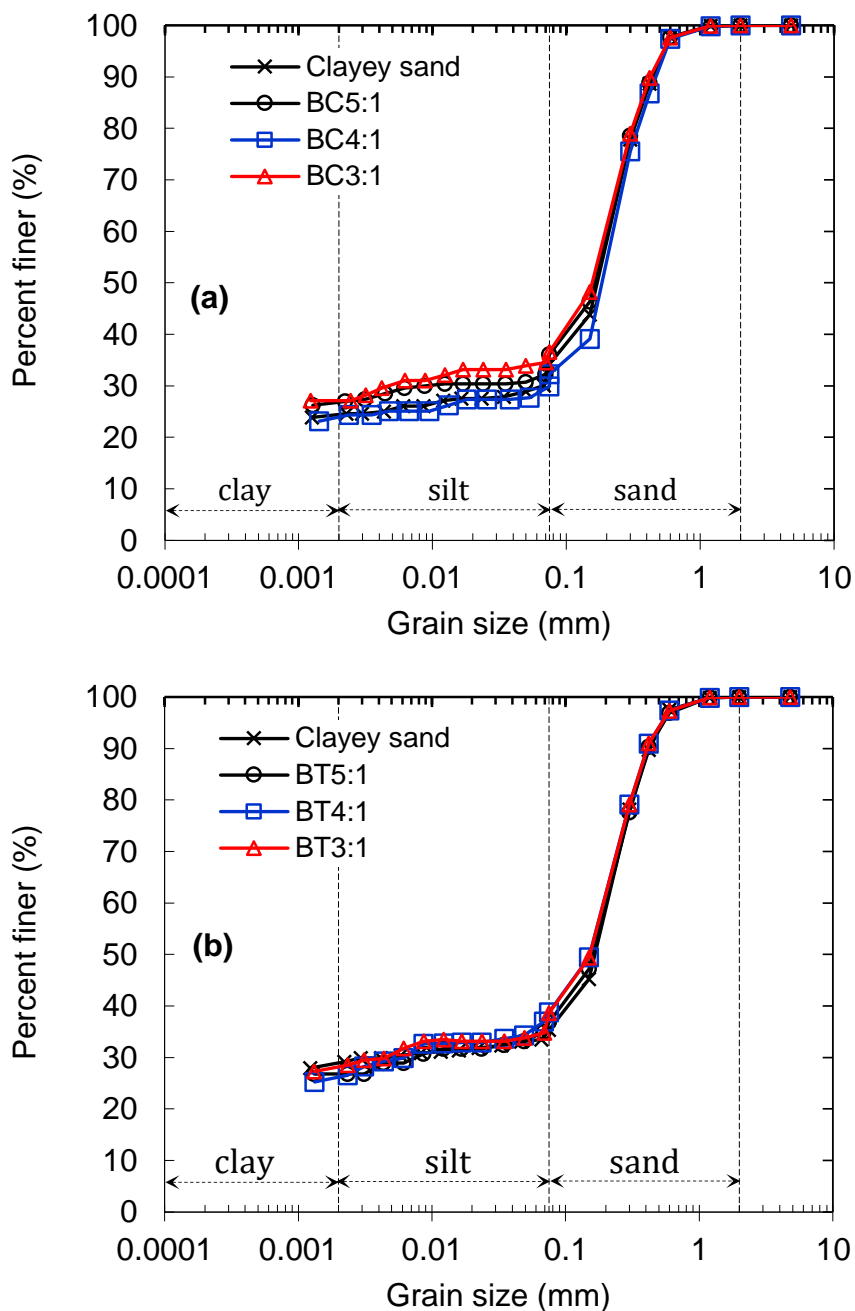
Two important aspects can be observed by comparing GSD curves from hydrometer and laser analyses: first, the laser-GSD for both WTS were coarser than the hydrometer-GSD; second, laser analyses were influenced by the initial state of the sample, i.e. wet or dry, since higher fines content was obtained for wet samples.

Figure 37 – GSD curves from laser analyses: a) Cubatão-WTS; b) Taiapuêba-WTS.



Source: author.

Figure 38 shows the grading curves of the mixtures. Addition of WTS to the soils did not significantly alter the GSD curves. Mixtures of Botucatu clayey sand with Cubatão WTS (BC mixtures) presented only a slight increment in fines content (Figure 38a) compared to the soil. Mixtures of the clayey sand with Taiapuêba WTS (BT mixtures) showed GDS practically equal to that of the soil.

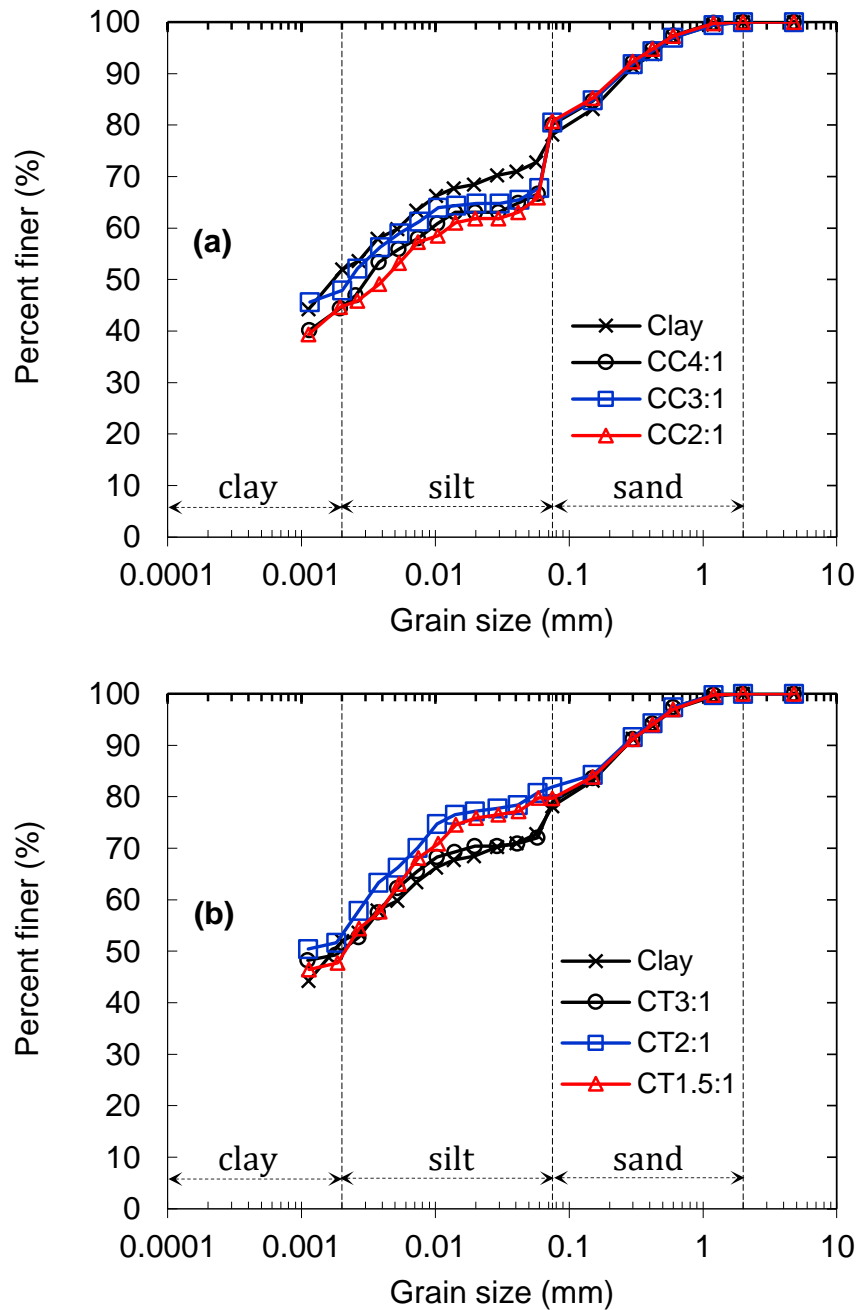
Figure 38 – GSD curves of clayey sand and mixtures: (a) BC¹; (b) BT².

Source: ¹modified from Montalvan (2016); ²the author.

Mixtures of Campinas clay with Cubatão WTS (CC mixtures), on the contrary, tended to indicate lower fines content with increasing sludge addition, although Cubatão WTS contains about 98% fines. This behavior could be related to the occurrence of micro-aggregation of the clay particles due to the incorporation of sludge with a coagulant agent (ferric chloride). That should not occur because of the use of

dispersant on the hydrometer tests. Nonetheless, such behavior was not observed in the clayey sand, maybe because of the lower fines content.

Figure 39 – GSD curves of Campinas clay and mixtures: (a) CC mixtures; (b) CT mixtures.

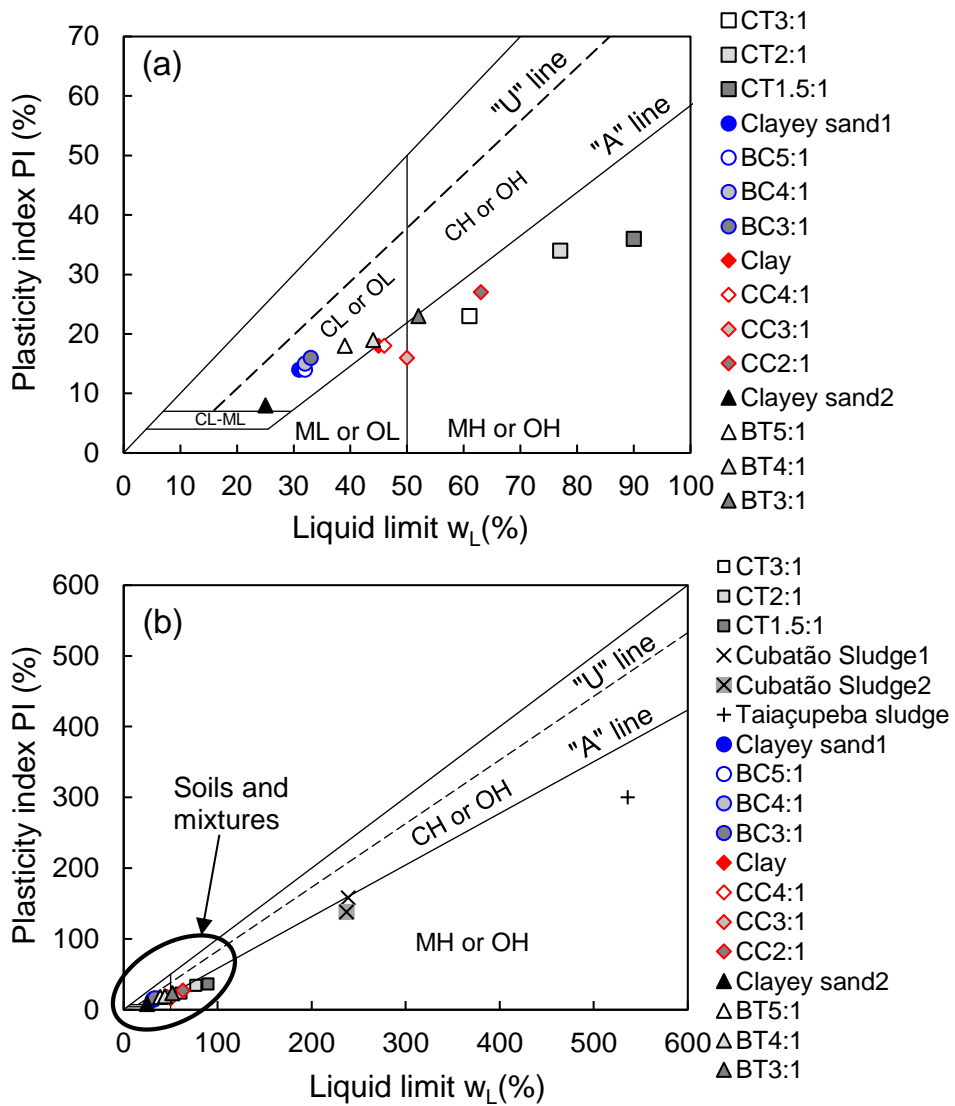


Source: author.

4.4.4 Atterberg limits

The values of liquid limit (w_L) and plasticity index (PI) for the soils, Cubatão WTS, Taiapuêba WTS and mixtures are plotted in the Casagrande plasticity chart in Figure 40. A summary of Atterberg limits and the corresponding classification according to the Unified Soil Classification System – USCS is presented in Table 14.

Figure 40 – Casagrande’s plasticity chart: (a) soils and mixtures; (b) sludges.



Source: prepared by the author.

Cubatão WTS presented liquid limit of 237% and plasticity index of 138%. Taiçupeba WTS presented values of liquid limit and plasticity index more than twice those of Cubatão WTS, 536 and 300%, respectively.

Based on the Atterberg limits and GSD, the clayey sand is classified as clayey sand (SC), the clay is classified as lean clay (CL), Cubatão WTS, as elastic silt (MH), and Taiçupeba WTS, as organic silt (OH) according to the Unified Soil Classification System (ASTM, 2017).

The soil-WTS mixtures showed a trend of increment of liquid limit and plasticity index with increasing WTS content. This was observed for both soils independently of the sludge. Even though, the classification of the mixtures was the same of the natural soil for the clayey sand mixtures.

It is important to remember that USCS is not totally adequate for classification of soils with especial characteristics. For instance, lateritic fine-grained soils classified as CH and MH, or CL and ML by the USCS do not differ significantly in geotechnical behavior. Additionally, most lateritic soils classified as MH do not have properties of typical silts, e.g. Brazilian red clay known as *terra roxa* (NOGAMI; VILLIBOR, 1991).

Both Cubatão WTS and Taiçupeba WTS became non-plastic after air and oven drying, not only due to organic matter but also related to the presence of coagulants (iron and aluminum hydroxides), therefore the criteria to define organic soils according to USCS was considered unsuitable for WTS.

The criteria adopted to define organic soils was presented in (item 4.4.2).

Table 14 – Geotechnical characterization of tested soils, sludges and mixtures.

Sample	w _L (%)	PI (%)	G _s	Clay (%<2μm)	Fines (%<75μm)	Sand (%)	OM (%)	USCS
Cubatão WTS ¹	239	158	2.85–2.95	69.3	95.4	4.6	-	MH
Cubatão WTS ²	237	138	2.95	78.1	98.3	1.7	19.2	MH
Taiáçupeba WTS ²	536	300	2.42	-	95.0	5.0	49.0	OH
Clayey sand ¹	31	14	2.69	24.4	34.2	65.8	-	SC
BC5:1 ¹	32	14	2.71	26.8	36.1	63.9	-	SC
BC4:1 ¹	32	15	2.70	23.9	32.2	67.8	-	SC
BC3:1 ¹	33	16	2.69	27.1	36.6	63.4	-	SC
Clayey sand ²	25	8	2.80	28.9	35.3	64.7	3.5	SC
BT5:1 ²	39	18	2.72	26.8	36.8	63.2	-	SC
BT4:1 ²	44	19	2.70	26.1	38.8	61.2	-	SC
BT3:1 ²	52	23	2.68	28.1	38.7	61.3	-	SM
Clay ²	45	18	2.98*	52.0	78.1	21.9	11.7	CL
CC4:1 ²	46	18	2.98*	44.7	80.1	19.9	-	ML
CC3:1 ²	50	16	2.98*	47.9	80.5	19.5	-	ML-MH
CC2:1 ²	63	27	2.98*	45.0	80.8	19.2	-	MH
CT3:1 ²	61	23	2.95*	49.6	79.1	20.9	-	MH
CT2:1 ²	77	34	2.94*	52.0	81.9	18.1	-	MH
CT1.5:1 ²	90	36	2.92*	48.0	79.7	20.3	-	MH

w_L= liquid limit; PI= plasticity index; G_s= specific gravity; OM= organic matter
*calculated by weighted average

Source: ¹Montalvan (2016); ²author.

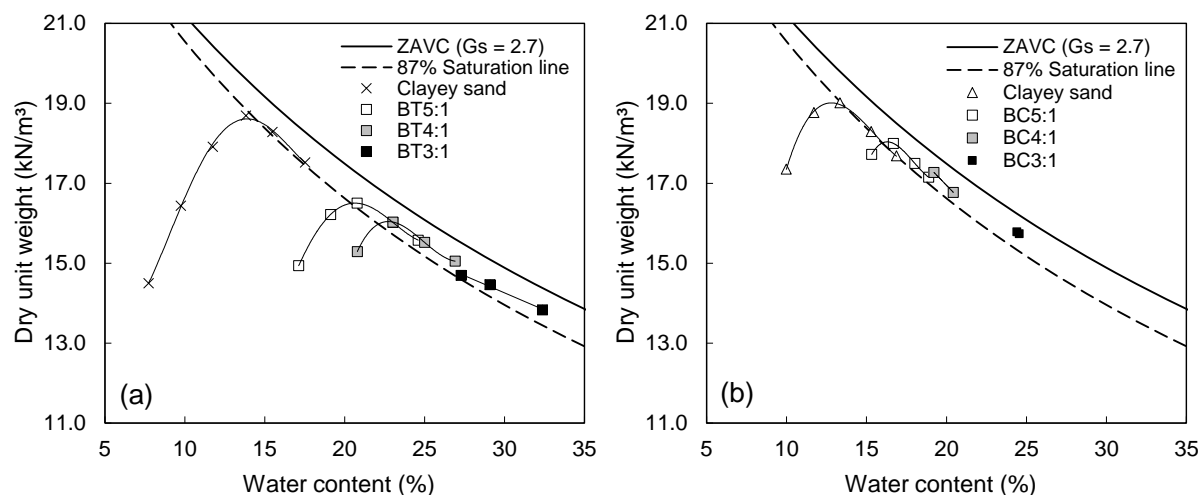
4.5 COMPACTION

Compaction curves of Botucatu clayey sand, BC mixtures and BT mixtures are presented in Figure 41. The clayey sand showed maximum dry unit weight of 19.0 kN/m³ and optimum water content of 13.5%. BC and BT mixtures presented maximum dry unit weight decreasing and optimum water content increasing with increasing WTS content.

This behavior is explained by the increment in fines, since WTS contains essentially only fines fraction (particles < 75 μm). The same trend has been observed for compaction parameters of sand-bentonite mixtures and silt-bentonite mixtures (DE MAGISTRIS; SILVESTRI; VINALE, 1998; BOSCOV et al., 2009; CHEN, Y.; MEEHAN, 2012). Nonetheless, when a fine material such as bentonite is added to a poorly graded sand or a sand with low or no fines content, the maximum dry unit weight may increase

and the optimum water the content may decrease (e.g. KENNEY et al., 1992; DE MAGISTRIS; SILVESTRI; VINALE, 1998).

Figure 41 – Compaction curves of: (a) Clayey sand and BT mixtures¹; (b) Clayey sand and BC mixtures².



ZAVC = zero air voids curve

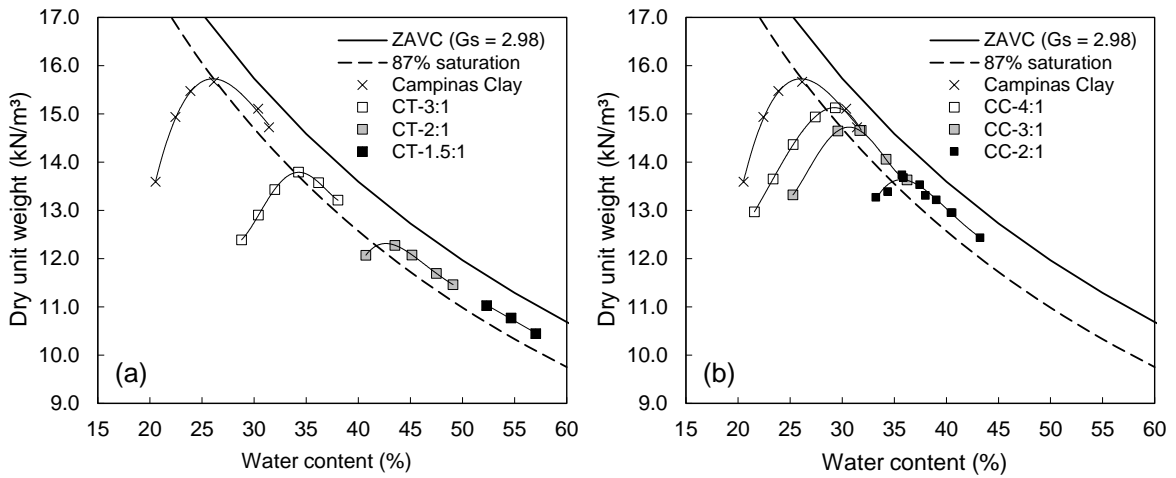
Source: ¹author; ²modified from Montalvan (2016).

Compaction curves for Campinas clay, CC mixtures and CT mixtures are shown in Figure 42. The clay presented maximum dry unit weight of 15.7 kN/m³ and optimum water content of 26%. CC and CT mixtures presented lower maximum dry unit weight and higher optimum water content with WTS increase, similar to the behavior of clayey sand-WTS mixtures.

Mixtures were prepared using air-dried soils and wet WTS (at their natural moisture, 268% for Cubatão WTS and 495% for Taiaçupeba WTS). Therefore, the higher the WTS content, the higher the initial water content of the mixture.

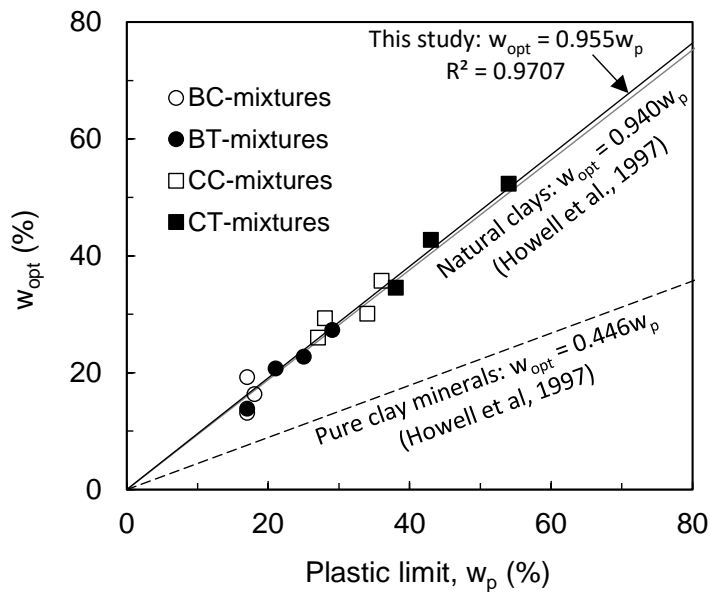
In the literature, compaction parameters have been correlated to Atterberg limits. For instance, it has been proposed that the optimum water content is approximately 94% the plastic limit (HOWELL et al., 1997). Figure 43 shows that the same relationship is valid for the tested mixtures.

Figure 42 – Compaction curves of: (a) Campinas clay and CT mixtures; (b) Campinas clay and CT mixtures.



Source: prepared by the author.

Figure 43 – Relationship between optimum water content and plastic limit.



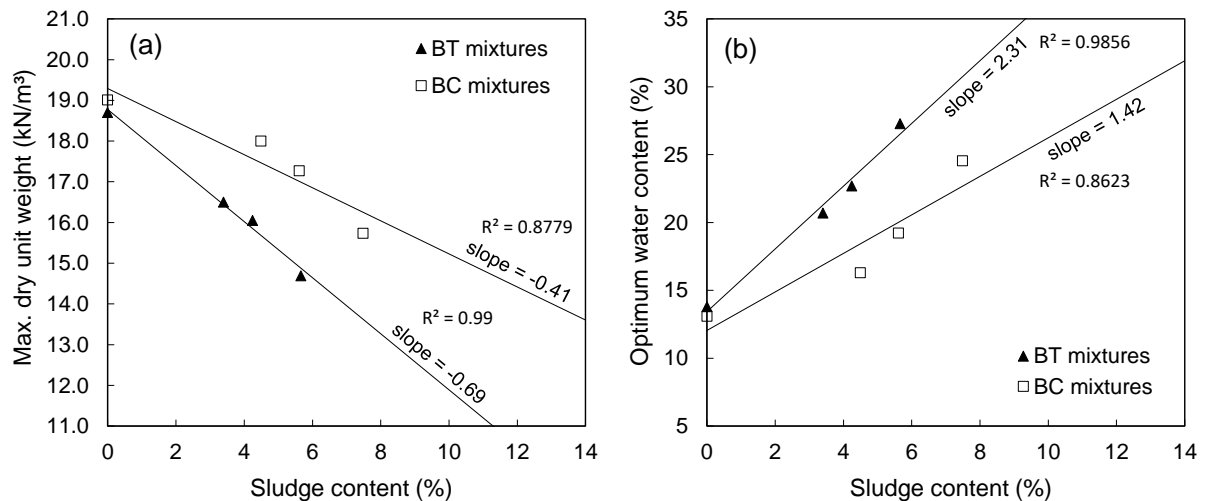
Source: prepared by the author.

The compaction curves presented in Figure 41 and Figure 42 were determined with samples of the mixtures without previous drying, i.e. at the resultant moisture right after mixing (as-mixed water content). Thus, mixtures with low WTS content had as-mixed water content lower than optimum, while with increasing WTS content the as-mixed water content of the mixtures tended to approach or even surpass optimum.

That explains why some compaction curves have points only on the wet side of the compaction curve, e.g. BC3:1 (Figure 41). For those mixtures, the first point was considered as the optimum for comparisons purposes, as in Figure 43.

Additionally, the incorporation of Taiapuêba WTS into the soils affected the compaction parameters more than the addition of Cubatão WTS. This can be observed in Figure 44 and Figure 45, where the trend lines for the variation of maximum dry unit weight and optimum water content with WTS content (by dry mass) (Figure 44a and Figure 45a) show a steeper slope for Taiapuêba WTS than for Cubatão WTS (Figure 44b and Figure 45b).

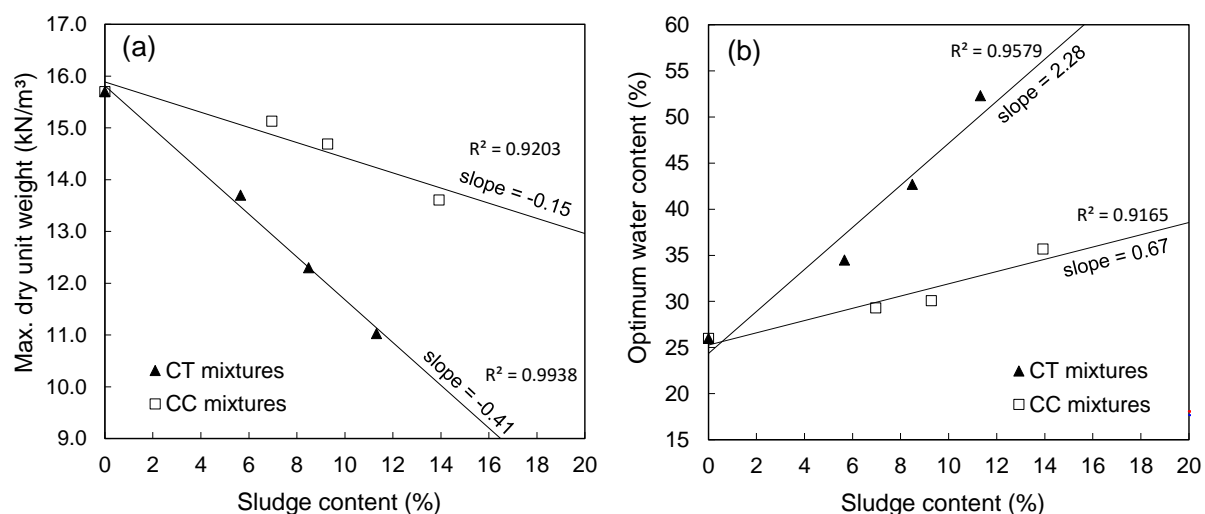
Figure 44 – Variation of compaction parameters as a function of WTS content for BC and BT mixtures: (a) Maximum dry unit weight; (b) Optimum water content.



Source: author.

The effect of Taiapuêba WTS on the reduction of maximum dry unit weight and increase of optimum water content, measured by the slope of the trend lines, was almost twice that of Cubatão WTS. This behavior may be explained by the higher organic matter content, liquid limit and plasticity index of Taiapuêba WTS compared to Cubatão WTS.

Figure 45 – Variation of compaction parameters as a function of WTS content for CC and CT mixtures: (a) Maximum dry unit weight; (b) Optimum water content



Source: author.

The finding that both sludges underwent irreversible changes after air drying (e.g. cementation and loss of plasticity), stated in item 4.4.1, prompted the investigation of the effect of drying on the compaction parameters of the mixtures. Thus, compaction tests were carried out with mixtures subjected to air drying prior testing, as detailed in 3.2.6.

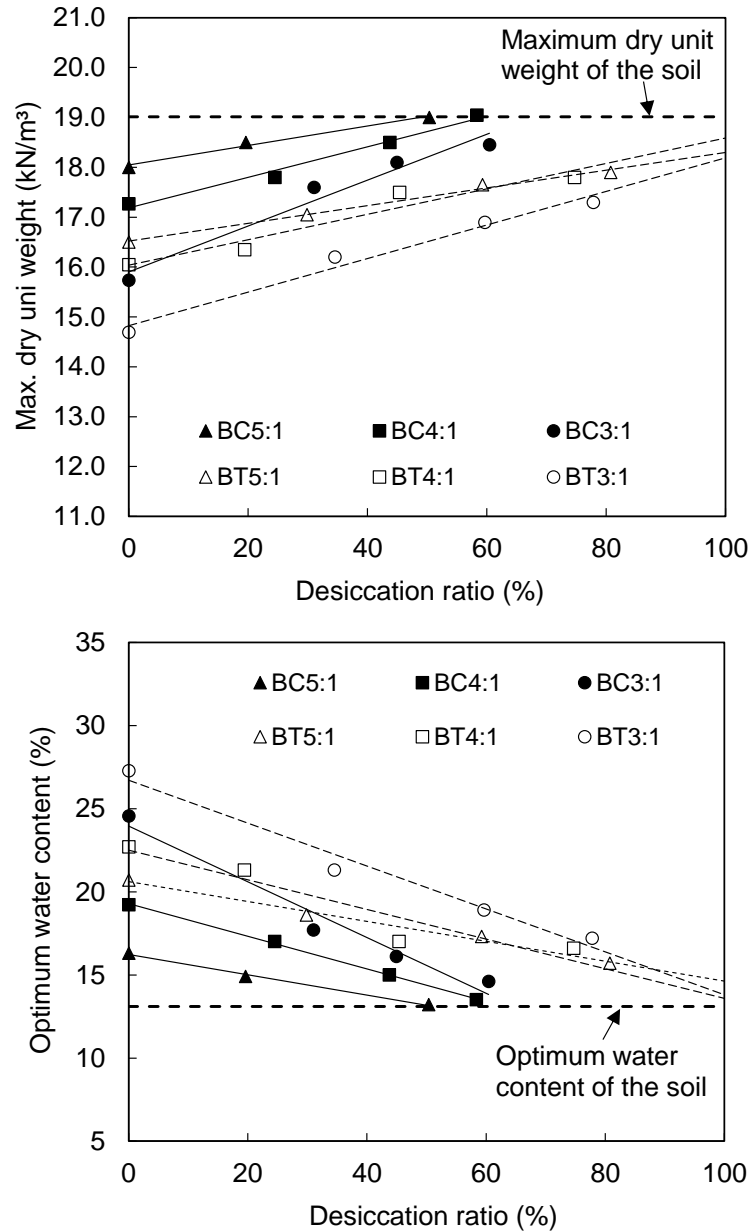
Drying was observed to remarkably affect compaction parameters: maximum dry unit weight increased and optimum water content decreased. Montalvan (2016) reported such behavior for BC mixtures, pointing out that air drying of mixtures was easier and faster than air-drying WTS alone.

Figure 46 and Figure 47 depict the variation of compaction parameters as a function of desiccation ratio. These values were determined from compaction curves from APPENDIX C. Maximum dry unit weights of the mixtures for zero desiccation ratio, i.e. without drying prior compaction, were lower than that of the corresponding soil (dashed line on Figure 46a and Figure 47a). Optimum water contents of the mixtures were higher than that of the soils (dashed line on Figure 46b and Figure 47b). By drying the mixtures prior to compaction an improvement of compaction parameters, proportional to the desiccation ratio, is evident.

At desiccation ratio between 50 to 60%, BC mixtures achieved the same values of compaction parameters as those of the soil (Figure 46). BT mixtures at desiccation

ratios up to 80% did not reach compaction parameters equal to those of the soil, while linear trend lines suggest that these would be reached at 100% desiccation ratio.

Figure 46 – Variation of compaction parameters as a function of desiccation ratio: (a) γ_{dmax} of BC and BT mixtures; (b) w_{opt} of BC and BT mixtures.

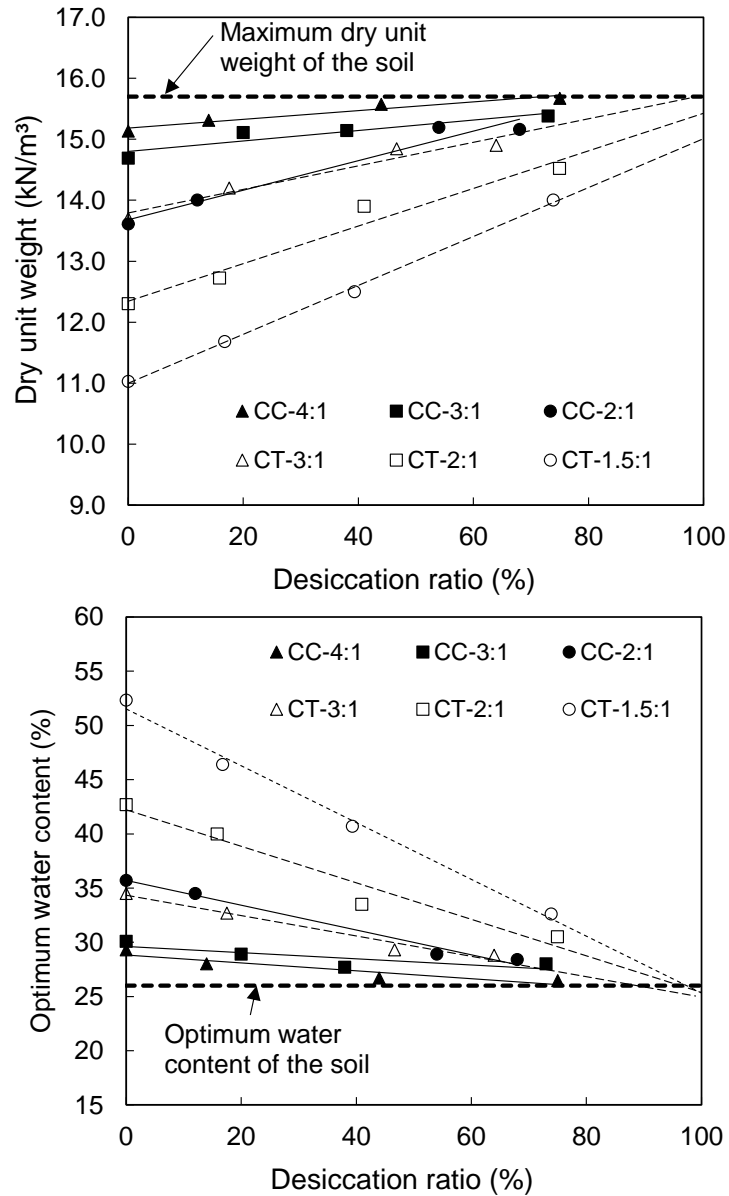


Source: prepared by the author.

Additionally, CC mixtures reached the same values of compaction parameters as those of the clay at desiccation ratios about 70 to 80% (Figure 47), higher than those of BC mixtures. CT mixtures at 80% desiccation ratio did not reach compaction

parameters equal to those of the clay. Linear trend lines suggest that would happen at 100% desiccation ratio.

Figure 47 – Variation of compaction parameters as a function of desiccation ratio: (a) γ_{dmax} of CC mixtures; (b) w_{opt} of CC mixtures.

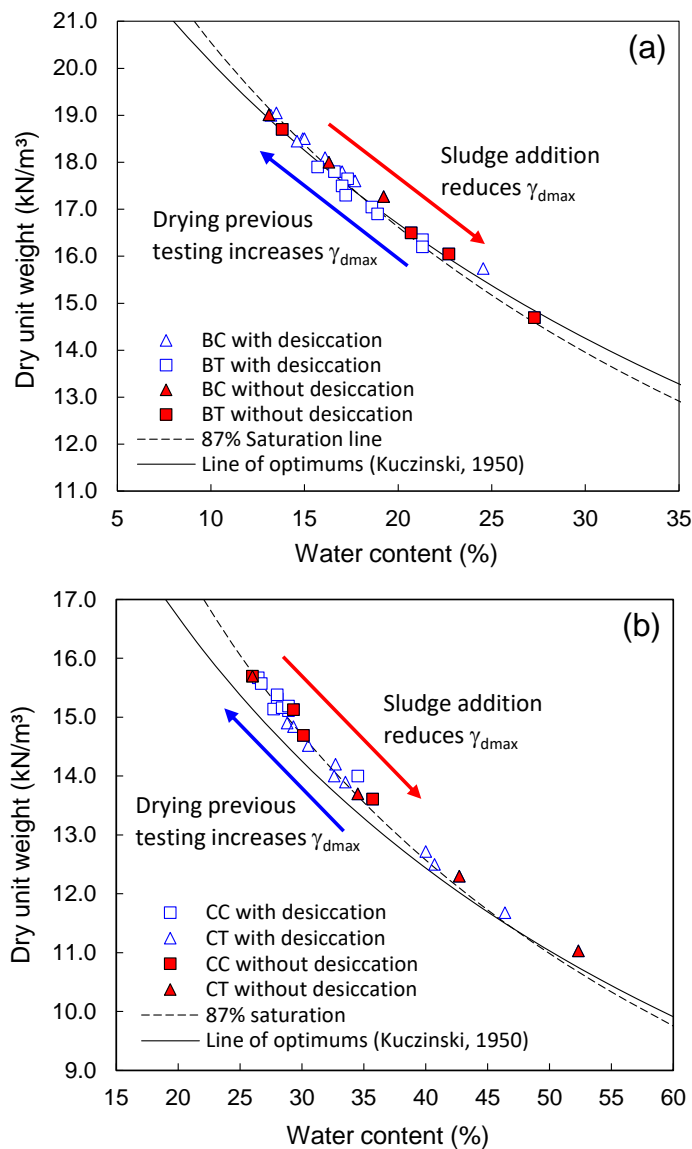


Source: prepared by the author.

Previous air-drying evidently affected the compaction parameters of all mixtures, independently of soil and WTS. Such influence may be a consequence of irreversible changes on WTS physical properties, such as loss of plasticity and cementation of particles, thus improving the compaction behavior of the mixtures.

All obtained pairs of compaction parameters (w_{opt} , γ_{dmax}) for soils and mixtures, with and without desiccation, were observed to move along a line-of-optimums, corresponding approximately to the 87%-saturation-curve, as illustrated in Figure 48. Kuczinski's line-of-optimums (Kuczinski, 1950, apud Massad, 2016) fitted well to the compaction parameters data for the clayey sand and BC and BT mixtures (Figure 48a), and remained below the data of CC and CT mixtures (Figure 48b).

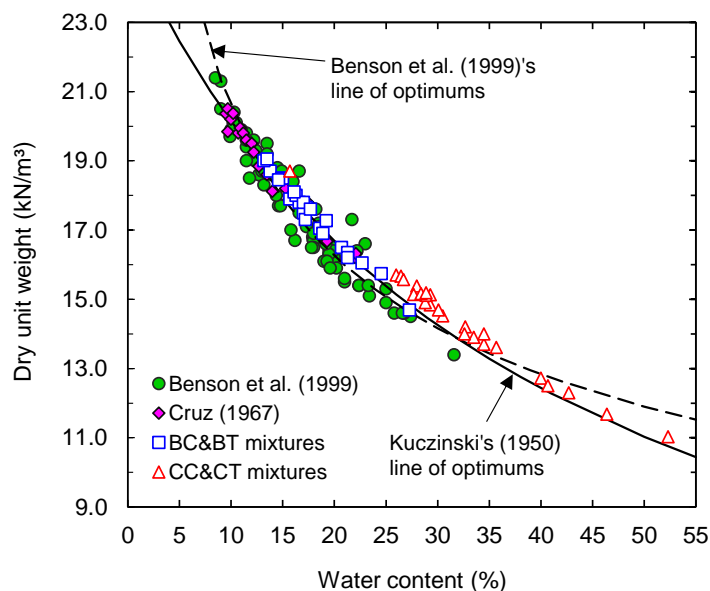
Figure 48 – Variation of compaction parameters with WTS addition and desiccation of: (a) BC and BT mixtures; (b) CC and CT mixtures.



Source: author.

Figure 49 shows a comparison of optimum compaction points of tested mixtures and several soils used in earthworks such as compacted clay liners (BENSON; DANIEL; BOUTWELL, 1999) and embankments (CRUZ, 1967).

Figure 49 – Comparison of optimum compaction parameters.



Source: prepared by the author.

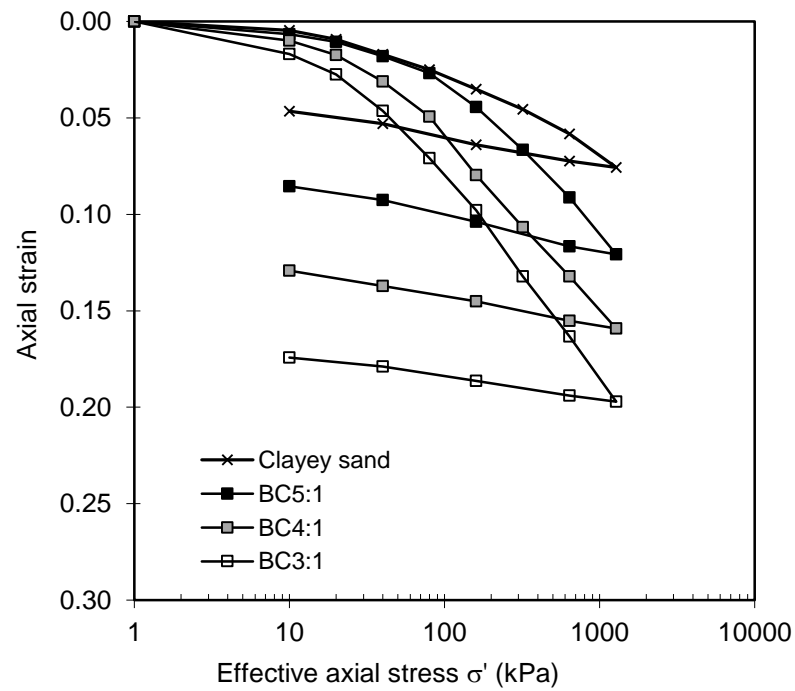
4.6 COMPRESSIBILITY

Oedometric compression curves (stress vs strain) of the clayey sand, BC and BT mixtures, clay, and CC and CT mixtures are shown in Figure 50 to Figure 53. The compacted mixtures were more compressible than the soils. The higher the WTS content, the higher the compressibility of the mixtures. Such behavior was expected since WTS addition causes reduction of dry unit weight and increases plasticity.

A summary of samples' characteristics and indexes computed from the oedometric compression tests is presented in Table 15. Virgin compression indexes (C_c) and swelling indexes (C_s) were determined from the oedometric compression curves (void ratio vs vertical stress) in APPENDIX D.

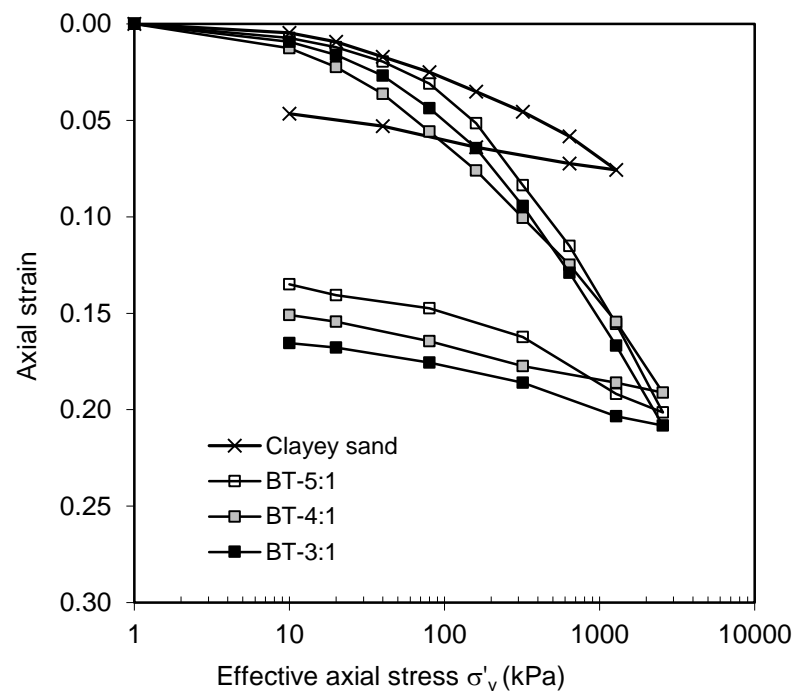
Since WTS addition causes reduction of dry unit weight of the soils, as discussed in the last section, the initial void ratio increases, as can be observed in Table 15. The clay and CC mixtures presented higher void ratios than those of the clayey sand and BC mixtures, coherent with the higher dry unit weight of the compacted clayey sand.

Figure 50 – Stress-strain curves from oedometric compression tests of Botucatu clayey sand and BC mixtures.



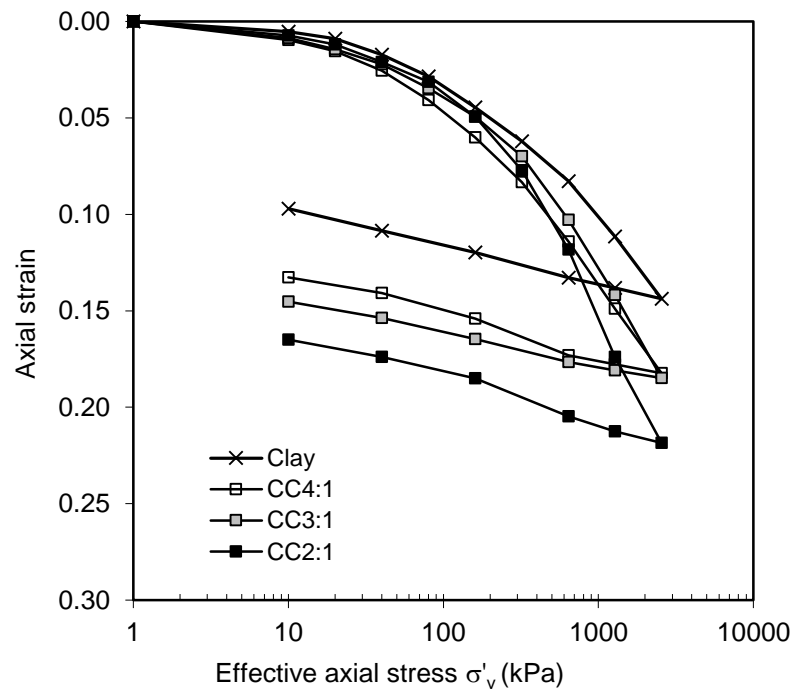
Source: Montalvan (2016)

Figure 51 – Stress-strain curves from oedometric compression tests of Botucatu clayey sand and BT mixtures.



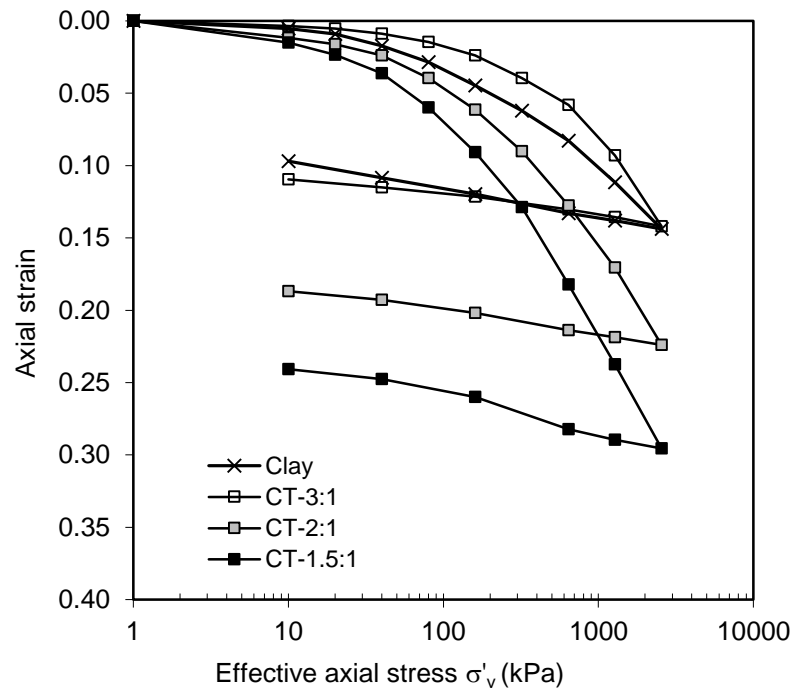
Source: author.

Figure 52 – Stress-strain curves from oedometric compression tests of Campinas clay and CC mixtures.



Source: author.

Figure 53 – Stress-strain curves from oedometric compression tests of Campinas clay and CT mixtures.



Source: author.

Table 15 – Summary of samples characteristics and indexes computed from oedometric compression tests.

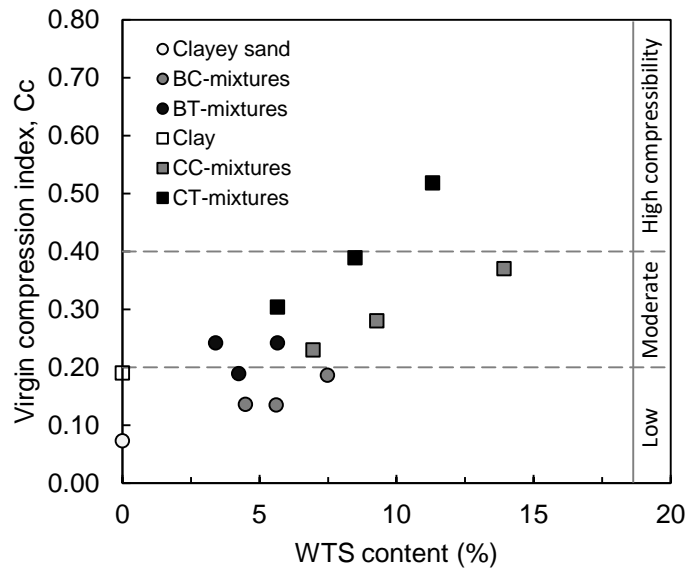
Sample	WTS content (%)	e_0	C_s	C_c	$C_c/(1+e_0)$	Compressibility*
Clayey sand	0.00	0.450	0.02	0.07	0.16	Low
BC5:1	4.49	0.510	0.03	0.14	0.27	Low
BC4:1	5.61	0.540	0.02	0.13	0.25	Low
BC3:1	7.48	0.720	0.02	0.19	0.26	Low
BT-5:1	3.39	0.683	0.05	0.24	0.35	Moderate
BT-4:1	4.24	0.722	0.03	0.19	0.26	Low
BT-3:1	5.66	0.836	0.03	0.24	0.29	Moderate
Clay	0.00	0.853	0.04	0.19	0.22	Low
CC4:1	6.96	1.039	0.04	0.23	0.22	Moderate
CC3:1	9.28	1.072	0.03	0.28	0.26	Moderate
CC2:1	13.92	1.217	0.05	0.37	0.30	Moderate
CT-3:1	5.66	1.176	0.03	0.30	0.26	Moderate
CT-2:1	8.49	1.432	0.04	0.39	0.27	Moderate
CT-1.5:1	11.32	1.752	0.07	0.52	0.30	High

e_0 = void ratio; C_c = compression index; C_s = swelling index

*Classification from Mitchell and Soga (2005)

Figure 54 shows the variation of the virgin compression index (C_c) with WTS content (by dry mass). Values of C_c were higher for Campinas clay mixtures (ranging from 0.19 to 0.52) than for Botucatu clayey sand mixtures (in the range of 0.07 to 0.24), for the same WTS content. However most mixtures presented medium to low compressibility according to the classification of Mitchell and Soga (2005), except for CT1.5:1 mixture. As comparison, average virgin compression index of compacted Brazilian residual soils is about 0.15 (ASSIS; HERNANDEZ; COLMANETTI, 2014). A compacted lateritic soil used in Tucuruí earth dam presented C_c of 0.19 (DIB; ONO, 1985). Some residual saprolitic soils used for highway embankments in the state of São Paulo presented C_c values ranging between 0.16 and 0.44 with average of 0.31 (POZZEBON, 2017).

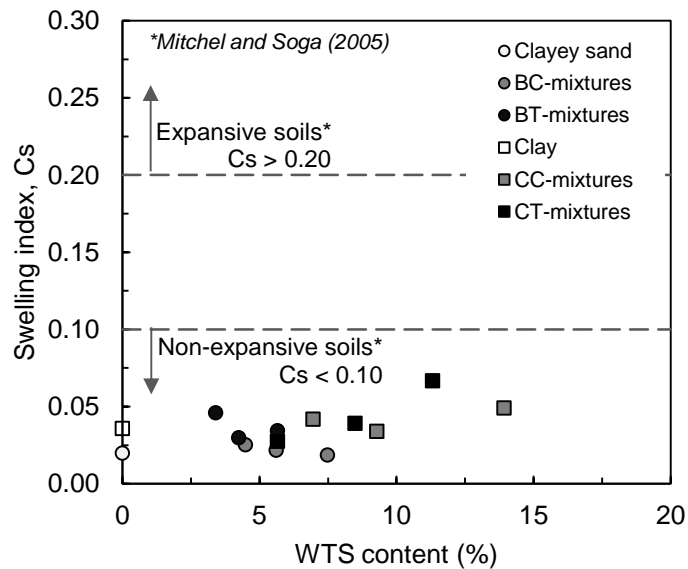
Figure 54 - Variation of compression index with WTS content.



Source: prepared by the author.

WTS addition did not significantly affect the swelling index (C_s), as illustrated in Figure 55, which shows the variation of C_s with WTS content (by dry mass). All tested mixtures presented C_s values below 0.10, and most of them below 0.05, therefore classified as non-expansive soils according to Mitchell and Soga (2005).

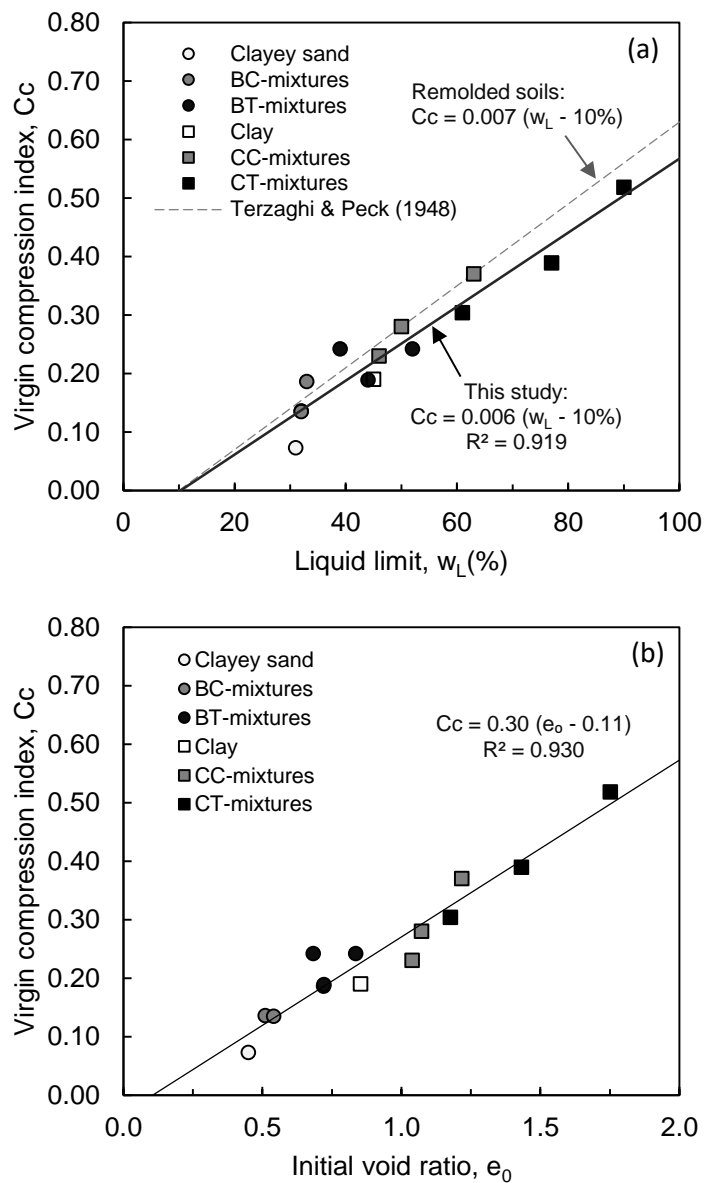
Figure 55 - Variation of swelling index with WTS content.



Source: prepared by the author.

C_c values have been correlated in the literature to state parameters, such as liquid limit, initial void ratio, and natural or initial water content. C_c of the mixtures presented a linear correlation with both liquid limit and initial void ratio. The linear correlation between C_c and liquid limit ($R^2 = 0.92$) was close to the correlation proposed by Terzaghi and Peck (1948) for remolded soils, even though the soils in this research have different genesis and lithology.

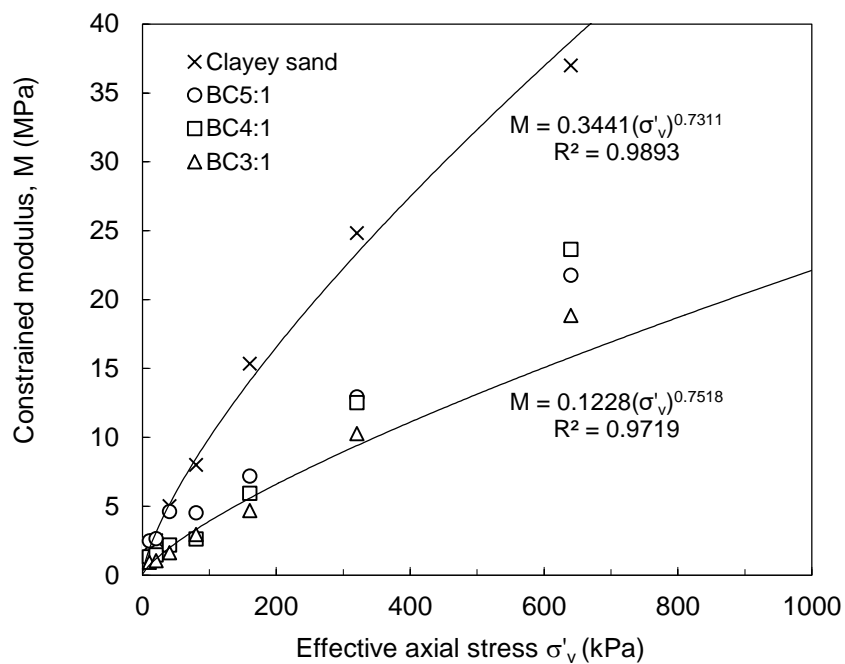
Figure 56 – Correlations of virgin compression index (C_c) with state parameters: (a) C_c – Liquid limit (w_L); (b) C_c – initial void ratio (e_0).



Source: author.

For the calculation of settlements of earthworks such as embankments, the constrained or oedometric modulus (M) of compacted soils is of great significance. The secant constrained modulus for each load increment of the consolidation test was computed and plotted against the lower value of the vertical stress interval. The variation of constrained modulus with vertical stress of all tested soils and mixtures is presented in Figure 57 to Figure 60.

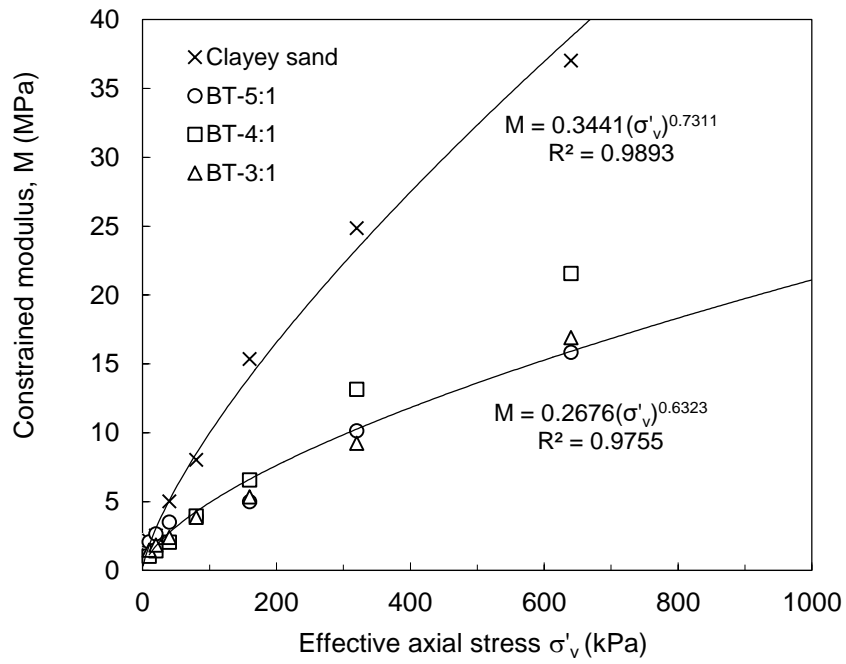
Figure 57 – Variation of constrained modulus (M) with effective vertical stress for Botucatu clayey sand and BC mixtures.



Source: prepared by the author.

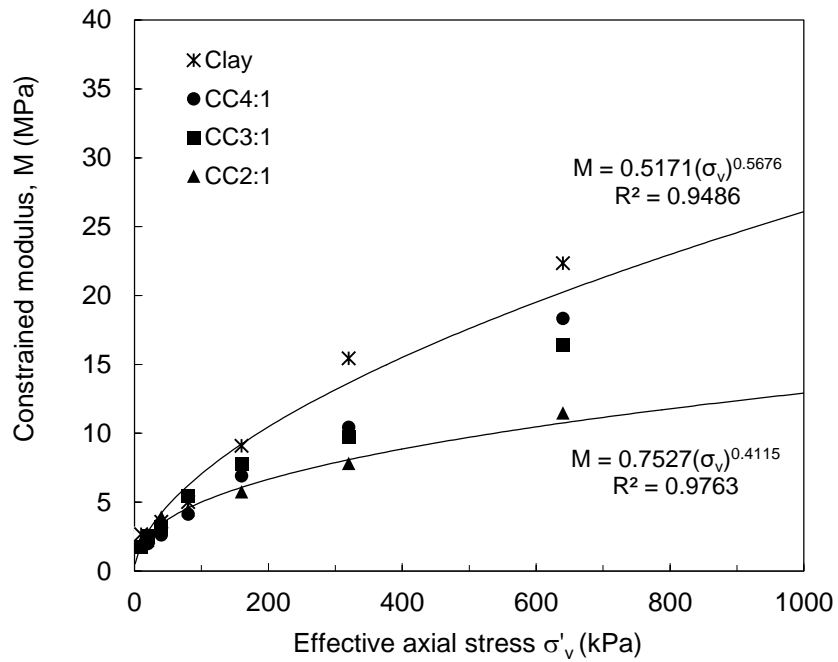
Angelim, Cunha, and Sales (2016) and Pozzebon (2017) reported similar values of constrained modulus of compacted residual soils, ranging from 14 to 47 MPa and from 12 to 30 MPa, respectively, for effective axial stress up to 1000 kPa. Evidently, the clay and its mixtures showed lower values of constrained modulus than the clayey sand and its mixtures, indicating that they are more compressible, as already discussed.

Figure 58 – Variation of constrained modulus (M) with effective vertical stress for Botucatu clayey sand and BT mixtures.



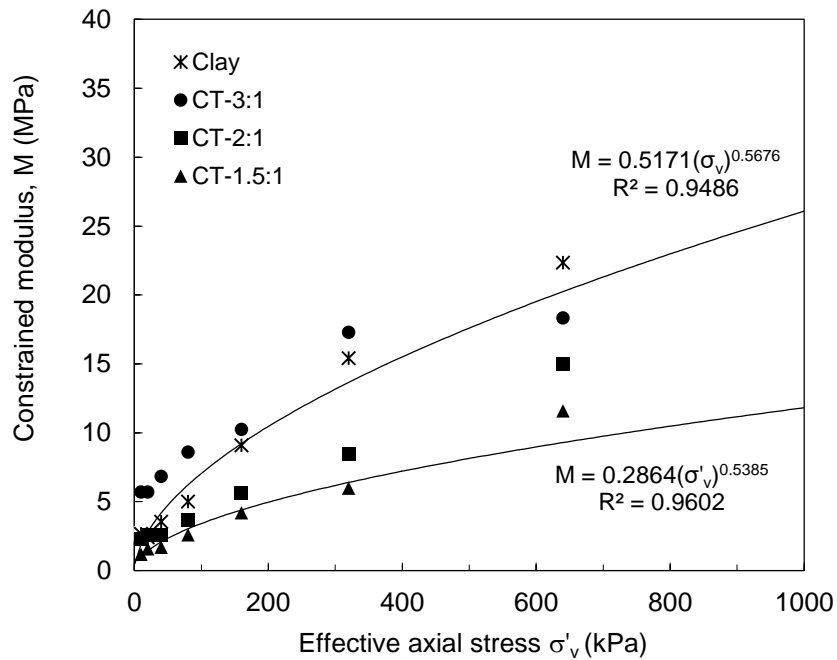
Source: prepared by the author.

Figure 59 – Variation of constrained modulus (M) with effective vertical stress for Campinas clay and CC mixtures.



Source: prepared by the author.

Figure 60 – Variation of constrained modulus (M) with effective vertical stress for Campinas clay and CT mixtures.



Source: prepared by the author.

4.7 PERMEABILITY

All values of hydraulic conductivity presented in this section are referred to a temperature of 20 °C (k_{20}). The variation of hydraulic conductivity with testing time for all mixtures is shown in APPENDIX E, except for BC mixtures whose tests were previously conducted by Montalvan (2016). A summary of samples characteristics, testing conditions and hydraulic conductivity values determined for each material are presented in Table 16.

Although the samples were saturated by backpressure to achieve B-value equal or greater than 0.96, the hydraulic conductivity of all samples decreased over time, tending to stabilize only after long periods of time (weeks). Samples of compacted lateritic soils presented similar behavior (BOSCOV (1997); ZANÓN; LUNARDI; BOSCOV, 2014). Lack of initial saturation would cause permeability to increase rather than to decrease over time. One possibility is migration of colloids inside the sample, eventually causing partial clogging, and reducing permeation flow rate. Dispersion of clay particles and internal swelling can also reduce hydraulic conductivity. Besides, particles migration, void ratio redistributions and fabric changes caused by effective stress can cause changes in flow rate (MITCHELL; SOGA, 2005).

Table 16 – Summary of permeability test samples, testing conditions, and results.

Sample	WTS content (%)	R.C. (%)	Δw (%)	$i=\Delta h/L$	Hydraulic conductivity k_{20} (m/s)		
					$\sigma'_c= 50\text{kPa}$	$\sigma'_c= 100\text{kPa}$	$\sigma'_c= 200\text{kPa}$
Campinas clay	0.0	95.9	-1.00	10	7.0×10^{-9}	3.5×10^{-9}	1.5×10^{-9}
CC4:1	7.0	99.4	0.01	10	4.5×10^{-10}	2.2×10^{-10}	1.2×10^{-10}
CC3:1	9.3	96.2	-0.20	10	2.0×10^{-10}	5.0×10^{-10}	5.0×10^{-10}
CC2:1	13.9	100.3	0.10	10	2.0×10^{-10}	1.5×10^{-10}	1.1×10^{-10}
CT3:1	5.7	95.4	-0.12	20	1.0×10^{-9}	-	-
CT2:1	8.5	100.2	0.04	20	2.0×10^{-9}	-	-
CT1.5:1	11.3	100.3	0.10	20	3.5×10^{-10}	-	-
Botucatu Clayey sand	0.0	97.2	-0.40	10	1.0×10^{-8}	-	-
BT5:1	3.4	99.5	0.50	10	6.0×10^{-10}	-	-
BT4:1	4.2	96.1	-0.04	10	3.5×10^{-9}	-	-
BT3:1	5.7	102	-0.05	10	3.0×10^{-10}	-	-

Source: author.

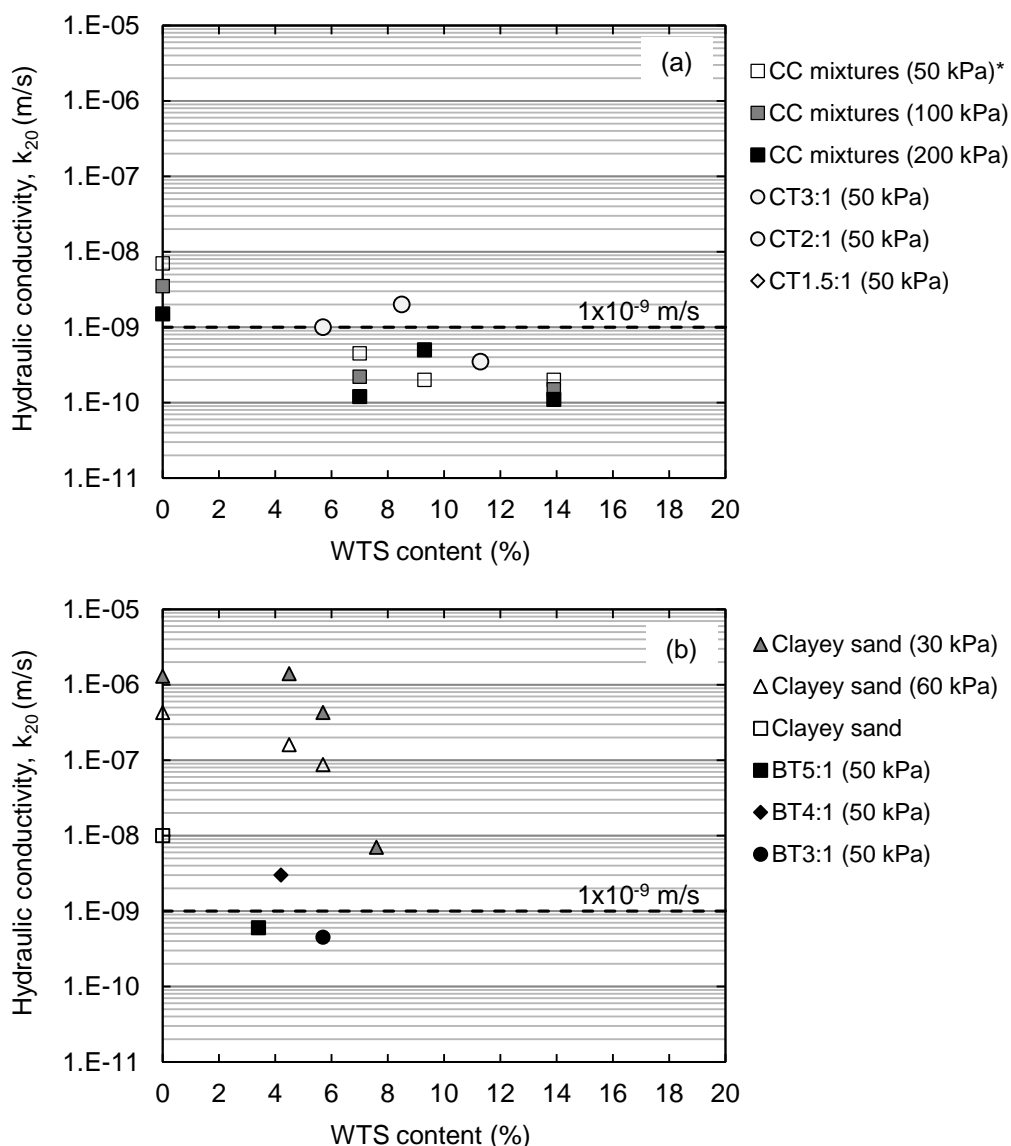
The clay presented hydraulic conductivity about 7×10^{-9} m/s for confining pressure of 50 kPa, reducing to 1.5×10^{-9} m/s for confining pressure of 200 kPa. The clayey sand (first sampling) tested by Montalvan (2016) showed hydraulic conductivity around 1×10^{-6} m/s for confining pressure equal to 30 kPa, and 4×10^{-7} m/s for confining pressure of 60 kPa. The clayey sand from the second sampling presented lower hydraulic conductivity, of 1×10^{-8} m/s for 50 kPa confining pressure.

Figure 61 shows the variation of hydraulic conductivity with WTS addition. WTS addition reduced the permeability of the soils, and the effect was more drastic for BC mixtures. However, all BC mixtures presented permeability higher than 1×10^{-9} m/s (minimum recommended for clay liners). On the other hand, all CC mixtures reached k-value smaller than 1×10^{-9} m/s.

The BT and CT mixtures presented hydraulic conductivity slightly higher than 1×10^{-9} m/s. Since those mixtures were compacted at optimum water content, it is likely that a hydraulic conductivity lower than 1×10^{-9} m/s will be obtained when compacted at wet-of-optimum.

CT and BT mixtures were only tested with 50 kPa confining pressure, since the k-value took very long to stabilize (APPENDIX E).

Figure 61 – Hydraulic conductivity variation with WTS content for: (a) CC¹ and CT¹ mixtures; (b) BC² and BT¹ mixtures.



*Values in parentheses correspond to the consolidation confining pressure

Source: ¹prepared by the author; ²Montalvan (2016).

Incorporation of small WTS contents into natural soils results in a reduction of permeability, indicating the possible use of mixtures of lateritic soils with WTS as CCLs. Mixtures that did not attend the criteria of k equal or lower than 1×10^{-9} m/s should be tested at wet-of-optimum to define an acceptable compaction zone for this application.

Besides, the capacity of lateritic soils and WTS for retention of heavy metals makes them excellent buffer materials for waste containment (BASSO; PARAGUASSÚ, 2006; GABAS; SARKIS; BOSCOV, 2014; ABO-EL-ENEIN; SHEBL; ABO EL-DAHAB, 2017).

4.8 TRIAXIAL COMPRESSION

Compaction conditions (w and γ_d) of tested specimens in consolidated undrained triaxial compression tests (CU) and obtained values of maximum principal stress ratio, maximum deviator stress and parameter A at failure are presented in Table 17 and Table 18. Interpretation and discussion of the results is divided in two parts: undrained shear strength and shear strength in terms of effective stress.

4.8.1 Undrained shear strength

The undrained shear strength (s_u) of tested samples was taken as half the maximum deviator stress from *deviator stress vs axial strain* graphs presented in APPENDIX F. The obtained values of A -coefficient at failure (A_f) correspond to those of overconsolidated clays, in the range of -0.5 to 0.7 (LAMBE; WHITMAN, 1969), which reflects the overconsolidated condition of the tested samples due to compaction-induced pre-stress. Moreover, the values of s_u/σ'_{1c} are also similar to those of overconsolidated soils (TERZAGHI; PECK; MESRI, 1996).

Power function curves fitted to undrained strengths are depicted in Figure 62 and Figure 63. Although the general trend is that WTS addition reduces undrained strength, some CC- and CT-mixtures presented higher undrained strength than Campinas clay for the same effective consolidation stress (σ'_c).

On the other hand, Botucatu clayey sand presented higher undrained strength than all BC- and BT- mixtures, and the influence of WTS addition on the reduction of s_u is evident. The undrained strength values of Botucatu clayey sand from CIU tests are compatible with those from CAU tests (Montalvan, 2016), except for the CIU test with effective consolidation stress of 200 kPa, which presented a much lower value. This value should be disregarded, since the general trend in all tests was the increase of undrained strength with increasing effective consolidation stress, as expected.

Table 17 – Characteristics of specimens and parameters from triaxial compression tests (CU) on Campinas clay and mixtures.

Sample	w (%)	γ_d (kN/m ³)	Δw (%)	RC (%)	σ'_{1c} (kPa)	$(\sigma'_1/\sigma'_3)_{max}$	$(\sigma_1-\sigma_3)_{max}$ (kPa)	Δu_f (kPa)	\bar{A}_f	s_u (kPa)	s_u/σ'_{1c}
Campinas Clay	26.4	15.6	+0.4	99.3	50	5.46	164.7	0.4	0.00	82.4	1.65
(CIU)	26.4	15.6	+0.4	99.3	100	4.97	182.4	26.1	0.14	91.2	0.91
	26.4	15.6	+0.4	99.3	200	4.21	295.3	100.6	0.34	147.7	0.74
CC4:1	29.0	14.8	-0.3	97.6	50	5.42	150.9	2.1	0.01	75.5	1.51
(CIU)	29.0	14.8	-0.3	97.6	100	5.03	217.5	32.2	0.15	108.8	1.09
	29.5	14.8	+0.2	97.7	200	4.67	337.8	85.2	0.25	168.9	0.84
CC3:1	29.8	14.3	-0.3	97.0	50	5.82	179.1	-7.6	-0.04	89.5	1.79
(CIU)	29.8	14.3	-0.3	97.0	100	5.32	224.3	28.9	0.13	112.1	1.12
	30.4	14.3	+0.3	97.6	200	4.96	229.0	131.9	0.58	114.5	0.57
CC2:1	36.0	13.3	+0.3	97.9	50	5.48	120.5	10.3	0.09	60.2	1.20
(CIU)	36.0	13.3	+0.3	97.9	100	4.89	132.6	57.1	0.43	66.3	0.66
	36.0	13.3	+0.3	97.9	200	4.48	199.4	134.1	0.67	99.7	0.50
CT3:1	34.2	13.3	+0.1	96.2	50	7.78	214.2	-8.4	-0.04	107.1	2.14
(CIU)	34.2	13.3	+0.1	96.2	100	6.75	220.5	41.8	0.19	110.3	1.10
	34.2	13.3	+0.1	96.2	200	5.59	302.6	117.3	0.39	151.3	0.76
CT2:1	42.1	12.4	-0.6	100.7	50	7.70	176.7	2.6	0.02	88.4	1.77
(CIU)	42.1	12.4	-0.6	100.7	100	6.49	214.8	41.0	0.19	107.4	1.07
	42.1	12.4	-0.6	100.7	200	5.57	268.2	121.7	0.45	134.1	0.67
CT1.5:1	52.7	11.0	+0.4	100.2	50	8.00	141.3	12.3	0.09	70.7	1.41
(CIU)	52.7	11.0	+0.4	100.2	100	5.91	175.8	53.5	0.30	87.9	0.88
	52.7	11.0	+0.4	100.2	200	5.08	233.4	131.4	0.56	116.7	0.58

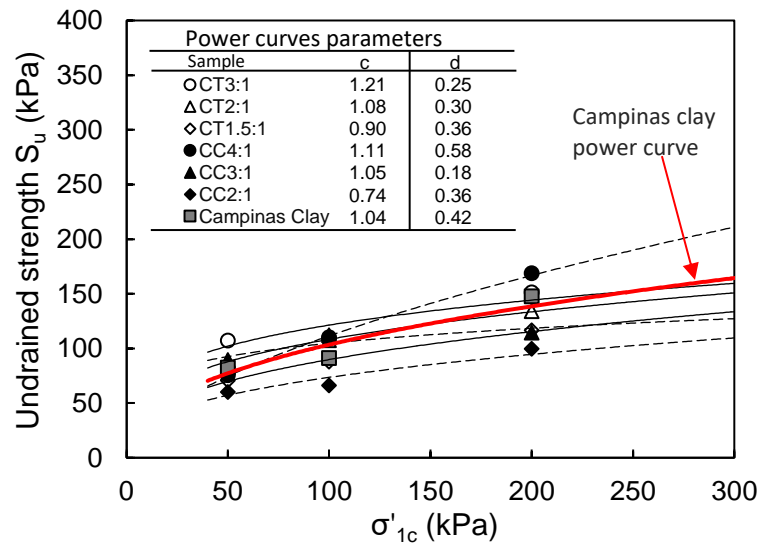
* Δu_f at maximum deviator stress $(\sigma_1-\sigma_3)_{max}$

Table 18 – Characteristics of specimens and parameters from triaxial compression tests (CU) on Botucatu clayey sand and mixtures.

Sample	w (%)	γ_d (kN/m ³)	Δw (%)	RC (%)	σ'_{1c} (kPa)	$(\sigma'_1/\sigma'_3)_{max}$	$(\sigma_1-\sigma_3)_{max}$ (kPa)	Δu_f^* (kPa)	\bar{A}_f	s_u (kPa)	s_u/σ'_{1c}
Clayey sand (CAU)	12.8	18.6	-0.4	97.9	63	6.05	264.1	-26.4	-0.10	132.1	2.95
	12.8	18.6	-0.4	97.9	125	4.63	351.0	-8.7	-0.03	175.5	1.68
	12.8	18.6	-0.4	97.9	250	4.25	494.6	46.8	0.09	247.3	0.65
BC5:1(CAU)	15.3	17.6	-	-	63	5.91	171.9	6.4	0.04	86.0	2.11
	15.3	17.6	-	-	125	5.00	201.6	42.4	0.21	100.8	1.40
	15.3	17.6	-	-	250	4.44	354.3	86.1	0.24	177.2	0.99
BC4:1(CAU)	19.2	17.3	-	-	62	6.34	202.8	-1.0	-0.01	101.4	1.38
	19.2	17.3	-	-	125	5.15	231.0	36.8	0.16	115.5	0.81
	19.2	17.3	-	-	250	4.47	300.3	123.1	0.41	150.2	0.71
BC3:1(CAU)	24.5	15.7	-	-	63	7.08	105.4	28.7	0.27	52.7	1.62
	24.5	15.7	-	-	125	5.53	136.4	67.2	0.49	68.2	0.92
	24.5	15.7	-	-	250	5.08	207.4	151.0	0.73	103.7	0.60
Clayey sand (CIU)	13.8	18.3	0.0	96.7	50	5.01	295.2	-51.0	-0.17	147.6	0.84
	13.8	18.3	0.0	96.7	100	4.48	336.2	-21.1	-0.06	168.1	0.55
	13.5	18.0	-0.3	95.0	200	3.99	260.9	108.1	0.41	130.4	0.41
BT5:1 (CIU)	21.3	16.1	+0.6	97.7	50	5.97	186.0	-11.7	-0.06	93.0	1.86
	21.3	16.1	+0.6	97.7	100	4.67	191.2	38.2	0.20	95.6	0.96
	21.3	16.1	+0.6	97.7	200	4.54	290.7	101.8	0.35	145.3	0.73
BT4:1 (CIU)	22.0	15.5	-0.8	96.5	50	5.29	159.2	4.8	0.03	79.6	1.59
	22.0	15.5	-0.8	96.5	100	4.94	232.7	25.8	0.11	116.3	1.16
	23.0	15.4	+0.2	95.7	200	4.31	266.0	111.1	0.42	133.0	0.67
BT3:1 (CIU)	27.4	14.7	+0.1	99.8	50	5.11	145.9	13.7	0.09	72.9	1.46
	27.4	14.7	+0.1	99.8	100	4.81	188.6	43.2	0.23	94.3	0.94
	27.4	14.7	+0.1	99.8	200	4.60	253.4	122.2	0.48	126.7	0.63

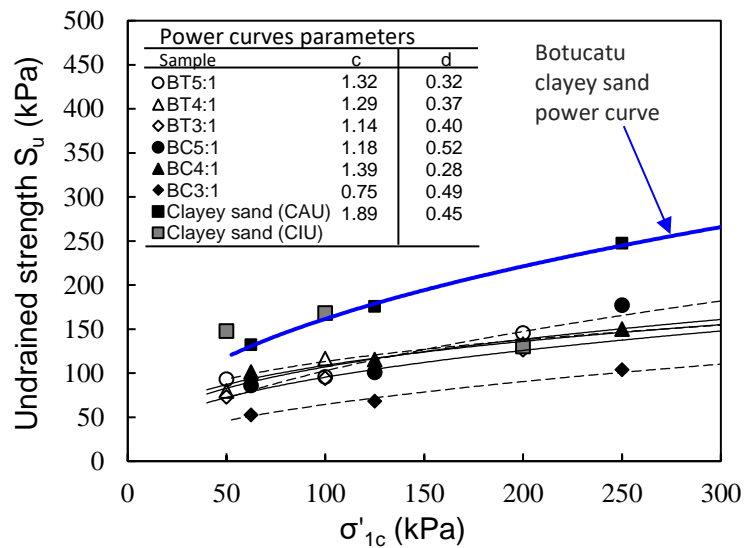
* Δu_f at maximum deviator stress $(\sigma_1-\sigma_3)_{max}$

Figure 62 – Undrained shear strength (s_u) versus consolidation principal major stress (σ'_{1c}) for Campinas clay and mixtures.



Source: author.

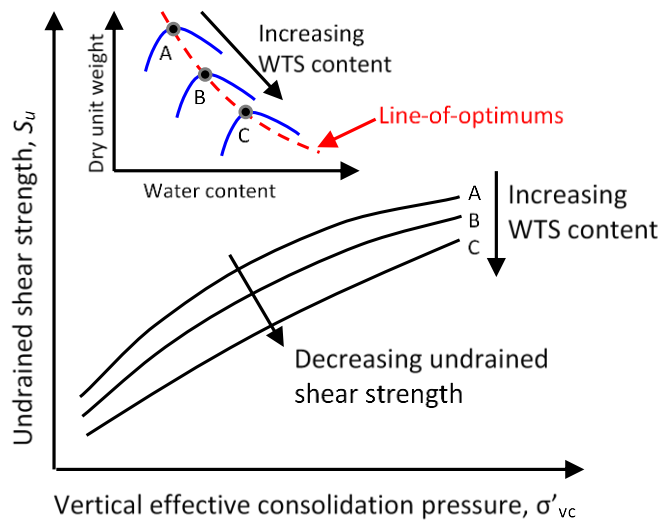
Figure 63 – Undrained shear strength (s_u) versus consolidation principal major stress (σ'_{1c}) for Botucatu clayey sand and mixtures.



Source: author.

The influence of WTS on the relationship $s_u-\sigma'_{1c}$ is analogous to the influence of relative compaction on the undrained shear strength (Vandenberge; Brandon; Duncan, 2014): s_u tends to decrease with increasing WTS content (decreasing dry unit weight) as shown in Figure 64.

Figure 64 – Influence of WTS addition on dry unit weight and undrained shear strength

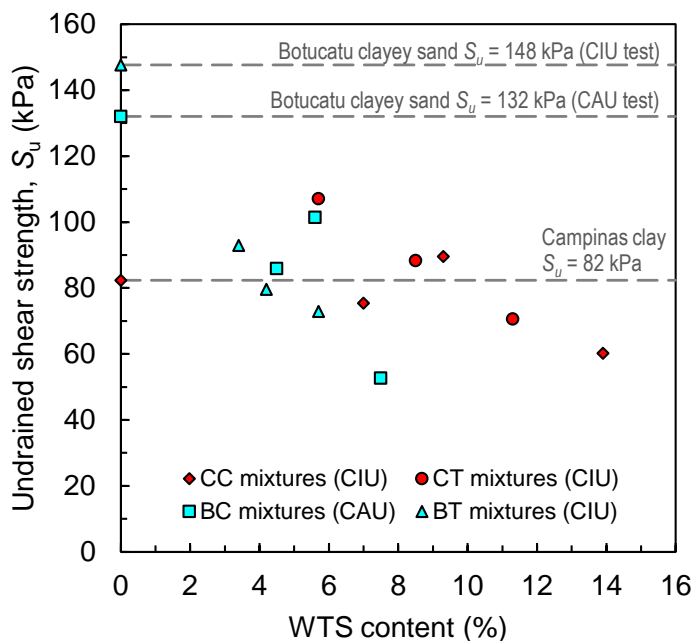


Source: Modified from Vandenberg; Brandon; Duncan (2014).

To evaluate the suitability of mixtures as construction material for earthworks, the lower undrained strength was considered, i.e. correspondent to the lower effective consolidation stress (50 kPa). Figure 65 shows the variation of s_u (for $\sigma'_c = 50$ kPa) with WTS content (by dry mass). Botucatu clayey sand presented the highest undrained shear strength values, 148 kPa for CIU tests and 132 kPa for CAU tests. In general, undrained strength was reduced with increasing WTS content. BC mixtures presented S_u in the range of 53 to 101 kPa, and BT mixtures in the range of 73 to 93 kPa.

On the other hand, Campinas clay presented undrained shear strength of 82 kPa. s_u values of CC mixtures ranged from 60 to 90 kPa, and those of CT mixtures from 71 to 107 kPa. CC3:1, CT3:1, and CT2:1 mixtures showed higher undrained shear strength than Campinas clay.

BC3:1 and CC2:1 presented the lowest values of undrained shear strength, 53 and 60 kPa. As discussed in section 2.5.2, the minimum undrained shear strength usually adopted as requirement for earthworks usually ranges from 40 to 50 kPa. However, these values are indicated for as-compacted undrained shear strength and for unconfined condition or very low confining pressure. This discussion will be resumed after presenting the results from unconfined compression tests.

Figure 65 – Variation of undrained shear strength (for $\sigma'_{3c} = 50\text{kPa}$) with WTS content.

Source: author.

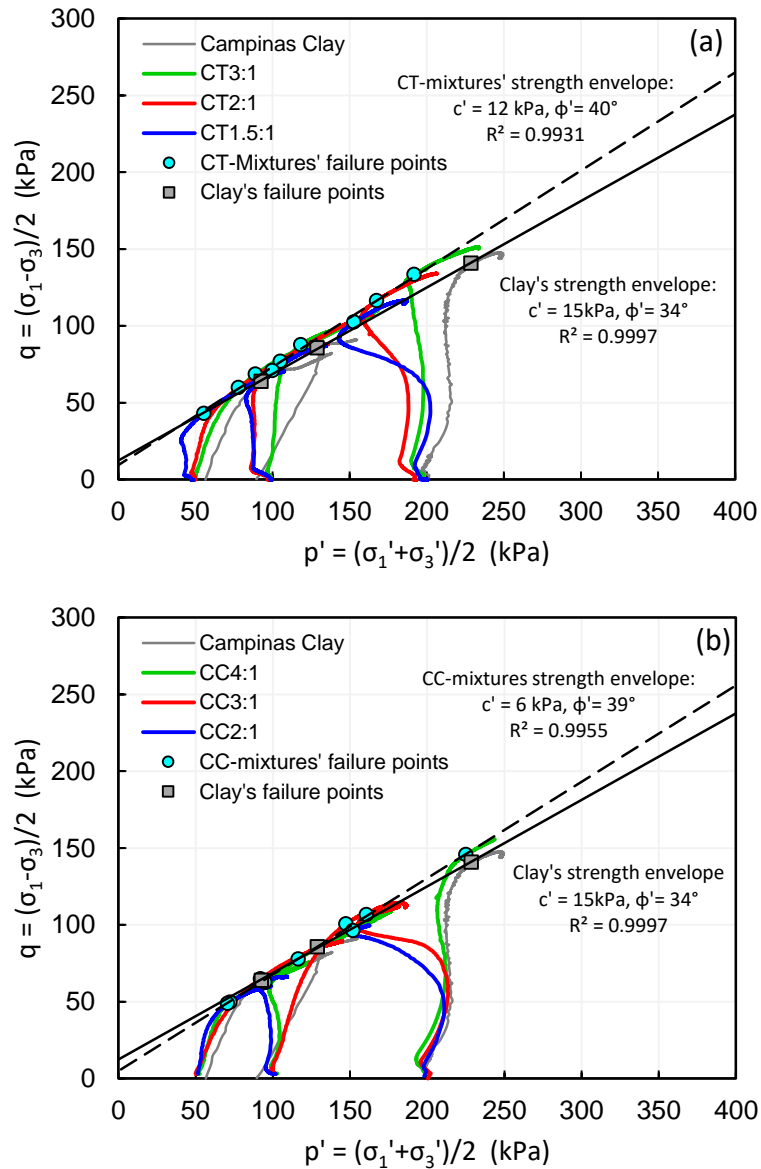
4.8.2 Shear strength in terms of effective stresses

The effective stress paths obtained from the consolidated undrained triaxial tests of Campinas clay and CC- and CT-mixtures are depicted in Figure 66. Failure points were considered at maximum principal effective stress ratio (σ'_1/σ'_3), see graphs in APPENDIX F.

The effective friction angle (ϕ') and the cohesion intercept (c') for Campinas clay were 34° and 15 kPa, respectively. The ϕ' and c' values for CT and CC mixtures are presented in Table 19. All mixtures presented higher friction angle than Campinas clay, ranging from 36 to 39° . A single strength envelope for mixtures with the same WTS fitted well ($R^2 > 0.99$). For CC mixtures (considering all failure points), a friction angle of 39° and intercept cohesion of 6 kPa were computed, and for CT mixtures (considering all failure points), the friction angle and cohesion were 40° and 12 kPa, respectively.

Figure 67 shows failure points of all the tests, the lower bound, the lower bound shear strength envelope of Campinas clay, the upper bound envelope of CT mixtures, and an average strength envelope considering all failure points of the clay and the mixtures.

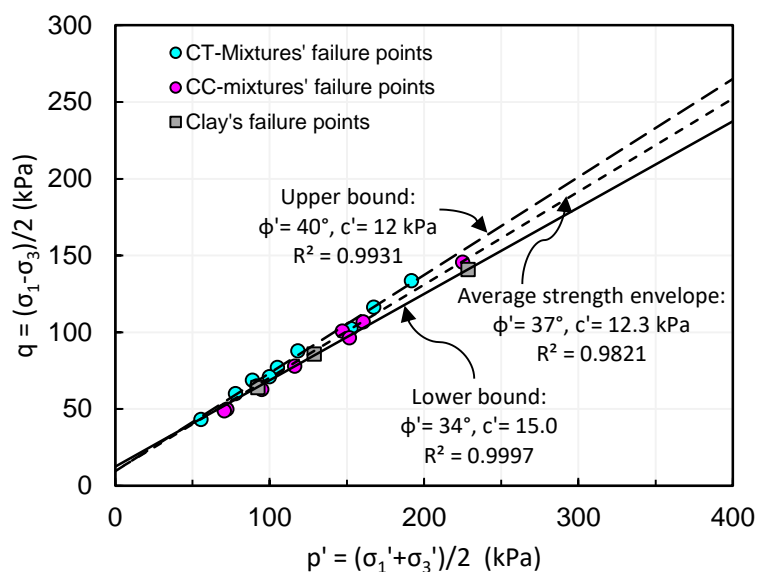
Figure 66 – Effective stress paths for Campinas clay and: (a) CT mixtures; (b) CC mixtures.



Source: author.

The effective stress paths for Botucatu clayey sand and its mixtures are depicted in Figure 68. The ϕ' and c' values of Botucatu clayey sand, from CIU tests, were 32° and 15 kPa, respectively, whereas from CAU tests were 34° and 22 kPa, respectively.

Figure 67 – Effective strength envelope for Campinas clay, and CC and CT mixtures.



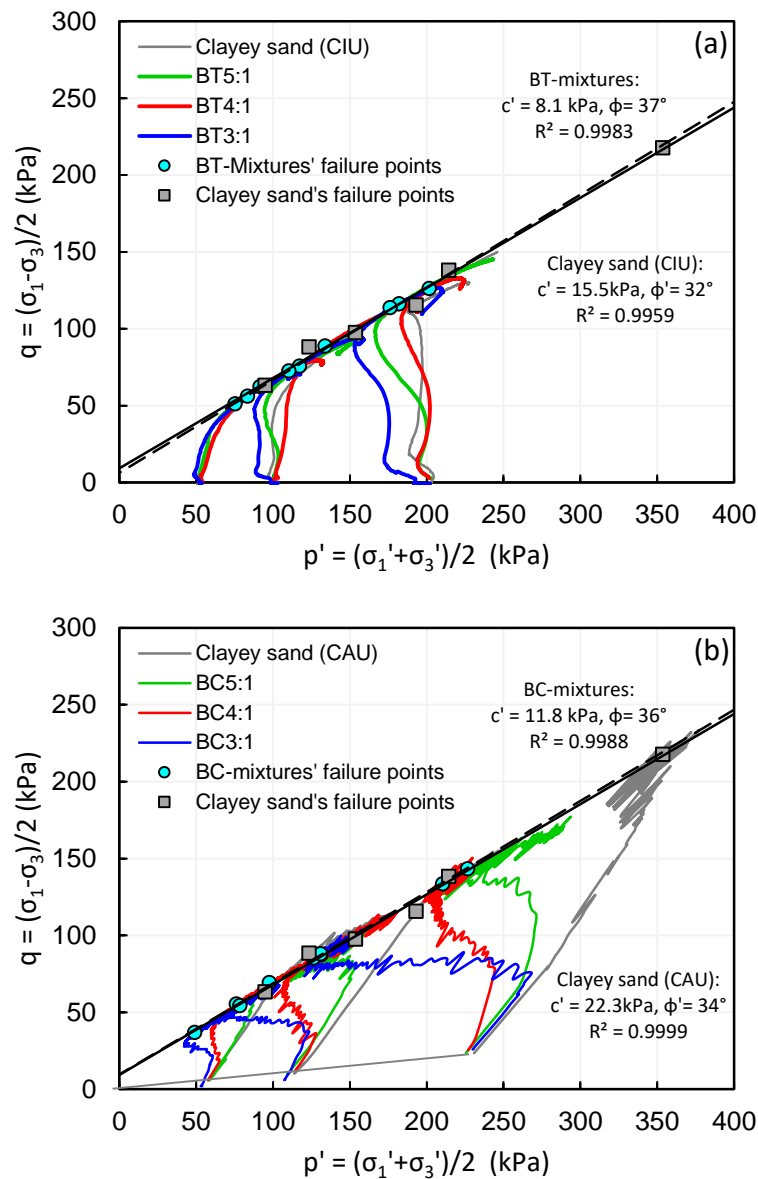
Source: author.

Table 19 – Mohr-Coulomb effective shear strength parameters of soils and mixtures.

Sample	c' (kPa)	φ' (°)
Botucatu Clayey sand ¹	22	34
Botucatu Clayey sand ²	15	32
BC5:1 ¹	17	34
BC4:1 ¹	15	35
BC3:1 ¹	10	37
BT5:1 ²	6	38
BT4:1 ²	13	35
BT3:1 ²	6	38
Campinas Clay ²	15	34
CC4:1 ²	6	39
CC3:1 ²	10	38
CC2:1 ²	9	36
CT3:1 ²	17	39
CT2:1 ²	14	39
CC1.5:1 ²	12	38

Source: ¹Montalvan(2016) ; ²author.

Figure 68 – Effective stress paths for Botucatu clayey sand and: (a) BT mixtures; (b) BC mixtures.



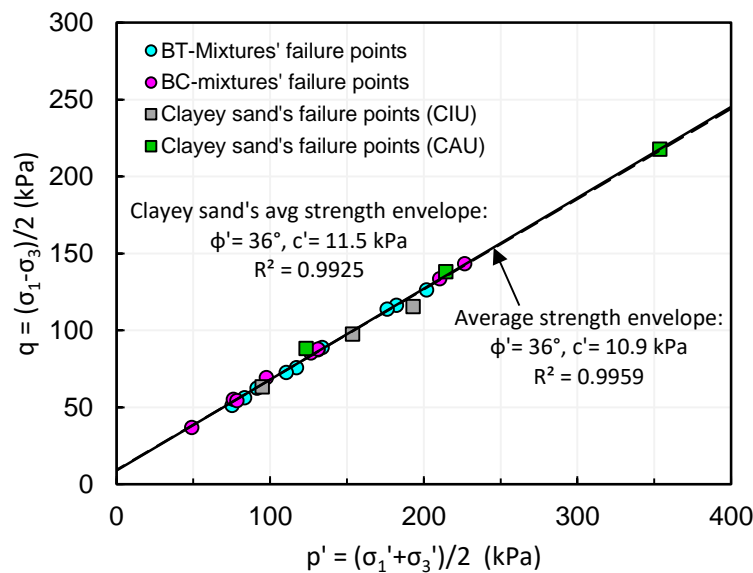
Source: (a) author; (b) modified from Montalvan (2016).

It is not a surprise that both soils presented relatively high values of ϕ' . Compacted lateritic soils usually exhibit high ϕ' values, even those with predominant clay fraction as Campinas clay. Moreover, excellent engineering behavior in many earthworks, such as embankments and road pavement bases, has been reported for those soils (CRUZ, 1967; NOGAMI; VILLIBOR, 1991).

BC and BT mixtures presented ϕ' ranging from 34 to 38°, and c' in the range of 6 to 17 kPa. The ϕ' of BT and BC mixtures when considering all failure points were equal to 37 and 36°, respectively, whereas c' values were 8 and 12 kPa, respectively.

Figure 69 shows failure points for the clayey sand and its mixtures. The average strength envelope computed using all failure points (soil and mixtures) presented ϕ' and c' values equal to 36° and 11 kPa ($R^2 > 0.99$), respectively. It seems that addition of WTS did not alter the effective shear strength parameters of Botucatu clayey sand.

Figure 69 – Effective strength envelope for Botucatu clayey sand, and BC and BT mixtures.



Source: author.

Most mixtures presented friction angle slightly higher and cohesion slightly lower than those of the soils, indicating a slight influence of WTS incorporation into the soils. Addition of clayey material with high plasticity index was expected to reduce the friction angle. Nonetheless, values of c' around zero kPa (O'KELLY; QUILLE, 2010), and ϕ' higher than 40° (O'KELLY; QUILLE, 2010; ROQUE; CARVALHO, 2006) have been reported for WTS. Besides, Balkaya (2015) reported that mixtures of zeolite and WTS exhibit increase of ϕ' and decrease of c' with increasing WTS content.

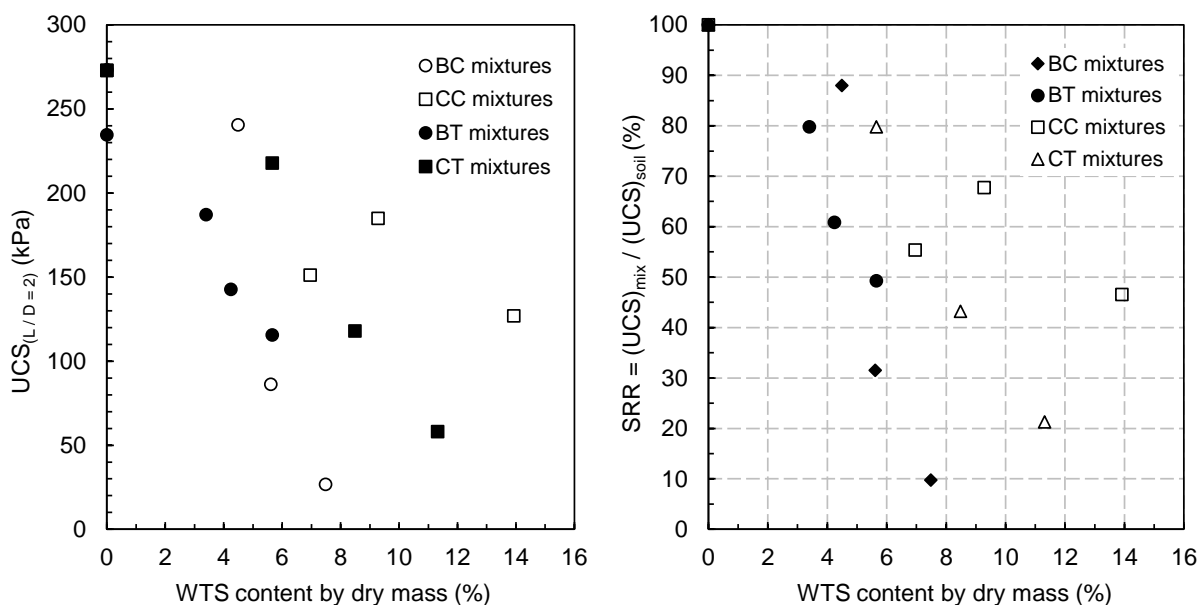
Effective stress paths show that development of excess pore pressure (PWP) increased with increasing WTS content, which can be better observed in the graphs of *excess-PWP vs. axial strain* presented in APPENDIX F. This may be explained by the increment in compressibility with increasing WTS content, and possibly also by lower

compaction-induced pre-stress. Development of higher excess PWP would explain the lower values of undrained shear strength of the mixtures.

4.9 UNCONFINED COMPRESSION

Diagrams of *axial stress vs. axial strain* obtained from unconfined compression tests (UC) are presented in APPENDIX G. Maximum axial stresses were corrected relative to L/D relation using equation (11). The unconfined compressive strength (UCS), i.e. the corrected maximum axial stress, tended to reduce and the axial strain at failure to grow with increasing WTS content. Figure 70a shows the variation of unconfined compressive strength with WTS content. Figure 70b illustrates the UCS of mixtures as percentage of the UCS of the respective soil, represented by the Strength Reduction Ratio (SRR).

Figure 70 – As-compacted UCS of soils and mixtures: (a) UCS variation with WTS content; (b) Strength Reduction Ratio (SRR) variation with WTS content.



Source: author.

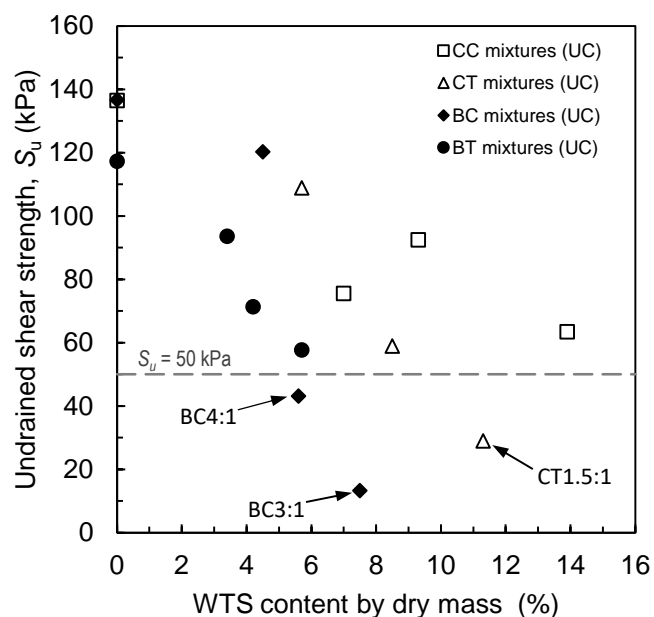
Since UC tests were conducted at a high shear rate (1%/min), an undrained condition at failure can be assumed. Therefore, the undrained shear strength, for as-compacted condition, was computed as half the unconfined compression strength.

The unconfined compressive strength of as-compacted samples is representative of field conditions, at least for small soil depth, where confining pressures are low. In view that confining pressures will increase with depth, causing

shear strength to increase as well, as-compacted undrained shear strength was considered as a lower bound. Hence, this value can be used to evaluate the material suitability for earthworks comparing to a minimum acceptable value (e.g. 50 kPa).

The variation of as-compacted undrained shear strength with WTS content of tested soils and mixtures is presented in Figure 71. Considering a minimum acceptable undrained shear strength of 50 kPa, only three of the mixtures (BC4:1, BC3:1, and CT1.5:1) are below the threshold.

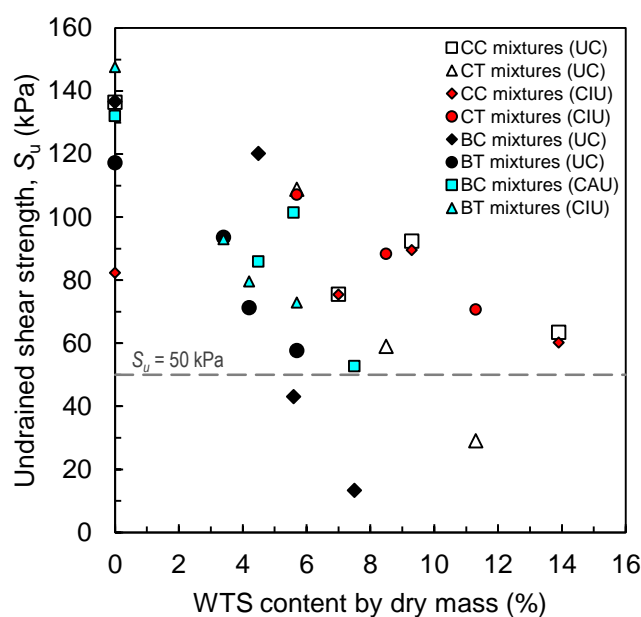
Figure 71 – Variation of as-compacted undrained shear strength with WTS content.



Source: author.

Figure 72 shows the as-compacted undrained shear strength (unsaturated) from UC tests compared to the undrained shear strength (saturated) from CU tests for 50 kPa confining pressure. The undrained shear strength from UC tests was equal or smaller than that from CU tests. The undrained shear strength from UC tests is greatly influenced by matric suction, due to the unsaturated condition. When undrained strength from UC and CU tests are equal, matric suction could be considered to be causing an increment in undrained shear strength equivalent to an effective confining pressure of 50 kPa. On the other hand, mixtures with higher compaction water content, with probably lower suction values and a lower strength gain due to suction, presented undrained shear strength from UC test much lower than from CU test.

Figure 72 – Comparison of undrained shear strength from UC (as-compacted) and CU tests (50 kPa confining pressure).



Source: author.

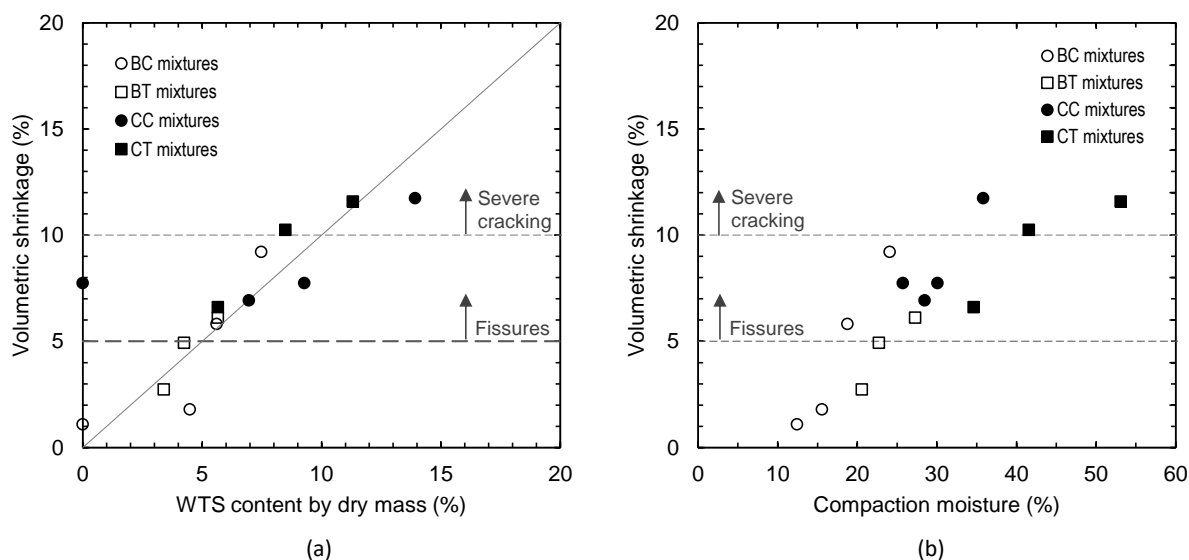
4.10 VOLUMETRIC SHRINKAGE

For some geotechnical applications, e.g. compacted landfill covers and liners, soil shrinkage must be limited to avoid cracking. Kleppe and Olson (1985) indicated that cracks may begin to appear at volumetric shrinkage of 4 to 5%, and at around 10% severe cracking may develop.

To avoid shrinkage-induced cracking due to desiccation, it is important to define a maximum acceptable limit of shrinkage, especially for landfill covers in arid areas. This parameter is seldom considered in earthworks, although it is of great importance.

Figure 73 shows the maximum volumetric shrinkage of tested soils and mixtures after full desiccation. Campinas clay and Botucatu clayey sand presented volumetric shrinkage of 7.7 and 1.1 %, respectively. The volumetric shrinkage of the mixtures was greater than that of the corresponding soil. As expected, the greater the WTS content, the higher the volumetric shrinkage of the mixture. Interestingly, the volumetric shrinkage of the mixtures was almost equal to the WTS content. The increment in the volumetric shrinkage is related to the increase in compaction moisture caused by WTS addition, as illustrated in Figure 73b.

Figure 73 – Variation of total volumetric shrinkage with: (a) WTS content; (b) Compaction moisture.

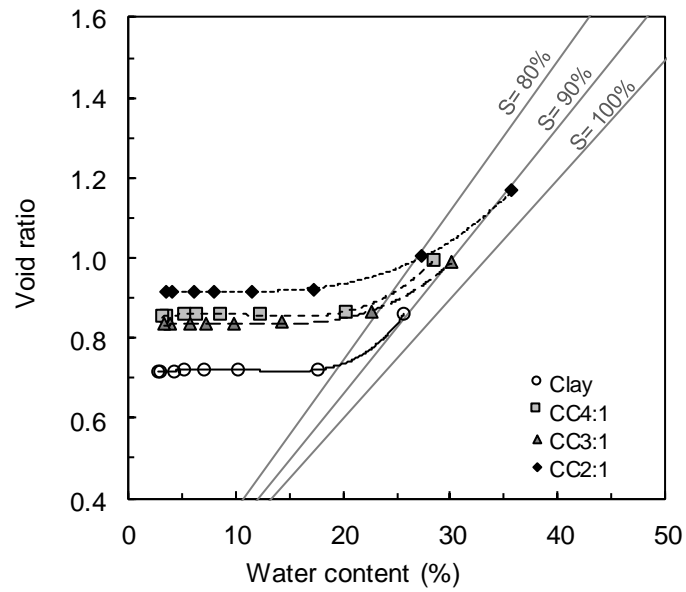


Source: author.

Among the tested soils and mixtures, the only samples that presented volumetric shrinkage lower than 5% were Botucatu clayey sand, BC5:1, BT5:1, and BT4:1. All samples underwent volumetric shrinkage smaller than 10%, except for CC2:1, CT2:1, and CT1.5:1. The shrinkage curves (*void ratio vs. water content*) of soils and mixtures are presented in Figure 74 to Figure 77. Saturation at compaction of most samples was about 90%, coherent with compaction near the optimum condition.

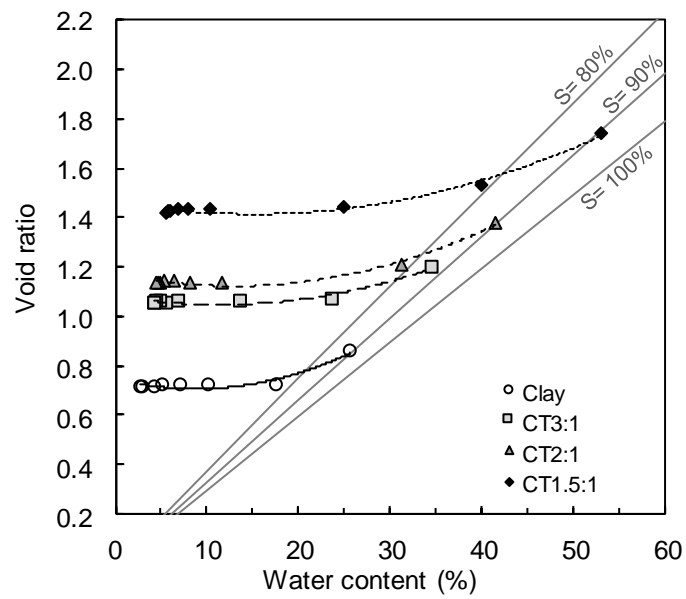
In all cases, the two mixtures with lower WTS content presented similar shrinkage curve and final void ratio, probably because the difference in WTS content is small.

Figure 74 – Shrinkage curves of Campinas clay and CC mixtures.



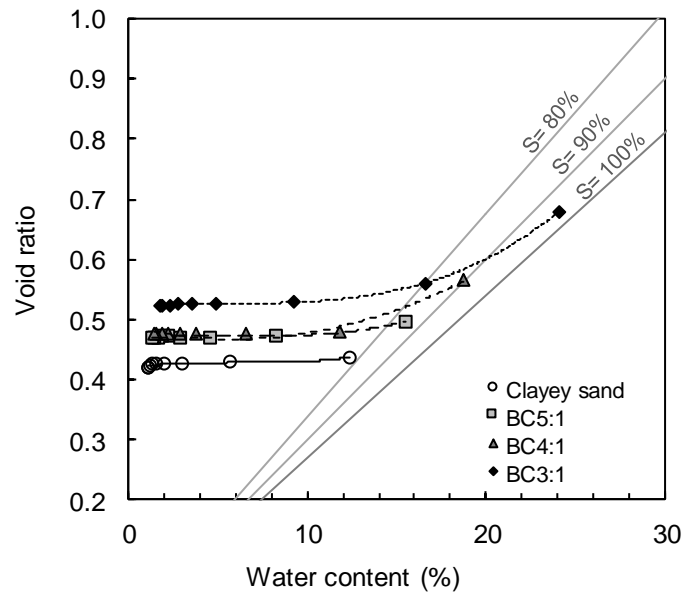
Source: author.

Figure 75 – Shrinkage curves of Campinas clay and CT mixtures.



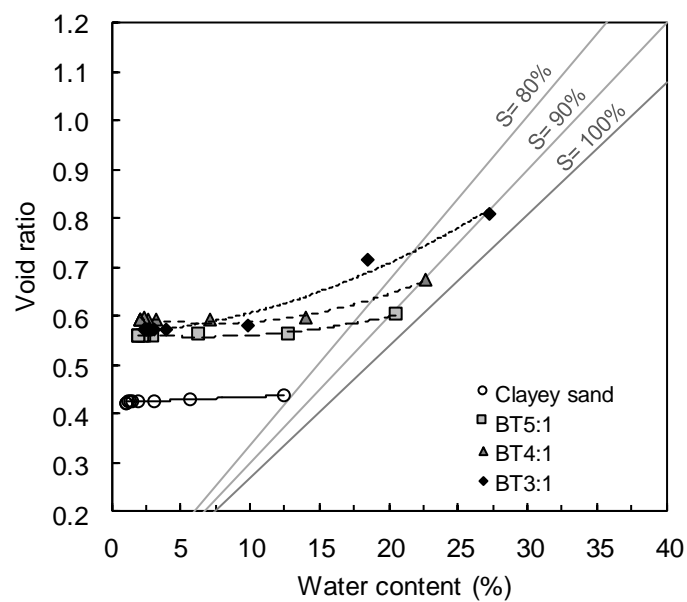
Source: author.

Figure 76 – Shrinkage curves of Botucatu clayey sand and BC mixtures.



Source: author.

Figure 77 – Shrinkage curves of Botucatu clayey sand and BT mixtures.

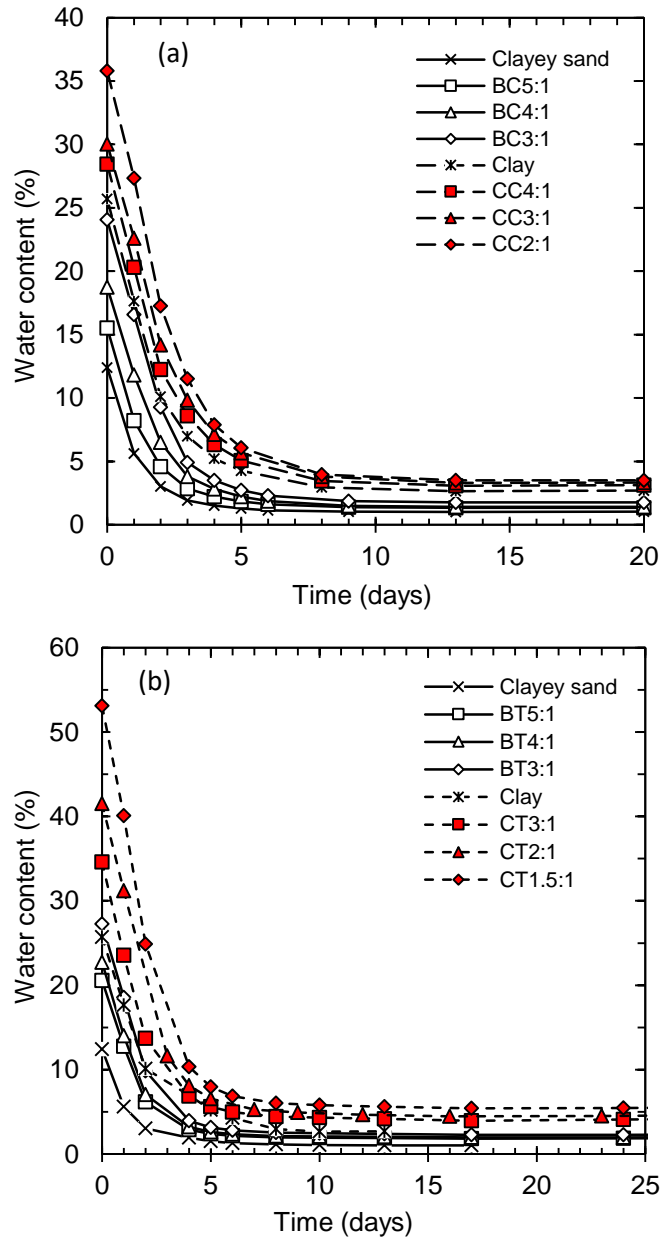


Source: author.

4.11 MERCURY INTRUSION POROSIMETRY

The specimens used for mercury intrusion porosimetry (MIP) were air-dried prior testing, since it is a pre-condition for the execution of this test. Figure 78 shows the variation of specimens' water content over time.

Figure 78 – Water content variation over time of samples during air-drying prior MIP tests.



Source: author.

The residual water content of the clayey sand was 0.9%. This value increased slightly with WTS addition: 1.2, 1.5, and 1.7% for BC5:1, BC4:1, and BC3:1 mixtures, respectively, indicating that WTS fines helped to retain more water after air-drying. BT5:1, BT4:1, and BT3:1 mixtures presented residual water content of 1.8, 2.0, and 2.3%, respectively. Similarly, CC mixtures had higher residual water content than the clay. The measured residual water content of the clay and CC4:1, CC3:1, and CC2:1 mixtures were 2.7, 3.1, 3.3, and 3.5%, respectively. CT3:1, CT2:1, and CT1.5:1 mixtures presented residual water content of 4.1, 4.5, and 5.4%, respectively.

Table 20 presents a comparison of samples porosity obtained from MIP and from index properties. Two important aspects can be highlighted from that data.

First, the clay and the clayey sand presented lower porosity than their mixtures with WTS, as already mentioned. The porosity increased with increasing WTS content. Such behavior is in accordance with compaction results (WTS addition reduced dry unit weight and increased void ratio).

Second, all porosity values obtained from MIP were lower than those obtained from index properties. This is explained by the volume change that samples underwent during drying prior testing. Shrinkage was higher for greater values of WTS content, as would be expected, since the samples become more plastic and compressible.

Table 20 – Porosity and void ratio values computed from MIP and as-compacted condition.

Sample	As-compacted		MIP	
	e	n (%)	e _{MIP}	n _{MIP} (%)
Clayey sand	0.42	30	0.40	29
BC5:1	0.49	33	0.47	32
BC4:1	0.54	35	0.48	33
BC3:1	0.67	40	0.54	35
Clay	0.88	47	0.76	43
CC4:1	0.95	49	0.84	46
CC3:1	1.09	52	0.96	49
CC2:1	1.15	54	0.98	50

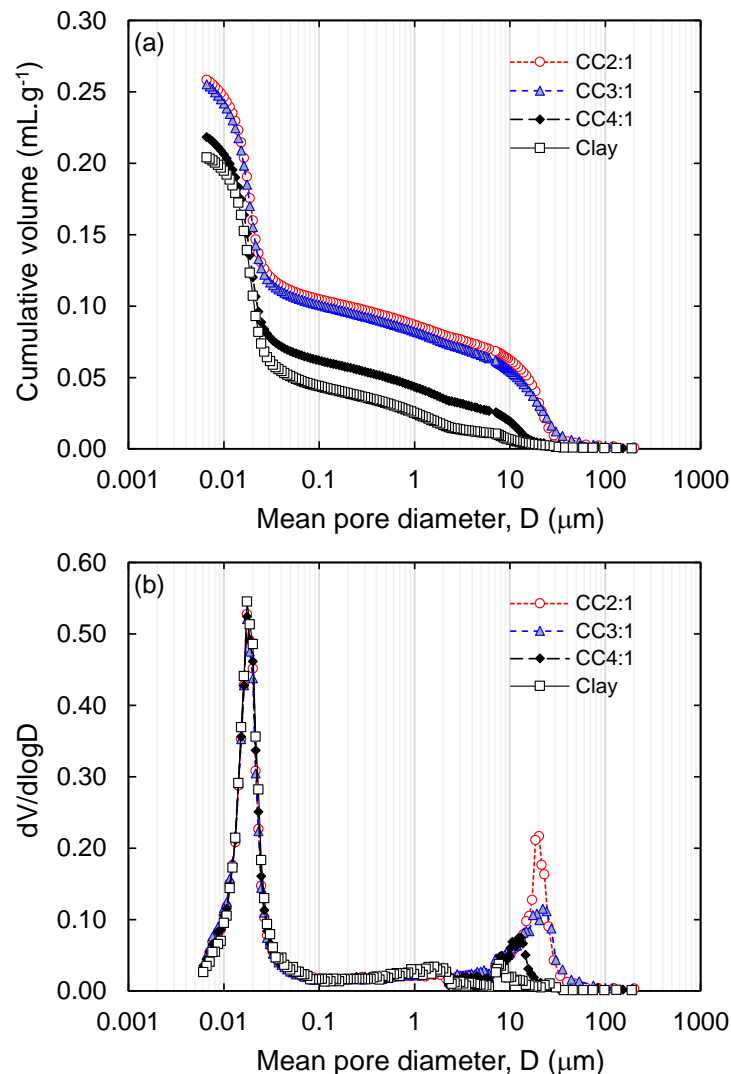
Source: author.

Results from MIP are usually displayed in two graphs: cumulative intruded volume (V) versus mean pore diameter (D), and differential-log volume (dV/dlogD) versus mean pore diameter (D). The latter is known as derivative curve (BRUAND; PROST, 1987) and is useful to analyze pore size distribution (PSD), i.e. pore sizes and frequency.

Pore sizes and frequencies vary among different soils due to differences in microstructure. There are PSD showing one, two or more major (high frequency) pore sizes, which are called unimodal, bimodal, and multimodal PSD, respectively.

Figure 79 and Figure 80 show the cumulative volume and derivative curves of the clay and CC mixtures, and the clayey sand and BC mixtures, respectively. The cumulative volume curves show that the total cumulative intruded volume for the clay and clayey sand was lower than that of the mixtures, indicating that the soils had lower effective porosity, as indicated in Table 20.

Figure 79 – Results from MIP for the clay and CC mixtures: (a) cumulative volume curves; (b) derivative curves.

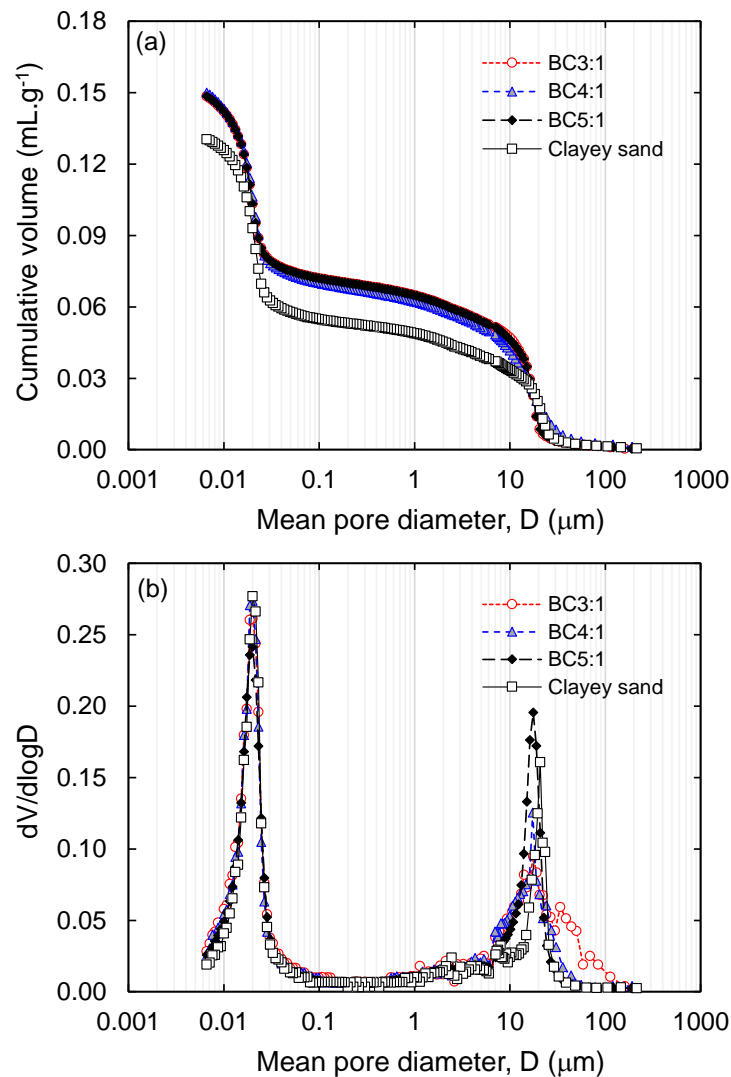


Source: author.

The derivative curves revealed that the clay presented unimodal PSD and high frequency of micropores with mean diameter about of 0.02 μm . However, WTS addition induced an increase in the occurrence of macropores. CC mixtures showed increasing frequency and mean pore diameter of macropores, ranging from 15 to 20 μm , with the

increase in WTS content. However, the mean pore diameter and frequency of micropores were not affected by WTS addition, suggesting that the increase in porosity with WTS content is only due to formation of more macropores. These macropores may have been formed by the flocculation of clay particles by WTS addition.

Figure 80 – Results from MIP for the clayey sand and CC mixtures: (a) cumulative volume curves; (b) derivative curves.



Source: author.

The clayey sand showed bimodal PSD, what agrees with some previous studies of Brazilian compacted lateritic soils (Borges et al., 2019; Neto et al., 2018). The highest frequency of macropores and micropores for the clayey sand (Figure 80) occurred at mean pore diameter about of 20 and $0.02 \mu\text{m}$, respectively.

On the one hand, the frequency of macropores was affected by WTS incorporation into the soil, resulting in lower volume of macropores for BC4:1 and BC3:1 mixtures. However, for the BC5:1 mixture the volume of macropores increased. Such behavior may be due to compaction conditions, since BC5:1 was compacted slightly dry-of-optimum, and BC4:1 and BC3:1 slightly wet-of-optimum.

Otálvaro, Neto, and Caicedo (2015), when comparing samples compacted with different water contents, observed that the sample compacted dry-of-optimum produced a structure with higher occurrence of macropores than the samples compacted at optimum and wet-of-optimum. On the other hand, micropores of Botucatu clayey sand remained unaltered with WTS addition, as observed for Campinas clay.

Surprisingly, the highest frequency of macropores and micropores of both the clayey sand and the clay with and without WTS addition occurred at similar mean pore diameter values: around 20 and 0.02 μm , respectively.

Moreover, undisturbed samples from different subsoil depths of Campinas lateritic clay presented bimodal PSD with similar major diameter of macropores and micropores: 30 and 0.02 μm (Miguel and Bonder, 2012).

4.12 SOIL-WATER RETENTION CURVES

4.12.1 SWRC from suction tests

Results from suction tests following a drying path on samples of Campinas clay and CC mixtures are presented in Figure 81. The soil-water retention curves (SWRCs) plotted in terms of volumetric water content (θ_w), gravimetric water content (w), and saturation (S), against matric suction are displayed in Figure 81a, Figure 81b, and Figure 81c, respectively. SWRCs of CT mixtures are presented in Figure 82.

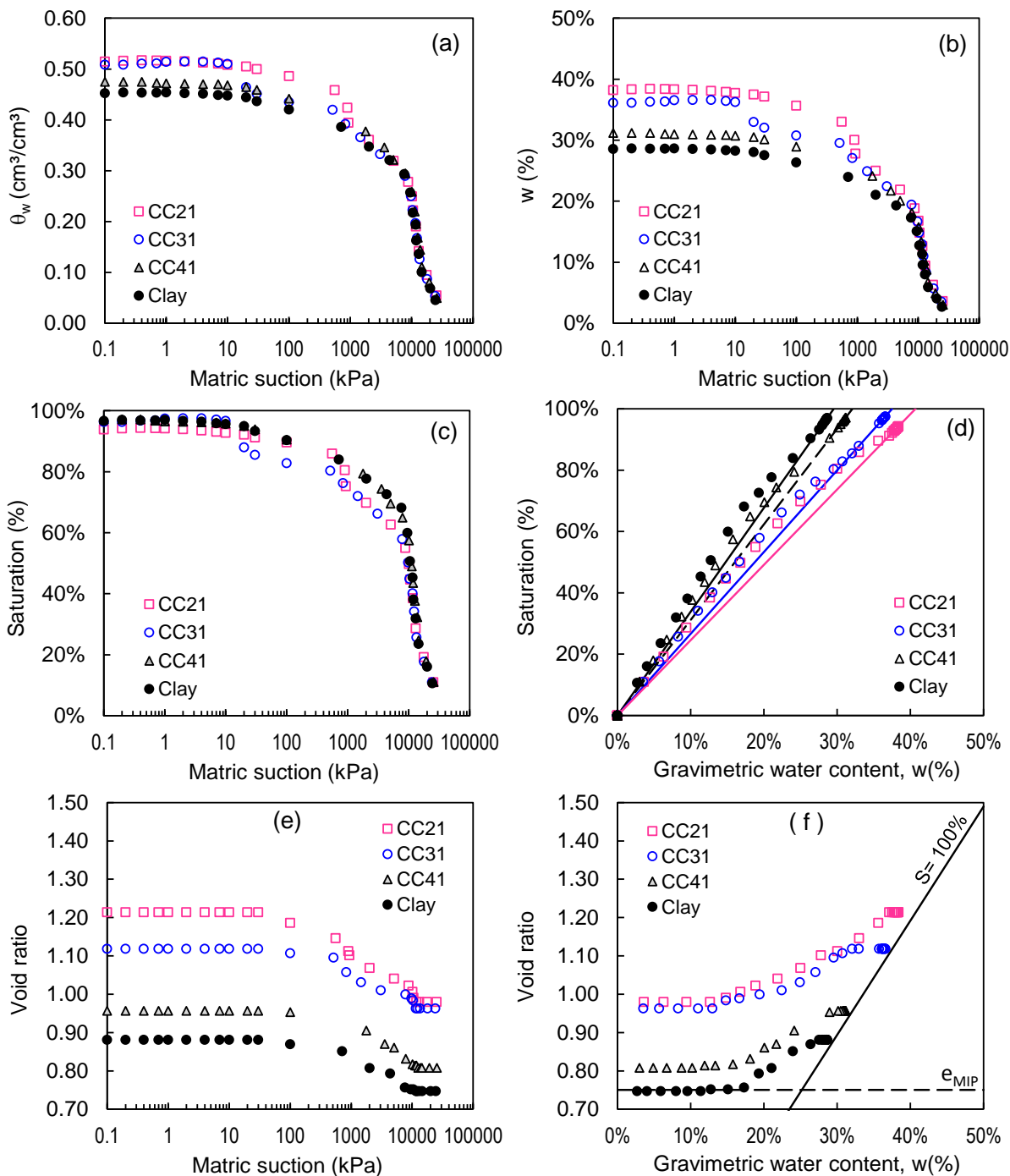
The air-entry value (AEV) for the clay occurred at approximately 20 kPa, as well as for the CC mixtures. Moreover, a second inflection of the curve seems to occur at approximately 10000 kPa.

SWRCs were similar in terms of saturation, and different in terms of volumetric and gravimetric water content for suction values up to 2000 kPa. Mixtures are indeed expected to present saturated volumetric and gravimetric water content increasing with increasing WTS content, since WTS addition causes increments in porosity.

All SWRCs tended to align and to follow the same path after the second AEV. This behavior may be due to volume change stabilization, i.e. no more shrinkage. In the shrinkage curves (graphs of void ratio variation with matric suction), void ratio is indeed constant for suction values higher than 10000 kPa (Figure 81e). These results confirm that, as indicated by MIP analyses, WTS addition did not alter micropores, which are related to high suction values according to the capillary equation.

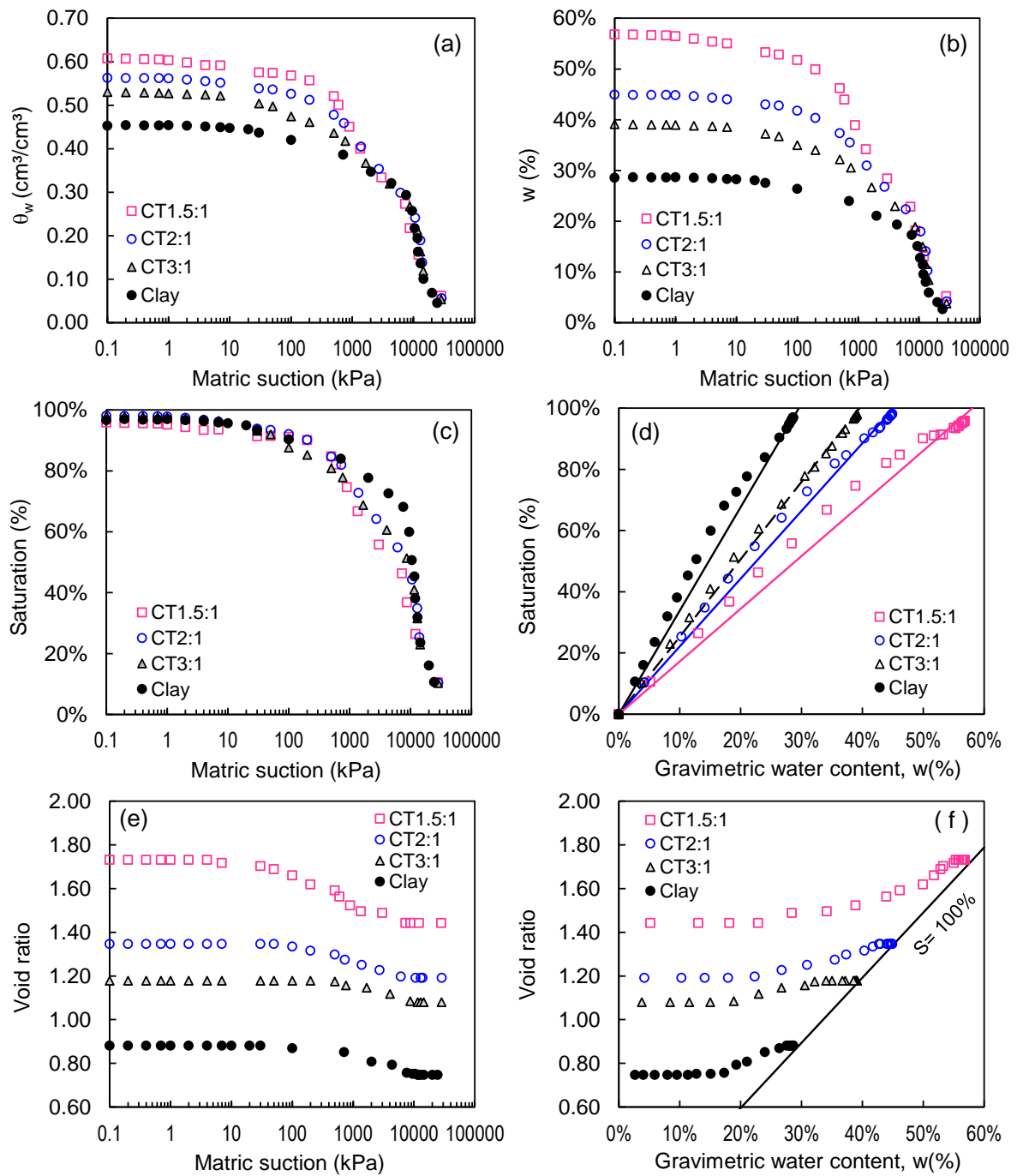
Figure 81e shows shrinkage caused by sample drying during suction tests. It can be noticed that Campinas clay underwent significant void reduction. The mixtures suffered even higher void reduction, as they had higher water content, higher plasticity, and higher compressibility, as already discussed. The void ratio of the clay sample after shrinkage (Figure 81e) was close to that obtained from MIP.

Figure 81 – SWRCs of Campinas clay and CC mixtures.



Source: author.

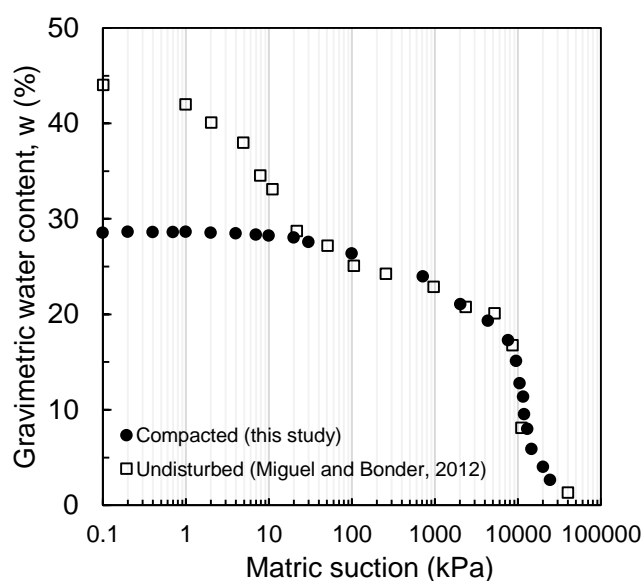
Figure 82 – SWRCs of Campinas clay and CT mixtures.



Source: author.

It is interesting to compare SWRCs of Campinas clay for compacted and natural undisturbed samples (Figure 83). The undisturbed sample was collected at 1.5 m depth, showing porosity of 68% (MIGUEL; BONDER, 2012). Micropores and some macropores were not affected by compaction-induced stresses, since the two curves are coincident for suctions higher than 20 kPa. For lower suctions, the undisturbed sample present higher volume of larger pores (macropores).

Figure 83 –SWRC of undisturbed and compacted samples of Campinas clay.

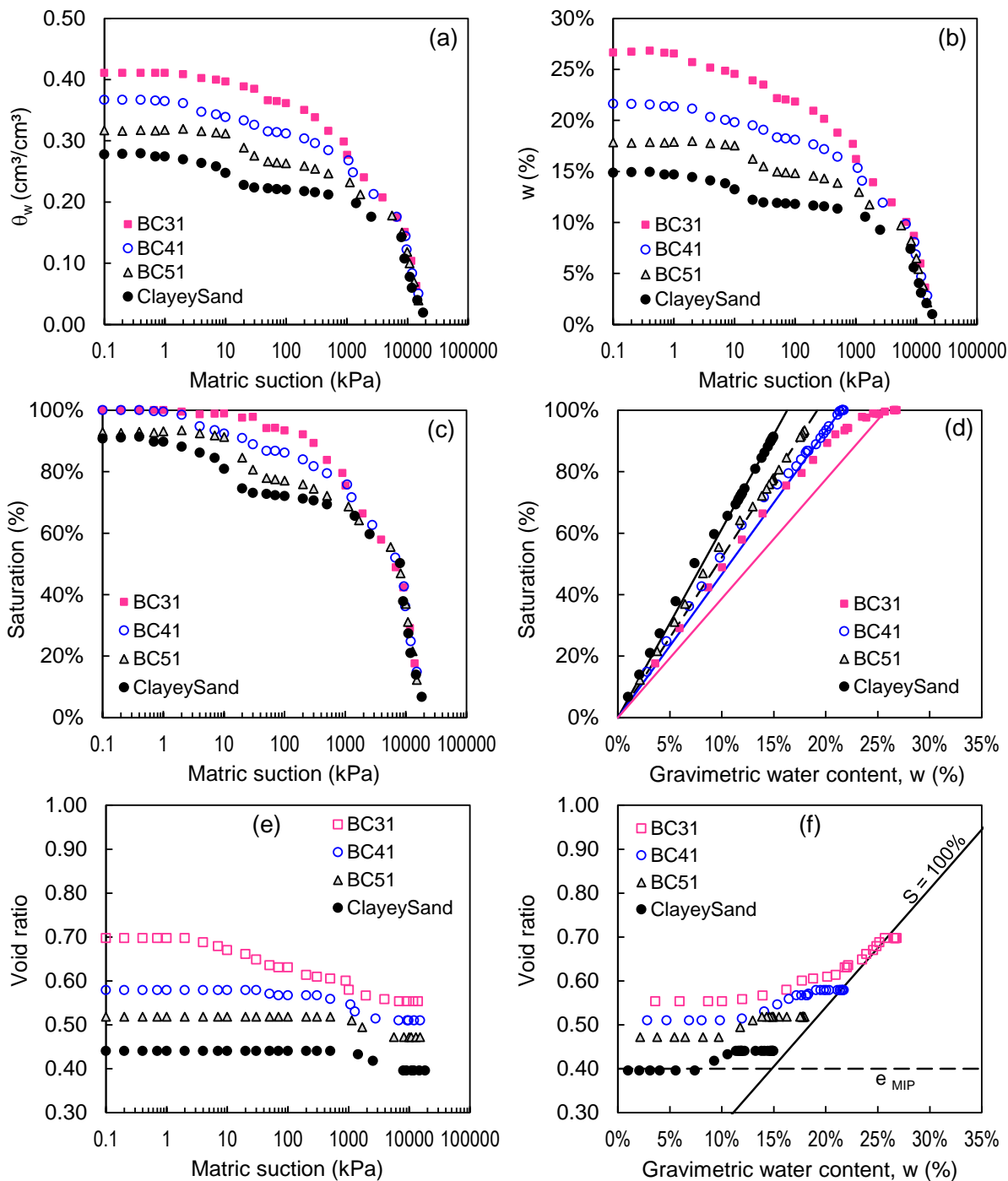


Source: prepared by author.

According to Gerscovich and Sayão (2002), compaction causes a reduction of the volume of macropores compared to undisturbed soil structure, and it has slight or no effect on the micropores. Hence, the percentage of pores with intermediate volume increases, resulting in a flatter shape of the SWRC for low suction values.

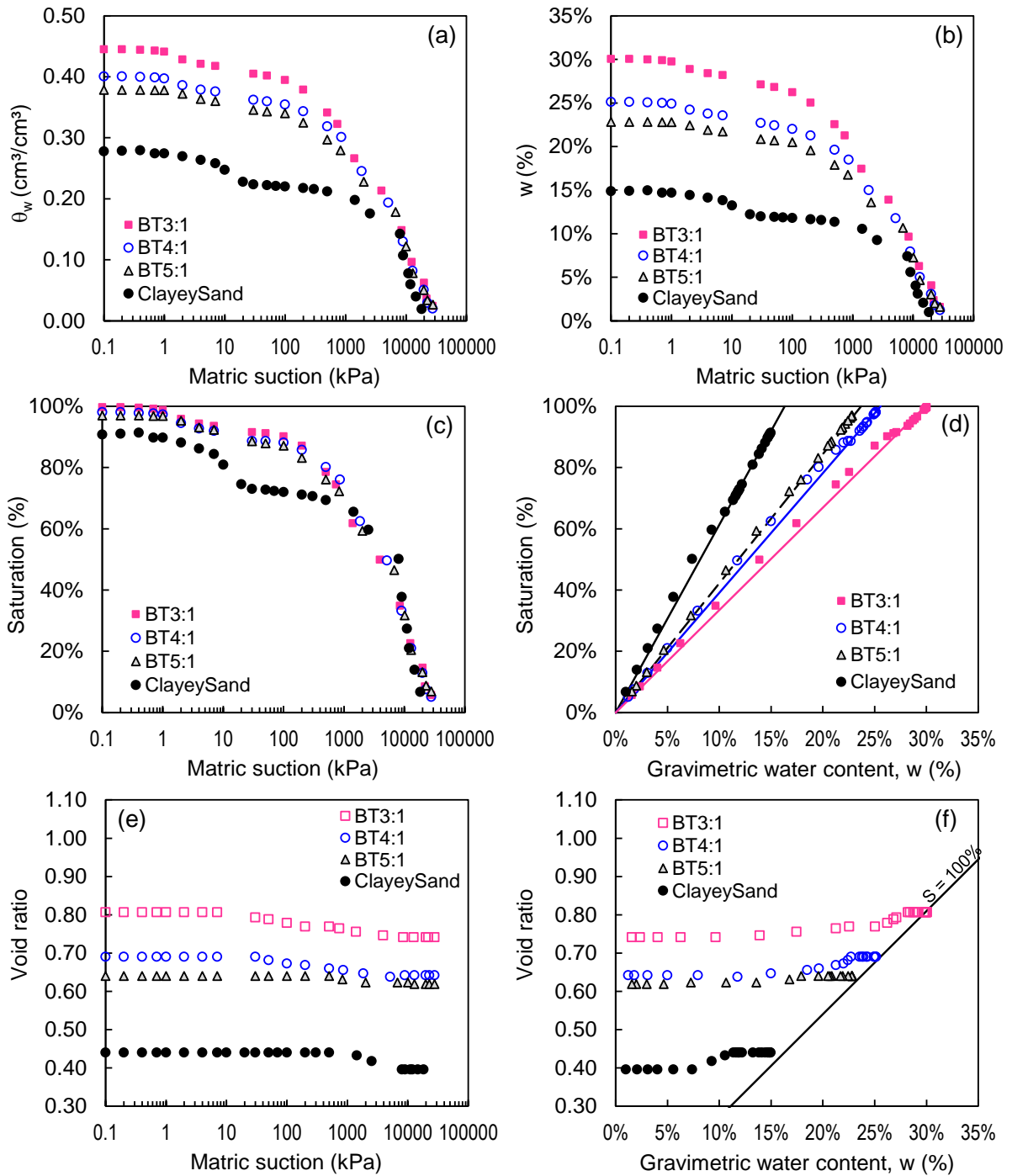
The SWRCs of Botucatu clayey sand and BC mixtures are depicted in Figure 84. Evidently, these curves presented bimodal behavior, similar to results from MIP tests. However, bimodality tended to diminish with increasing WTS content (Figure 84a, Figure 84b, and Figure 84c). The first AEV for the clayey sand occurred at circa 1 kPa, and the second nearby 5000 kPa. These values are a bit lower than those of Campinas clay. For higher suction values, all SWRCs tended to line up, indicating that micropores were not affected by WTS addition. The SWRCs of BT mixtures are presented in Figure 85.

Figure 84 – SWRCs of Botucatu clayey sand and BC mixtures.



Source: author.

Figure 85 – SWRCs of Botucatu clayey sand and BT mixtures.



Source: author.

The clayey sand and the BC5:1 mixture presented very close SWRCs. However, complete saturation for these samples was not achieved (around 90 to 95%), although BC4:1 and BC3:1 were completely saturated (Figure 84c).

SWRCs of the clayey sand show higher saturated volumetric and gravimetric water content (initial condition in suction tests) with increasing WTS content, similar to Campinas clay.

Figure 84d, Figure 84e, and Figure 84f show that the clayey sand suffered very low volume change (shrinkage). However, for the mixtures shrinkage increased with increasing WTS content. Furthermore, shrinkage of all samples ceased at suction values around 5000 kPa, which corresponds to the second AEV.

Similarly to Campinas clay, shrinkage of Botucatu clayey sand stabilized at a void ratio very close to that obtained from MIP analysis (Figure 84f).

4.12.2 SWRC from MIP

SWRCs of Campinas clay, Botucatu clayey sand and all mixtures, estimated using PSD from MIP tests, are presented in Figure 86 and Figure 87 in terms of saturation and volumetric water content versus matric suction.

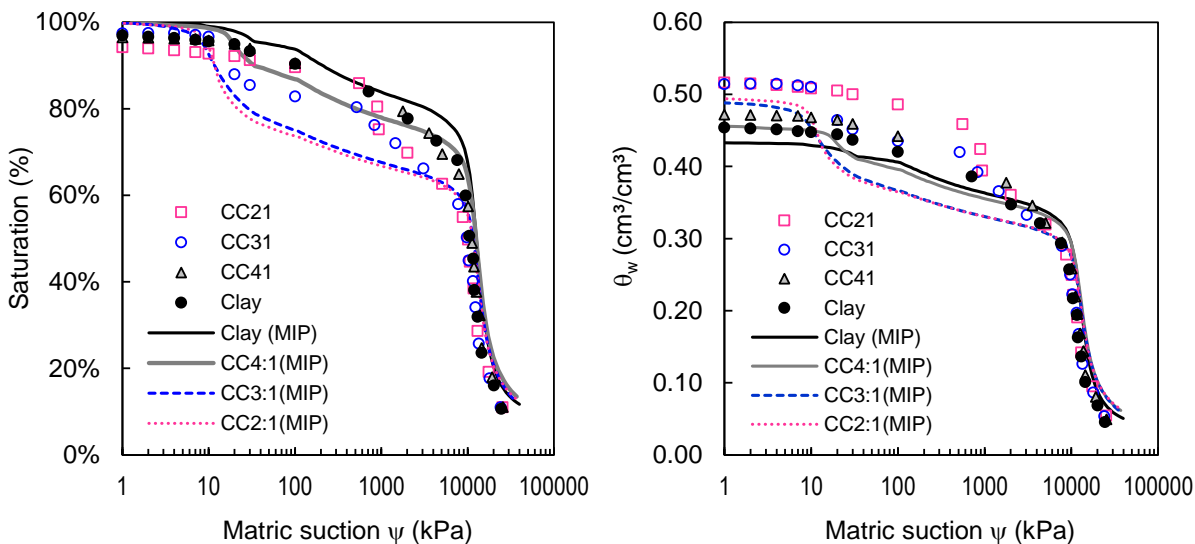
The estimated SWRC for Campinas clay was remarkably similar to that from the conventional suction test. The estimated SWRC for the clayey sand was also similar only for high suction values, greater than 2000 kPa. That may be related to lack of full saturation at the beginning of the suction test, as abovementioned, and also to sample shrinkage prior MIP testing.

The estimated SWRC for the mixtures was completely different from that obtained from suction tests for suction values up to about 5000 kPa. For higher suctions, all curves tend to line up and follow the same path. According to the capillary equation, matric suctions higher than 5000 kPa occur within pores smaller than 0.05 μm diameter. Therefore, this pore diameter could be defined as the limit between macro and micropores.

WTS addition significantly altered SWRCs and shrinkage behavior of Campinas clay and Botucatu clayey sand. MIP analyses showed that WTS addition caused increase of porosity only due to the increase of macropores volume. Suction tests showed that shrinkage did not affect micropores. Finally, since MIP tests were

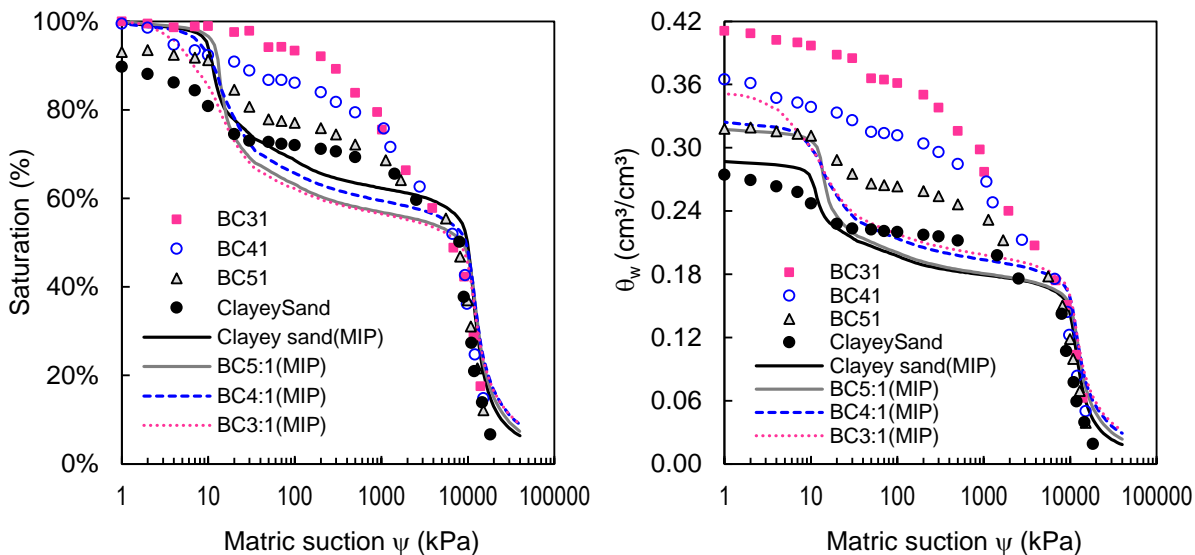
conducted on air-dried samples, most macropores were not detected, because they were reduced by desiccation-induced shrinkage. Hence, SWRCs estimated from MIP give reliable results only for micropores, i.e. high suction values.

Figure 86 – SWRCs estimated from MIP for the clay and CC mixtures.



Source: author.

Figure 87 – SWRCs estimated from MIP for the clayey sand and BC mixtures.



Source: author.

5 EVALUATION OF THE MIXTURES FOR USE IN EARTHWORKS

5.1 WASTE LANDFILLS

Table 21 presents a summary of the results of hydraulic conductivity, undrained shear strength (from unconfined compression tests) and volumetric shrinkage for the studied mixtures.

In the following sections the suitability of the mixtures as construction material for landfill liner and final cover is evaluated considering requirements for hydraulic conductivity $k < 10^{-9}$ m/s, volumetric shrinkage $VS < 10\%$, and undrained shear strength $s_u > 40$ kPa. The suitability as material for daily covers in landfills is evaluated considering only a requirement for undrained shear strength ($s_u > 10$ kPa), which is related to workability of the material in the field. Requirements for hydraulic conductivity or volumetric shrinkage are not usually considered for daily covers.

Table 21 Summary of hydraulic conductivity, undrained shear strength and volumetric shrinkage of the studied mixtures.

Sample	k (m/s)	s_u (kPa)*	VS (%)
Clayey sand	1.3×10^{-6}	137	1.1
BC5:1	1.4×10^{-6}	120	1.8
BC4:1	4.3×10^{-7}	43	5.8
BC3:1	7.0×10^{-9}	13	9.2
Clayey sand	1.0×10^{-8}	117	1.1
BT5:1	6.0×10^{-10}	94	2.7
BT4:1	3.5×10^{-9}	71	4.9
BT3:1	3.0×10^{-10}	58	6.1
Clay	7.0×10^{-9}	136	7.7
CC4:1	4.5×10^{-10}	76	6.9
CC3:1	2.0×10^{-10}	92	7.7
CC2:1	2.0×10^{-10}	63	11.7
CT3:1	1.0×10^{-9}	109	6.6
CT2:1	2.0×10^{-9}	59	10.2
CT1.5:1	3.5×10^{-10}	29	11.6

*Undrained shear strength from unconfined compression tests.

Although Campinas clay and Botucatu clayey sand presented adequate values of shear strength and volumetric shrinkage, they are not suitable for landfill liners and final covers due to the hydraulic conductivity. Addition of WTS to the soils decreased

the hydraulic conductivity, but with side effects on shear strength and volumetric shrinkage, which restricts the amount of WTS that could be added to the soils.

5.1.1 BC mixtures

None of the studied BC mixtures presented adequate values of hydraulic conductivity for landfill liner and final cover. The amount of WTS necessary to achieve $k < 10^{-9}$ m/s could have been determined, however, the undrained shear strength of BC3:1 mixture was already low (13 kPa), thus adding more WTS would not be a solution. The volumetric shrinkage of all of the mixtures was below 10%.

All the studied BC mixtures are adequate materials for daily cover in landfills.

5.1.2 BT mixtures

BT5:1 and BT3:1 mixtures presented hydraulic conductivity lower than 10^{-9} m/s, and BT4:1 mixture, a value slightly higher than 10^{-9} m/s. The relative compaction of BT4:1 sample was around 96% (Table 16). For lateritic soils, samples compacted at such relative compaction may present hydraulic conductivity 10 to 100 times lower than samples compacted at 100% (Bosco, 1997). Thus, BT mixtures compacted at relative compaction close to 100% might meet the hydraulic conductivity requirement; the same if compacted slightly wet-of-optimum. In terms of volumetric shrinkage and undrained shear strength, all BT mixtures presented adequate values. Since the undrained shear strength of BT3:1 mixture is still higher than the minimum requirement, more WTS could be added to Botucatu clayey sand.

All the studied BT mixtures are adequate materials for daily cover in landfills.

5.1.3 CC mixtures

These mixtures presented acceptable hydraulic conductivity and shear strength values for landfill liner and cover. The critical parameter for these mixtures is the volumetric shrinkage. CC2:1 mixture presented VS greater than 10%, while CC4:1 and CC3:1 can be considered suitable materials.

All the studied CC mixtures are adequate for use as daily cover in landfills.

5.1.4 CT mixtures

Mixtures CT3:1, CT2:1 and CT1.5:1 presented values of hydraulic conductivity equal to, slightly higher than, and lower than 10^{-9} m/s, respectively. According to these values CT2:1 mixture would not be acceptable for landfill liner or final cover. CT3:1 mixture (with lower WTS content than CT2:1) presented lower hydraulic conductivity, inconsistent with the general trend of hydraulic conductivity reduction with increasing WTS content, probably caused by experimental error (data noise). CT2:1 mixture compacted wet-of-optimum would probably present hydraulic conductivity lower than 10^{-9} m/s. Nonetheless, the most critical values, in this case, are actually the volumetric shrinkage and the undrained shear strength. CT2:1 and CT1.5:1 presented volumetric shrinkage higher than 10%. CT1.5:1 presented undrained shear strength lower than 40 kPa. These values may be reduced to acceptable values if the mixtures are compacted dry-of-optimum, however, this would probably cause an undesired increase in the hydraulic conductivity. Therefore, the only acceptable mixture for use as material for landfill liner and final cover is the CT3:1 mixture.

All CT mixtures, however, are adequate materials for use as landfill daily cover.

5.2 EMBANKMENTS

The shear strength parameters in terms of effective stress (c' and ϕ') of the mixtures were compared to those from a database of Brazilian residual soils used for the construction of earth dam embankments with satisfactory behavior. Figure 88 shows the average strength envelopes of the mixtures compared to strength envelopes of the soils from the database. Evidently, the mixtures presented similar or even higher strength in terms of effective stresses than the soils from the database.

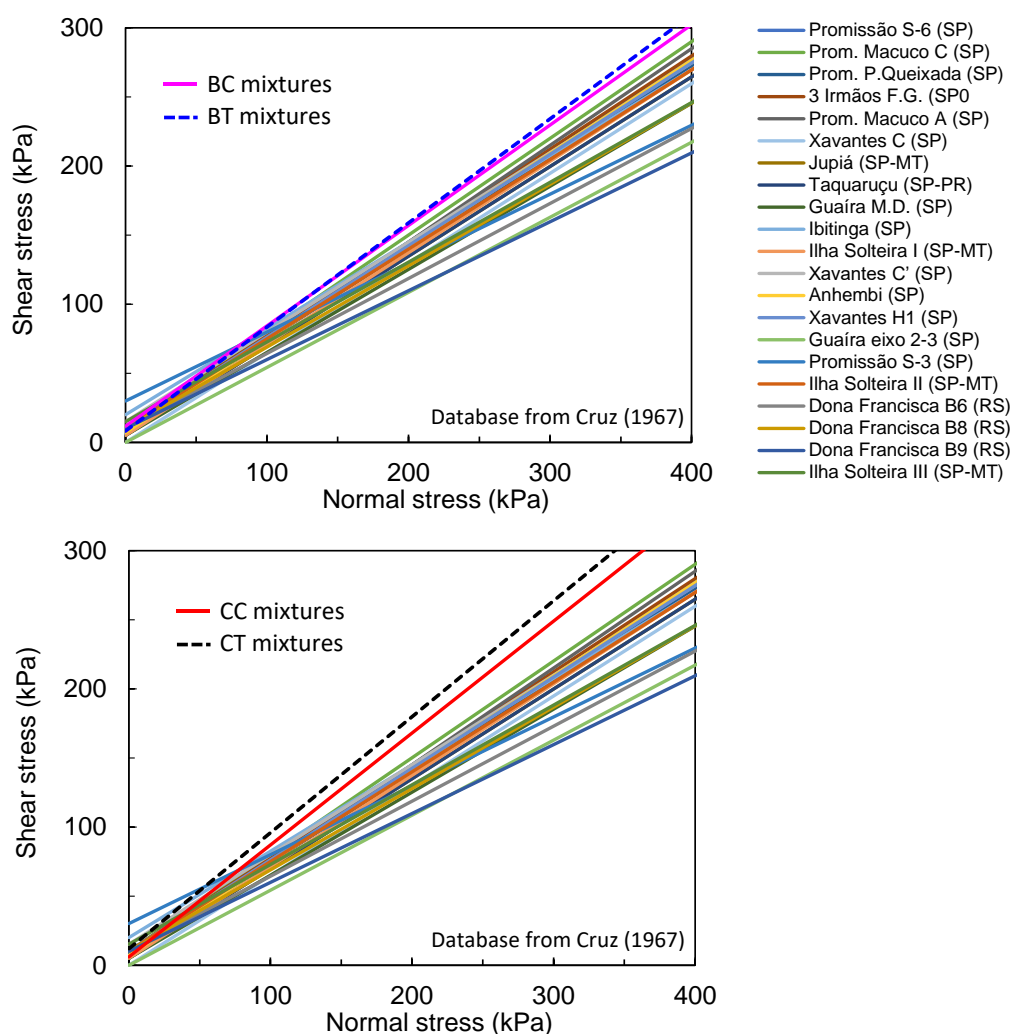
Since long-term stability (drained condition) depends on the effective strength parameters, embankments constructed with the studied mixtures would be expected to present satisfactory behavior (drained condition).

On the other hand, the short-term or during construction stability depends on the undrained shear strength of the construction material. Thus, the evaluation of the suitability of the mixtures as construction materials for embankments was based on the as-compacted undrained shear strength (Figure 71) and compressibility behavior (Table 15). The maximum acceptable values for the compression index and the undrained shear strength (from unconfined compression tests) were considered as

equal to 0.40 and 50 kPa, respectively. The definition of these values was discussed in the literature review.

Both studied soils, Campinas clay and Botucatu clayey sand, are suitable materials for construction of embankments based on their compressibility and shear strength parameters. Addition of WTS to the soils was expected to worsen their behavior, thus the maximum amount of WTS that can be added is restricted by the requirements of compressibility and undrained shear strength.

Figure 88 – Comparison of strength envelopes in terms of effective stresses.



Source: prepared by the author.

5.2.1 BC mixtures

All studied BC mixtures presented low compressibility (compression index lower than 0.20). Hence, these mixtures are adequate from a compressibility point of view. However, from a stability point of view, only the BC5:1 mixture comply with the minimum undrained shear strength.

5.2.2 BT mixtures

In terms of undrained shear strength, all BT mixtures are adequate. The compressibility of the mixtures varied between low to moderate, with compression index lower than 0.40. Hence, all of the studied BT mixtures are suitable as construction material for small embankments.

5.2.3 CC mixtures

All CC mixtures presented values of undrained shear strength higher than the 50 kPa, and values of compression index lower than 0.40 and higher than 0.20 (moderate compressibility). Hence, these mixtures are suitable as construction material for small embankments.

5.2.4 CT mixtures

CT3:1 and CT2:1 mixtures presented moderate compressibility, however acceptable, and values of undrained shear higher than 50 kPa. CT1.5:1 mixture, however, presented high compressibility (compression index higher than 0.40) and undrained shear strength lower than 50 kPa. Hence, only CT3:1 and CT2:1 mixtures are considered to be suitable for construction of small embankments.

6 CONCLUSIONS

- WTS sampling

The methodology used for WTS sampling revealed that both Cubatão WTS and Taiaçupeba WTS present considerable variations in water content over time. For a month of sampling, the water content of Cubatão WTS ranged from 232 to 308%, with average 268% and coefficient of variation 8.7%. The water content of Taiaçupeba WTS ranged from 456 to 530%, with average 496% and coefficient of variation 4.0%.

For researches using WTS, the sampling methodology herein employed is highly recommended to provide representative samples. A unique sample of WTS collected in a short period of time (a few days) may not be adequate.

- Mineralogical and chemical characterization

The mineralogical composition of Cubatão WTS (quartz, goethite, muscovite, and kaolinite) coincides with that of residual soils located within Cubatão River's basin. Taiaçupeba WTS presented predominantly amorphous phase even after treatment with hydrogen peroxide, with possible occurrence of quartz, gibbsite, and kaolinite. The probable sources of amorphous material are organic matter, amorphous metal (hydr)oxides and polymers.

Scanning electron microscopy imaging showed that particles of both WTS are coated by amorphous material, e.g. metal (hydr)oxides. Besides, presence of diatoms was revealed in Taiaçupeba WTS. There was no significant difference between Taiaçupeba WTS samples untreated or treated with hydrogen peroxide.

Water source in WTPs was shown to influence volatiles content (Loss on ignition, LOI), as indicated in the literature. Cubatão WTS (water from river) and Taiaçupeba WTS (water from reservoir) presented LOI of 22 and 53%, respectively. These values indicate that WTS produced by treatment of water from rivers usually contains lower volatiles content than WTS produced from reservoir water.

Chemical composition of Cubatão WTS and Taiaçupeba WTS comprises mainly aluminum, iron, and silicon. The highest concentrations in Cubatão WTS and Taiaçupeba WTS corresponded to iron and aluminum, respectively. These values are related to the type of coagulant used in the water treatment process. Cubatão WTP uses ferric chloride (FeCl_3) and Taiaçupeba WTP used aluminum sulfate ($\text{Al}_2(\text{SO}_4)_3$).

pH (in H₂O) of Cubatão WTS was neutral (7.0) and that of Taiaçupeba WTS was slightly acidic (6.4). Organic matter (*Walkley-Black* method) of Cubatão WTS and Taiaçupeba WTS were equal to 2.4 and 26.7%, respectively. The cation exchange capacity (CEC) were equal to 32.5 and 7.3 cmolc.kg⁻¹, respectively. CEC values in soils are usually correlated to organic matter content, however, such behavior was not observed for the studied WTS. This suggests that correlations from soils should always be verified instead of directly applied to WTS.

- Geotechnical characterization

Air-drying of samples showed that Taiaçupeba WTS is more hydrophilic than Cubatão WTS. Besides, drying causes irreversible alterations on WTS, e.g. loss of plasticity and particles cementation. The author suggests that WTS should not be dried for the geotechnical characterization unless it will be also be dried in the foreseen geotechnical application.

Specific gravity of solids of Cubatão WTS and Taiaçupeba WTS ranged from 2.94 to 2.97, and 2.37 to 2.45, respectively. These values reveal the influence of the coagulant and organic matter content on the specific gravity of solids.

Cubatão WTS presented fines content, liquid limit and plasticity index equal to 98%, 237% and 138%, while respective parameters for Taiaçupeba WTS were 95%, 536% and 300%. These values indicate that both WTS are materials of high plasticity. Based on the Unified Soil Classification System (USCS) with modified organic matter criteria, Cubatão WTS is an inorganic elastic silt (MH) and Taiaçupeba WTS is an organic silt (OH). USCS criteria for classifying a soil as *organic* is not adequate for WTS, since this material may undergo loss of plasticity not only due to organic matter, but because of coagulants as well. Therefore, the author classified WTS as organic if organic matter by ignition at 440 °C is greater than 20% or organic carbon content is greater than 8% (SANTOS et al., 2018).

Addition of WTS to the soils tended to increase Atterberg limits. Specific gravity of solids and grain-size distribution underwent only slight variation, as expected, since the added WTS solids content was low. Mixtures of WTS and Botucatu clayey sand presented the same classification as the soil (Clayey sand, SC), except for BT3:1 mixture classified as silty sand (SM). Mixtures of WTS and Campinas clay (lean clay, CL) were classified as elastic silt (MH), except for CC4:1 classified as silt (ML).

- Compaction

Addition of WTS to both Campinas clay and Botucatu clayey sand affected compaction parameters: maximum dry unit weight decreased and optimum water content increased. The effect of Taiaçupeba WTS on compaction parameters was more noticeable than the effect of Cubatão WTS for the same WTS content.

A linear correlation between optimum water content and plastic limit ($w_{opt} = 0.955w_p$; $R^2 = 0.97$) was defined including all mixtures, very close to the correlations for natural soils in the literature, indicating that classical correlations for soils could be used for mixtures of WTS and soils as long as their validity is previously verified.

Drying of mixtures prior to compaction affects compaction parameters and causes the opposite effect of WTS addition: maximum dry unit weight increases and optimum water content decreases. BC mixtures can achieve the same values of compaction parameters as the clayey sand at desiccation ratio in the range of 50 to 60%, while linear trend lines indicate that for the BT mixtures these values would be achieved at 100% desiccation ratio. CC mixtures can reach the same compaction parameters as those of the clay at desiccation ratio of 70 to 80%, while CT mixtures might reach them at 100 % desiccation ratio, based on linear trend lines.

The line-of-optimums for CC- and CT-mixtures (with $G_s = 2.98$) and the BC- and BT mixtures ($G_s = 2.70$) can be approximated by the 87% saturation line as well as by Kuczinski's line-of-optimums.

- Compressibility

Based on the virgin compression index (C_c), the compacted soils have low compressibility and most of the mixtures have low to moderate compressibility. Most tested mixtures present acceptable compressibility as construction material for earthworks such as small embankments (e.g. highways and foundation for small buildings).

The swelling index (C_s) of tested soils and mixtures indicate that all tested materials can be considered as non-expansive ($C_s < 0.10$).

A high correlation between virgin compression index and liquid limit ($C_c = 0.006(w_L - 10)$, $R^2 = 0.92$) was found, similar to the classical correlation for remolded soils (TERZAGHI; PECK, 1948).

- Hydraulic conductivity

WTS addition caused reduction of the soil hydraulic conductivity. The reduction was more drastic for BC mixtures. However, all BC mixtures presented hydraulic conductivity higher than 10^{-9} m/s (minimum value for landfill liners). BT and CT mixtures presented hydraulic conductivity slightly higher than 10^{-9} m/s. On the other hand, all CC mixtures presented hydraulic conductivity lower than 10^{-9} m/s, which enables them as suitable material for compacted landfill liners.

Mixtures were compacted at optimum water content. A hydraulic conductivity lower than 10^{-9} m/s might be obtained by wet-of-optimum compaction. The author suggests that permeability be evaluated with samples compacted wet-of-optimum.

- Shear strength

Incorporation of WTS into Campinas clay and Botucatu clayey sand increased the effective friction angle. Fine materials with high plasticity generally present low values of effective friction angle, nonetheless such behavior agrees with the high friction angles of WTS reported in the literature. Therefore, in the author's view WTS addition to natural soils is beneficial from the perspective of effective shear strength.

On the other hand, the undrained shear strength, obtained from consolidated undrained (CU) tests, was reduced by WTS addition. The higher the WTS content, the lower the undrained shear strength. The general variation of undrained shear strength with WTS content can be considered as being analogous to the undrained strength variation with compactive effort or relative compaction for constant saturation.

The as-compacted undrained shear strength (unsaturated), obtained from unconfined compression (UC) tests, was greatly reduced by WTS addition. Notwithstanding, only three out the twelve studied mixtures did not comply with the requirement of minimum acceptable undrained shear strength equal to 50 kPa (BC4:1, BC3:1, and CT1.5:1). Since as-compacted undrained shear strength is highly influenced by matric suction, the author considers that compaction slightly dry-of-optimum would greatly increase the undrained shear strength of the mixtures.

- Volumetric shrinkage

WTS addition to the soils increases the volumetric shrinkage as a consequence of the increase in plasticity and optimum water content with increasing WTS content.

Most tested mixtures presented volumetric shrinkage in the range of 5 to 10%, therefore they are likely to develop small fissuring to moderate cracking. However, further studies on shrinkage-induced cracking should be conducted.

- Mercury intrusion porosimetry and Soil-water retention curves

Botucatu clayey sand and Campinas clay compacted at optimum water content and standard effort present bimodal and unimodal pore-size distribution, respectively, indicated by both MIP and SWRCs. WTS addition tends to diminish bimodality.

The reduction of dry unit weight or increase of void ratio caused by addition of WTS to the soils is only related to the increase in macropores ($D > 1 \mu\text{m}$), whereas micropores ($D < 1 \mu\text{m}$) remain unaltered.

Incorporation of WTS into the studied soils causes changes on SWRC only for suction values below 1000 kPa.

WTS addition increases shrinkage, therefore SWRC estimation from MIP for the studied samples was only satisfactory for high suction values ($> 5000 \text{ kPa}$).

- Concluding remarks

WTS can be incorporated to local soils for geotechnical applications, provided the feasible mixtures are evaluated by means of geotechnical testing and criteria coherent with the intended applications. WTS-soil mixtures can be regarded as traditional geomaterials. However, attention must be given to the obtention of WTS representative samples, mainly due to seasonal variability of composition, and adaptation of characterization tests may be necessary for this material. The complete characterization of WTS may be useful to indicate field procedures that improve geotechnical properties, e.g. partial air-drying of mixtures prior compaction. Environmental evaluation, also necessary for the acceptance of the new geomaterial., was not in the scope of this thesis, however, the risk of release of contaminants is not expected to be detrimental according to on-going research and the literature.

REFERENCES

ABO-EL-ENEIN, S. A.; SHEBL, A.; ABO EL-DAHAB, S. A. Drinking Water Treatment Sludge as an Efficient Adsorbent for Heavy Metals Removal. **Applied Clay Science**, v. 146, p. 343–349, 2017.

ABOY, N. **Secagem natural e disposição final de lodos de estações de tratamento de água**. 1999. 101p. Dissertação (Mestrado) – Programa de Pós-graduação em Engenharia de Recursos Hídricos e Saneamento Ambiental, Universidade Federal do Rio Grande do Sul, Porto Alegre, 1999.

AHMAD, T.; AHMAD, K.; ALAM, M. Sustainable management of water treatment sludge through 3'R' concept. **Journal of Cleaner Production**, v. 124, p. 1–13, 2016.

ALBRECHT, B. A.; BENSON, C. H. Effect of desiccation on compacted natural clays. **Journal of Geotechnical and Geo-environmental Engineering**, v. 127, n. 1, p. 67–75, 2001.

ALDEEB, A. A.; QUASIM, S. R.; PUPPALA, A. J.; ANDERSON, C. F. Physical and Engineering Properties of Treatment Plant Residuals and Disposal. **Journal - American Water Works Association**, v. 95, n. 8, p. 127–137, 2003.

ANDRADE, C.; MYNRINE, V.; SILVA, D. A.; MAYER, S. L.; SIMETTI, R.; MARCHIORI, F. Compósito para a construção civil a partir de resíduos industriais. **Matéria (Rio de Janeiro)**, v. 21, n. 2, p. 321–329, 2016.

ANGELIM, R. R.; CUNHA, R. P.; SALES, M. M. Determining the Elastic Deformation Modulus from a Compacted Earth Embankment via Laboratory and Ménard Pressuremeter Tests. **Soils and Rocks**, v. 39, n. 3, p. 285–300, 2016.

ASSIS, A. P.; HERNANDEZ, H. M.; COLMANETTI, J. P. Notas de Aula de Barragens. Publicação G.AP-AA006/02 ed. Brasília, DF, Brasil: Departamento de Engenharia Civil & Ambiental, Universidade de Brasília, 2014.

ASSOCIAÇÃO BRASILEIRA DE NORMAS TÉCNICAS – ABNT. **NBR 6459**: Determinação do Limite de Liquidez. Rio de Janeiro, 1984, 6p.

_____. **NBR 6508**: Grãos de solos que passam na peneira de 4,8 mm - Determinação da massa específica, Rio de Janeiro, 1984, 8p.

_____. **NBR 6457**: Amostras de solo - Preparação para ensaios de compactação e ensaios de caracterização, Rio de Janeiro, 1986, 9p.

_____. **NBR 7180**: Determinação do Limite de Plasticidade, Rio de Janeiro, 1988, 3p.

_____. **NBR 7181**: Solo - Análise granulométrica, Rio de Janeiro, 1988, 13p.

_____. **NBR 12007:** Solo - Ensaio de adensamento unidimensional - Método de ensaio, Rio de Janeiro, 1988, 13p.

_____. **NBR 7182:** Solo – Ensaio de compactação, Rio de Janeiro, 1988, 10p.

_____. **NBR 13896:** Solo – Aterros de resíduos não perigosos – Critérios para projeto, implantação e operação, Rio de Janeiro, 1997, 12p.

_____. **NBR 10004:** Resíduos sólidos – Classificação, Rio de Janeiro, 2004, 71p.

ASTM. **ASTM D698-12e2:** Test Methods for Laboratory Compaction Characteristics of Soil Using Standard Effort (12 400 Ft-Lbf/Ft³ (600 KN-m/M³)). West Conshohocken, PA: ASTM International, 2012.

_____. **ASTM D2435 / D2435M-11:** Test Methods for One-Dimensional Consolidation Properties of Soils Using Incremental Loading. West Conshohocken, PA: ASTM International, 2011a.

_____. **D422-63(2007) E2:** Test Method for Particle-Size Analysis of Soils. . West Conshohocken, PA: ASTM International, 2007.

_____. **D854-14:** Test Methods for Specific Gravity of Soil Solids by Water Pycnometer. West Conshohocken, PA: ASTM International, 2014a.

_____. **D2487-17:** Practice for Classification of Soils for Engineering Purposes (Unified Soil Classification System). West Conshohocken, PA: ASTM International, 2017a.

_____. **D2974-14:** Test Methods for Moisture, Ash, and Organic Matter of Peat and Other Organic Soils. West Conshohocken, PA: ASTM International, 2014b.

_____. **D4318-17e1:** Test Methods for Liquid Limit, Plastic Limit, and Plasticity Index of Soils. West Conshohocken, PA: ASTM International, 2017b.

_____. **D4767-11:** Test Method for Consolidated Undrained Triaxial Compression Test for Cohesive Soils. West Conshohocken, PA: ASTM International, 2011b.

_____. **D5084-16a:** Test Methods for Measurement of Hydraulic Conductivity of Saturated Porous Materials Using a Flexible Wall Permeameter. West Conshohocken, PA: ASTM International, 2016a.

_____. **D6836-16:** Test Methods for Determination of the Soil Water Characteristic Curve for Desorption Using Hanging Column, Pressure Extractor, Chilled Mirror Hygrometer, or Centrifuge. West Conshohocken, PA: ASTM International, 2016b.

_____. **D7928-17:** Standard Test Method for Particle-Size Distribution (Gradation) of Fine-Grained Soils Using the Sedimentation (Hydrometer) Analysis. West Conshohocken, PA: ASTM International, 2017c.

BABATUNDE, A. O.; ZHAO, Y. Q. Constructive Approaches toward Water Treatment Works Sludge Management: An International Review of Beneficial Reuses. **Critical Reviews in Environmental Science and Technology**, v. 37, n. 2, p. 129–164, 2007.

BAGCHI, A. **Design of Landfills and Integrated Solid Waste Management**. New York: John Wiley & Sons, 2004.

BALKAYA, M. Evaluation of the Geotechnical Properties of Alum Sludge, Zeolite, and Their Mixtures for Beneficial Usage. **Environmental Progress & Sustainable Energy**, v. 34, n. 4, p. 1028–1037, 2015.

BASIM, S. C. **Physical and Geotechnical Characterization of Water Treatment Plant Residuals**. 1999. 208p. PhD thesis—New Jersey Institute of Technology, Department of Civil and Environmental Engineering, 1999.

BASSO, J. B.; PARAGUASSÚ, A. B. Column tests of a compacted mixture of tropical soils for use in liners in Brazil. *In*: 10th International Congress of the International Association of Engineering Geology and the Environment, 2006. **Proceedings [...]**. London: IAEG, 2006.

BENSON, C. H.; DANIEL, D. E.; BOUTWELL, G. P. Field performance of compacted clay liners. **Journal of Geotechnical and Geoenvironmental Engineering**, v. 125, n. 5, p. 390–403, 1999.

BENSON, C. H.; ZHAI, H.; WANG, X. Estimating Hydraulic Conductivity of Compacted Clay Liners. **Journal of Geotechnical Engineering**, v. 120, n. 2, p. 366–387, 1994.

BERNUCCI, L. B.; BALDUZZI, F. Use of Lateritic Soils in Low Volume Road Pavements in Brazil. *In*: of the XIITH World Meeting of the International Road Federation, Toronto, Ontario, June 16 to 20, 1997. **Proceedings [...]**. 1997.

BERNUCCI, L. L. B. **Expansão e contração de solos tropicais compactados e suas aplicações às obras viárias. Classificação de solos tropicais com base na expansão e contração**. 1987. Master's dissertation— Escola Politécnica, Universidade de São Paulo, 1987.

BIZARRETA, J.; DE CAMPOS, T. Water Retention Curve and Shrinkage of Sludge from a Leachate Treatment Plant. 2012, Berlin, Heidelberg. **Proceedings [...]**. Berlin, Heidelberg: Springer, 2012. p. 409–414.

BOSCOV, M. E. G. **Contribuição ao projeto de sistemas de contenção de resíduos perigosos utilizando solos lateríticos**. 1997. Doctoral Thesis—Escola Politécnica da Universidade de São Paulo, São Paulo, Brazil, 1997.

BOSCOV, M. E. G.; SOARES, V.; VASCONCELOS, F. G.; FERRARI A. A. P. Geotechnical properties of a silt-bentonite mixture for liner construction. *In*: 17th

Conference on Soil Mechanics and Geotechnical Engineering, ICSMGE, 2009, Alexandria, Egypt. **Proceedings [...]**. ICSMGE, 2009. pp. 217–220.

BOSCOV, M. E. G. **Geotecnia Ambiental**. São Paulo: Oficina de Textos, 2008.

BOSCOV, M. E. G.; HACHICH, W. C.; MAHLER, C. F.; OLIVEIRA, E. Properties of a Lateritic Red Soil for Pollutant Containment. **Journal of Environmental Protection**, v. 02, p. 923, 2011.

BRADY, N. C.; WEIL, R. R. **The nature and properties of soils**. Fifteenth edition ed. Columbus: Pearson, 2016.

BRASIL. **DNIT 108-ES** -Terraplenagem - Aterros - Especificação de Serviço. Rio de Janeiro, Brazil: IPR, 2009.

BREESEM, K. M.; FARIS, F. G.; ABDEL-MAGID, I. M. Reuse of alum sludge in construction materials and concrete works: a general overview. **Research Journal**, p. 20, 2014.

BRUAND, A.; PROST, R. Effect of Water Content on the Fabric of a Soil Material: An Experimental Approach. **Journal of Soil Science**, v. 38, n. 3, p. 461–472, 1987.

CAMAPUM DE CARVALHO, J.; de REZENDE, L. R.; CARDOSO, F. B.; LUCENA, L. C.; GUIMARÃES, R. C.; VALENCIA, Y. G. Tropical soils for highway construction: Peculiarities and considerations. **Transportation Geotechnics**, Lateritic and Tropical Geomaterials in Construction of Transportation Infrastructures. v. 5, p. 3–19, 2015.

CHANDLER, R.; CRILLY, M.; SMITH, M. A low-cost method of assessing clay desiccation for low-rise buildings. **Proceedings of the Institution of Civil Engineers - Civil Engineering**, v. 92, n. 2, p. 82–89, 1992.

CHEN, H.; MA, X.; DAI, H. Reuse of water purification sludge as raw material in cement production. **Cement and Concrete Composites**, v. 32, n. 6, p. 436–439, 2010.

CHEN, Y.; MEEHAN, L. C. Undrained Strength Characteristics of Compacted Bentonite/Sand Mixtures. *In*: Geo-Frontiers, 2012. **Proceedings [...]**. American Society of Civil Engineers, 2012. p. 2699–2708.

CHU, T. Y.; DAVIDSON, D. T. Some Laboratory Tests for the Evaluation of Stabilized Soils. Methods for testing engineering soils, Iowa Engineering Experiment Station, **Bulletin 192**, p. 243–256, 1960.

COELHO, R. V. et al. Uso de Lodo de Estação de Tratamento de Água na Pavimentação Rodoviária. REEC - **Revista Eletrônica de Engenharia Civil**, v. 10, n. 2, 2015.

CONAMA, Conselho Nacional do Meio Ambiente. **Resolução Conama No 430**, DE 13-05-2011. 430. 2011.

CORDEIRO, J. S. Importância do tratamento e disposição adequada dos lodos de ETAs. *In*: REALI, M. A. P. **Noções gerais de tratamento e disposição final de lodos de estações de tratamento de água**. 1. ed. Rio de Janeiro: ABES, 1999. p. 1–19.

CORNWELL, D. A. **Water Treatment Residuals Engineering**. AWWA Research Foundation and American Water Works Association, 2006.

CORNWELL, D. A.; MACPHEE, M. J.; MUTTER, R. N. **Self-Assessment of Recycle Practices**. Washington D.C.: AWWA Research Foundation and American Water Works Association, 2003.

CRUZ, P. T. **Propriedades de engenharia de solos residuais compactados da região Centro-Sul do Brasil**. DLP, São Paulo, Brazil, 002, 1967.

CULLITY, B. D.; STOCK, S. R. **Elements of X-Ray Diffraction**. 3rd International ed. London, England: Pearson, 2014.

DANIEL, D. E. **Geotechnical Practice for Waste Disposal**. Springer Science & Business Media, 2012.

DANIEL, D. E.; BENSON, C. H. Water Content-Density Criteria for Compacted Soil Liners. **Journal of Geotechnical Engineering**, v. 116, n. 12, p. 1811–1830, 1990.

DANIEL, D. E.; WU, Y. K. Compacted Clay Liners and Covers for Arid Sites. **Journal of Geotechnical Engineering**, v. 119, n. 2, p. 223–237, 1993.

DE MAGISTRIS, F. S.; SILVESTRI, F.; VINALE, F. Physical and mechanical properties of a compacted silty sand with low bentonite fraction. **Canadian Geotechnical Journal**, v. 35, n. 6, p. 909–925, 1998.

DELGADO, J. V. C. **Avaliação da Aplicação do Lodo da ETA Guandu na Pavimentação Como Disposição Final Ambientalmente Adequada**. 2016. 132 p. Master's dissertation–UFRJ/COPPE, Programa de Engenharia Civil, Rio de Janeiro, 2016.

DIB, P. S.; ONO, S. Compressibility of the Soils Used in the Construction of Tucuruí Dam. *In*: Geomechanics in Tropical, Lateritic and Saprolitic Soils, 1985, Brasília, Brazil. **Proceedings [...]**. Brasília, Brail: ABMS, Committee on Tropical Soils of the ISSMFE, 1985.

DEPARTAMENTO NACIONAL DE INFRAESTRUTURA DE TRANSPORTES. **Pavement Manual**. IPR 719. 3rd. ed. Rio de Janeiro, Brazil: Instituto de Pesquisas Rodoviárias IPR, 2006.

DEPARTAMENTO DE ESTRADAS E RODAGEM DO ESTADO DE SÃO PAULO. **Sub-Base ou Base de Solo Arenoso Fino de Comportamento Laterítico – SAFL**. 2005. São Paulo: DER/SP, 2005. 19p.

- DONAGEMA, G. K. et al. **Handbook of methods for soil analysis**. 2nd. ed. Rio de Janeiro, Brazil: Embrapa Solos, 2011.
- EDELMANN, L.; HERTWECK, M.; AMANN, P. Mechanical behavior of landfill barrier systems. **Proceedings of the Institution of Civil Engineers - Geotechnical Engineering**, v. 137, n. 4, p. 215–224, 1999.
- EDZWALD, J. K. (Org.). **Water quality & treatment**. 6th ed. New York: McGraw-Hill, 2011. American Water Works Association, 2011.
- FADIGAS, F. de S. et al. Natural contents of heavy metals in some Brazilian soil classes. **Bragantia**, v. 61, n. 2, p. 151–159, 2002.
- FERREIRA, K. S. **Comportamento geotécnico de misturas de argila laterítica com lodo de estação de tratamento de água para uso em obras de terra**. 2020. 88p. Dissertação (mestrado) –Programa de Pós-Graduação em Engenharia Civil Escola Politécnica da Universidade de São Paulo, São Paulo, Brazil, 2020.
- FORTES, R. M.; AMARAL S.N.; MAZUR, N.; ANJOS, L. H. C.; FREIXO, A. A. Estudo da dosagem de cal em lodo oriundo do tratamento de água para utilização em reaterro de valas. *In: VII Jornadas Luso-Brasileiras De Pavimentos*, 2006, Recife, PE, Brazil. **Proceedings [...]**. Recife, PE, Brazil, 2006.
- FORTES, R. M.; MERIGHI, J. V.; PAULI, D. R.; BARROS, M. A. L.; DE CARVALHO, M. H.; CÉSAR, N.; BARBOSA, A. S.; RIBEIRO, F.B.; BENTO, B. B. Study of Dry Sludge Stabilization from Water Treatment Plant (WTP) in Taiaçupeba to Use as Compacted Soil in Earthwork Ditches. *In: Bearing Capacity of Roads, Railways and Airfields*, 2009, Champaign, Illinois, USA. **Proceedings [...]**. Champaign, Illinois, USA: CRC Press, 2009. p. 37–44.
- FOTH, H. D. **Fundamentals of Soil Science**. 8th. ed. New York: John Willey & Sons, 1991.
- FREDLUND, D. G.; RAHARDJO, H. **Soil mechanics for unsaturated soils**. 1. ed. New York: John Wiley & Sons, 1993.
- FURIAN, S.; BARBIERO, L.; BOULET, R.; CURMI, P; GRIMALDI, M.; GRIMALDI, C. Distribution and dynamics of gibbsite and kaolinite in an oxisol of Serra do Mar, southeastern Brazil. **Geoderma**, v. 106, n. 1–2, p. 83–100, 2002.
- GABAS, S. G.; SARKIS, J. E. S.; Boscov, M. E. G. Heavy Metal Diffusion and Retention in A Mineral Barrier of Compacted Lateritic Soil. **Revista Brasileira de Geologia de Engenharia e Ambiental**, v. 4, n. 2, p. 14, 2014.
- GERSCOVICH, D. M. S.; SAYÃO, A. S. F. J. Evaluation of the Soil-Water Characteristic Curve Equations for Soils from Brazil. *In: UNSAT2002*, 2002, Recife, PE, Brazil. **Proceedings [...]**. Recife, PE, Brazil: 2002. p. 295–300.

GERVASONI, R. **Caracterização e avaliação do potencial de destinação do lodo de estações de tratamento de água do Estado do Paraná**. 2014. 144 p., Master's dissertation – Universidade Federal do Paraná, Curitiba, 2014.

GODOY, L. G. G.; ROHDEN, A. B.; GARCEZ, M. R.; COSTA, E. B.; DA DALT, S.; ANDRADE, J. J. Valorization of water treatment sludge waste by application as supplementary cementitious material. **Construction and Building Materials**, v. 223, p. 939–950, 2019.

GODOY H.; BERNUCCI, L. L. B. Tablets method for understanding basic geotechnical properties of soils: a didactic resource. *In: Proc of the National Perspective of Transport Research, Natal, Brazil*. **Proceedings [...]**. Brazil, 2002. p. 145–156 [In Portuguese]

GODOY, H.; BERNUCCI, L. B.; NOGAMI, J. S. Diretrizes para a identificação expedita de solos lateríticos para uso em obras viárias. *In: XXX Reunião Anual de Pavimentação, 1996, Salvador, BA, Brazil*. **Proceedings [...]**. Salvador, BA, Brazil: 1996. p. 556–568.

GOMES, S. de C.; ZHOU, J. L.; LI, W.; LONG, G. Progress in manufacture and properties of construction materials incorporating water treatment sludge: A review. **Resources, Conservation and Recycling**, v. 145, p. 148–159, 2019.

GONÇALVES, F., DE SOUZA, C. H. U.; TAHIRA, F. S.; FERNANDES, F.; TEIXEIRA, R. S. Incremento de lodo de ETA em barreiras impermeabilizantes de aterro sanitário. **Revista DAE**, p. 5–14, 2017.

GORDON, M. E. Design and performance monitoring of clay-lined landfills. *In: Geotechnical Practice for Waste Disposal'87*. **Proceedings [...]**. ASCE, 1987. p. 500–514.

GUERRA, R. C. **Caracterização e biodegradação de lodo de estações de tratamento de água para descarte em aterro sanitário**. 2005. 88p. Master's dissertation - UNESP, 2005.

GÜNEYLI, H.; RÜŞEN, T. Effect of Length-to-Diameter Ratio on the Unconfined Compressive Strength of Cohesive Soil Specimens. **Bulletin of Engineering Geology and the Environment**, v. 75, n. 2, p. 793–806, 2016.

HEMSI, P. S. **Um estudo da adsorção de poluentes em um latossolo Paulista considerando a carga variável e o ponto de carga**. 2001. Master's dissertation – Departamento de Engenharia de Estruturas e Geotécnica, Escola Politécnica, Universidade de São Paulo, São Paulo, 2001.

HENDRICKS, D. W. **Fundamentals of Water Treatment Unit Processes**. Boca Raton: CRC Press, 2011.

- HIDALGO, A. M.; MURCIA, M. D.; GÓMEZ, M.; GÓMEZ, E.; GARCÍA-ISQUIERDO, C. Possible Uses for Sludge from Drinking Water Treatment Plants. **Journal of Environmental Engineering**, v. 143, n. 3, p. 04016088, 2017.
- HOPPEN, C. et al. Co-disposição de lodo centrifugado de Estação de Tratamento de Água (ETA) em matriz de concreto: método alternativo de preservação ambiental. **Cerâmica**, v. 51, n. 318, p. 85–95, 2005.
- HOWELL, J. L.; SHACKELFORD, C. D.; AMER, N. H.; STERN, R. T. Compaction of Sand-Processed Clay Soil Mixtures. **Geotechnical Testing Journal**, v. 20, n. 4, p. 443–458, 1997.
- HSIEH, H. N.; RAGHU, D. **Criteria Development for Water Treatment Plant Residual Monofills**. American Water Works Association, 1997.
- HUAT, B. B.; PRASAD, A.; ASADI, A.; KAZEMIAN, S. **Geotechnics of organic soils and peat**. London, UK: CRC press/Balkema, 2014.
- IAC, INSTITUTO AGRONÓMICO DE CAMPINAS. **Métodos de Análise Química, Mineralógica e Física de Solos do Instituto Agrônomo de Campinas**. 2009. Boletim Técnico 106. Campinas, SP, Brazil: Instituto Agronomico, 2009. Available: <http://www.iac.sp.gov.br/produtoseservicos/analisedosolo/docs/Boletim_Tecnico_106_rev_atual_2009.pdf>. Accessed: 23 September 2020.
- IBGE, INSTITUTO BRASILEIRO DE GEOGRAFIA E ESTATÍSTICA. **Mapa de Solos do Brasil**. 2001. Rio de Janeiro: IBGE, 2001.
- _____. **Pesquisa nacional de saneamento básico 2008**. IBGE, Coordenação de População e Indicadores Sociais. Rio de Janeiro: IBGE, 2010. Available: <<https://www.ibge.gov.br/estatisticas/multidominio/meio-ambiente/9073-pesquisa-nacional-de-saneamento-basico.html?=&t=publicacoes>>. Accessed: 19 May 2019.
- _____. **Pesquisa nacional de saneamento básico 2017**. IBGE, Coordenação de População e Indicadores Sociais. Rio de Janeiro: IBGE, 2020. 124p. Available: <<https://www.ibge.gov.br/estatisticas/multidominio/meio-ambiente/9073-pesquisa-nacional-de-saneamento-basico.html?=&t=publicacoes>>. Accessed: 20 October 2020.
- IWAKI, G. **Destinação Final de Lodos de ETAs e ETEs**. Available: <<https://www.tratamentodeagua.com.br/artigo/destinacao-final-de-lodos-de-etas-e-etes/>>. Accessed: 20 June 2019.
- KAISHA, K. K. K. Kurita **Handbook of Water Treatment**. Shinjuku-ku, Tokyo: Kurita Water Industries, 1985.
- KAMON, M.; KATSUMI, T.; RAJASEKARAN, G.; INAZUMI, S. Waste sludges utilization as landfill cover. *In*: ISRM International Symposium, 19-24 November, Melbourne, Australia 2000. **Proceedings [...]**. ISRM, 2000.

- KENNARD, M. F. et al. Shear strength specification for clay fills. *In: Clay fills, Conference held at the Institution of Civil Engineers, 14-15 November 1978. Proceedings [...]*. Thomas Telford Publishing, 1979. p. 143–147.
- KENNEY, T. C.; VEEN, W. A.; SWALLOW, M. A.; SUNGAILA, M. A. Hydraulic Conductivity of Compacted Bentonite–Sand Mixtures. **Canadian Geotechnical Journal**, v. 29, n. 3, p. 364–374, 1992.
- KLEPPE, J.; OLSON, R. Desiccation Cracking of Soil Barriers. In: JOHNSON, A. et al. (Org.). **Hydraulic Barriers in Soil and Rock**. 100 Barr Harbor Drive, PO Box C700, West Conshohocken, PA 19428-2959: ASTM International, 1985. p. 263-263–13.
- KOMLOS, J. et al. Feasibility Study of As-Received and Modified (Dried/Baked) Water Treatment Plant Residuals for Use in Storm-Water Control Measures. **Journal of Environmental Engineering**, v. 139, n. 10, p. 1237–1245, 2013.
- LADD, C. C.; FOOTT, R. New Design Procedure for Stability of Soft Clays. **Journal of the Geotechnical Engineering Division**, v. 100, n. 7, p. 763–786, 1974.
- LADE, P. V. **Triaxial testing of soils**. Hoboken: John Wiley & Sons Inc, 2016.
- LAMBE, T. W.; WHITMAN, R. V. **Soil Mechanics**. 2nd. ed. New York: John Wiley & Sons, 1969.
- MARINHO, F. A. M.; SOTO, M. A. A.; GIRITANA JUNIOR, G. F. N. **Unsaturated soils in the geotechnical context**. São Paulo: ABMS, 2015. v. Chapter 9. (Organized by de Carvalho, J. C; Gitirana Junior, G. F. N.; Machado, S. L.; Mascarenha, M. M. A., Silva Filho, F. C). [In Portuguese]
- MARTINS, B. E. D. B. S.; YOKOYAMA, L.; ALMEIDA, V. C. Avaliação da Influência do Coagulante Contido no Lodo Gerado na ETA em Corpos Cerâmicos. *In: XXI CBECIMAT - Congresso Brasileiro de Engenharia e Ciência dos Materiais, 2014, Cuiabá, MT, Brasil. Proceedings [...]*. Cuiabá, MT, Brasil, 2014. p. 1777–1783.
- MASCARENHA, M. M. dos A. et al. Utilização da porosimetria por injeção de mercúrio (MIP) na determinação de curvas características em solos deformáveis. *In: XIV Congresso Brasileiro de Mecânica dos Solos e Engenharia Geotécnica, 2008. Proceedings [...]*. São Paulo, Brazil: ABMS, 2008. p. 1839–1845.
- MASSAD, F. **Mecânica dos solos experimental**. São Paulo, Brazil: Oficina de Textos, 2016.
- MEDINA, J. Tropical soils in pavement design. In: II Intern. Symposium on Pavement Evaluation and Overlay Design, 1989. **Proceedings [...]**. Rio de Janeiro, Brazil: ABPV, 1989. p. 543–546.
- MICROMERITICS INSTRUMENT CORPORATION. **Mercury Intrusion Porosimetry Theory**. Retrieved from:

<https://www.micromeritics.com/Repository/Files/Mercury_Porosemity_Theory_poster.pdf>. Accessed: 21 July 2019.

MIGUEL, M. G.; BONDER, B. H. Soil–Water Characteristic Curves Obtained for a Colluvial and Lateritic Soil Profile Considering the Macro and Micro Porosity. **Geotechnical and Geological Engineering**, v. 30, n. 6, p. 1405–1420, 2012.

MIGUEL, M. G.; VILAR, O. M. Study of the water retention properties of a tropical soil. **Canadian Geotechnical Journal**, v. 46, n. 9, p. 1084–1092, 2009.

MIKUTTA, R. et al. Review: Organic Matter Removal from Soils Using Hydrogen Peroxide, Sodium Hypochlorite, and Disodium Peroxodisulfate. **Soil Science Society of America Journal**, v. 69, n. 1, p. 120, 2005.

MITCHELL, J. K.; SOGA, K. **Fundamentals of soil behavior**. 3rd ed. Hoboken, N.J: John Wiley & Sons, 2005.

MONTALVAN, E. L. T. **Investigação do comportamento geotécnico de misturas de solo arenoso com lodo da Estação de Tratamento de Água do Município de Cubatão**. 2016. 133 p. Master's dissertation–Escola Politécnica, Universidade de São Paulo, São Paulo, 2016.

MONTALVAN, E. L. T.; BOSCOV, M. E. Geotechnical Parameters of Mixtures of a Tropical Soil with Water Treatment Sludge. *In*: Zhan L., Chen Y., Bouazza A. (eds), 8th International Congress on Environmental Geotechnics, Volume 1. ICEG 2018. Environmental Science and Engineering. **Proceedings [...]**. Singapore, Netherlands: Springer, 2018. p. 235–242.

MONTALVAN, E. L. T.; BOSCOV, M. E. G. Geotechnical Characterization of a Soil-Water Treatment Sludge Mixture. *In*: GeoChicago 2016, Chicago, Illinois, US. **Proceedings [...]**. Chicago, Illinois, US: ASCE, 2016. p. 418–427.

MURRAY, E. J.; DIXON, N.; JONES, D. R. V. Properties and testing of clay liners. *In*: symposium held at the Nottingham Trent University Department of Civil and Structural Engineering on 24 September 1998. **Proceedings [...]**. London, England: Thomas Telford Services Limited, 1998. p. 37.

MURRAY, E. J.; RIX, D. W.; HUMPHREY, R. D. Clay linings to landfill sites. **Quarterly Journal of Engineering Geology and Hydrogeology**, v. 25, n. 4, p. 371–376, 1992.

NATIONAL RIVERS AUTHORITY. **Policy and practice for the protection of groundwater**. 1998. 2nd ed. Bristol, England: Environment Agency, 1998.

NOGAMI, J. S.; VILLIBOR, D. F. Additional considerations about a new geotechnical classification for tropical soils. 1985, São Paulo, Brazil. **Anais...** São Paulo, Brazil: ABMS, 1985. p. 327–337.

_____. Pavimentação de baixo custo com solos lateríticos. 1995.

_____. Use of Lateritic Fine-Grained Soils in Road Pavement Base Courses. **Geotechnical & Geological Engineering**, v. 9, n. 3, p. 167–182, 1991.

O'KELLY, B. C. Geotechnical properties of a municipal water treatment sludge incorporating a coagulant. **Canadian Geotechnical Journal**, v. 45, n. 5, p. 715–725, 2008.

O'KELLY, B. C.; QUILLE, M. E. Compressibility and consolidation of water treatment residues. **Proceedings of the ICE-Waste and Resource Management**, v. 162, n. 2, p. 85–97, 2009.

O'KELLY, B. C.; QUILLE, M. E. Shear strength properties of water treatment residues. **Proceedings of the ICE-Geotechnical Engineering**, v. 163, n. 1, p. 23–35, 2010.

O'KELLY, B.C. AND SIVAKUMAR, V. Water content determinations for peat and other organic soils using the oven-drying method. **Drying Technology: An International Journal**, v. 32, 13 p., 2014.

OLIVEIRA, E. M. S.; MACHADO, S. Q.; HOLANDA, J. N. F. Caracterização de resíduo (lodo) proveniente de estação de tratamento de águas visando sua utilização em cerâmica vermelha. **Cerâmica**, v. 50, p. 324–330, 2004.

OSINUBI, K. J.; NWAIWU, C. M. Design of Compacted Lateritic Soil Liners and Covers. **Journal of Geotechnical and Geoenvironmental Engineering**, v. 132, n. 2, p. 203–213, 2006.

OTÁLVARO, I. F.; NETO, M. P. C.; CAICEDO, B. Compressibility and microstructure of compacted laterites. **Transportation Geotechnics: Lateritic and Tropical Geomaterials in Construction of Transportation Infrastructures**. v. 5, p. 20–34, 2015.

PAN-ICSD. **PANalitycal Inorganic Cristal Structure Database (ICSD)**. Germany: Fach informations zentrum Karlsruhe (FIZ) and National Institute of Standards and Technology (NIST), 2007.

PARSONS, A. W.; BODEN, J. B. The Moisture Condition Test and Its Potential Applications in Earthworks. No. SR 522. Wokingham, Berkshire, United Kingdom: Transport and Road Research Laboratory (TRRL), 1979.

PASINI, F.; DA SILVA, M. G.; DA SILVA, L. D. Análise Físico-Química do Lodo Gerado na ETA de Caçapava do Sul-Rs. *In: Salão Internacional de Ensino, Pesquisa e Extensão*, 2017. **Anais...**, v. 8, n. 2, 2017.

PETRUZZELLI, D.; VOLPE, A.; LIMONI, N.; PASSINO, R. Coagulants removal and recovery from water clarifier sludge. **Water Research**, v. 34, n. 7, p. 2177–2182, 2000.

PINHEIRO, B. C. A.; ESTEVÃO, G. M.; SOUZA, D. P. Lodo proveniente da estação de tratamento de água do município de Leopoldina, MG, para aproveitamento na

indústria de cerâmica vermelha Parte I: caracterização do lodo. **Matéria (Rio de Janeiro)**, v. 19, n. 3, p. 204–211, 2014.

PINTO, C. de S. **Curso básico de mecânica dos solos**. 3. ed., com exercícios resolvidos ed. São Paulo, SP: Oficina de Textos, 2006.

PINTO, C. S. et al. Propriedades dos solos residuais. In: **Solos do Interior de São Paulo**. São Paulo: ABMS, 1993.

PIZZI, N. G. **Water treatment plant residuals field guide**. Denver, CO: American Water Works Association, AWWA, 2010.

PORTELLA, K. F. et al. Caracterização físico-química do lodo centrifugado da estação de tratamento de água Passaúna–Curitiba–PR. 2003, SANEPAR. Available: <http://www.sanepar.com.br/Sanepar/Gecip/Congressos_Seminarios/Lodo_de_agua/Caracterizacao_do_lodo_de_ETA.pdf> Accessed: 18 August 2019.

POZZEBON, B. H. **Parâmetros de solos residuais compactados da Região Metropolitana de São Paulo: comparação com dados de outras localidades no Brasil**. 2017. 284 p. Master's dissertation–University of São Paulo, São Paulo, 2017.

PRAPAHARAN, S.; ALTSCHAEFFL, A. G.; DEMPSEY, B. J. Moisture Curve of Compacted Clay: Mercury Intrusion Method. **Journal of Geotechnical Engineering**, v. 111, n. 9, p. 1139–1143, 1985.

PREFEITURA DO MUNICÍPIO DE SÃO PAULO. IR-01/2004 **Instrução de reparação de pavimentos flexíveis danificados por abertura de valas**. São Paulo, Brazil: 2004. Available: <http://avisocgvias.prefeitura.sp.gov.br/Recurso/Legislacao/IR_01.pdf>. Accessed: 16 November 2019.

QASIM, S. R.; CHIANG, W. **Sanitary landfill leachate: generation, control and treatment**. Boca Raton, Florida: CRC Press, Taylor & Francis Group, 1994.

RAGHU, D.; HSIEH, H. N.; NEILAN, T.; YIH, C. T. Water Treatment Plant Sludge as Landfill Liner. In: **Geotechnical Practice for Waste Disposal '87**, 1987. **Proceedings [...]**. Reston, Virginia, US: ASCE, 1987. p. 744–758.

RAMIREZ, K. G. et al. Physico-Chemical Characterization of Centrifuged Sludge from the Tamanduá Water Treatment Plant (Foz Do Iguaçu, PR). **Matéria (Rio de Janeiro)**, v. 23, n. 3, 2018.

ROCCA, A. C. C.; IACOVONE, A. M. M.; BARROTTI, A. J. **Resíduos sólidos industriais**. 2nd ed. São Paulo, SP: CETESB, 1993.

RODRIGUES, L. P.; HOLANDA, J. N. F. Recycling of Water Treatment Plant Waste for Production of Soil-Cement Bricks. In: **Procedia Materials Science, International Congress of Science and Technology of Metallurgy and Materials SAM - CONAMET 2013. Proceedings [...]**. 2015, v. 8, p. 197–202.

ROQUE, A. **Comportamento geotécnico de misturas de areia argilosa laterítica e lodo da estação de tratamento de água taiáçupeba, município de Suzano, São Paulo**. 2020. 159p. Qualificação (mestrado)–Programa de Pós-Graduação em Engenharia Civil Escola Politécnica da Universidade de São Paulo, São Paulo, Brazil, 2020.

ROQUE, A. J.; CARVALHO, M. Possibility of using the drinking water sludge as geotechnical material. *In: IV International Congress on Environmental Geotechnics, ICEG 2006. Proceedings [...]*. London, England: Thomas Telford Services Limited, 2006, p. 1535–1542.

SABESP. SABESP- **Tratamento de água**. São Paulo, Brazil: SABESP, 2019a. Available: <<http://site.sabesp.com.br/site/interna/Default.aspx?secaold=47>>. Accessed: 19 May 2019a.

_____. **Taiáçupeba Water Treatment Plant**. São Paulo, Brazil: SABESP, 2019b Available: <<http://www.setechidrobrasileira.com.br/en/Projetos/saneamento---agua/estacao-de-tratamento-de-agua-de-taiacupeba-->>. Accessed: 18 August 2019b.

SANTOS, H. G. dos et al. **Sistema Brasileiro de Classificação de Solos**. 5th revised ed. Brasília, DF, Brasil: EMBRAPA, 2018.

SANTOS, I. S. S. dos et al. Caracterização e identificação do resíduo: lodo da estação de tratamento do Município de São Leopoldo. *In: Congresso Interamericano de Ingeniería Sanitaria y Ambiental, 2000. Proceedings [...]*. São Paulo, Brazil: ABES, 2000. p. 1-8.

SARSBY, R. W. **Environmental Geotechnics**. London, England: Thomas Telford, 2000.

SEED, H. B.; MITCHELL, J. K.; CHAN, C. K. The Strength of Compacted Cohesive Soils. *In: Research Conference on Shear Strength of Cohesive Soils, 1960. Proceedings [...]*. Reston, Virginia, US: ASCE, 1960. p. 877–964.

SILVA, A. dos S.; HEMSI, P. S. Efeito do Teor de Sólidos na Resistência ao Cisalhamento de um Lodo de ETA Visando seu Uso em Cobertura Diária de Aterros Sanitários. *In: XIX Congresso Brasileiro de Mecânica dos Solos e Engenharia Geotécnica – COBRAMSEG, 2018, Salvador, Bahia, Brazil. Anais...* São Paulo, Brazil: ABMS, 2018.

SILVA, S. M. C. P.; FERNANDES, F. Co-compostagem de biosólidos, lodo de tratamento de água e resíduos de podas de árvores. *In: XXVI Congresso Interamericano de Ingeniería Sanitaria y Ambiental, 1998, Lima, Perú. Peru: APIS, 1998. p. 1–7.*

SIMMS, P. H.; YANFUL, E. K. Predicting soil-water characteristic curves of compacted plastic soils from measured pore-size distributions. **Geotechnique**, v. 52, n. 4, p. 269–278, 2002.

SIQUEIRA JÚNIOR, B. **Caracterização de resíduos de estação de tratamento de água e estudo de reaproveitamento na indústria de cerâmica vermelha**. 2011. 86 p. Master's dissertation—Programa de Pós-Graduação em Engenharia Mecânica, Universidade Federal de Pernambuco, Pernambuco, Recife, 2011.

SOCKANATHAN, S. **Water Treatment Plant Sludge as Sanitary Landfill Liner**. 1991. 104p. Master's dissertation - Department of Civil and Environmental Engineering, New Jersey Institute of Technology, Newark, NJ, US, 1991.

SOIL SURVEY STAFF. **Soil Taxonomy**. A basic system of soil classification for making and interpreting soil surveys. (Agriculture Handbook No. 436). 2nd. ed. Washington DC, US: United States Department of Agriculture - USDA, 1999.

SPARKS, D. L. **Environmental Soil Chemistry**. 2nd. ed. Amsterdam, Netherlands: Elsevier, 2003.

STEVENSON, F. J. **Humus chemistry**. 2nd ed. New York: John Wiley & Sons, 1994.

SUN, D.; YOU, G.; ANNAN, Z.; DAICHAO, S. Soil–Water Retention Curves and Microstructures of Undisturbed and Compacted Guilin Lateritic Clay. **Bulletin of Engineering Geology and the Environment**, v. 75, n. 2, p. 781–791, 2016.

TAN, K. H. **Principles of soil chemistry**. Boca Raton, Florida, US: CRC press, 2010.

TARTARI, R.; DÍAZ-MORA, N.; MONDÉNES, A. Lodo gerado na estação de tratamento de água Tamanduá, Foz do Iguaçu, PR, como aditivos em argila para cerâmica vermelha. Parte I: Caracterização do lodo e de argilas do terceiro planalto paranaense. **Cerâmica**, v. 57, n. 343, p. 288–293, 2011.

TEIXEIRA, S. R. et al. The effect of incorporation of a Brazilian water treatment plant sludge on the properties of ceramic materials. **Applied Clay Science**, v. 53, n. 4, p. 561–565, 2011.

TERZAGHI, K.; PECK, R. B. **Soil Mechanics in Engineering Practice**. 1st ed. New York: J. Wiley & Sons, 1948.

TERZAGHI, K.; PECK, R. B.; MESRI, G. **Soil mechanics in engineering practice**. 3rd ed. New York: John Wiley & Sons, 1996.

TRENTER, N. A. **Earthworks**. 1st ed. London, England: Thomas Telford, 2001.

TRENTER, N. A.; CHARLES, J. A. A Model Specification for Engineered Fills for Building Purposes. **Proceedings of the Institution of Civil Engineers - Geotechnical Engineering**, v. 119, n. 4, p. 219–230, 1996.

TSUGAWA, J. K. et al. Importance of Composing Representative Samples According to the Theory of a Sampling (TOS) for the Reuse of Water Treatment Sludge. *In: XVI PCSMGE*, 17 nov. 2019, Cancun, Mexico. **Proceedings [...]**. Cancun, Mexico: IOS Press ebooks, 17 November 2019. p. 2450–2457.

USEPA, US Environmental Protection Agency. **Hazardous Waste Management System**. Washington D.C.: US Environmental Protection Agency, 1986. v. 40. (Land Disposal Restrictions, Final Rule, Federal Register, Part II).

_____. **Criteria for solid waste disposal facilities**. Washington D.C.: U.S. Government Printing Office, 1993. Available: <<https://www.epa.gov/landfills/criteria-solid-waste-disposal-facilities-guide-ownersoperators>>. Accessed: 20 October 2016.

_____. Soil organic matter. **Soil Quality Kit**, Guide for Educators. US Department of Agriculture, Natural Resources Conservation Service, USDA-NRCS, 2020. Available: <https://www.nrcs.usda.gov/Internet/FSE_DOCUMENTS/nrcs142p2_053264.pdf>. Accessed 10 October 2020.

_____. **Management of water treatment plant residuals**. New York, N.Y. Reston, Virginia: ASCE, 1996. (ASCE manuals and reports of engineering practice, no. 88).

VANDENBERGE, D. R.; BRANDON, T. L.; DUNCAN, J. M. Triaxial tests on compacted clays for consolidated-undrained conditions. **Geotechnical Testing Journal**, v. 37, n. 4, p. 705–716, 2014.

VANDENBERGE, Daniel R.; DUNCAN, J. M.; BRANDON, T. L. Undrained strength of compacted clay under principal stress reorientation. **Journal of Geotechnical and Geoenvironmental Engineering**, v. 141, n. 8, p. 04015035, 2015.

VANDERMEYDEN, C.; CORNWELL, D. A. **Non-mechanical Dewatering of Water Plant Residuals**. Denver, CO: AWWA Research Foundation and American Water Works Association, 1998.

VERLICCHI, P.; MASOTTI, L. Reuse of drinking water treatment plants sludges in agriculture: problems, perspectives and limitations. *In: 9th International Conference on the FAO ESCORENA Network on recycling of agricultural, municipal and industrial residues in agriculture*. **Proceedings [...]**. 2000. p. 67–73.

VILLIBOR, D. F.; NOGAMI, J. S. **Economic pavements: Technology of the use of lateritic fine-grained soils employment**. São Paulo, Brazil: Arte & Ciência, 2009.

WANG, M. C.; HULL, J. Q.; JAO, M.; DEMPSEY, B. A.; CORNWELL, D. A. Engineering behavior of water treatment sludge. **Journal of Environmental Engineering**, v. 118, n. 6, p. 848–864, 1992.

WANG, M. C.; HULL, J. Q.; JAO, M. Stabilization Of Water Treatment Plant Sludge For Possible Use As Embankment Material. **Transportation Research Record**, n. 1345, p. 36–43, 1992.

WASHBURN, E. W. The dynamics of capillary. **Journal of the American Physical Society**, v. 17, n. 3, p. 273–283, 1921.

WATANABE, Y. et al. Batch Leaching Test Focusing on Clod Size of Drinking Water Sludge and Applicability to Long-Term Prediction Using Column Leaching Test. *In: Geo-Frontiers Congress*, March 13-16, 2011, Dallas, Texas, United States. **Proceedings [...]**. ASCE, 2011. p. 1075–1080.

WIKIMEDIA COMMONS CONTRIBUTORS. **File:SaoPaulo Municip Botucatu.svg**. Retrieved from: <https://commons.wikimedia.org/w/index.php?title=Special:CiteThisPage&page=File%3ASaoPaulo_Municip_Botucatu.svg&id=199618838>. Accessed: 16 September 2019a.

_____. **File:SaoPaulo Municip Campinas.svg**. Retrieved from: <https://commons.wikimedia.org/w/index.php?title=Special:CiteThisPage&page=File%3ASaoPaulo_Municip_Campinas.svg&id=230251041>. Accessed: 23 September 2019b.

_____. **File:SaoPaulo Municip Cubatao.svg**. Retrieved from: <https://commons.wikimedia.org/w/index.php?title=Special:CiteThisPage&page=File%3ASaoPaulo_Municip_Cubatao.svg&id=230251060>. Accessed: 23 September 2019c.

_____. **File:SaoPaulo Municip Suzano.svg**. Retrieved from: <https://commons.wikimedia.org/w/index.php?title=Special:CiteThisPage&page=File%3ASaoPaulo_Municip_Suzano.svg&id=230251297>. Accessed: 23 September 2019d.

WILLIAMS, C. E. Containment applications for earthen liners. *In: 1987 Specialty Conference on Environmental Engineering. Proceedings[...]*. ASCE, 1987. p. 122-128.

WU, T. H.; ZHOU, S. Z.; GALE, S. M. Embankment on sludge: predicted and observed performances. **Canadian Geotechnical Journal**, v. 44, n. 5, p. 545–563, 2007.

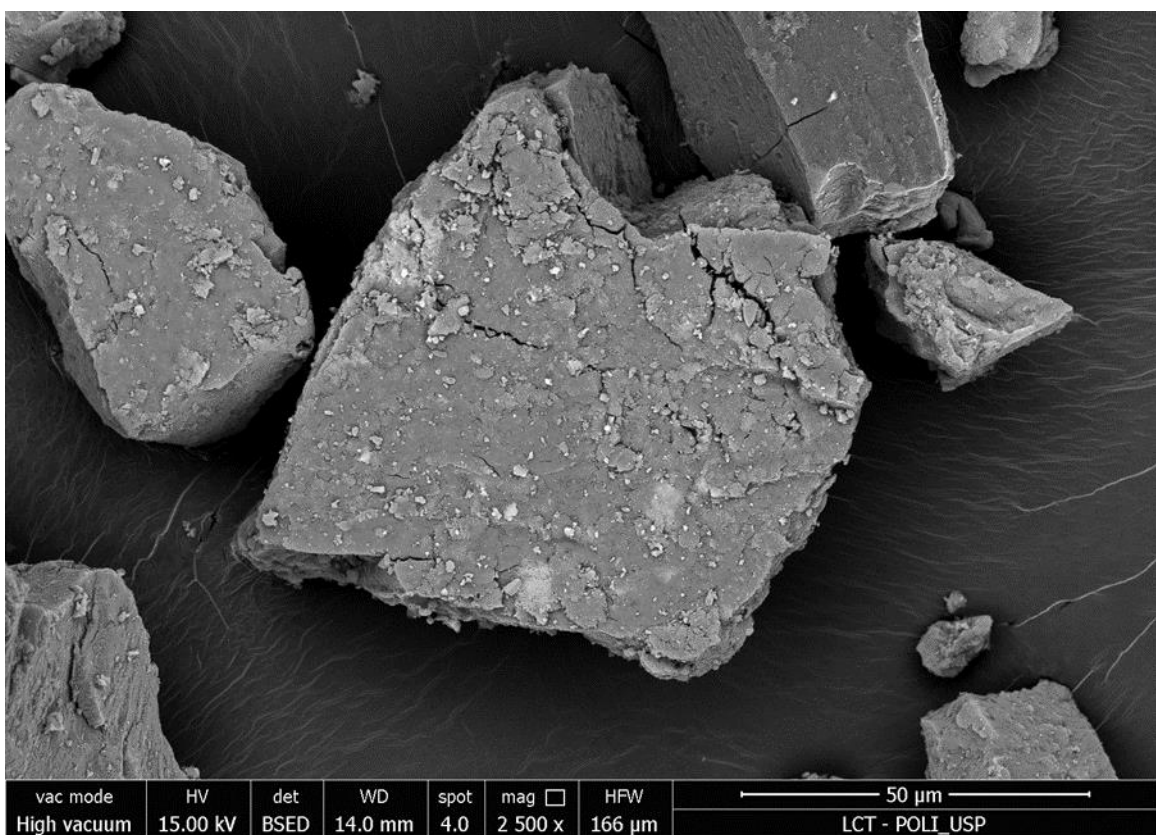
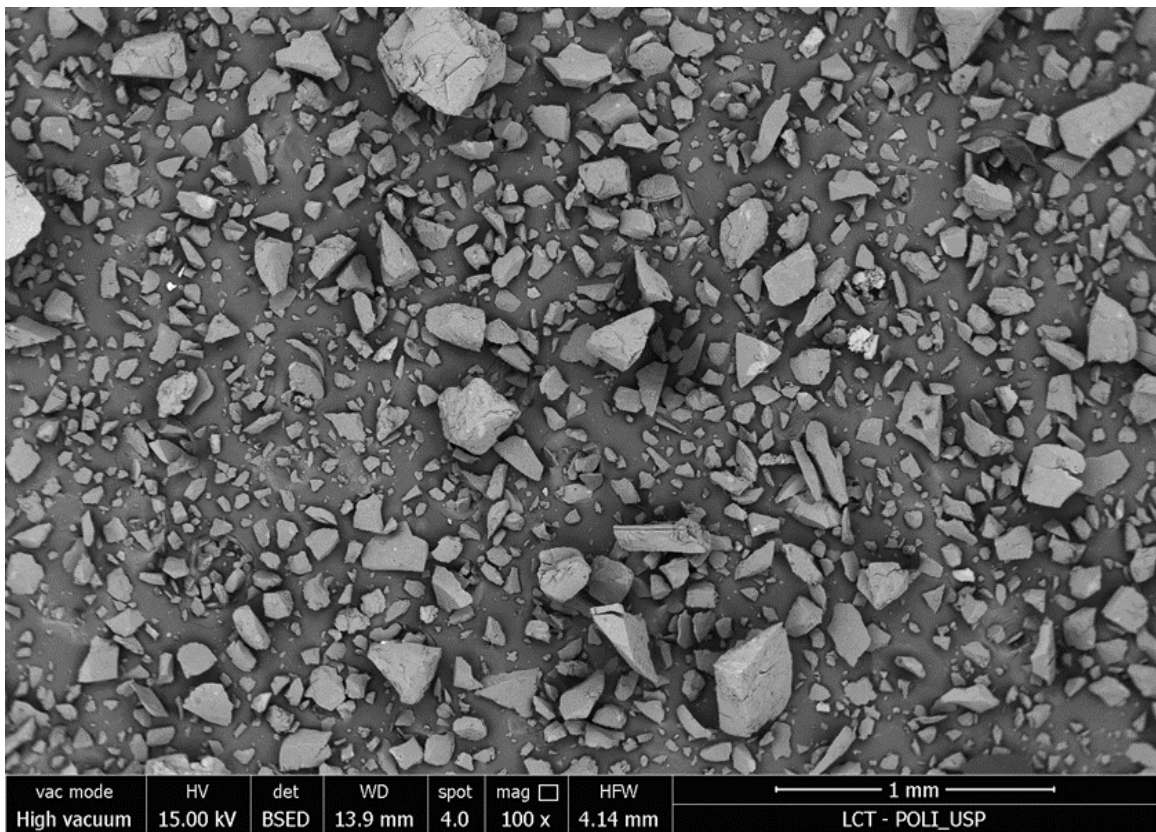
XIA, Z. **Geotechnical Characterization of Water Treatment Plant Residuals**. 1994. 88 p. Master's dissertation - New Jersey Institute of Technology, Department of Civil and Environmental Engineering, 1994.

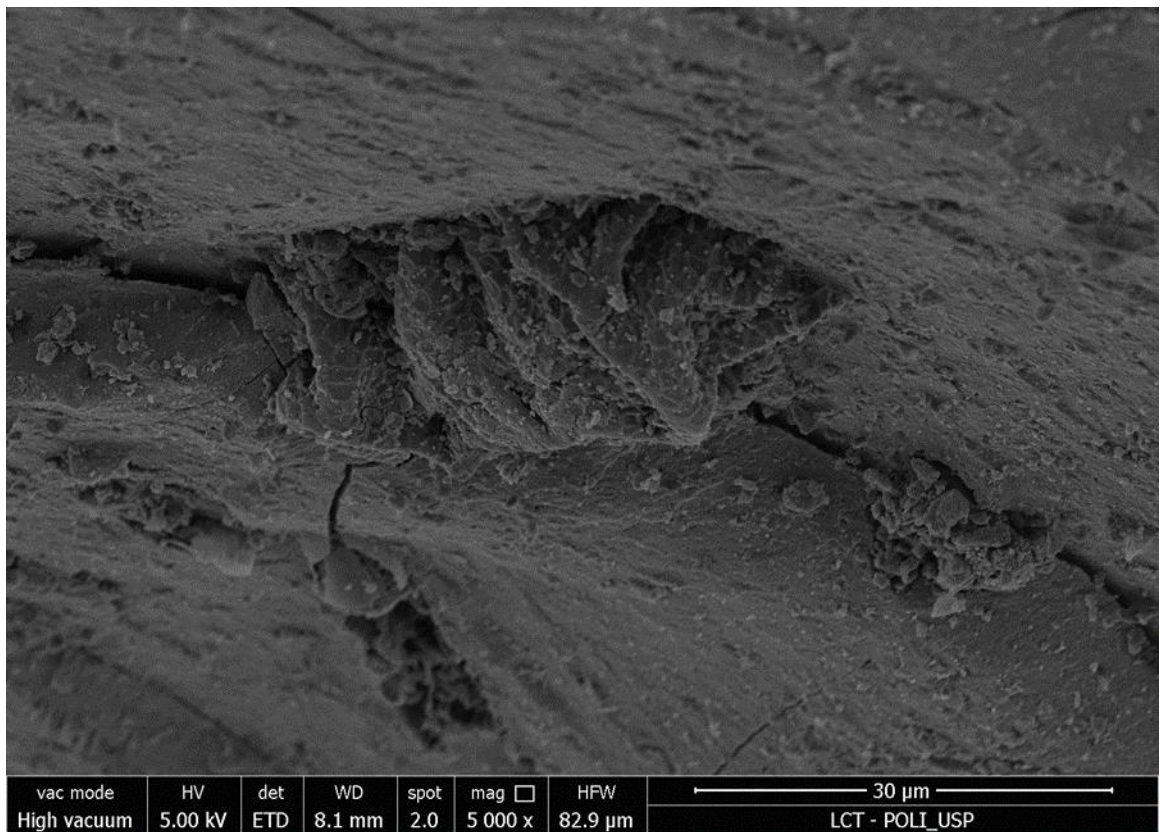
ZANON, T. V. B. **Avaliação da contaminação de um solo laterítico por lixiviado de aterro sanitário através de ensaios de laboratório e de retroanálise de campo**. 2014. 101 p. Dissertação de mestrado—Universidade de São Paulo, 2014.

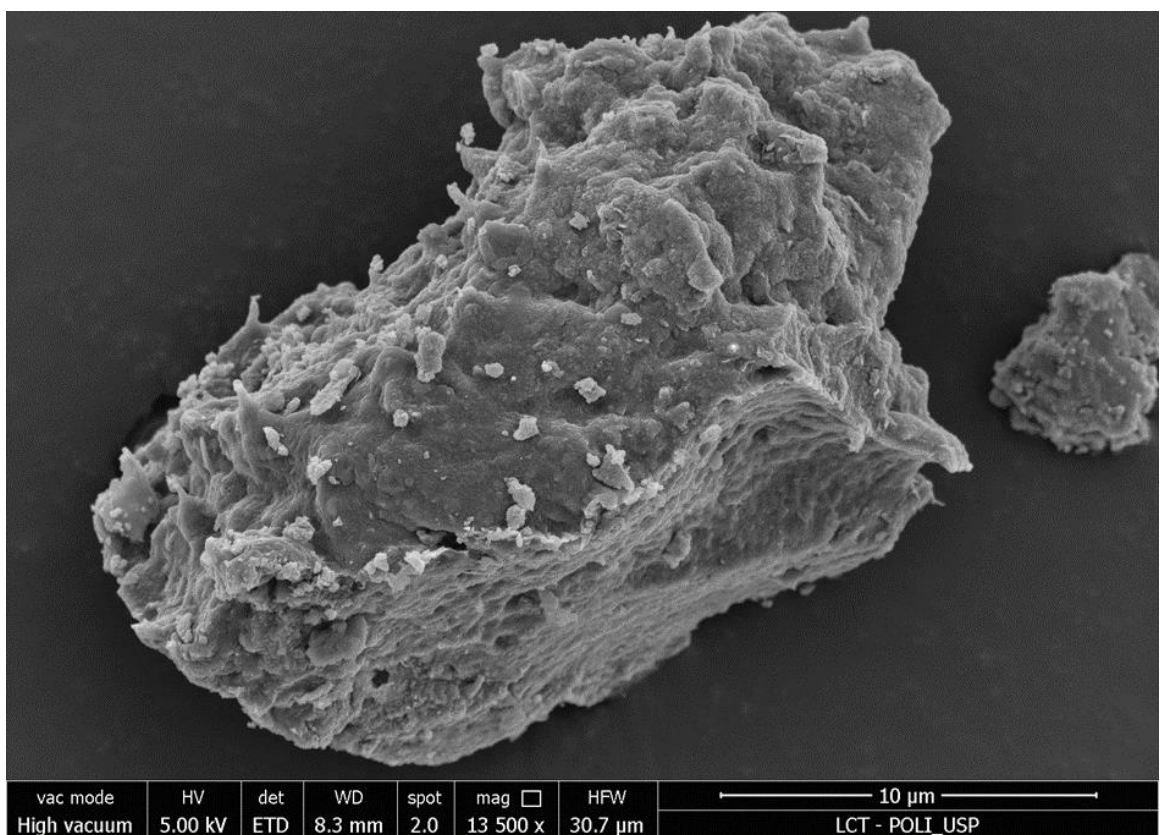
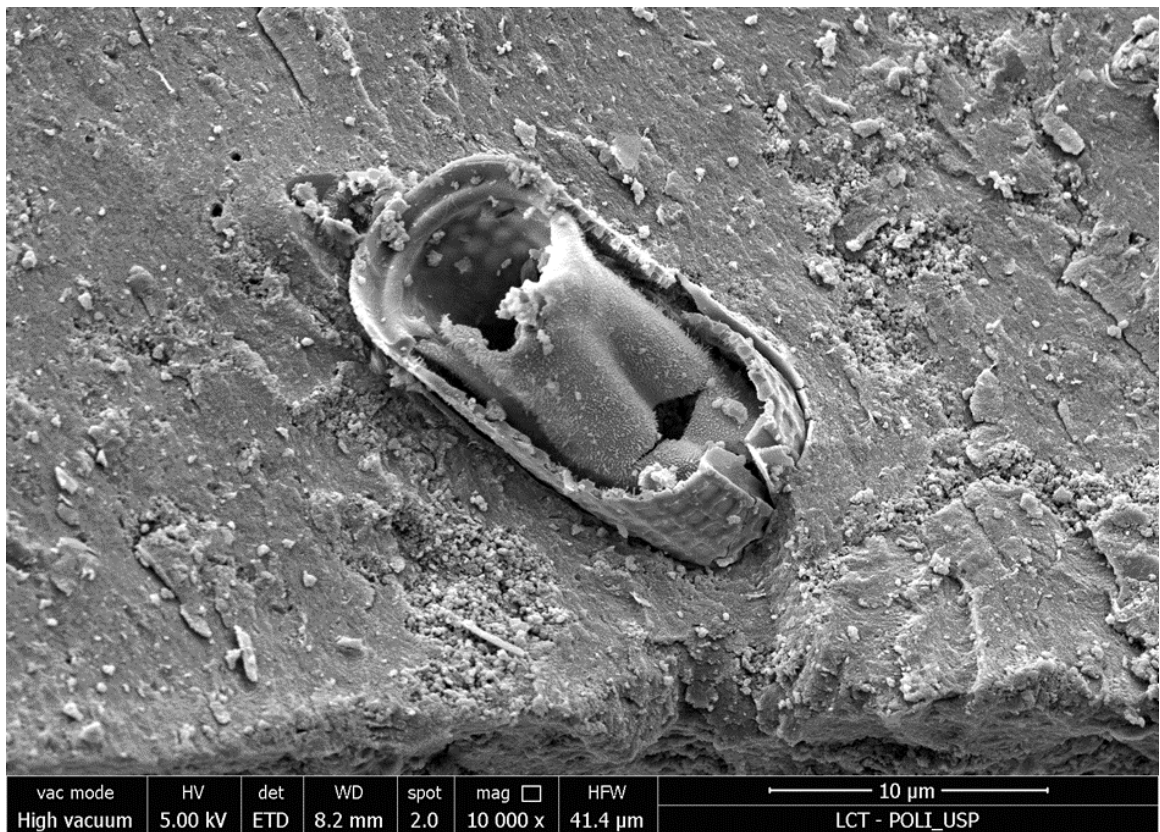
ZUQUETTE, L. V. **Análise crítica da cartografia geotécnica e proposta metodológica para condições brasileiras**. 1987. 673 p. Doctoral Thesis—Escola de Engenharia de São Carlos, Universidade de São Paulo, São Carlos, Brazil, 1987.

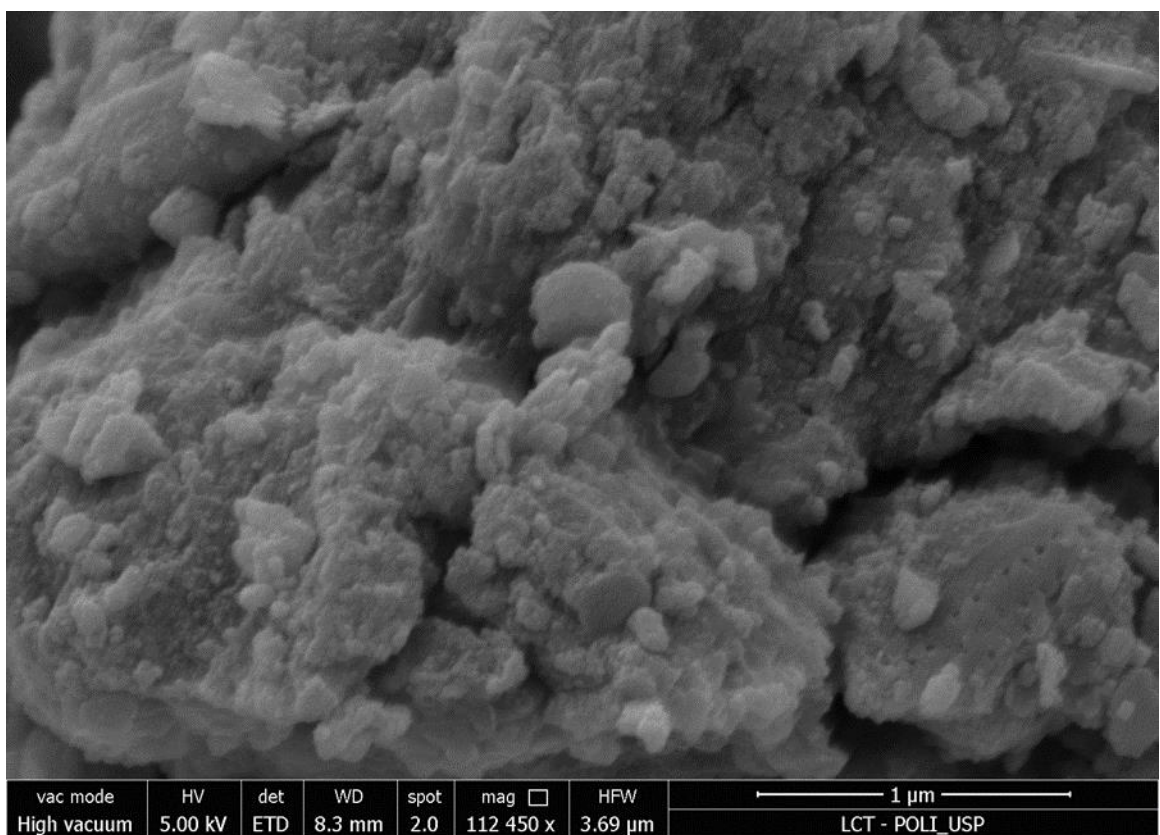
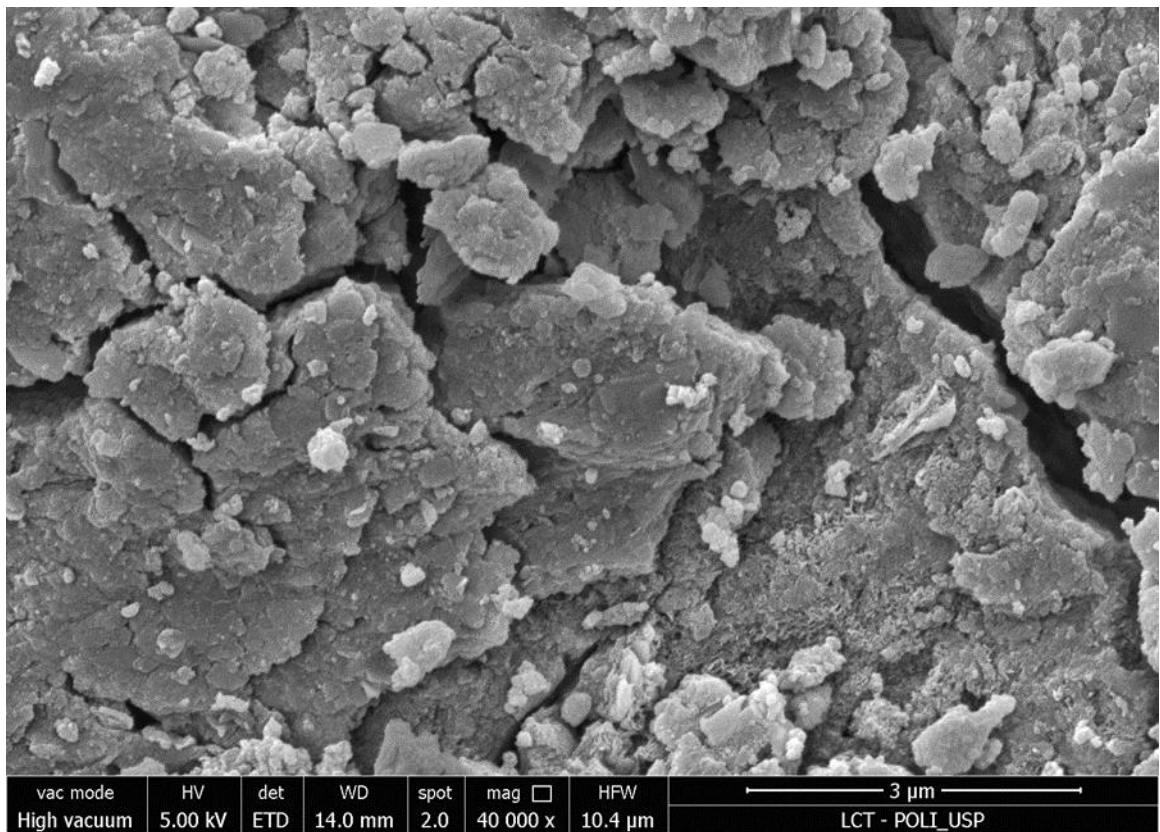
APPENDIX A

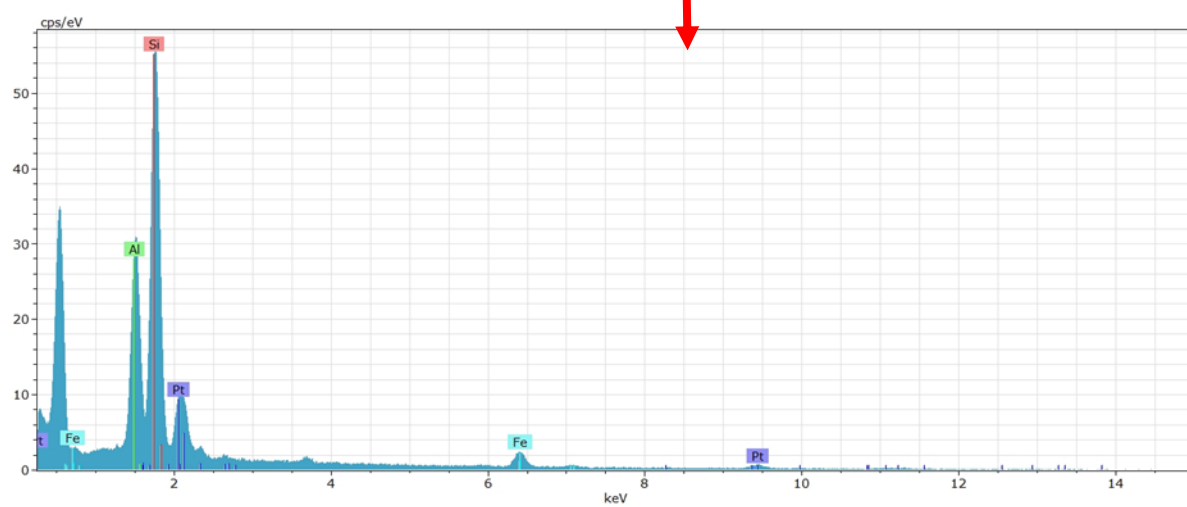
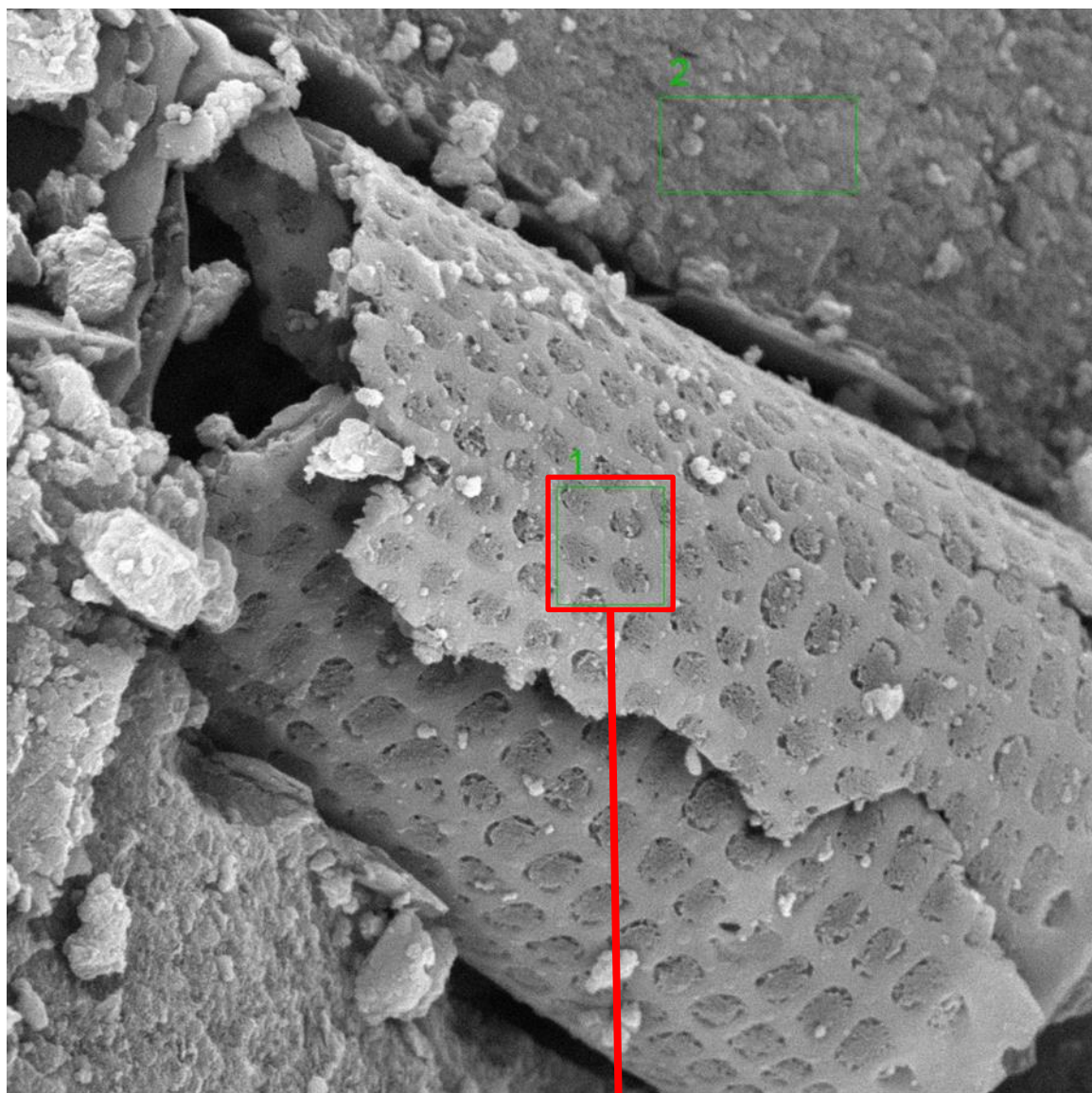
Scanning Electron Microscopy (SEM) images of Taiapuêba-WTS.





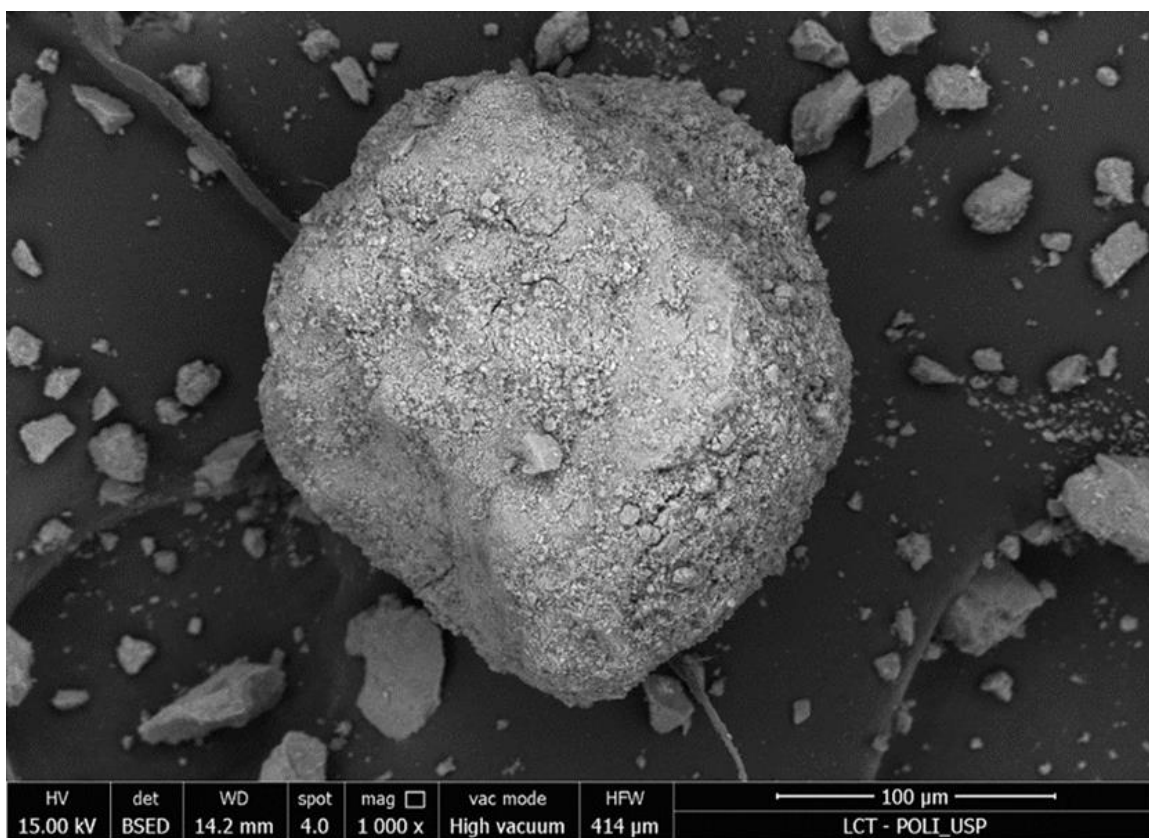
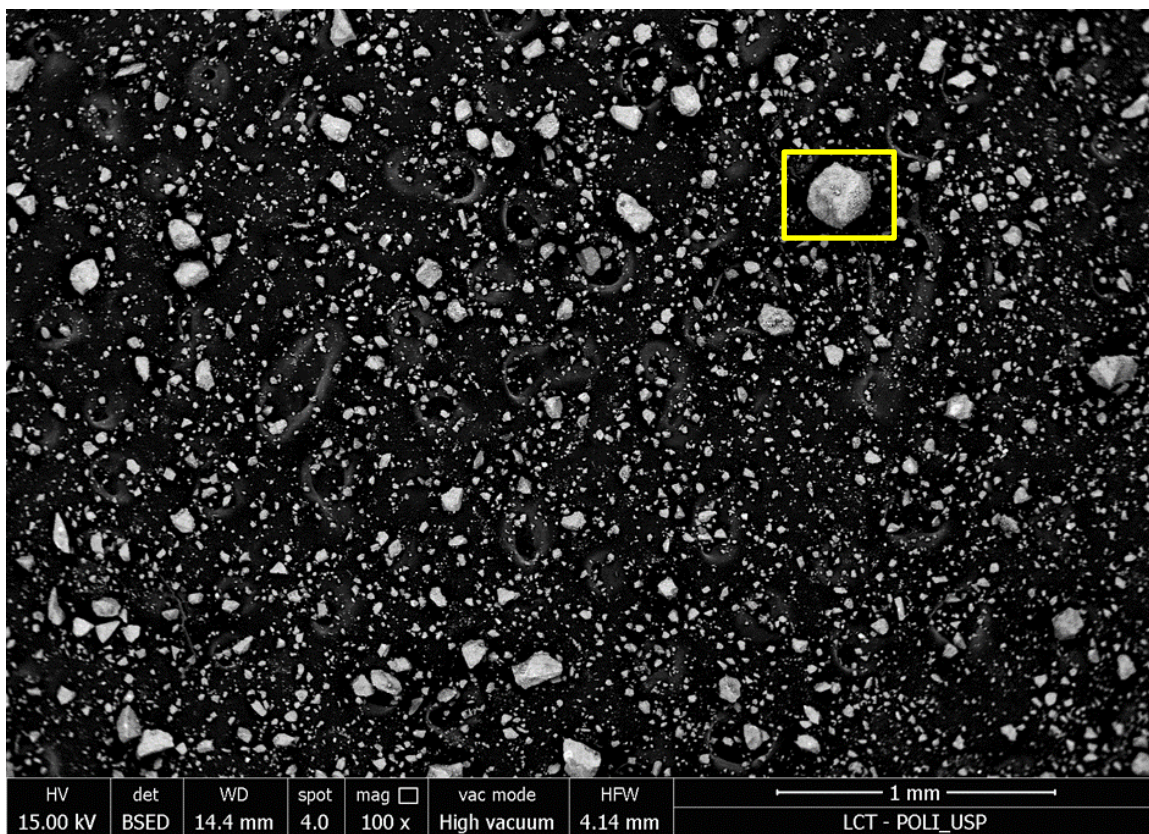


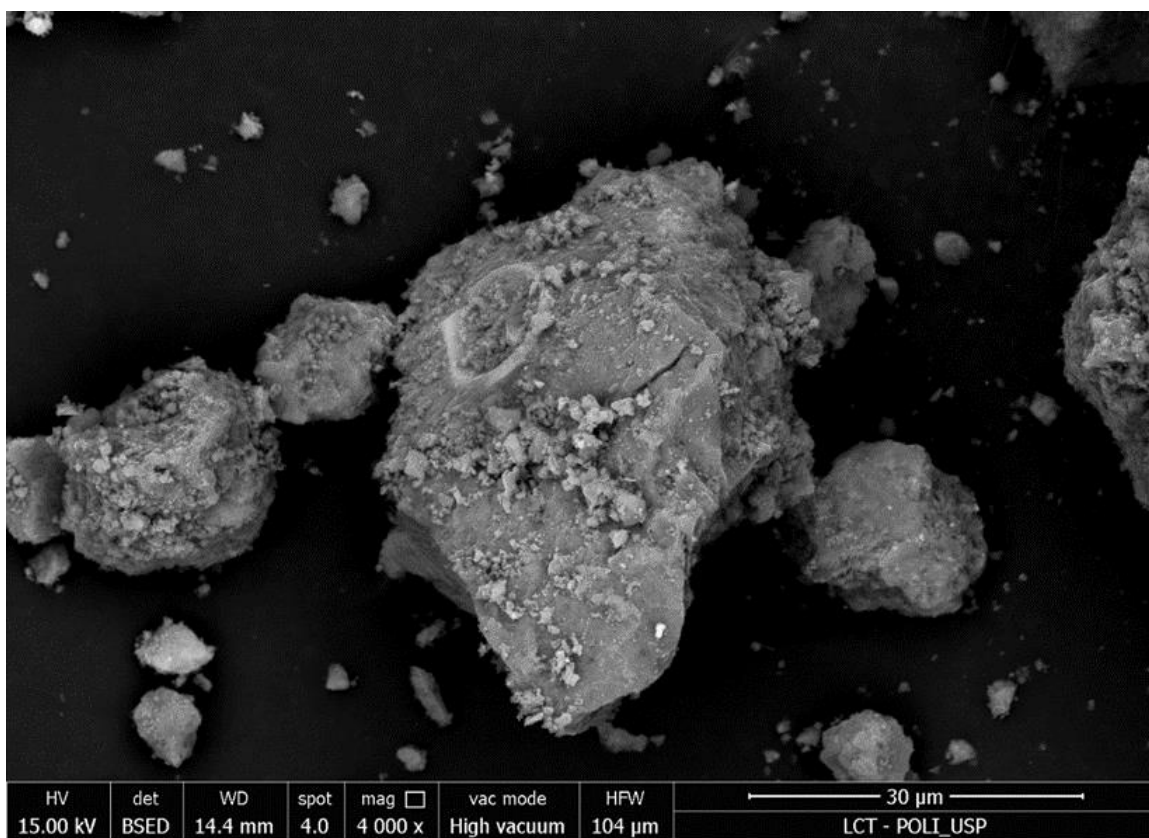
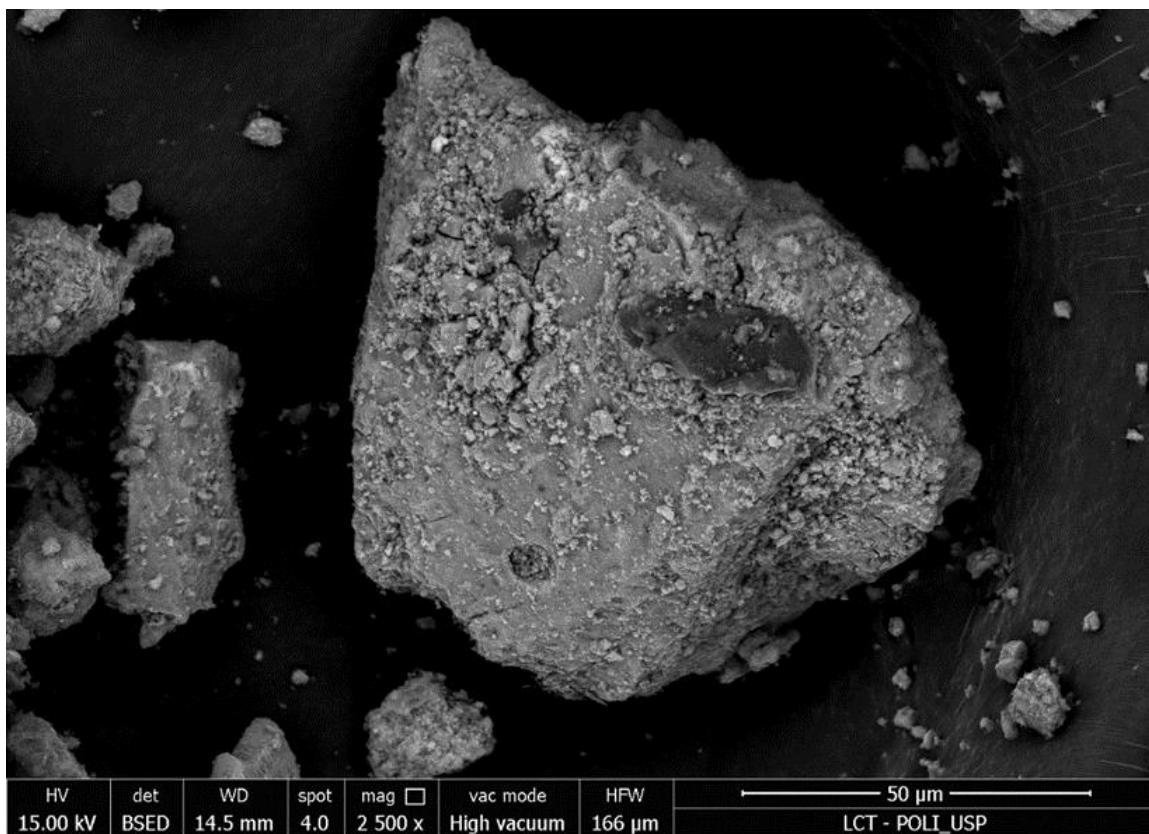


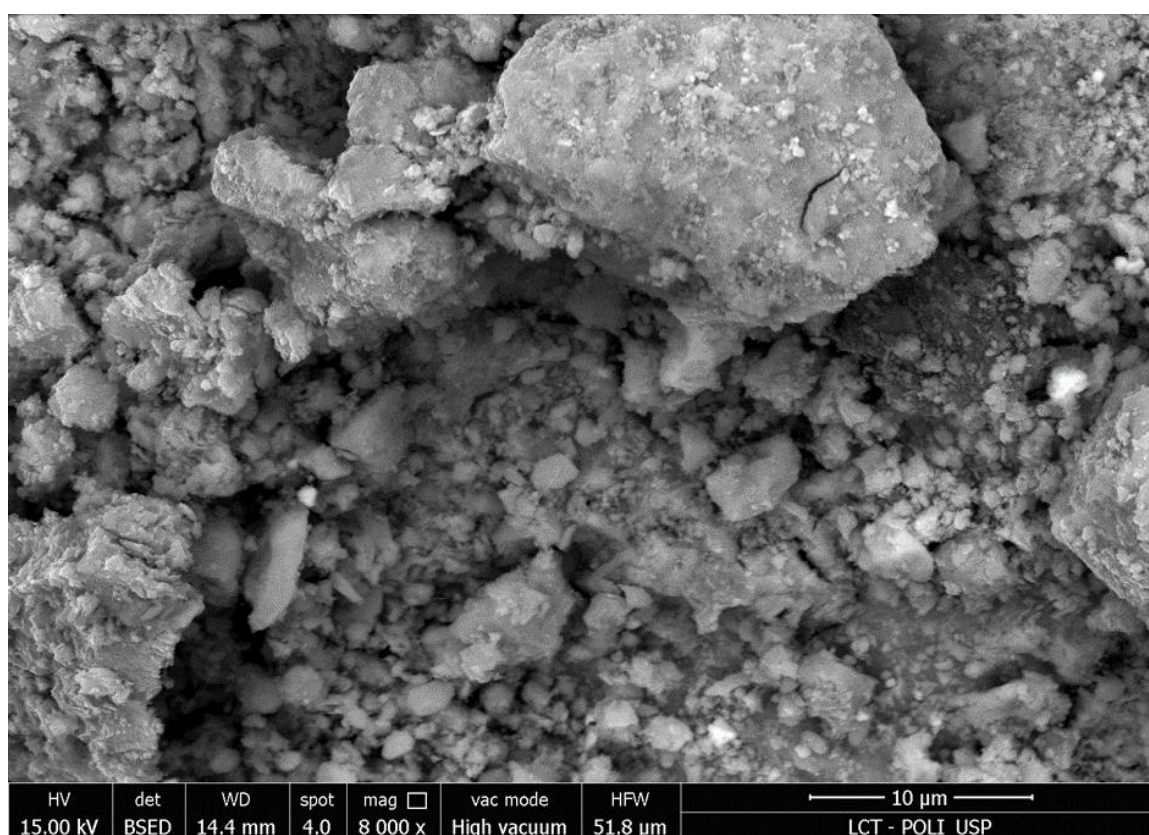
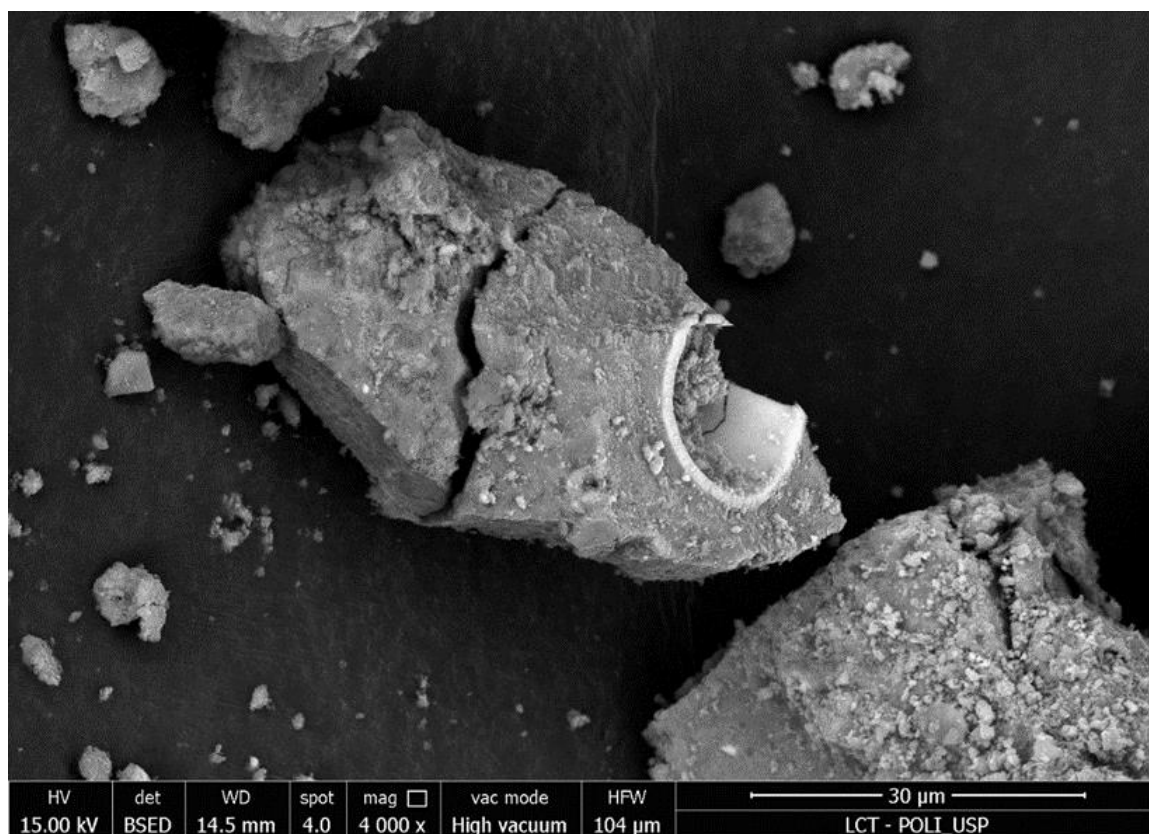


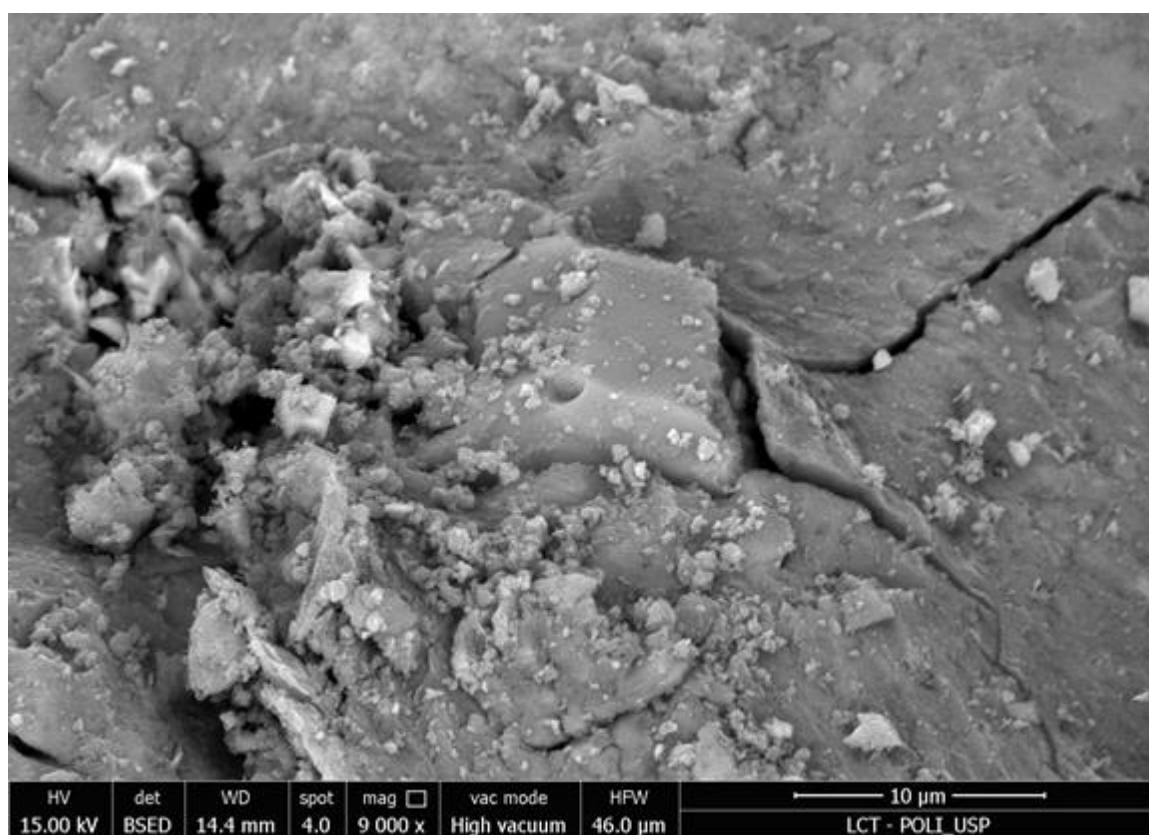
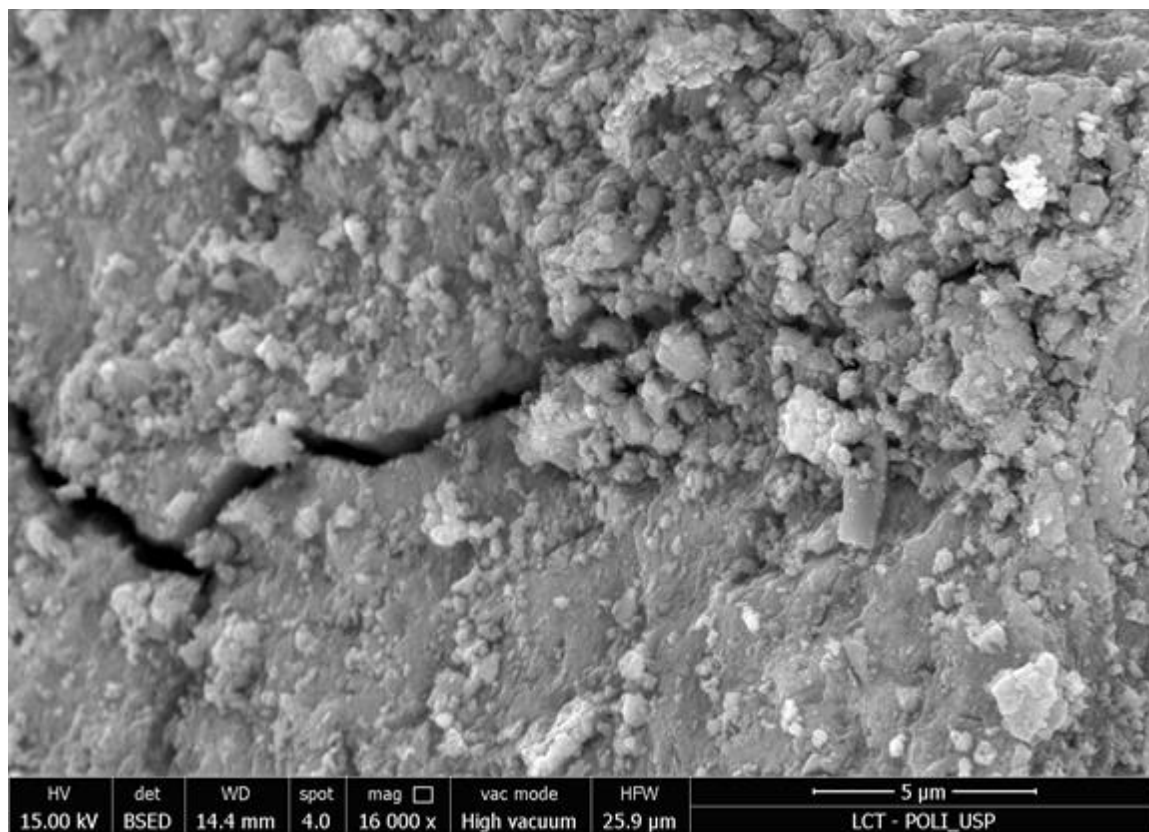
APPENDIX B

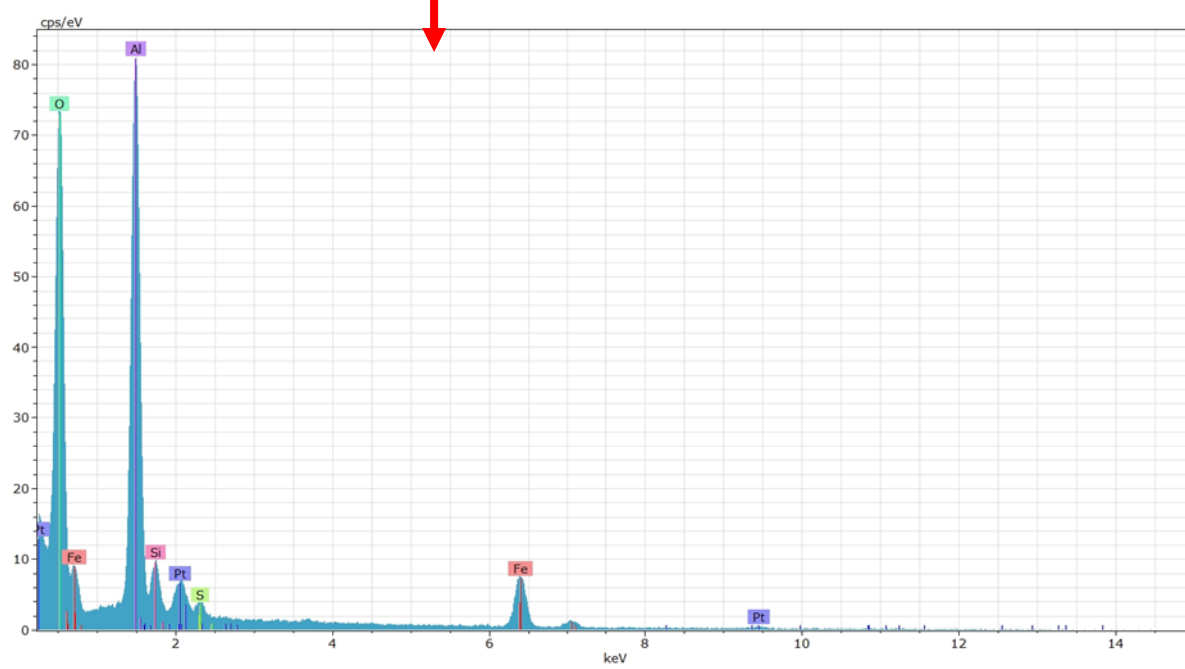
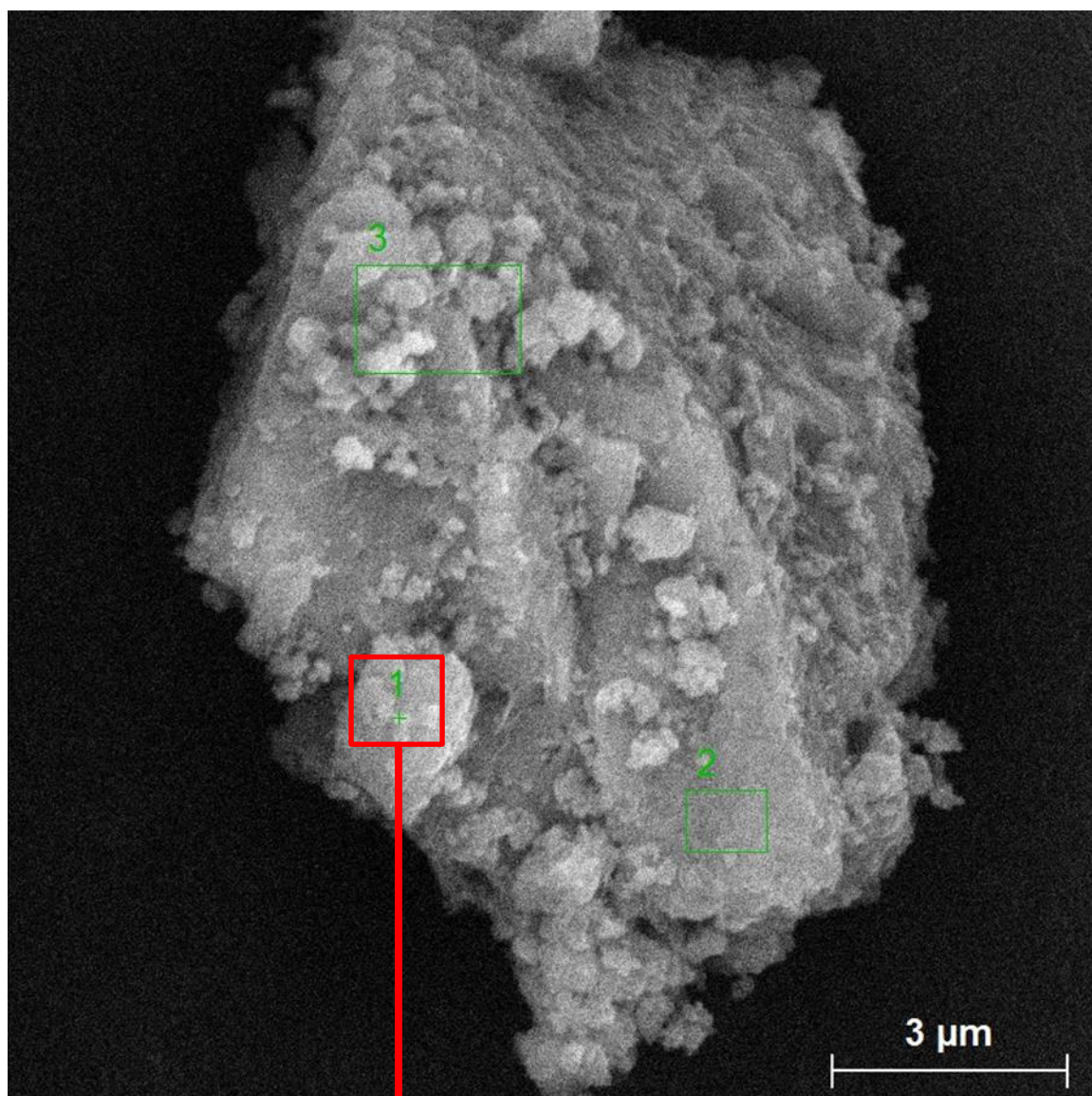
Scanning Electron Microscopy (SEM) images of Taiapuiba-WTS after treatment by H₂O₂ and heating.







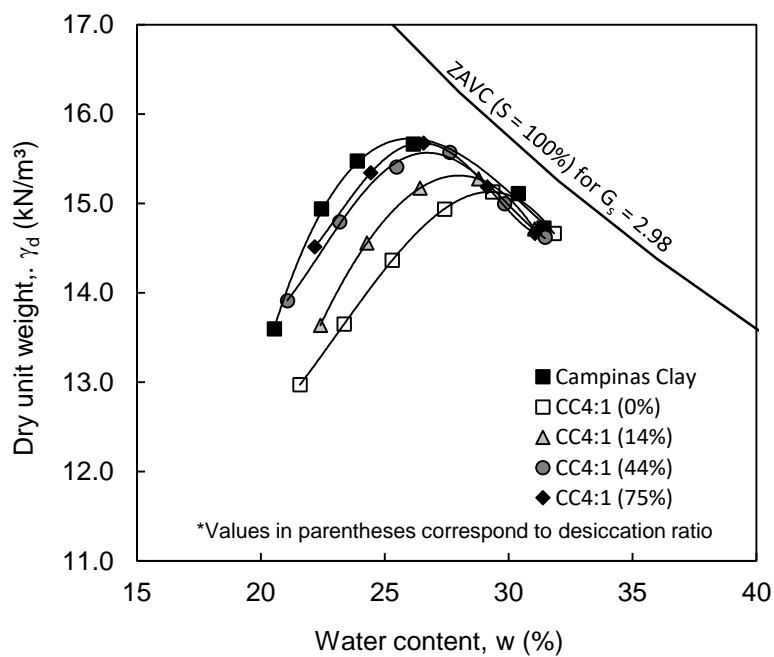




APPENDIX C

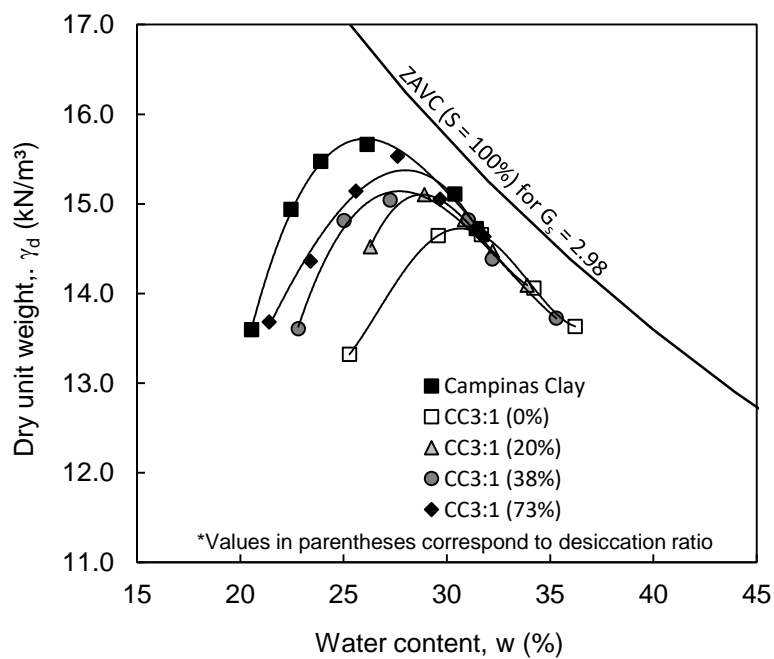
Compaction curves (γ_d vs. w) of mixtures with previous drying.

Figure 89 – Influence of previous drying on compaction curves of CC4:1 mixtures.



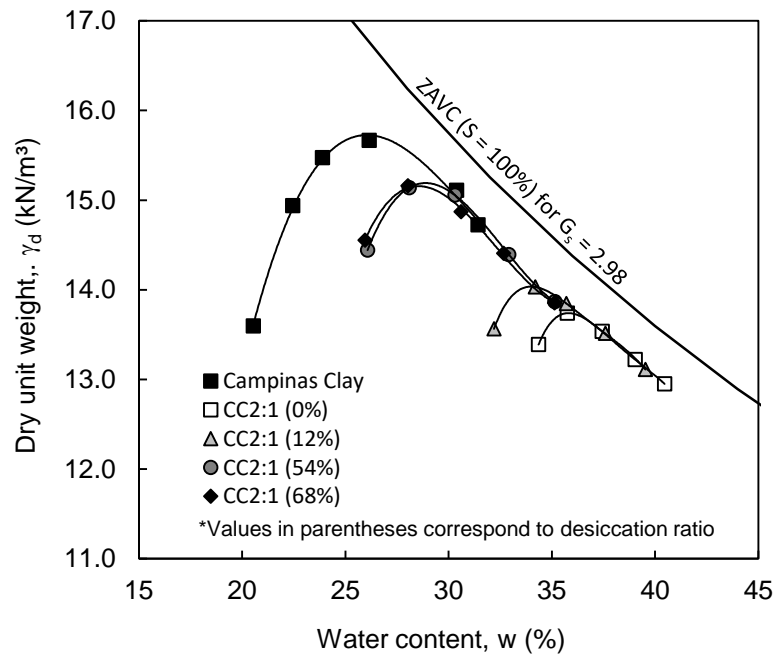
Source: author.

Figure 90 – Influence of previous drying on compaction curves of CC3:1 mixtures.



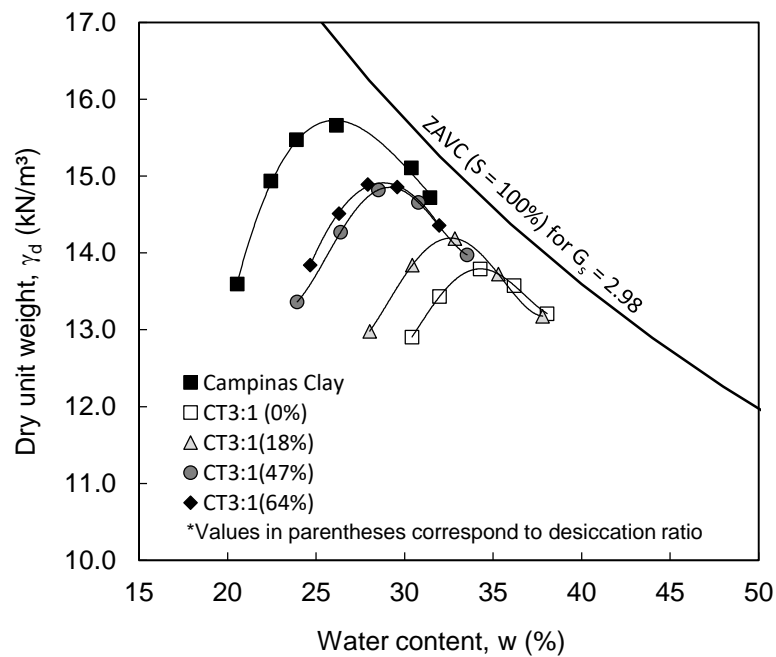
Source: author.

Figure 91 – Influence of previous drying on compaction curves of CC2:1 mixtures.



Source: author.

Figure 92 – Influence of previous drying on compaction curves of CT3:1 mixtures.



Source: author.

Figure 93 – Influence of previous drying on compaction curves of CT2:1 mixtures.

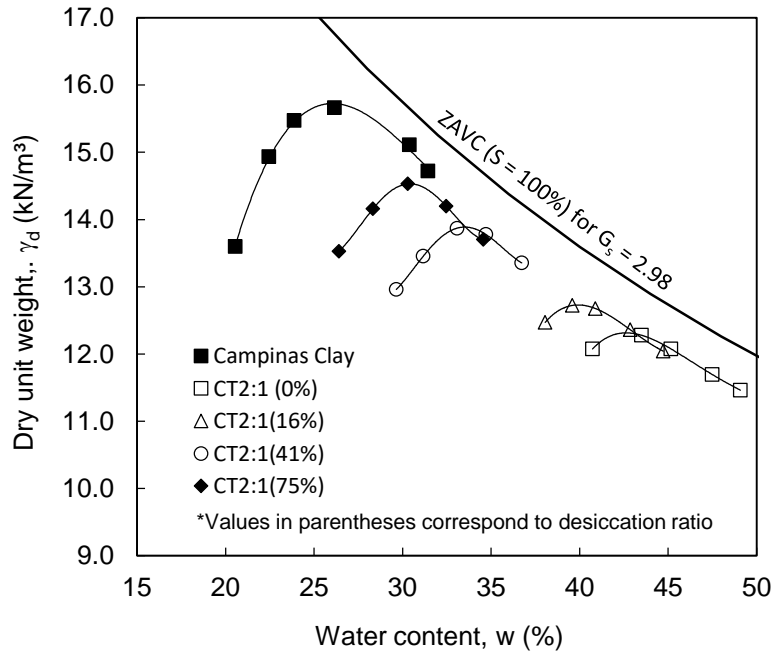


Figure 94 – Influence of previous drying on compaction curves of CT1.5:1 mixtures.

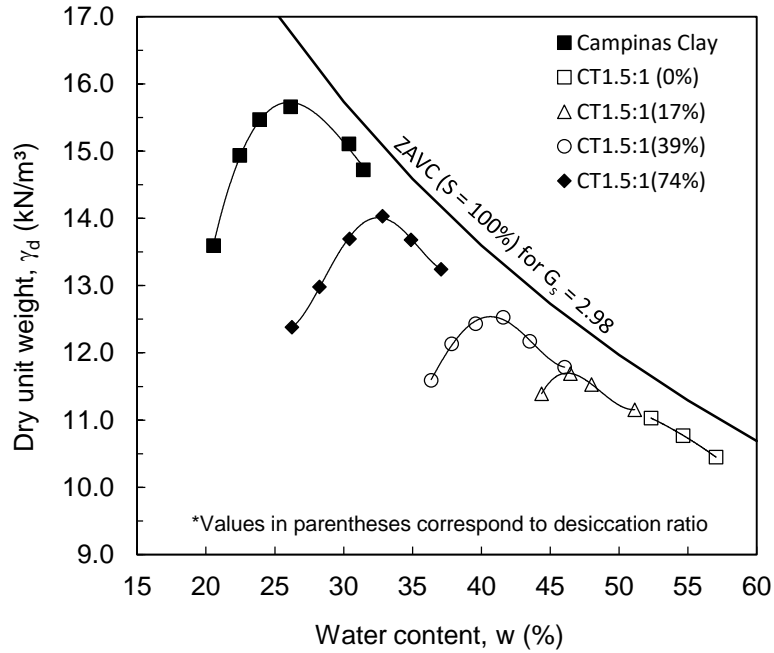
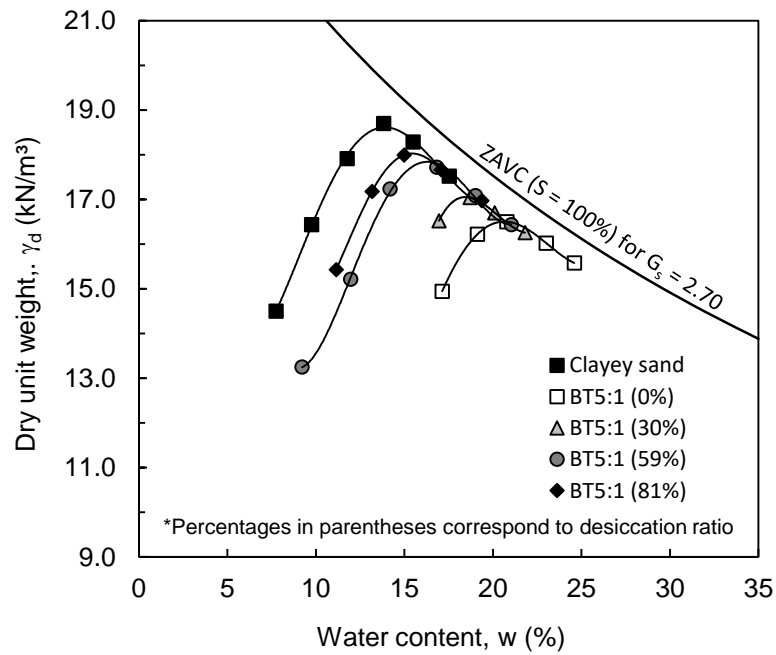
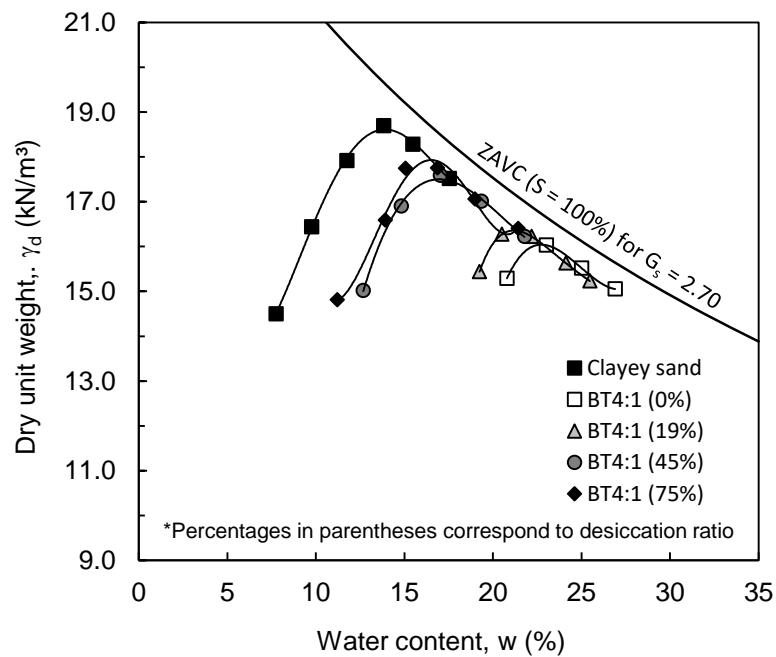


Figure 95 – Influence of previous drying on compaction curves of BT5:1 mixtures.



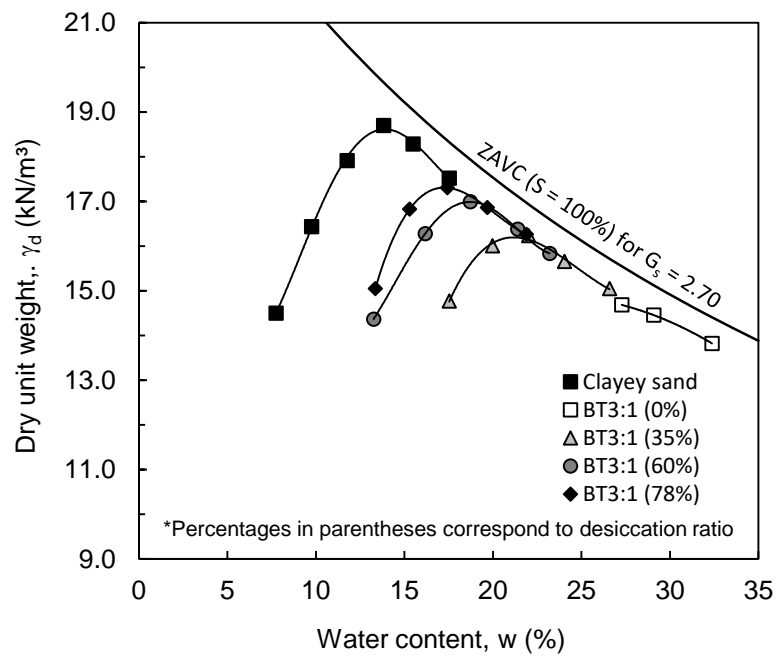
Source: author.

Figure 96 – Influence of previous drying on compaction curves of BT4:1 mixtures.



Source: author.

Figure 97 – Influence of previous drying on compaction curves of BT3:1 mixtures.

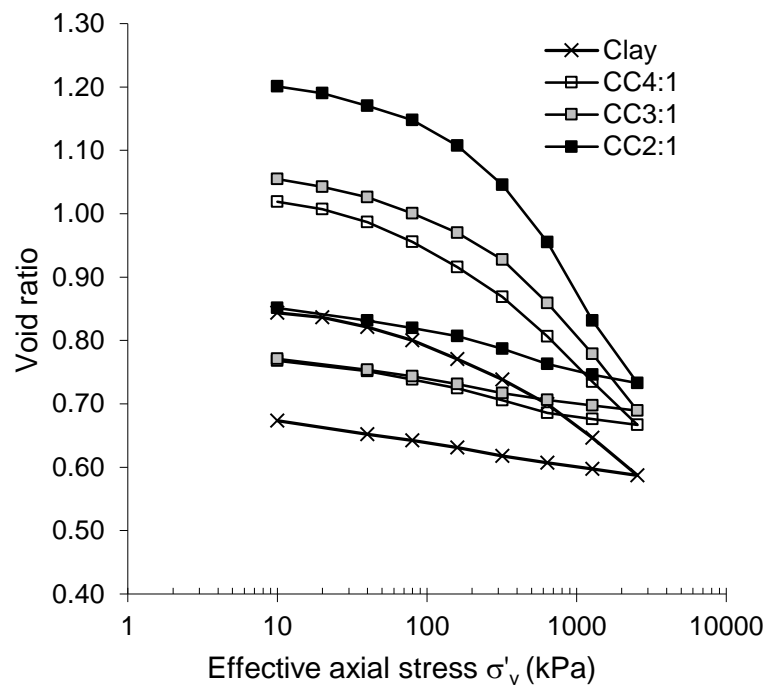


Source: author.

APPENDIX D

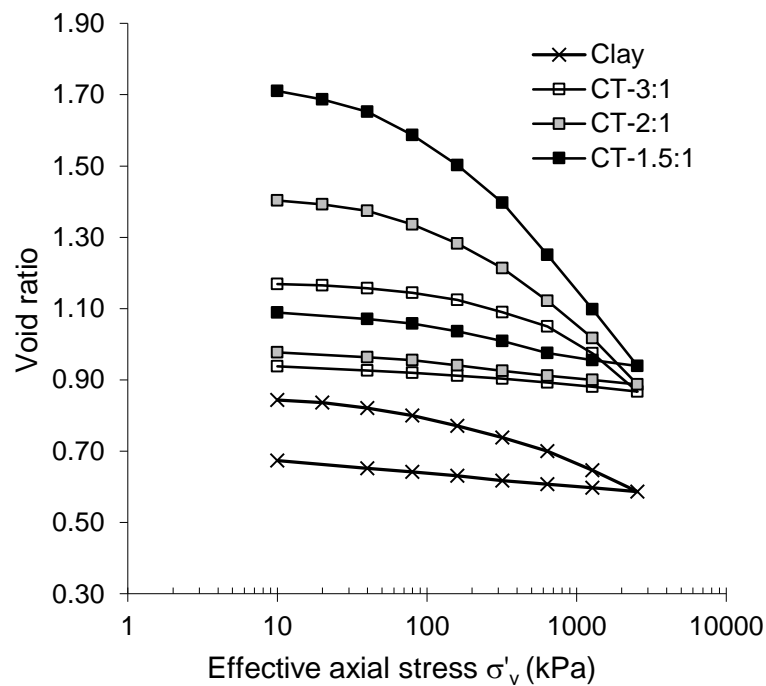
Oedometric compression curves (e vs. $\log\sigma'_v$) of studied soils and mixtures.

Figure 98 – Oedometric compression curves of Campinas clay and CC mixtures.



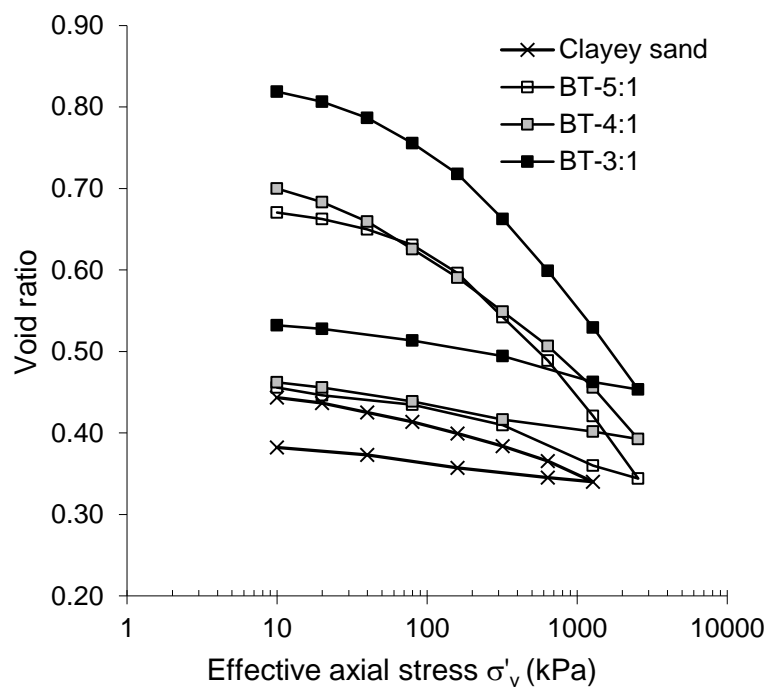
Source: author.

Figure 99 Oedometric compression curves of Campinas clay and CT mixtures.



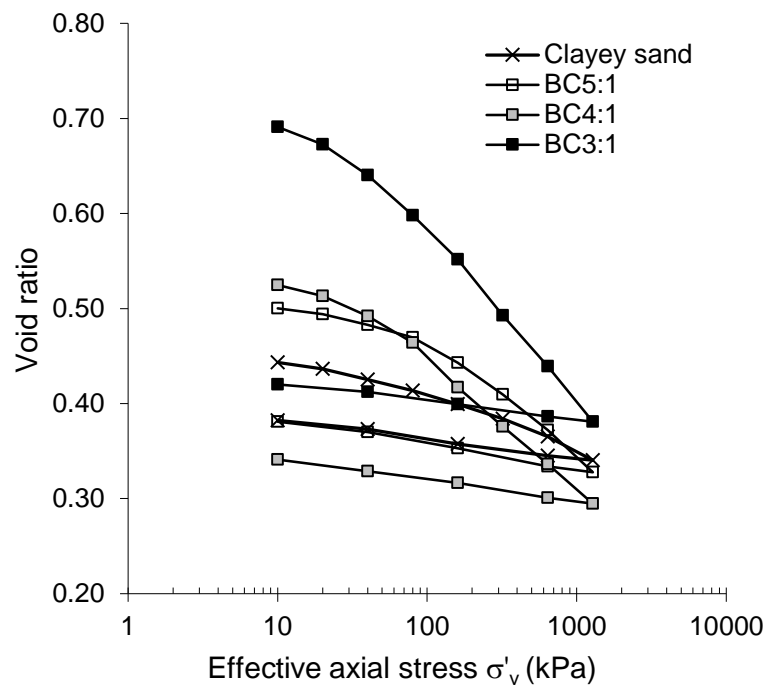
Source: author.

Figure 100 - Oedometric compression curves of Botucatu clayey sand and BT mixtures.



Source: author.

Figure 101 - Oedometric compression curves of Botucatu clayey sand and BC mixtures.

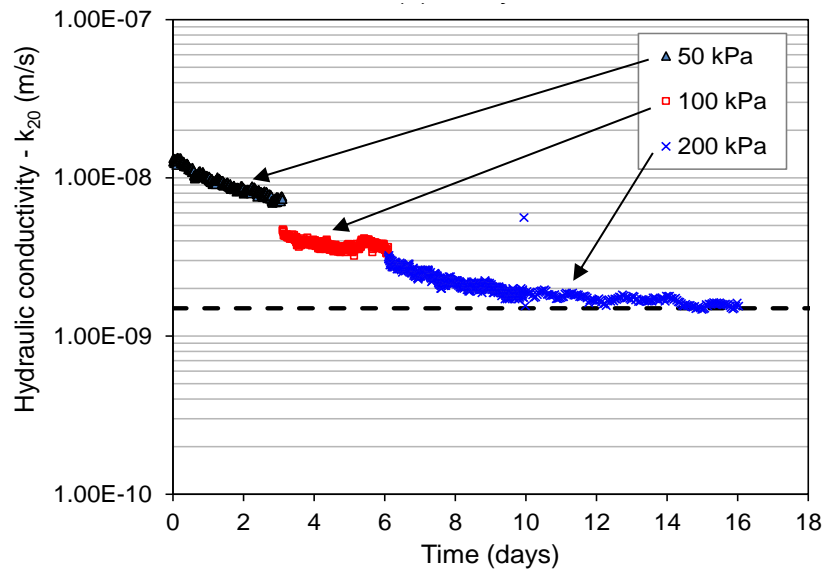


Source: Montalvan (2016).

APPENDIX E

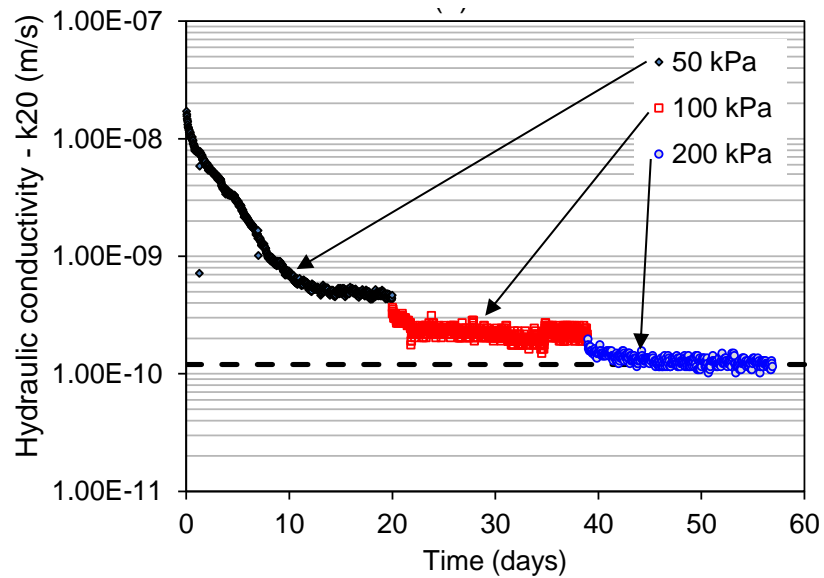
Graphs of hydraulic conductivity variation over time (k_{20} vs t) of studied soils and mixtures.

Figure 102 – Hydraulic conductivity of Campinas clay.



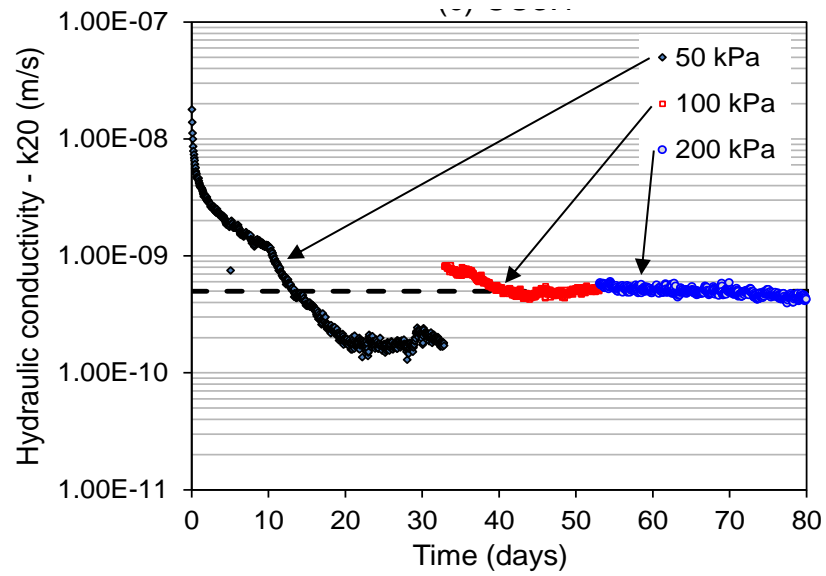
Source: author.

Figure 103 – Hydraulic conductivity of mixture CC4:1.



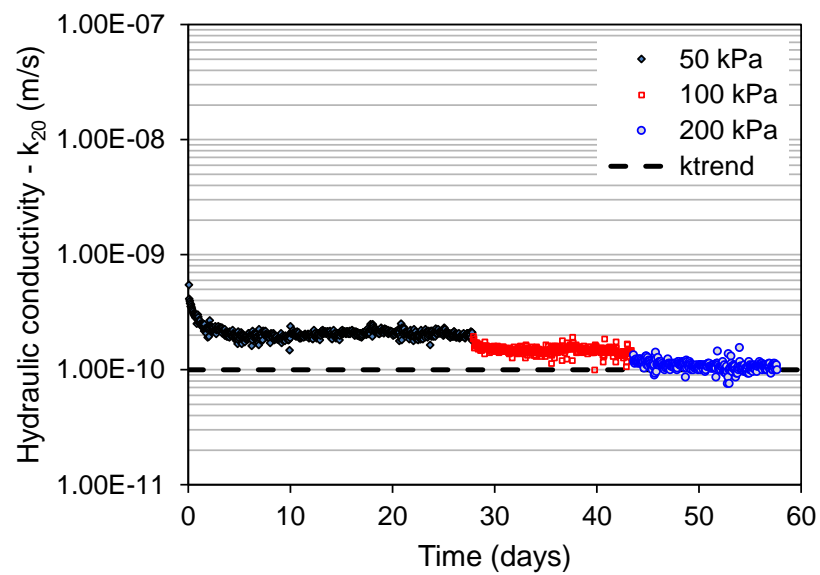
Source: author.

Figure 104 – Hydraulic conductivity of mixture CC3:1.



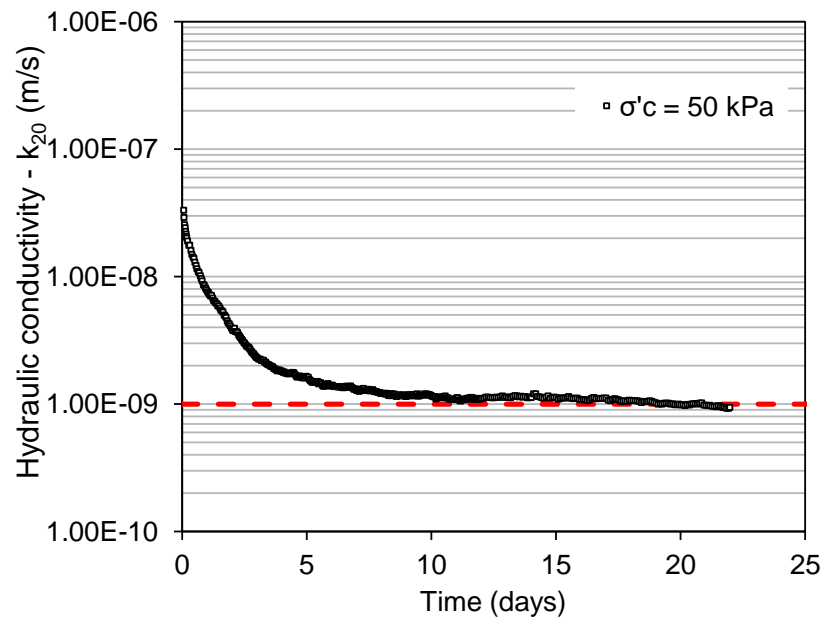
Source: author.

Figure 105 – Hydraulic conductivity of mixture CC2:1.



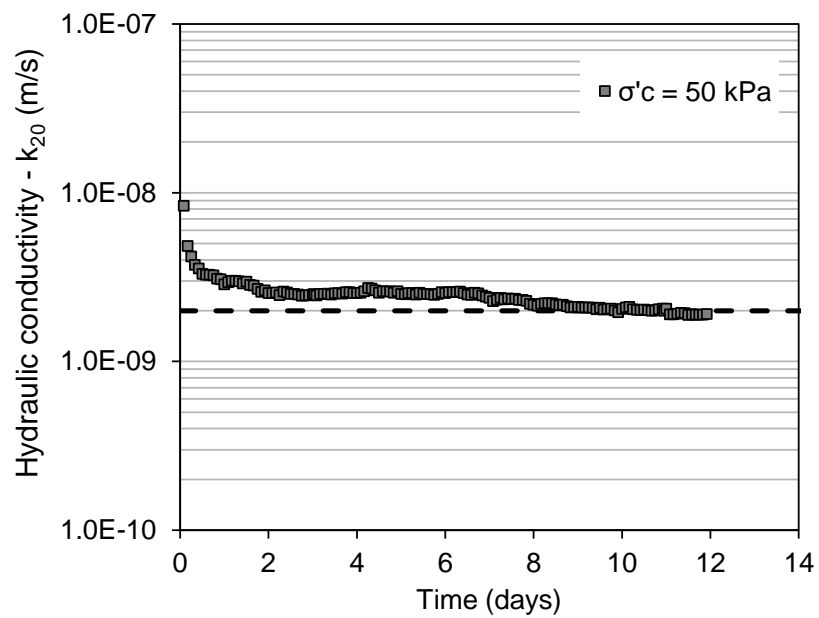
Source: author.

Figure 106 – Hydraulic conductivity of mixture CT3:1.



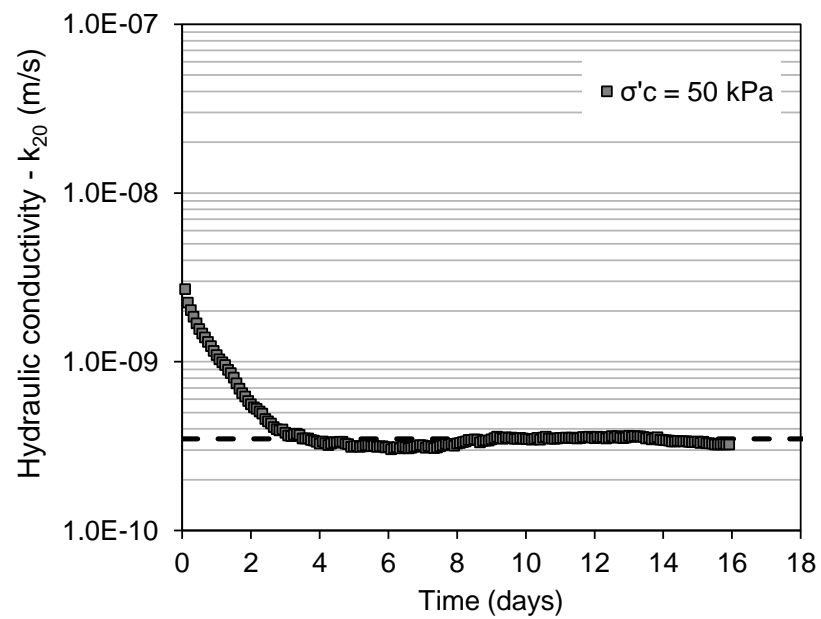
Source: author.

Figure 107 – Hydraulic conductivity of mixture CT2:1.



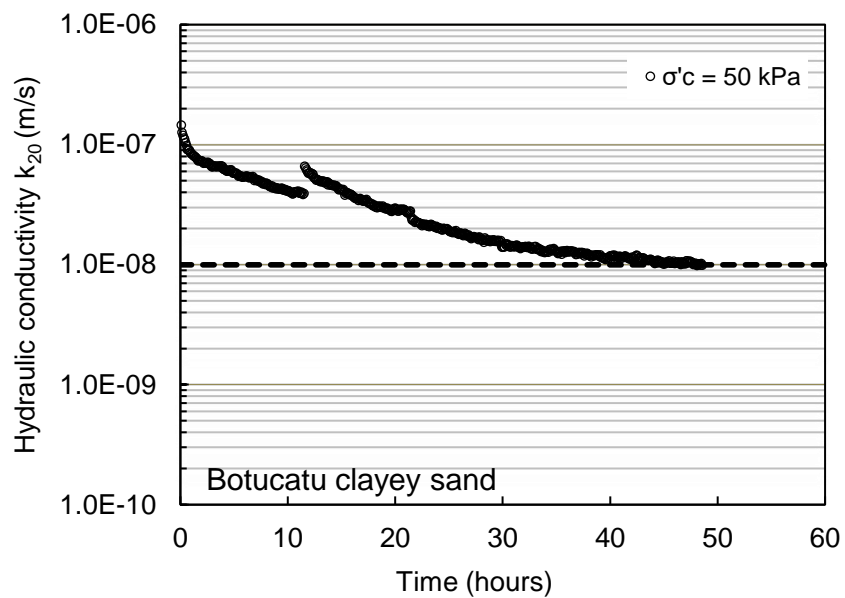
Source: author.

Figure 108 – Hydraulic conductivity of mixture CT1.5:1.



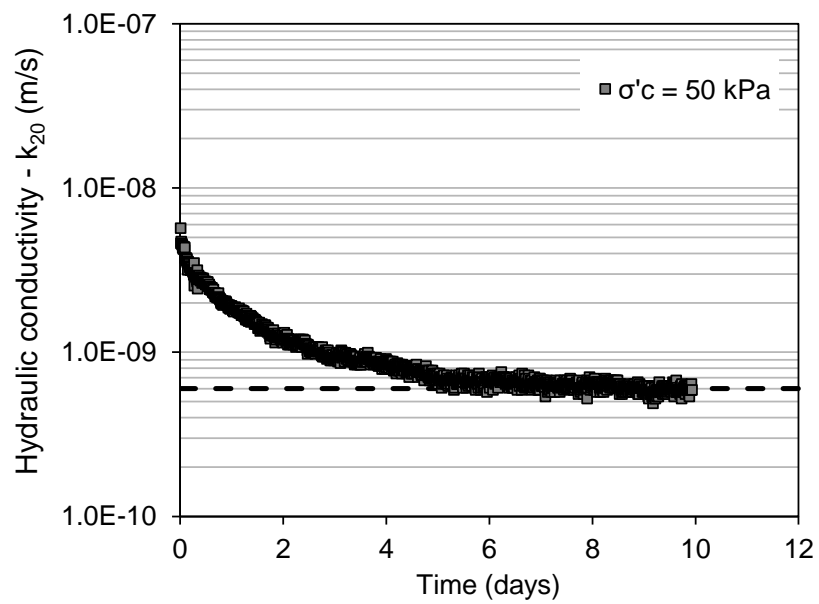
Source: author.

Figure 109 – Hydraulic conductivity of Botucatu clayey sand.



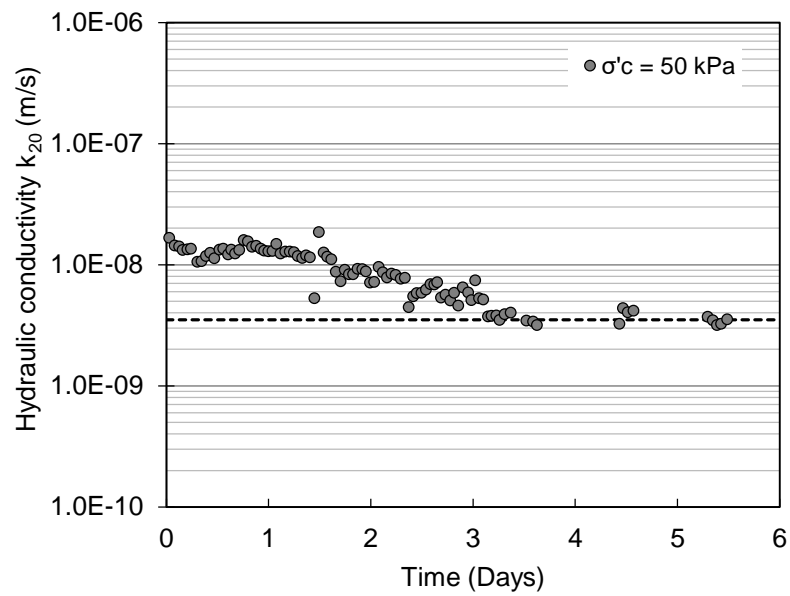
Source: author.

Figure 110 – Hydraulic conductivity of mixture BT5:1.



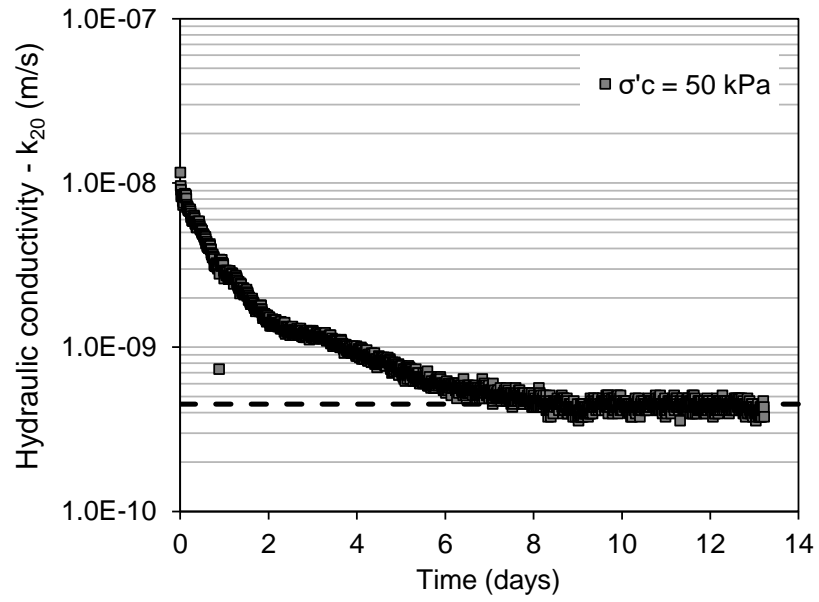
Source: author.

Figure 111 – Hydraulic conductivity of mixture BT4:1.



Source: author.

Figure 112 – Hydraulic conductivity of mixture BT3:1.



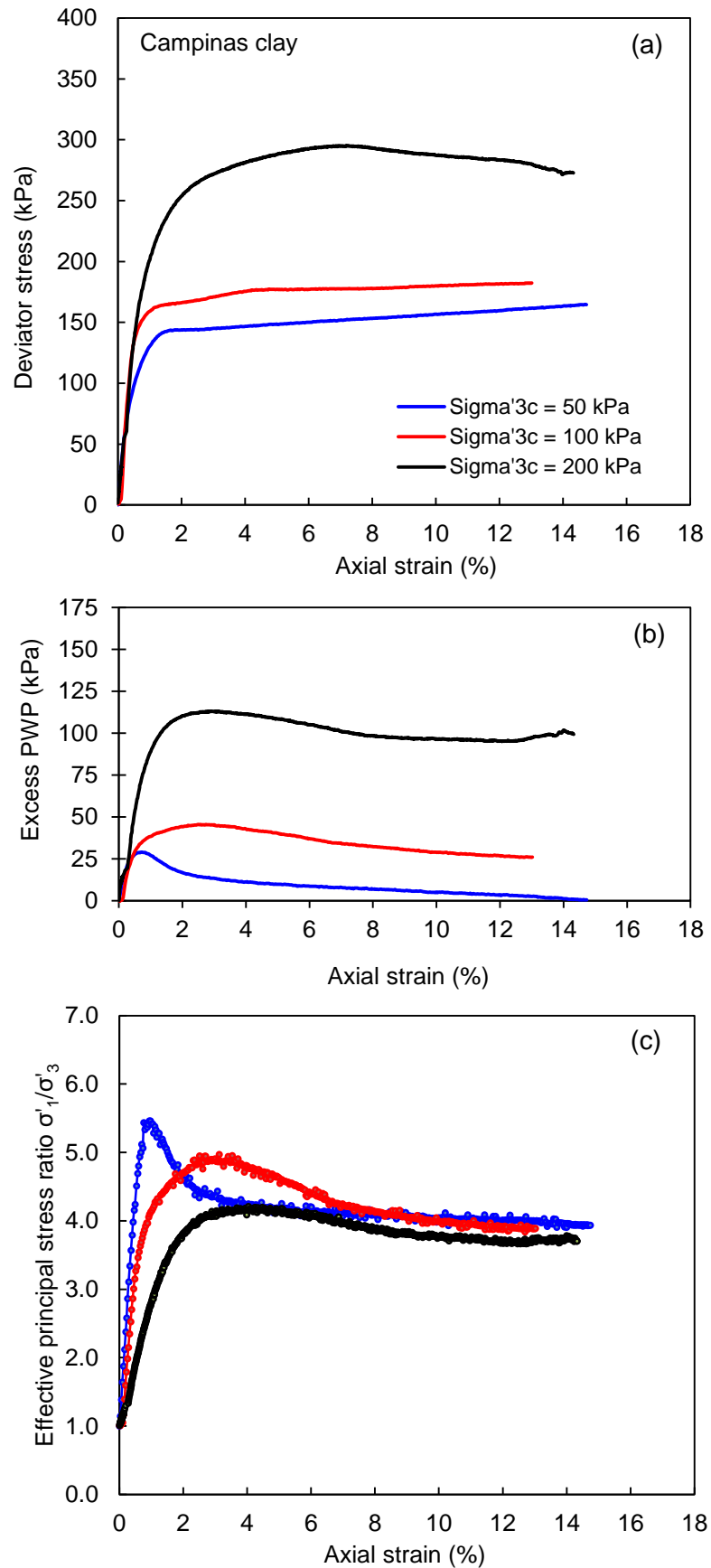
Source: author.

APPENDIX F

Results from Isotropically Consolidated Undrained (CIU) triaxial compression tests:

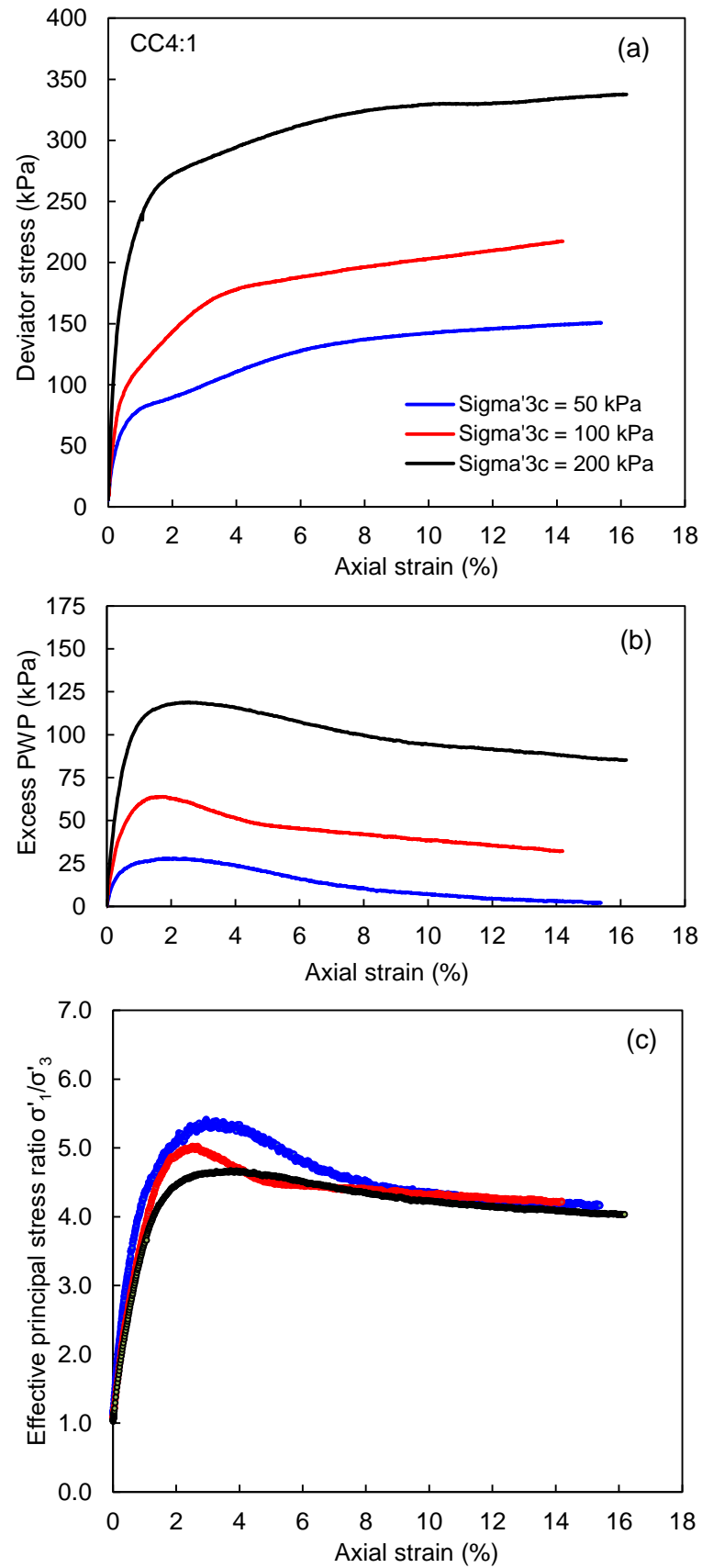
(a) stress-strain, (b) pore pressure-strain, and (c) principal effective stress ratio.

Figure 113 – Results of CIU tests on Campinas clay.



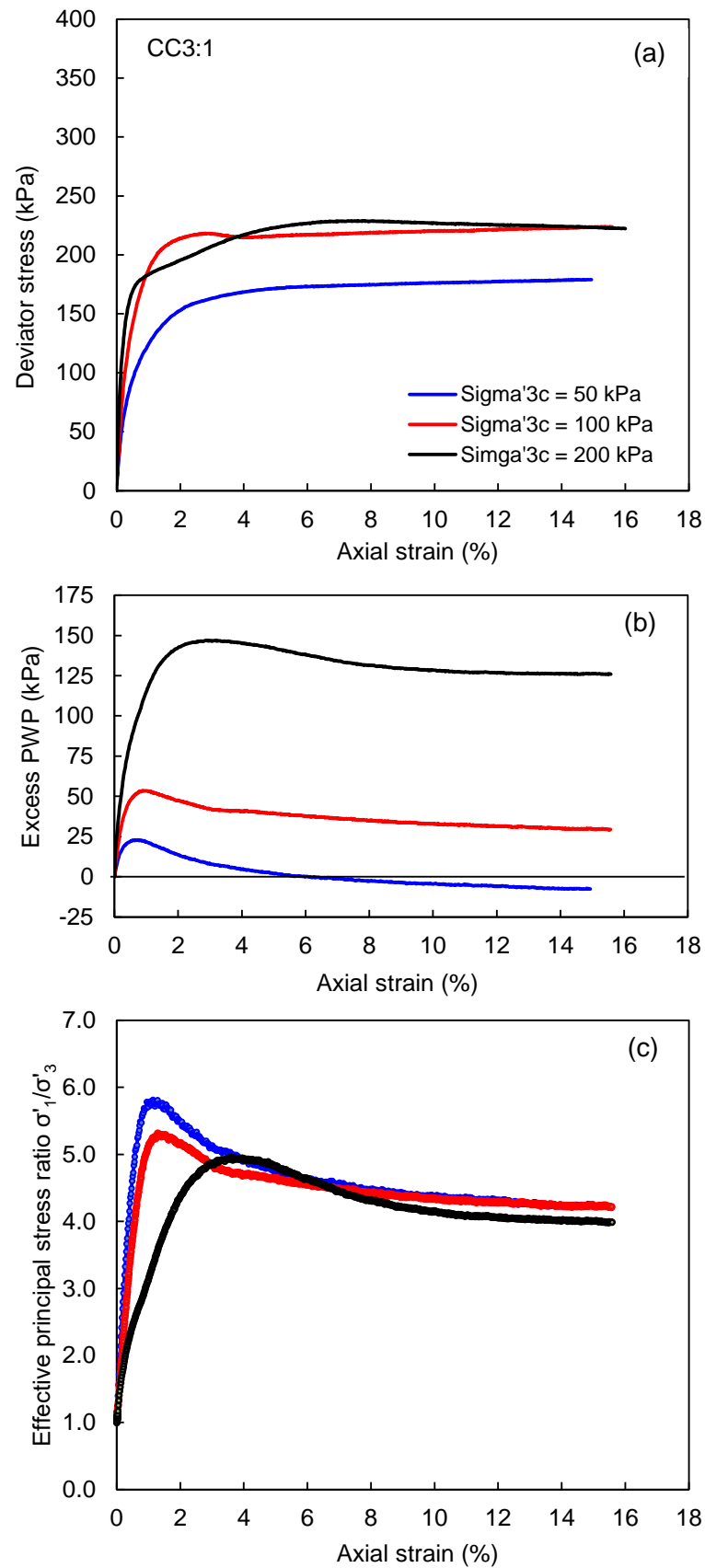
Source: author.

Figure 114 – Results of CIU tests on CC4:1 mixture.



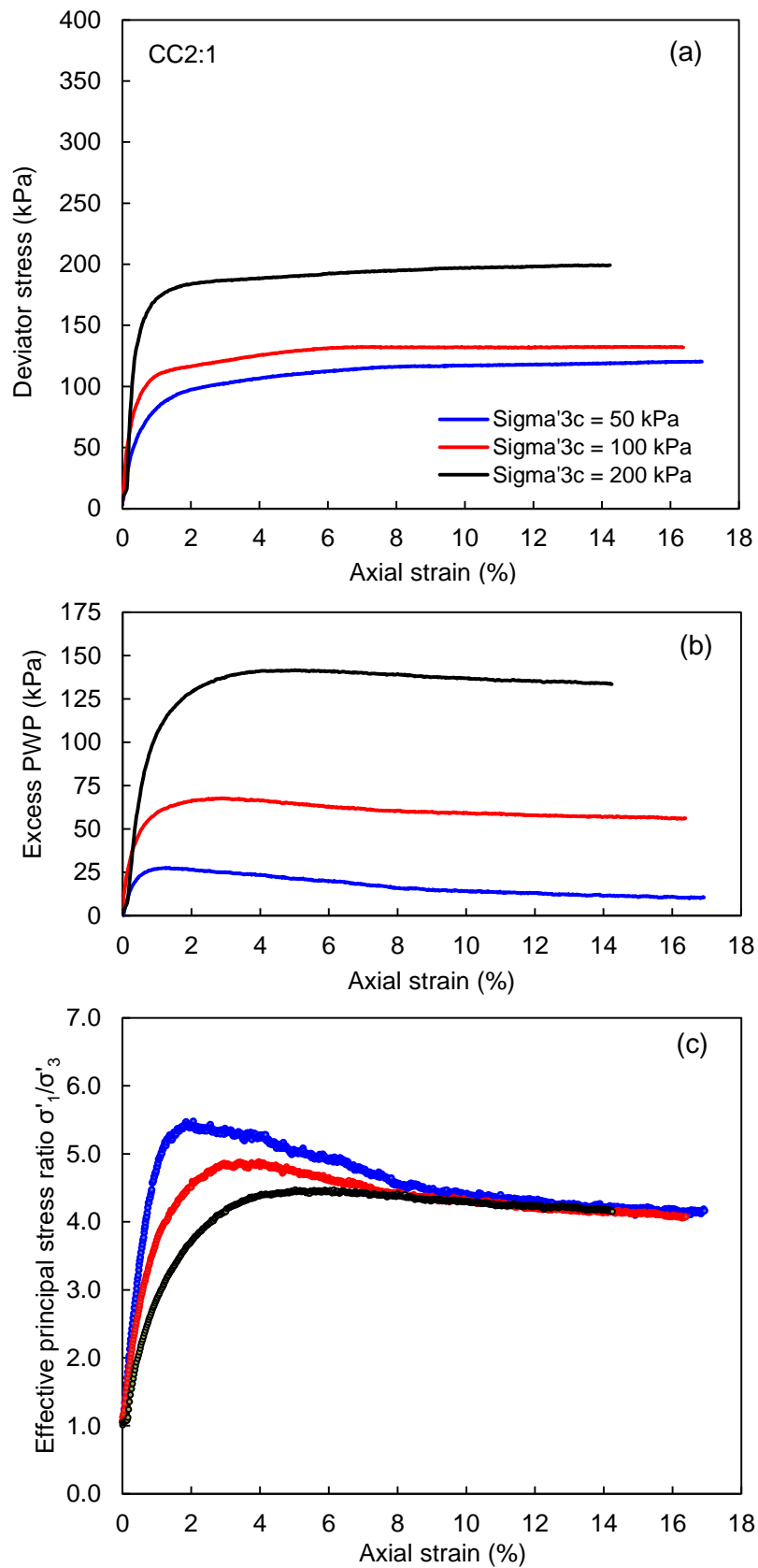
Source: author.

Figure 115 – Results of CIU tests on CC3:1 mixture.



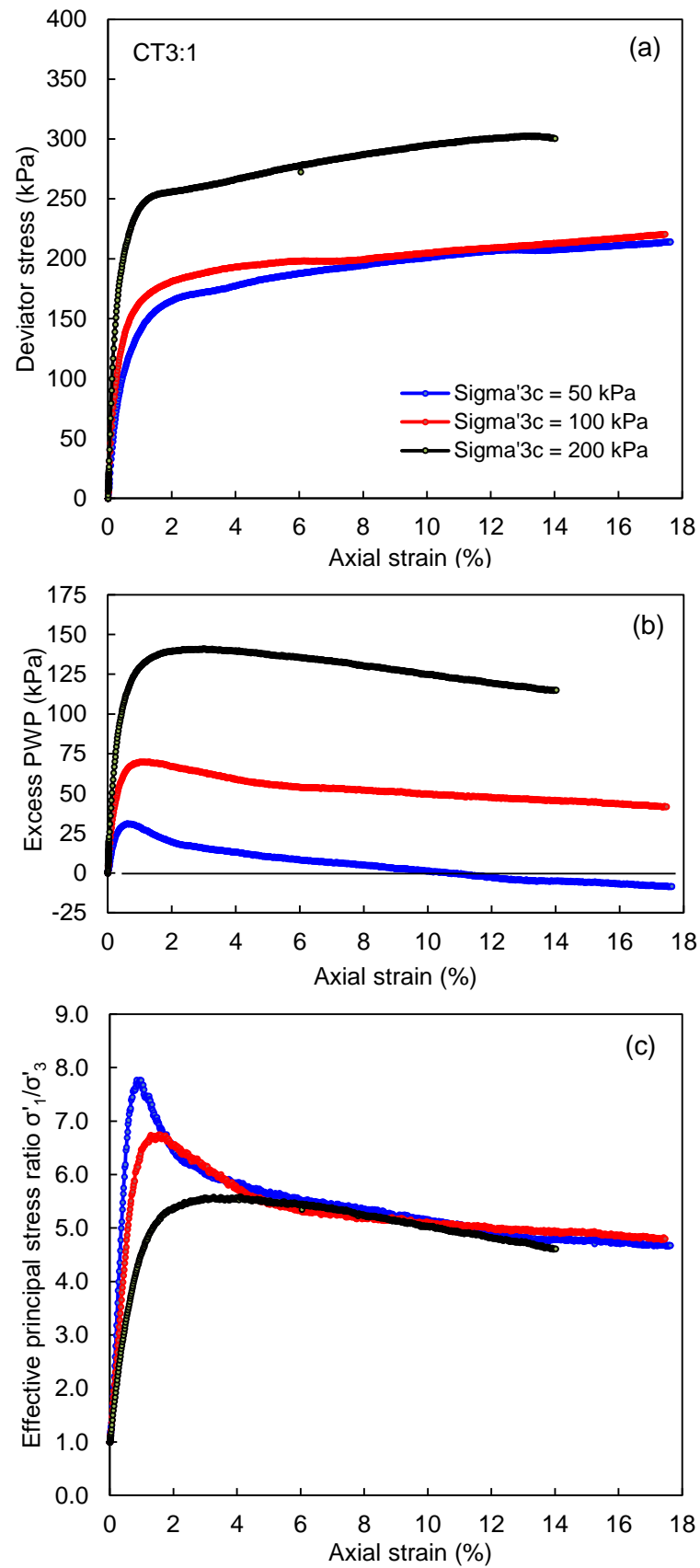
Source: author.

Figure 116 – Results of CIU tests on CC2:1 mixture.



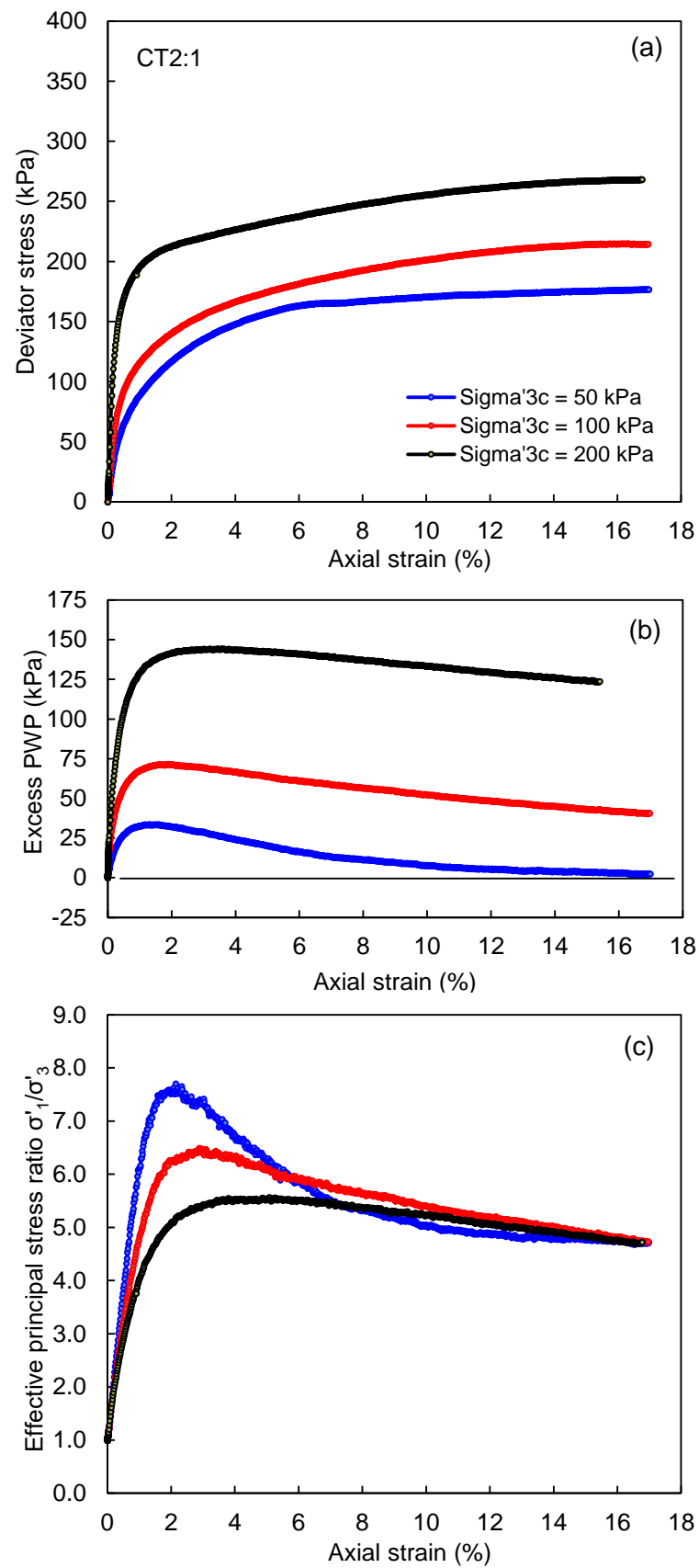
Source: author.

Figure 117 – Results of CIU tests on CT3:1 mixture.



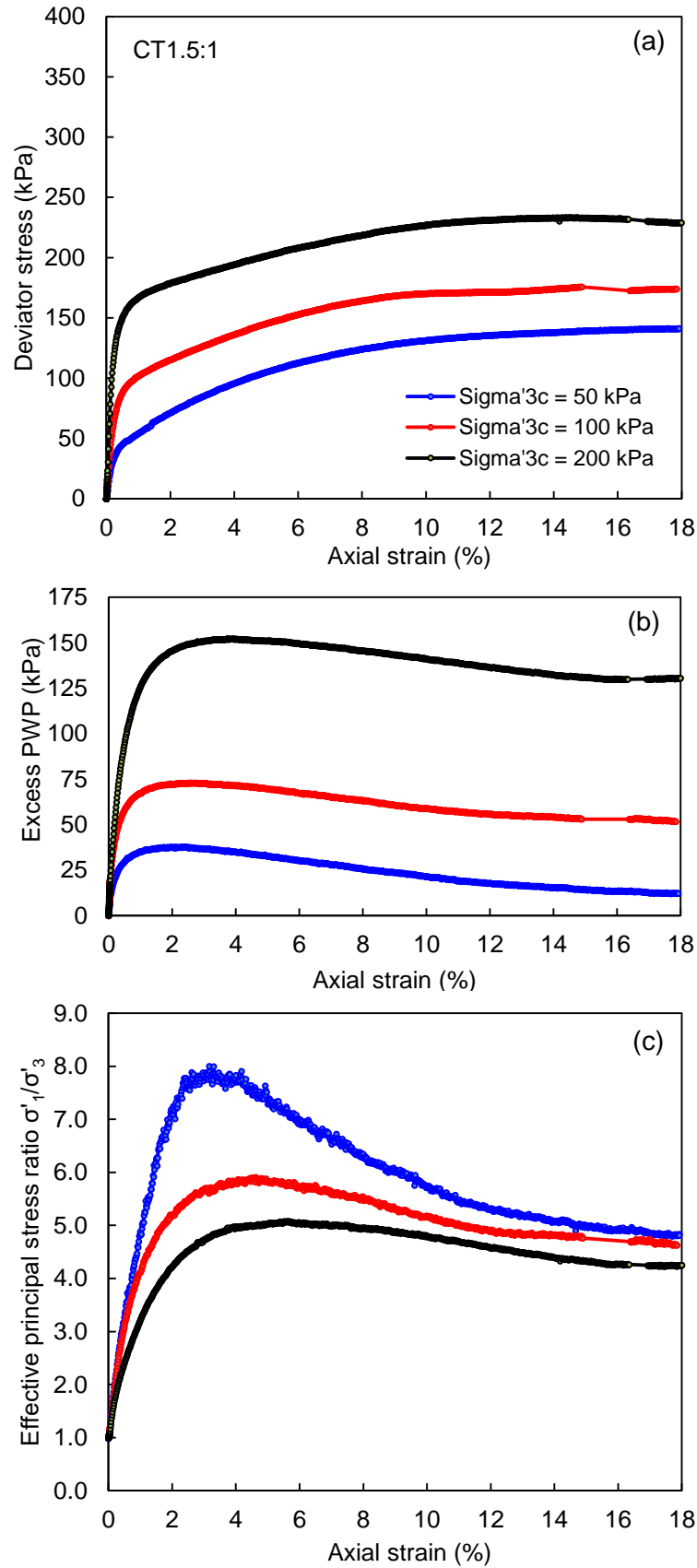
Source: author.

Figure 118 – Results of CIU tests on CT2:1 mixture.



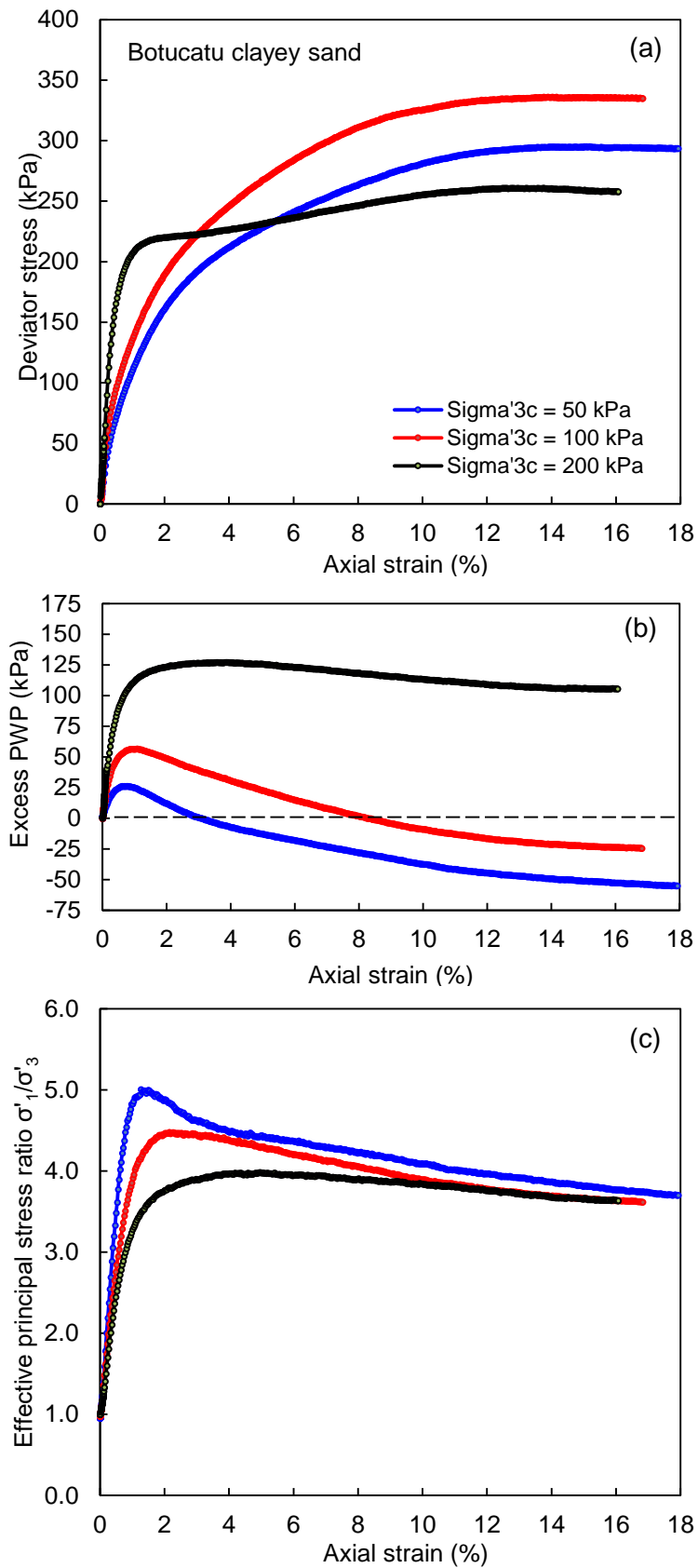
Source: author.

Figure 119 – Results of CIU tests on CT1.5:1 mixture.



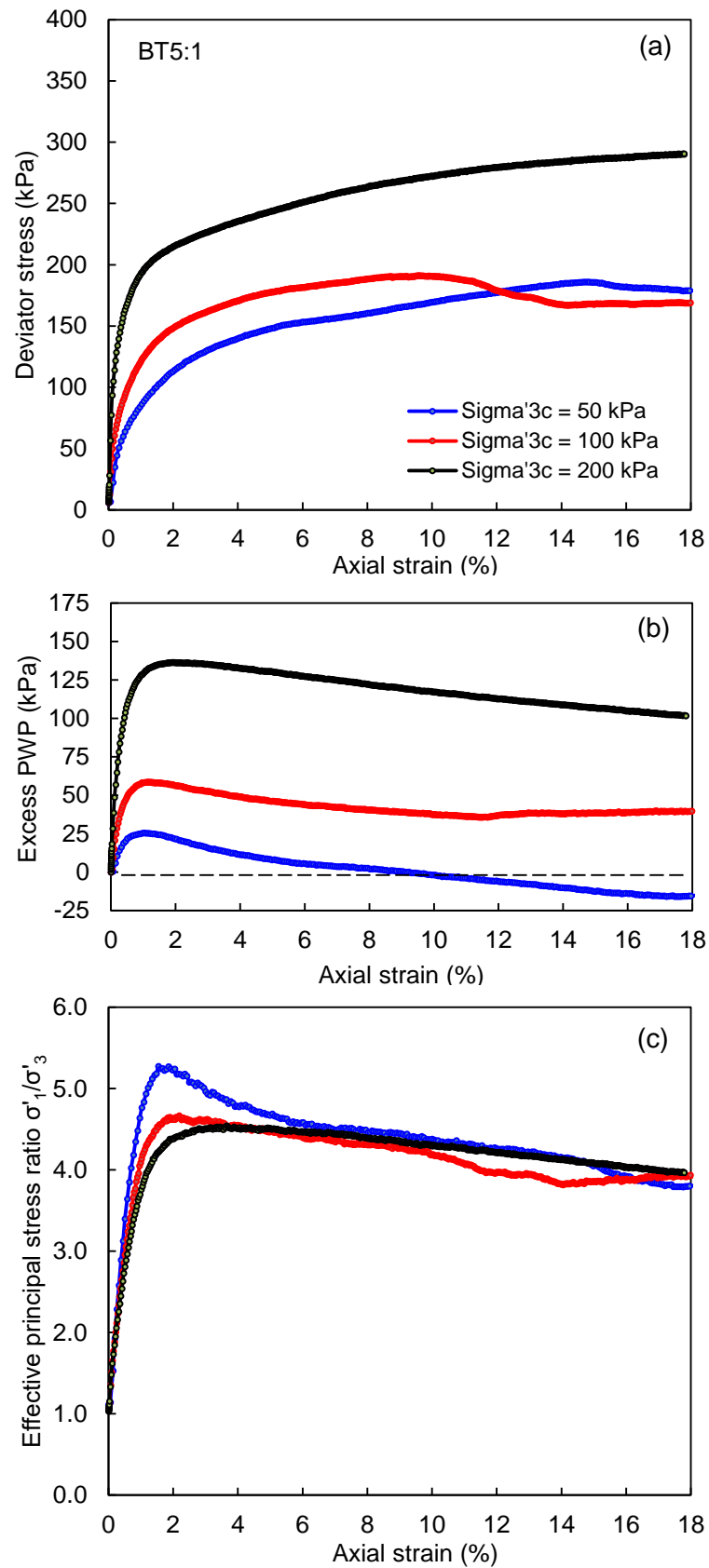
Source: author.

Figure 120 – Results of CIU tests on Botucatu clayey sand.



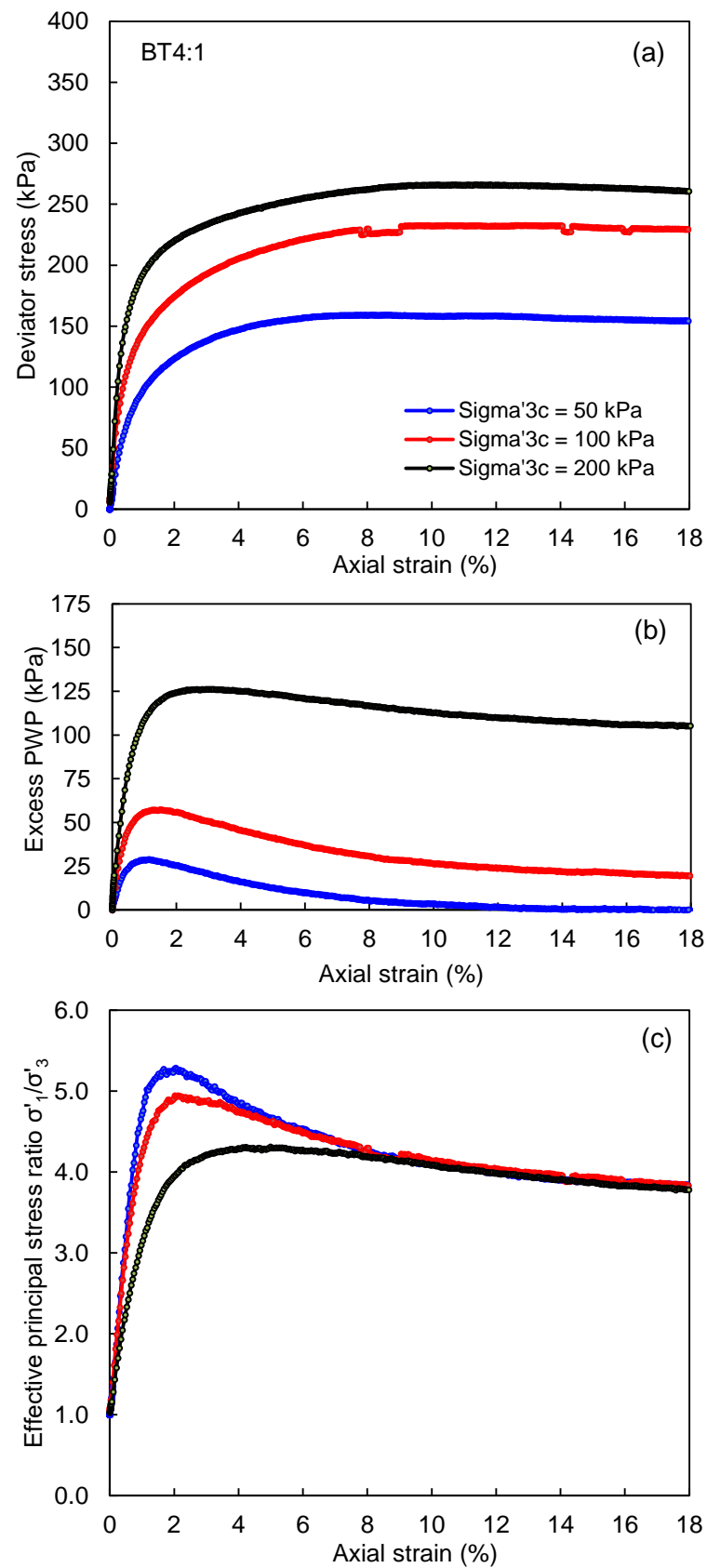
Source: author.

Figure 121 – Results of CIU tests on BT5:1 mixture.



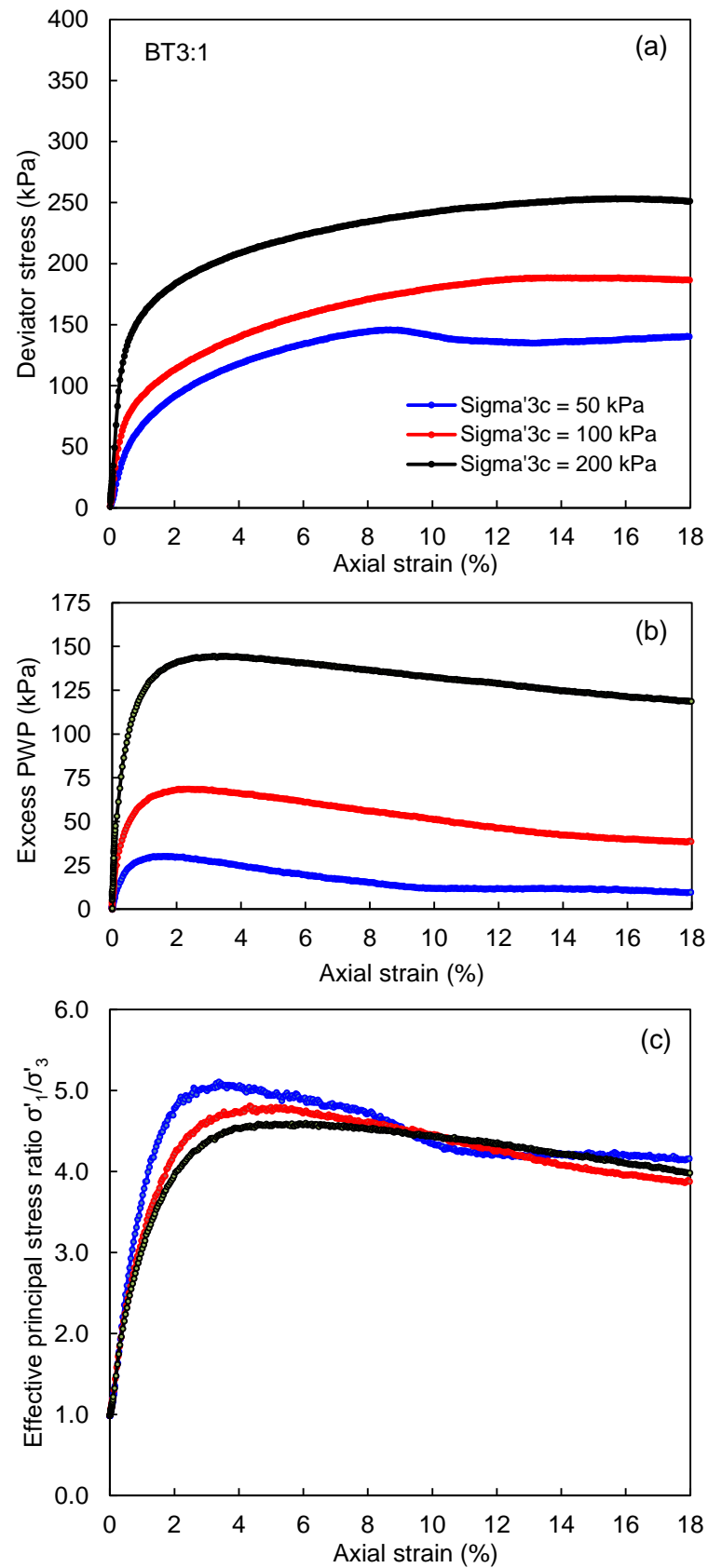
Source: author.

Figure 122 – Results of CIU tests on BT4:1 mixture.



Source: author.

Figure 123 – Results of CIU tests on BT3:1 mixture.

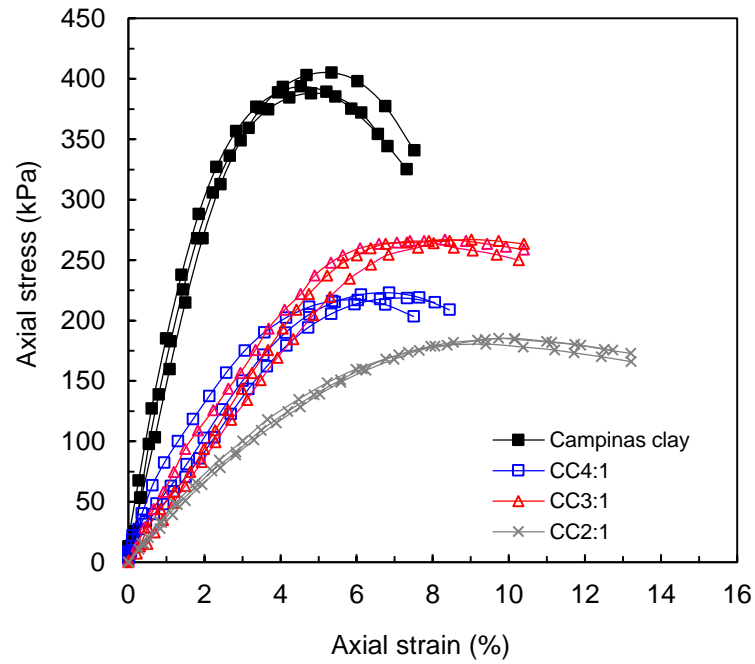


Source: author.

APPENDIX G

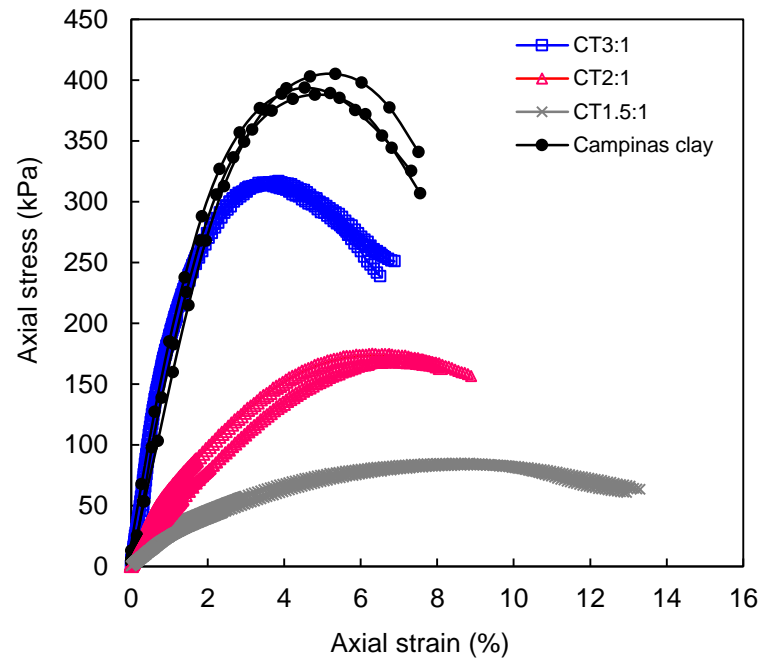
Results from unconfined compression tests (UC): *axial stress vs. axial strain* curves.

Figure 124 – Stress-strain curves from UC tests on Campinas clay and CC mixtures.



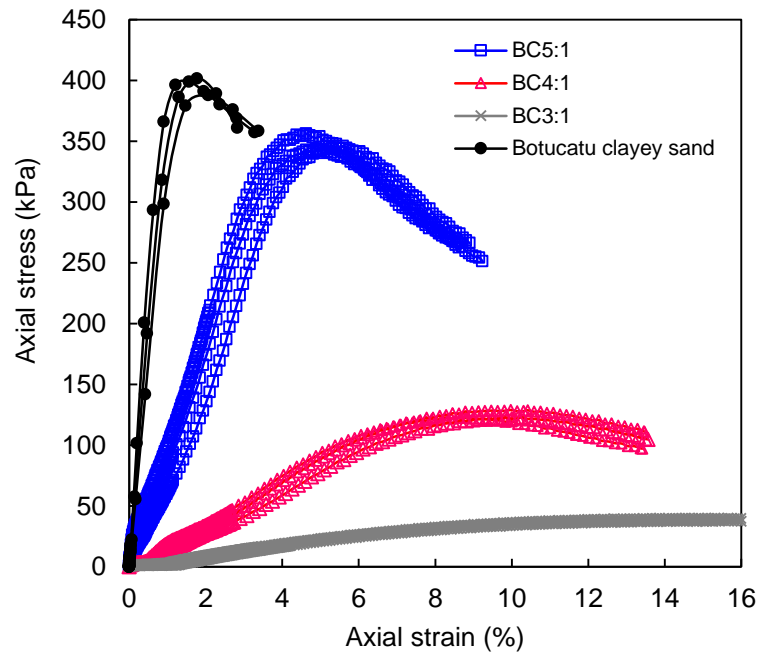
Source: author.

Figure 125 – Stress-strain curves from UC tests on Campinas clay and CT mixtures.



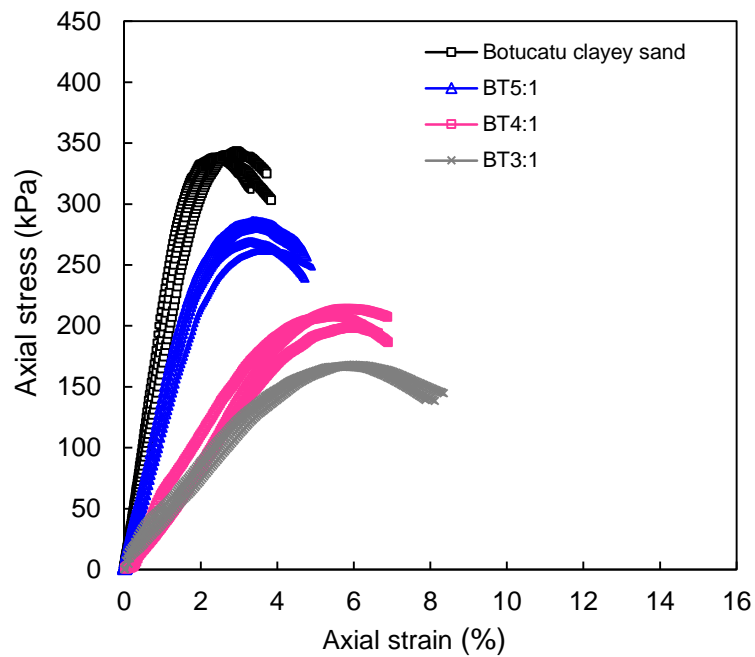
Source: author.

Figure 126 – Stress-strain curves from UC tests on Botucatu clayey sand and BC mixtures.



Source: author.

Figure 127 – Stress-strain curves from UC tests on Botucatu clayey sand and BT mixtures.



Source: author.